

A STRUCTURAL STUDY OF THE VARISCAN

FOLD BELT IN NORTHERN PORTUGAL

BY

DAVID WILLIAM COLLER

Thesis submitted in accordance with
the requirements of the Council for
National Academic Awards for the
degree of Doctor of Philosophy.

Research was Carried Out at Kingston Polytechnic

December 1979

BEST COPY AVAILABLE.

VARIABLE PRINT QUALITY

**VOLUME CONTAINS
CLEAR OVERLAYS**

**OVERLAYS HAVE BEEN
SCANNED SEPERATELY
AND THEN AGAIN OVER
THE RELEVANT PAGE**



IMAGING SERVICES NORTH

Boston Spa, Wetherby

West Yorkshire, LS23 7BQ

www.bl.uk

**CONTAINS MAPS
IN BACK POCKET**

To My Mother and Father

ABSTRACT

The Variscan Fold Belt in Northern Portugal comprises late Precambrian and Lower Palaeozoic sediments folded in three, N.W.-S.E. trending kilometric-scale folds, the Valongo Anticline, the Penacova Syncline and the Marão Syncline.

It is shown that prior to the Variscan deformation (post L. Devonian) the Complexo xisto-grauvaquico, an undifferentiated sequence of non-fossiliferous fine-grained sediments of late Precambrian to Cambrian age were gently folded during Upper Cambrian times resulting in a significant planar-linear alignment of conglomerate pebbles.

Variscan deformation was dominated by one major ductile phase, DV_1 , characterised by plane strain fabrics and an intense pervasive cleavage. A consistent sub-horizontal elongation lineation in the Ordovician rocks is shown to coincide with the bedding/ S_1 cleavage intersection lineation and F_1 minor fold axes. It is demonstrated that burial metamorphic chlorite porphyroblasts are preserved in the domainal structure of the S_1 cleavage in Ordovician slates.

Tight refolding of Upper Cambrian folds by DV_1 resulted in constrictional fabrics in deformed conglomerates with a maximum elongation plunging at various angles sub-parallel to F_1 fold axes.

The Armorican Quartzite sl, a thick succession of bedded orthoquartzites of Arenig age is shown to have behaved as a competent multilayered unit during DV_1 controlling the development of the three major F_1 folds in the belt. In the Marão Syncline a pre-syn-buckling spaced, pressure-solution cleavage, S'_1 , is recognised. This cleavage pre-dates the regional, grain alignment cleavage, S_1 which is either axial or non-axial-planar to F_1 folds.

Deformed conglomerates, fossils and spots in the Ordovician rocks, and a variation in texture in massive quartzites of the Santa Justa Formation all indicate an increase in strain north eastwards across the Fold Belt.

Post- DV_1 , inhomogenous, ductile shearing in a coastal area 70kms north of Valongo is recognised as an extension of the Douro Shear Belt.

A model of large-scale inhomogeneous simple shear for the Variscan deformation is described explaining the horizontal maximum elongation and DV_1 structures comprising the Fold Belt.

CONTENTS

SECTION A

Page No.

CHAPTER 1

INTRODUCTION

1.1	Regional Setting	1
1.2	Topography and exposure	7
1.3	Previous work	8
1.4	Main objectives and method of approach	9
1.5	Terminology	11
1.6	Stratigraphy	12
1.7	Structural Chronology of north Portugal	24
1.8	Metamorphism	32

SECTION B

CHAPTER 2

THE VALONGO ANTICLINE BETWEEN VALONGO AND SATÃO

2.1.	Introduction	38
2.2.	Stratigraphy	
	1. Complexo xisto - grauvaquico	38
	2. Ordovician	41
2.3	Major structure	46
2.4	Minor structures	52
	1. Cleavage	52
	2. Minor folds	58
	3. Elongation structures	61
2.5	Summary	61

CHAPTER 3THE COASTAL REGION AROUND APULIA AND VIANADO CASTELO

3.1	Introduction	69
3.2	Stratigraphy	
	Apulia	69
	Viana do Castelo	73
3.3	Structure at Apulia	
	General	73
	Deformed <u>Skolithos</u>	76
	Summary	84
	Late structures	85
3.4	Structure at Viana do Castelo	
	General	87
	Ductile Shear Zones	89

CHAPTER 4THE PENACOVA SYNCLINE BETWEEN LUSO AND PIORES

4.1.	Introduction	94
4.2	Stratigraphy	94
4.3	Structure	
	1. The Upper Cambrian Deformation	98
	2. The morphology of the Penacova Syncline	100
	3. Cleavage and minor structures	101
	4. Strain related to DV ₁	106
	5. The Penacova Deformation Zone	109
4.4	Summary	111

CHAPTER 5THE MARÃO SYNCLINE

5.1	Introduction	113
5.2	Stratigraphy and lithologies	
	1. The Complexo xisto-grauvaquico	114
	2. The Ordovician	115
5.3	Structure	
	1. Major structure of the Marão Syncline	123
	2. Minor folds	124
	3. Cleavage development	131
	4. Evolution of the Dv1 structures	140
	5. Pebble deformation and cleavage development in the Marão conglomerate	145
5.4	Summary	153

SECTION CCHAPTER 6

<u>FINITE STRAIN IN THE ORDOVICIAN ROCKS</u>	159	
6.1	Conglomerates	161
6.2	Ellipsoidal spots	163
6.3	Fossils	166
6.4	Summary	169

CHAPTER 7STRAIN IN THE COMPLEXO XISTO-GRAUVAQUICO

7.1	Introduction	172
-----	--------------	-----

7.2	The conglomerates in the Complexo Xisto- grauvaquico	
1.	Sedimentary features	173
2.	Tectonic features	173
3.	Composition of the conglomerates	176
7.3	Analysis of strain using the deformed conglomerates	
1.	Methods of measurement	182
2.	Pebbles and the strain ellipsoid	185
a.	pebble composition and grain size	185
b.	pre-tectonic fabric	187
c.	rotation of pebbles during deformation	190
d.	polyphase deformation	190
7.4	Representation and description of the strain	191
7.5	Interpretation of the strain	197
1.	Subtraction of the DV_1^V ariscan strain	199
2.	Theoretical superimposed strains	207
7.6	Summary	212

CHAPTER 8

THE DEVELOPMENT OF TEXTURES IN THE ORDOVICIAN

QUARTZITES

8.1	General features of the quartzites	214
8.2	Undeformed quartzites of the Penacova Syncline	215

8.3	Deformation textures in the quartzites of the Valongo Anticline	215
8.4	Deformation and annealed textures in quartzites of the Marao Syncline	222
8.5	Summary	226

CHAPTER 9LATE VARISCAN DUCTILE-BRITTLE STRUCTURES

9.1	Classification of structures	229
	Ductile-brittle deformation zones	231
	Kink bands	233
9.2	Discussion	235

CHAPTER 10SLATY CLEAVAGE AND CHLORITE PORPHYROBLASTS

10.1	Slaty cleavage	237
10.2	Crenulation cleavage	238
10.3	Nature of the chlorite porphyroblasts	241
10.4	Conclusions	249

SECTIONCHAPTER 11SUMMARY AND REGIONAL CONSIDERATIONS

1.	Folding and cleavage	252
2.	Variscan strain	253
3.	Superimposed strain in the Complexo xisto-grauvaquico	254
4.	Regional considerations	254

Page No.

ACKNOWLEDGEMENTS

262

REFERENCES

263

S E C T I O N A

CHAPTER 1

INTRODUCTION

In North Portugal the present level of erosion exposes Ordovician to Lower Devonian sediments in the hinge zones of kilometric scale folds comprising the Variscan Fold Belt. The structural geology of three such major folds forms the subject of this thesis. The geographic location of the areas studied are shown in Fig. 1.1.

1.1 REGIONAL SETTING

The majority of north-western Iberia comprises of late Precambrian and Palaeozoic sediments which have been deformed, regionally metamorphosed and extensively intruded by granites during the Variscan Orogeny. Older, deep crustal Precambrian rocks are present in three separate complexes each comprising ultrabasic and basic igneous rocks associated with polymetamorphic sediments and paragneisses. All three complexes are considered to be allochthonous, catazonal remnants of a thrustured plate which originated from the west (Ries and Shackleton, 1971). Ribeiro (1974), however, proposes a different origin for the Morais Complex in north-east Portugal suggesting that it was emplaced as an upthrustured diapir. Slices of Precambrian basement have also been recorded (Carta Geologica de Portugal, 1:500,000, 1972) outcropping along the Porto-Portalegre tectonic lineament (Fig. 1.2).

FIG. 1.1

Location of study areas in Northern Portugal

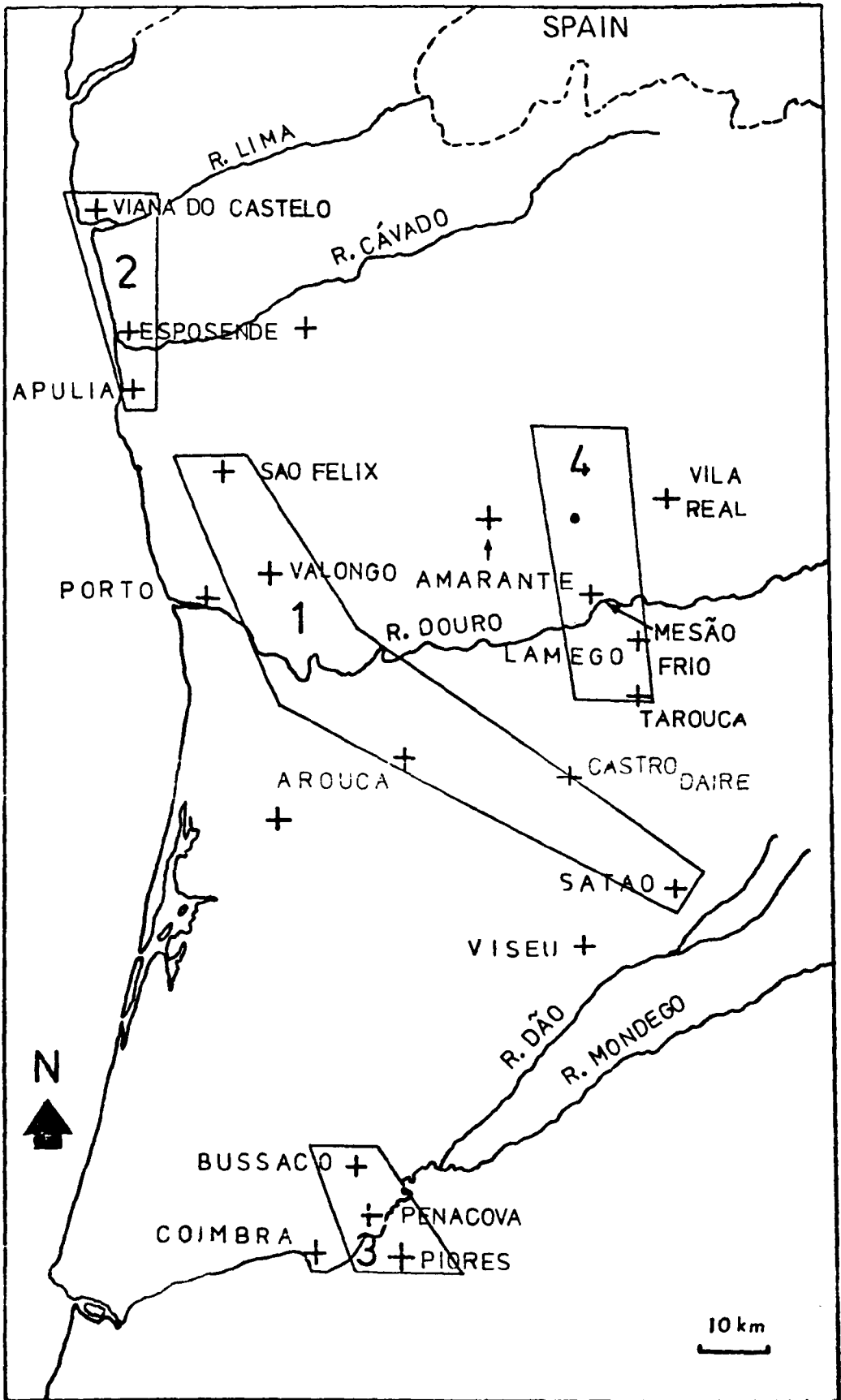
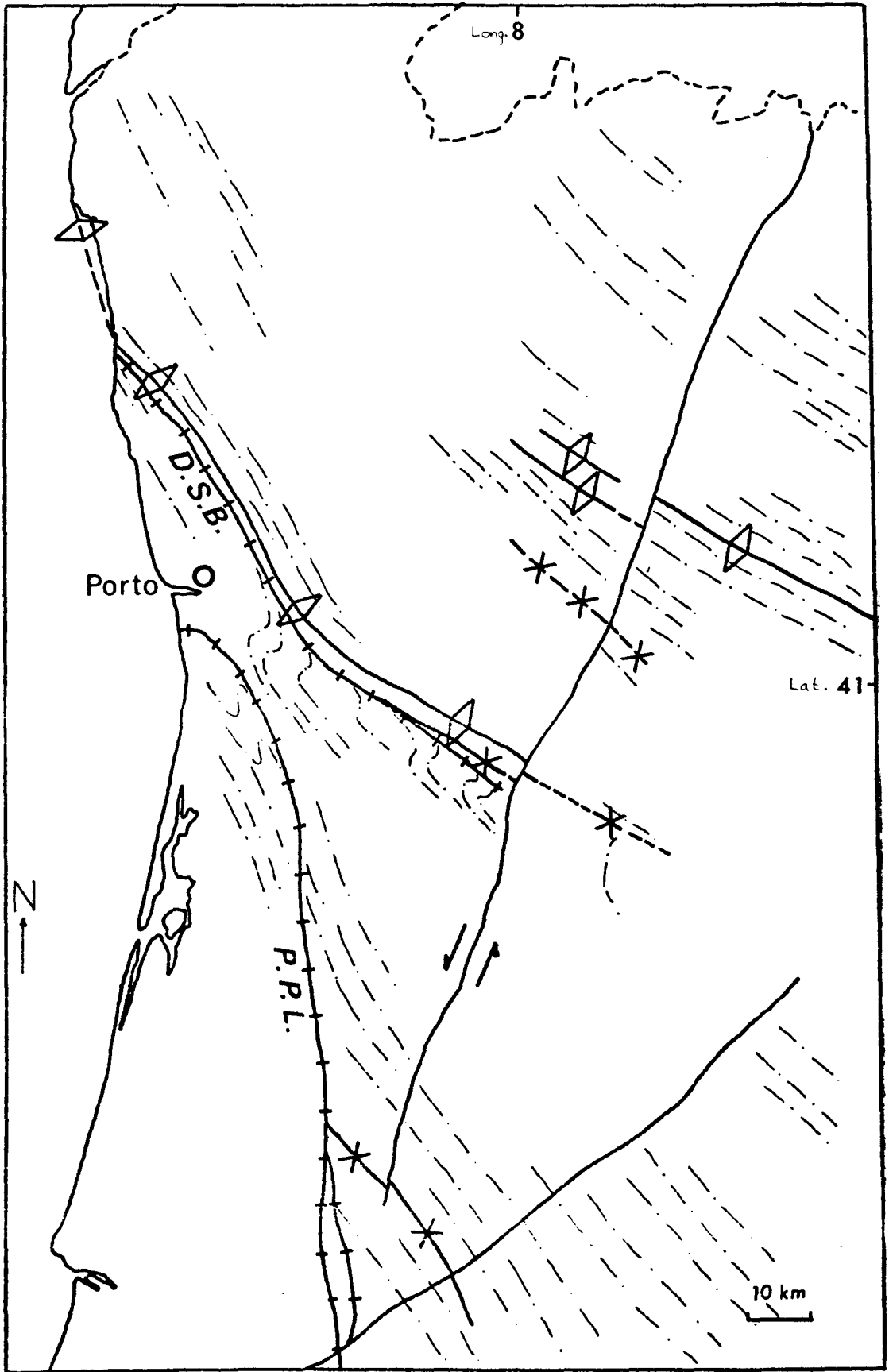


FIG. 1.2

Axial traces of major first phase Variscan folds and major lineaments.

D.S.B. Douro Shear Belt

P.P.L. Porto - Portalegre Lineament



The term Complexo xisto-grauvaquico (Teixeira , 1955; Bard et. al., 1971) is adopted in this thesis in preference to Beira Schists (Schermerhorn, 1955) to describe the late Precambrian to Cambrian sedimentary succession. The base of this succession is not defined, while the contact between Precambrian crystalline basement rocks and younger sediments is always recorded as a thrust or faulted one (Ries et. al., 1971, Ribeiro, 1974).

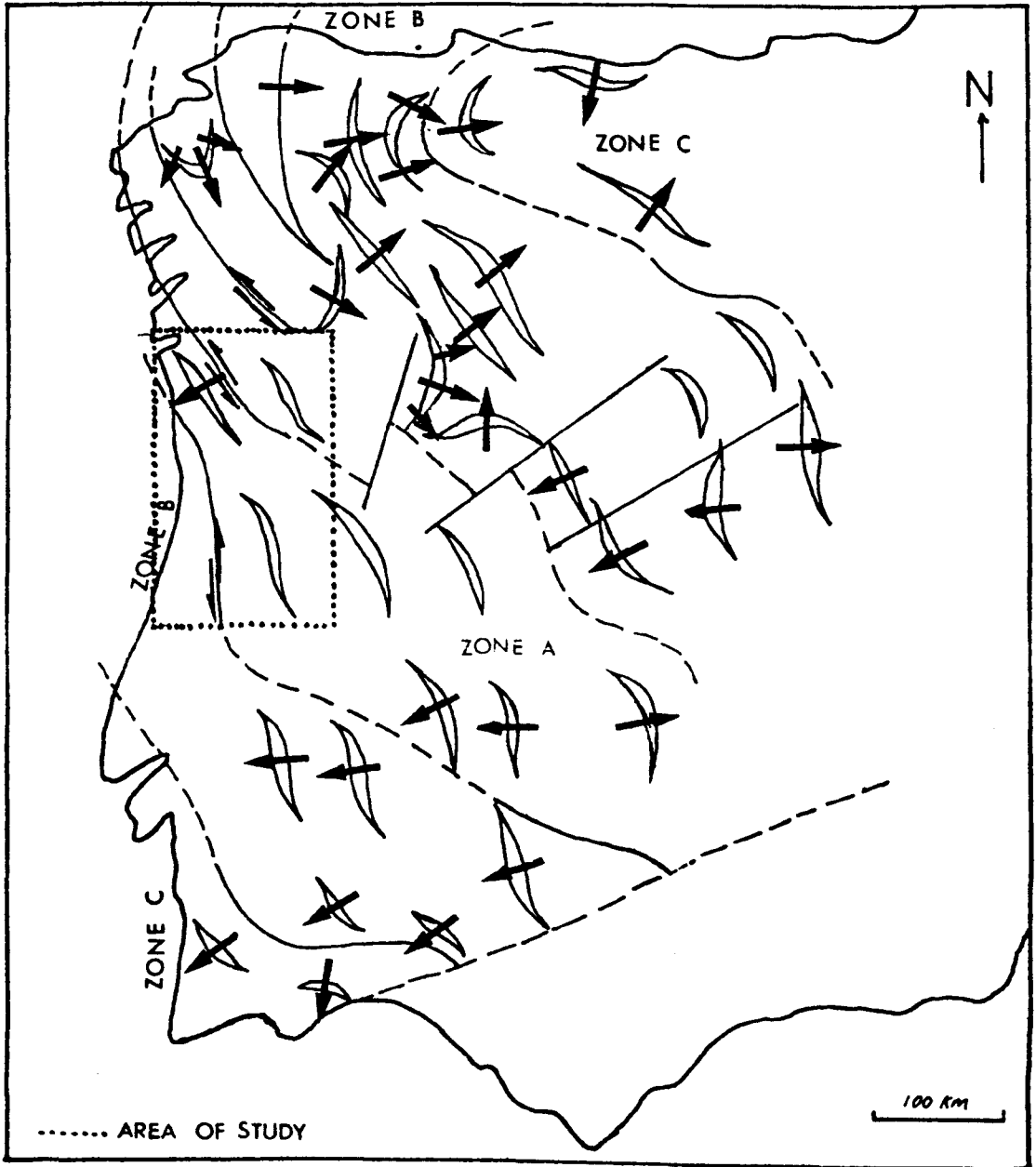
Bard, Capdevila and Matte (1971) usefully summarise the structure of the Variscan Belt in Iberia, largely by subdividing the Peninsula into zones of different palaeogeography, stratigraphy, tectonics, metamorphism and granite distribution (Fig. 1.3). Similar zones to those in the north-western part of Iberia are recognised in southern Brittany, France; the two regions are believed to have been adjoined at least until the end of the Variscan Orogeny (Bard et. al. op.cit.).

Several plate reconstruction models based on the closing, or partial closing of the Bay of Biscay to rejoin Iberia and Brittany have been proposed, most of which have been reviewed by Ries (1974) and Choukroune, Le Pichon, Seguret and Sibuet (1973). The most recent model of reconstruction involves restoring the Iberian Peninsula to a position due west of Brittany at the end of the Palaeozoic (Bless, 1977). Recent tentative correlation of late Palaeozoic Tethyan faunal provinces (Oliveira, pers comm), supports the proposal of Bless (1977) that the

FIG. 1.3.

Structural zonation of the Iberian Variscan Orogenic Belt.

Arrows indicate the vergence of major first phase folds



(Adapted from Bard et. al. 1973 Figure 1)

Iberian Variscan Orogenic Belt is a longitudinal extension of the Central European Moldanubian Zone (Read and Watson, 1975).

In Iberia, tectonic and metamorphic activity of Alpine age is largely restricted to the Pyrenees in north-east Spain, and the Betic chain in south Spain i.e. the area considered in this thesis is essentially unaffected by the Alpine Orogeny.

From the structural zonation erected by Bard et. al. (1971) and Bard et. al. (1973) the simplest interpretation of the Variscan Orogenic Belt is that it consists of an internal zone flanked by two roughly symmetrical external zones (Fig. 1.3). The external zones, in Cantabria and south-west Portugal, are characterised by high level nappe and thrust tectonics with a dominant transport direction away from the axis of the orogen.

The internal zone has been further subdivided by Bard et.al. (1973) into three tectono-metamorphic zones: a central, or axial zone characterised by folds with vertical hinge surfaces and a steeply inclined cleavage. Either side of the central zone are two roughly symmetrical zones characterised by folds with inclined hinge surfaces. The cleavage across the internal zone has a fan-like pattern related to the inclined folds which verge in a direction away from the axis of the central zone.

This thesis examines the main fold structures across a region which forms part of the Central Zone of the Variscan Orogenic Belt.

1.2 TOPOGRAPHY AND EXPOSURE

North Portugal is a region of low-lying topography rarely exceeding a thousand metres above sea level. The region receives moderately high seasonal rainfall which supports a varied, often dense vegetation; this is in stark contrast to the arid and sparsely vegetated south.

Three broad groups of rocks: granites, pelitic to semi-pelitic sediments, and quartzites, give rise to the diverse landscape. Granites underly two thirds of the region and generally form rounded, hummocky terrain of either exposed rock or forest. The pelitic to semi-pelitic sediments give rise to gently undulating, densely vegetated terrain often forested by eucalyptus. The quartzites generally form striking ridges and scarps with bare rock and scree partially covered by forest.

The region is drained essentially by the Douro and the Mondego rivers which have both eroded prominent valleys with gorge sections. Over much of the inland region, the best exposure is provided by natural cuttings made by rivers and streams, road cuttings, bullock and mine tracks. The Serra do Marão are the exception, composed of exposed quartzite mountains.

1.3 PREVIOUS WORK

Delgado (1908) published a comprehensive stratigraphy, including maps, of the Lower Palaeozoic of North Portugal, upon which almost all following work has been based. However, since Delgado's original mapping Portuguese and other workers have tended to present only discussions and notes on regional tectonic and stratigraphic problems (Teixeira, 1943, 1955a; Carrington da Costa, 1948, 1950; Schermerhorn, 1955), whilst there have been few detailed descriptions of the structures throughout the region.

One of the main discussion topics over the years has been the 'Caledonian Orogeny' in North Portugal.

Schermerhorn (1955) argues that there are no Caledonian effects, excepting epeirogenic movements, and the earliest recognisable phase of deformation is Pre-Variscan in age, and represents an Upper Cambrian orogenic event. This view contrasts with Teixeira (1943, 1955a) and Carrington da Costa (1948, 1950), who assign the Pre-Variscan deformation to a Caledonian orogenic phase.

The most significant contribution to the detailed structural geology of North Portugal has been the study, by Ribeiro (1974), of the Tragos-Montes region. This region lies approximately 50 kilometres north-east of the eastern limit of the area examined in this thesis, and contains two of the Precambrian complexes, Morais and Bragança, encircled by Silurian sediments. Ribeiro

(ibid.) presents detailed descriptions of minor structures and a chronology of events for the Variscan in north-east Portugal.

Relevant studies have been made by three other authors in areas encompassed by the region dealt with in this thesis. Firstly, Schermerhorn (1956) has described the geology, with particular emphasis on the granitoid rocks, around Castro Daire (Fig. 1.1). Oen (1958), again with the emphasis on the granitoid rocks, has described the geology between Porto and Viseu (Fig. 1.1). Priem (1962) has described the geology of the northern part of Serra do Marão, particularly the economic mineral deposits.

Most recently, Romano and Diggins (1974) have presented a revised stratigraphy and detailed description of the structure of the area around Valongo.

1.4 MAIN OBJECTIVES AND METHOD OF APPROACH

Preliminary studies by J. N. Diggins of Kingston Polytechnic and M. Romano of Sheffield University, primarily on the sedimentology and palaeontology of the Lower Palaeozoic rocks within the Variscan Fold Belt of North Portugal, prompted a detailed investigation, by the author, into the structural geology of that region.

The Lower Palaeozoic rocks within this area are repeated by three major Variscan fold structures separated

by the Complexo xisto-grauvaquico and Variscan granites. All three folds, in terms of their scale and geometry, are largely controlled by the Armorican quartzite(s.l.) generally regarded as being mainly Arenig, Lower Ordovician in age (Teixeira, 1968; Romano and Diggens, 1974).

The main object of the project was to map each of the folds along their axial lengths from well exposed traverse sections to examine the following:

i. To construct the accurate fold geometries from the measurement of minor structures; and to analyse the fold mechanisms.

ii. In relation to (i), to examine the internal deformation of the quartzites comprising the Armorican quartzite, in particular their microstructure and recrystallisation.

iii. To examine the patterns of strain within each fold and the whole fold belt by measuring the abundant deformed objects in the Ordovician rocks e.g. conglomerate pebbles, fossils and various spots, and in the Complexo xisto-grauvaquico e.g. conglomerate pebbles and spots. A second aim of the strain analysis was to resolve the magnitude and symmetry of the strain attributable to the Pre-Variscan and Variscan deformations.

Mapping was carried out using topographic maps of

scale 1:25,000 which were issued by the Servicos Cartograficos do Exercicio on authorisation from the Servicos Geologicos do Portugal.

The thesis is divided into four sections. In this first, introductory section the regional stratigraphy, geochronology, and metamorphism are described. In the second section the three kilometric scale folds are described in four separate areas: the Valongo Anticline outcropping between Valongo and Castro Daire, and Viana do Castelo and Apulia; the Penacova Syncline outcropping between Bussaco and Piores; the Marão Syncline outcropping between Pardelhas and Penajoia. The third section describes five different topics common to two or more of the areas. The final section presents the conclusions and discussion on the structural evolution of the fold belt.

1.5 TERMINOLOGY

The terms Variscan, Hercynian and Armorican are often used synonymously to describe the same orogenic belt. A certain amount of confusion has arisen by the use of the above terms to describe structural trends, timing of events and the geographical location of the orogen (Coe, 1962; Matte, 1968; Bennison et.al. 1969). For clarity in this thesis the term Variscan is used to describe the orogenic belt in Iberia without implying any specific time significance. For consistency the 'Older' and 'Younger' Hercynian Granites (Oen, 1970) will be referred to as the 'Older' and 'Younger' Variscan Granites. The

table in Fig. 1.4 lists the structural nomenclature and abbreviations used in this thesis.

1.6 STRATIGRAPHY

The stratigraphy of North Portugal is summarised in Fig. 1.5

i. Complexo xisto-grauvaquico

The Complexo xisto-grauvaquico comprises the oldest succession of sedimentary rocks exposed in the region. The upper sequences are considered to be laterally equivalent to the fossiliferous Cambrian in Spain and S.E. Central Portugal (Schermerhorn, 1955) although the exact age range of the succession remains conjectural. Except for several specimens of Lingulella (Ribeiro et.al., 1962; Teixeira et.al. 1964) proving a Palaeozoic age for part of the succession, the sediments are non-fossiliferous. The sediments also appear not to contain microfossils, although more material needs to be analysed (Romano, pers. com.).

Schermerhorn (1955) suggests, in a review of the stratigraphical evidence of the Complexo xisto-grauvaquico (Beira Schists), a Precambrian to Cambrian age for the succession. Bard et.al. (1971) prefer a Cambrian age for most of the succession.

The succession consists of very thick laterally homogeneous sequences of fine-grained greywackes, silts-tones and slates, and metamorphic rocks ranging from

FIG. 1.4

STRUCTURAL NOMENCLATURE AND ABBREVIATIONS

- DU Upper Cambrian Deformation
- DV₁ First phase Variscan Deformation
- DV₂ Second phase Variscan Deformation
- F₀ Upper Cambrian Folds
- F₁ First phase Variscan Folds
- F₂ Second phase Variscan Folds
- S₀ Bedding Surface
- S'₁ Early first phase Variscan pressure solution cleavage
- S₁ First phase regional Variscan cleavage
- S₂ Second phase Variscan cleavage

Strain Ellipsoid

- X Major axis
- Y Intermediate axis
- Z Minor axis
- K Parameter describing symmetry of strain ellipsoid
where $K = \frac{X}{Y/Z}$

Natural or logarithmic strain

FIG. 1.5

Precambrian and Lower Palaeozoic Stratigraphy of
Northern Portugal

		FORMATION	LITHOLOGY	
DEVONIAN	Upper		Quartzites, greywackes and slates	First phase of Variscan deformation
	Lower			
SILURIAN	Ashgill	Sobredo Formation	Greywackes Quartzites	Continuous sedimentation
	Caradoc ?			
ORDOVICIAN	Llandeilo?	Valongo Formation	Blue-grey slates	Continuous sedimentation
	Llanvirn	Santa Justa Formation (Armorican Quartzite)	Interbedded quartzites and shales Massive white quartzites Basal conglomerate Possible red beds ?	
CAMBRIAN	Arenig			Complexo xisto-grauvaquico
	Tremadoc			
	Upper			
PRECAMBRIAN	Middle		Massifs of Branca and Morais Polymetamorphic gneisses	Metamorphism
	Lower			

hornfelses to staurolite - kyanite - mica schists. Within the fine-grained sediments are single or multiple beds of quartz- and quartzite-pebble conglomerates. Subordinate limestone beds occur within the sequences in the Douro valley approaching the eastern border, while they become more extensive eastwards into Spain (Schermerhorn, 1955).

Most of the fine-grained sediments weather to a grey-green colour mainly due to the burial and regional metamorphic chlorite (Slide D70).

Bedding

The fine-grained sediments are ubiquitously very thinly bedded with an average thickness less than 10 centimetres. The general bed form is planar lamination with only very rare cross lamination or current bedding. The distinct bed units usually have a homogeneous grain size distribution, rarely showing any significant grading. The beds also have planar tops and bottoms, although in most cases it is not possible to distinguish their way up.

The total thickness of the succession has been previously estimated at 2½ kilometres at minimum by Schermerhorn (1955) for the Viseu region. Ribeiro (1974) reports a progressive diminution of the succession from Porto north-eastwards to Serra de la Culebra, Spain.

The fine clastic sediments comprising the Complexo

xisto-grauvaquico have been interpreted as a thick geosynclinal sequence deposited by turbidity currents (Schermmerhorn, 1955). Certainly many features of these sediments, namely: thin bedding; alternating greywackes and slates; large thickness and lateral extent; lack of shallow water fauna, are characteristic of a distal turbidite facies; however, there are several important features which are incompatible with this general interpretation. The beds, singularly or as sets, are not graded vertically in grain size as is generally found in turbidite flows or packages.

Secondly, the beds do not possess either bottom structures, such as groove marks or flute casts, or erosional bases generally common at the base of turbidite flows and indicating turbulent flow.

It remains open, being beyond the scope of this thesis, whether this thick, monotonous sequence of fine clastic deposits is a true distal turbidite facies or perhaps, a marine platform facies deposited in fairly deep water in a less turbid environment. The Complexo xisto-grauvaquico of North Portugal calls for a detailed sedimentological study.

ii. The Ordovician - The distribution of Ordovician sediments is shown in Fig. 1.6.

The sedimentary successions comprising the Ordovician,

FIG. 1.6

Principal exposures of the Ordovician (black) and
Silurian (dots) sediments in Northern Portugal.

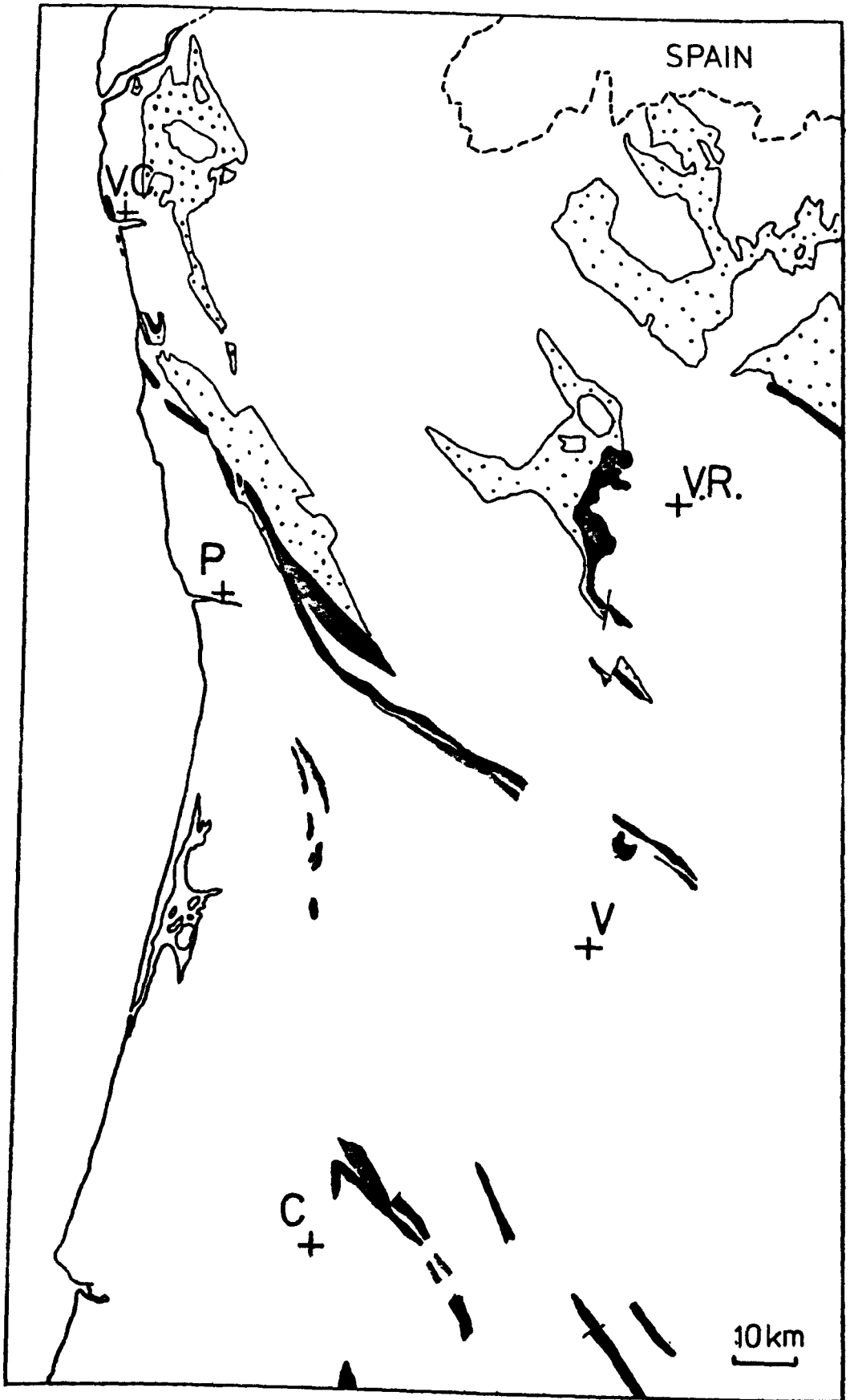
V.C. Viana do Castelo

P. Porto

V.R. Vila Real

C. Coimbra

V. Viseu



Silurian and Lower Devonian, although varied in their lithologies, form a conformable series of marine deposits which are interrupted only very locally during the Ordovician by volcanic rocks. They have been deformed together^{and} show the same structural histories and will therefore be considered in the main part of this thesis as a major tectonic unit.

In north and north-east Spain Cambrian sediments pass conformably up into those of Ordovician age (Schermerhorn, 1955); whereas in north Portugal the base of the Ordovician everywhere overlies the Complexo xisto-grauvaquico with either a slight to appreciable angular discordance or a concordance. The angular unconformity is well exposed in a road cutting on the N108, near the village of Sebolido on the north bank of the river Douro. A concordant relationship is exposed in a road cutting approximately 4 kilometres north-west of Mesão Frio (see chapter 5), however it is suspected that it is a discontinuity rather than a conformable contact. Most contacts are unfortunately tectonised. The regional unconformity has resulted from folding, uplift and erosion of the Complexo xisto-grauvaquico during the Upper Cambrian, tectonic activity which is largely localised to north Portugal (Schermerhorn, 1955).

The Ordovician is divisible into three distinct formations recognisable throughout most of the region (Fig. 1.5). A sequence of shallow water epiclastic deposits comprises the Armorican Quartzite, the basal formation of the Ordovician.

This formation is very distinctive and is present in many parts of Europe.

Although the formational term Armorican Quartzite is used it is often referred to as the 'Formation du Gres Armorican' (Babin 1972). Delgado (1908) originally used the two names: 'Quartzites a Bilobites' and 'Quartzites a Scolithos' to describe the same formation having subdivided it on the presence of different fauna. It has also been referred to in the Valongo area as the Santa Justa Formation (Romano and Diggins, 1974).

Lithologically the Armorican Quartzite is internally diverse and detailed descriptions of the sediments, including mineralogy, texture and sedimentary structures, in each area follow in the succeeding chapters 2 to 5. However, below is a general description of the succession, its age and depositional environment.

The formation begins with a variable conglomerate facies whose thickness ranges from less than 2 metres in the Valongo area to almost 200 metres in the Serra do Marão. Generally these are orthoconglomerates composed of self-supporting pebbles or cobbles of quartz and quartzite with subordinate slate, in either a quartzitic or semi-pelitic matrix.

The conglomerates pass up into a thick sequence (up to 200 metres) of massive to well bedded quartzites which

characterise the formation throughout much of Europe. In the westernmost areas where the quartzites are the least recrystallised (e.g. Penacova) they are texturally mature (i.e. well sorted and well rounded grains) and mineralogically mature, orthoquartzites. The predominant bed forms are small scale cross bedding (less than 10 metres) and planar bedding, with ripple lamination common towards the top of the sequence where they tend to become thinner and interbedded with thin shales.

In most areas there is an increase in the proportion of shale and siltstone in the upper part of the quartzite facies, with a transition upwards into homogeneous blue to black slates of the middle formation. This transitional passage of beds between the two formations is an important iron-bearing horizon which has proved economic in many areas of north Portugal. The sequence of slates is referred to as the Valongo Formation (Romano & Diggens, 1974) after the type locality where high grade slate is mined. The slates are typically composed of an assemblage of fine-grained quartz, muscovite, chlorite, white mica and opaques.

The slates pass abruptly into sandstones and pebbly greywackes which comprise the upper, or Sobredo Formation (Romano & Diggens, op.cit.) named after the type locality, 4 kilometres north-east of Valongo.

Ages of the Ordovician Formations

The sediments comprising the lower and middle formations

contain body and trace fossils from which they have been dated.

Of the ichnofauna preserved in the Armorican Quartzite, Cruziana furcifera and Cruziana rugosa occur in most areas, generally near the base and toward the top of the formation (Romano & Diggens, 1974). These two trace fossils are indicative of the Arenig (Crimes, 1968). It is noteworthy that the red, basal facies of the Armorican Quartzite at Penacova may be Tremadoc in age (Delgado, 1908).

A Llanvirnian age is well established from the graptolites Didymograptus geminus (Hisinger) and Didymograptus murchisoni (Beck) in the lower part of the Valongo Formation (Romano & Diggens, 1974), while trilobite fauna of the genus Placoparia Hawle and Corda, 1847, indicates a Llandeilo age for the upper part (Romano, 1976).

To date only unidentifiable fragments of brachiopod have been found in the Sobredo Formation (see Romano & Diggens, 1974). However, Romano & Diggens (op.cit.) suggest that at least part of the formation may be Caradoc in age, from lithostratigraphic correlation with the Ordovician succession at Caceres, Spain.

Depositional Environment of the Ordovician

The Armorican Quartzite is characterised by clean-washed, texturally mature sandstones deposited in a shallow water environment.

Common small-scale cross bedding and a cruziana and skolithos ichnofauna indicate that the environment was also one of high energy. The high degree of maturity of the sandstones maybe a result of reworking by bottom traction under prevailing high energy conditions. Alternatively, the sandstones may have been derived from a mature source. The basal conglomerates probably comprise a transgressive shoreline deposit, which in detail is very variable across the region. The great lateral extent of the thick orthoquartzite suggest conditions most likely approximated to a shallow, marine platform. Nabais Conde (1966) has suggested an estuarine or deltaic-like environment for the deposition, while Romano & Diggins, (1974) have argued that these conditions, with influxes of fresh water, are unlikely with the presence of trilobites.

From preliminary studies of the regional thickness changes of the Armorican Quartzite it appears that several fault controlled blocks were active during sedimentation in the Arenig (Romano, pers.comm.).

A general marine transgression in an eastward direction Nabais (Conde, 1966) is supported by a Llandeilo age obtained for the Armorican Quartzite at Vimioso, Spain (Ribeiro, 1974). However, in the Porto region the current directions suggest, locally, that transport movement was in a southerly direction (Romano & Diggins, 1974).

The incoming of shaly horizons towards the top of the quartzites marks a widespread change in the lithofacies

from sandstones to silty mudstones and mudstones. These sediments reflect deposition in a more distal and deeper water environment which supported a sporadically distributed fauna of trilobites, brachiopods and graptolites. The occasional sandy beds in the lower part of this formation may have resulted from sands being washed into the silty muds and muds being deposited in a pro-delta and offshore delta environment.

The Sobredo Formation is interpreted as a deposit of coarser clastic sediment introduced by turbidity currents into the offshore delta or basinal environment.

iii. The Silurian and Lower Devonian

A series of quartzites, greywackes and slates, which comprise the Silurian and Lower Devonian successions, conformably overlie the Sobredo Formation. Only parts of the Silurian succession have been described in any detail i.e. two sections in the hinge of the Penacova syncline (Chapter 4). Delgado (1908) has described the stratigraphy and palaeontology of the Silurian and Lower Devonian in north Portugal, however, it is not the intention of the author of this thesis to review the sedimentology.

In north Portugal there is no record of sedimentation between the end of the Lower Devonian and the Upper Carboniferous, approximately 70 million years, corresponding to the period of Variscan deformation. However, a thick

sequence of flysch-type sediments were deposited during the Lower Carboniferous in a developing basin in south-west Portugal.

Late in the tectonic history of north Portugal sediments of Westphalian (D) and Stephanian (B to C) age were deposited in two narrow intracontinental, limnic basins (Teixeira, 1968). The two, extremely elongate basins developed in the hinge regions of synclines which are complementary to the Valongo Anticline. The basin with the oldest sediments (Westphalian D), and perhaps the first to develop, extends from Apulia to east of Porto to the west of the Valongo Anticline. The other basin, containing Stephanian sediments, extends from Valongo to Satão. The sequences comprise continental polymictic conglomerates and breccias with locally developed coals, generally overlain by shales and greywackes.

Permian (Lower Autunian) sediments were deposited in the region around Bussaco in a third, separate local basin. In this same area, and further south Cretaceous and younger sediments unconformably overlie Palaeozoic and older sediments.

1.7 STRUCTURAL CHRONOLOGY OF NORTH PORTUGAL

The pre-Mesozoic chronology for north Portugal is summarised in Fig. 1.7.

FIG. 1.7

Table showing the structural chronology of Northern Portugal and the rest of Iberia.

The Variscan deformation is diachronous within Iberia with particular events localised in their effect to one area. The structural events, in terms of their age and style of deformation, across Iberia are compared (Fig.1.7).

The details of the structure in each of the areas studied are presented in Section B.

In north Portugal an Upper Cambrian deformation is recognised which precedes three main deformation phases of the Variscan Orogeny.

The Upper Cambrian Deformation

In north Portugal at least there is clear evidence of a significant Upper Cambrian deformation:

Refolding of the Complexo xisto-grauvaquico resulting in fold interference patterns not developed in Ordovician or younger rocks.

Folded bedding of the Complexo xisto-grauvaquico is truncated by the base of the Ordovician.

Deformed conglomerates record a Pre-Ordovician component of strain.

The unconformity at the base of the Ordovician provides an upper limiting age for the deformation. However, in north-west and west Spain Ordovician sediments rest conformably on the Cambrian, with no evidence in these areas of any pre-Variscan folding (Schermerhorn, 1955). In all landward directions away from north Portugal the unconformity

is less clear or absent with Cambrian sediments passing up into the Ordovician with no apparent break in sedimentation e.g. N.W. Spain (Schermerhorn, op.cit.). Schermerhorn (op.cit.) concludes, therefore, that the Upper Cambrian deformation was most intense in north Portugal and affected very little of the remainder of Iberia.

The Upper Cambrian deformation in north Portugal produced one set of folds on a decimetric to kilometric scale only. Although modified by the later, Variscan deformation these folds are open with upright axial planes whose traces trend approximately N.E - S.W. The resolved finite strain component for deformation indicates that there was little or no internal flattening of single beds, but that conglomerate pebbles experienced mainly rigid rotation during folding.

The metasediments of the Complexo xisto-grauvaquico exhibit only one cleavage, which is clearly the same cleavage as that developed in the Lower Palaeozoic rocks i.e. the regional Variscan cleavage S_1 . There is no textural evidence in thin section for the existence of an earlier cleavage related to the Upper Cambrian deformation.

The sediments of the Complexo xisto-grauvaquico are for the most part structurally anisotropic, composed of thinly bedded units. This strong anisotropic nature

considered collectively with the general absence of cleavage and the non-penetrative strain indicate the early folding was dominantly by a flexural slip mechanism.

The same age folds have been described in the Trás-os-Montes region by Ribeiro (1974) and here they are large scale, angular, box-type folds. Similarly, these folds must have developed by a flexural slip mechanism.

Schermerhorn (1955) has argued that equation, by some authors, of the Upper Cambrian folding with the Sardinian phase of the Caledonian Orogeny is not strictly accurate, according to Stille (1939), who defines it as post-Cambrian.

Therefore, apart from gradual facies changes and local sedimentary hiatuses within the Lower Palaeozoic succession which are correlated with epeirogenic movements (Carrington da Costa, 1948), there are no Caledonian effects in Iberia, as stated by Schermerhorn (1955).

The Variscan Deformation

In north Portugal the Variscan Orogeny commenced with a post-Lower Devonian, pre-Westphalian ductile deformation which gave rise to major folds and a regional penetrative cleavage. Two later, subordinate, phases of deformation extended into the Permian. These latter deformations folded Upper Carboniferous sediments, whilst locally refolding or coaxially tightening earlier folds. More

evident in the Lower Palaeozoic rocks is extensive ductile-brittle thrusting, kinking and faulting attributable to these later deformations.

Middle Carboniferous, Westphalian D conglomerates near Covelo, east of Porto, contain clasts of cleaved Lower Palaeozoic sediments which dates the main deformation as pre-Westphalian.

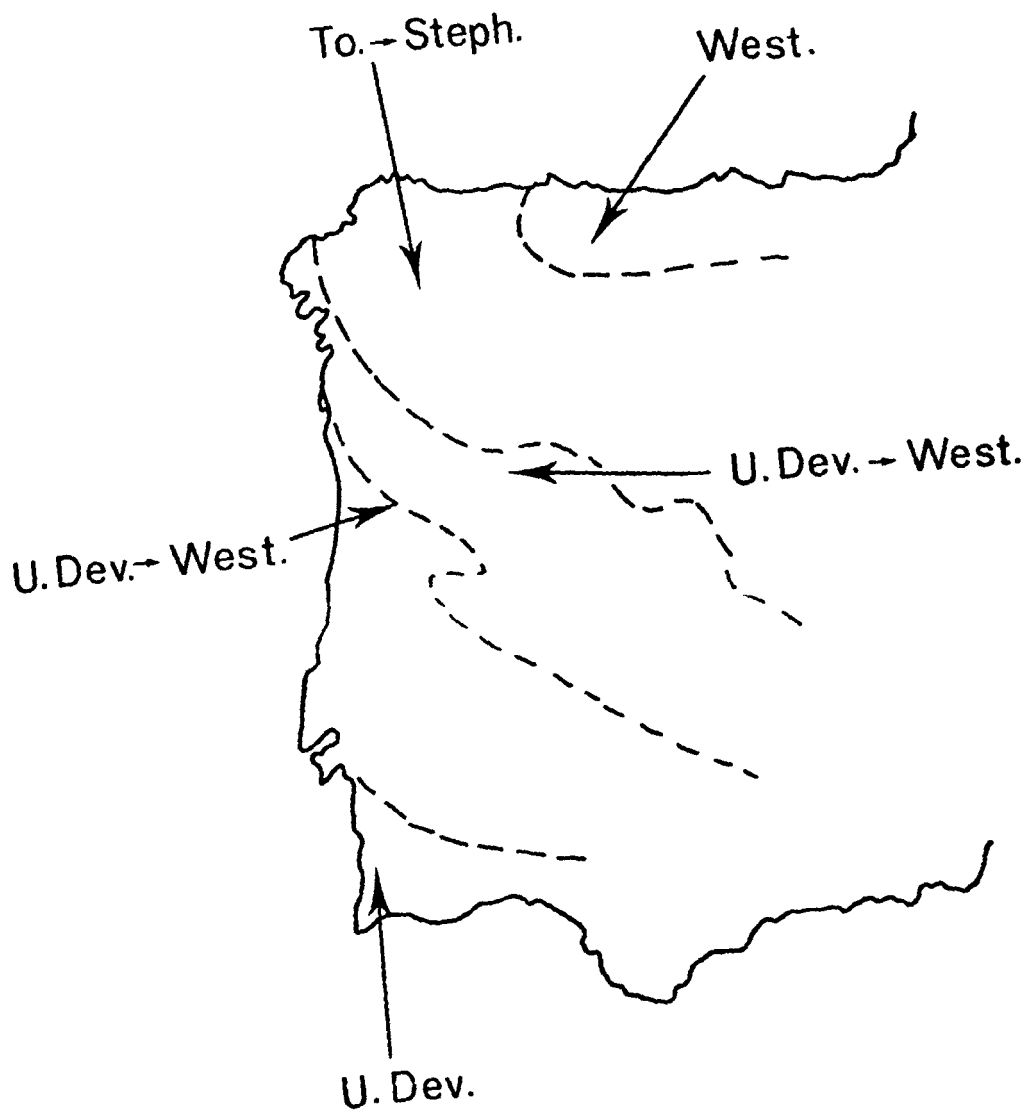
The age ranges of the main deformation throughout Iberia indicates that for the Central Zone of the Iberian Arc (Fig. 1.8) the deformation is post Lower Devonian to Westphalian, while in Cantabria, north Spain the earliest folding event dates more narrowly between Namurian and Westphalian (Julivert, 1971).

The dominant structures comprising the central zone of the Variscan Fold Belt are kilometeric scale folds whose curved, upright axial planes define the belts broad arcuate pattern. The folds of this age are much tighter in the Complexo xisto-grauvaquico where they refold the Upper Cambrian folds resulting in an elongate basin and dome interference pattern.

A ubiquitous cleavage (S_1), ranging from a slaty to a spaced cleavage, is developed for the most part axial

FIG. 1.8

Age of the first phase Variscan deformation in Iberia



planar to the main folds. In the Serra do Marão region a pre to syn-buckling cleavage (S_1') pre-dates the main grain flattening cleavage (S_1). In much of the Complexo xisto-grauvaquico, the main cleavage is parallel or sub-parallel to the bedding.

The largest component of finite strain in both the Complexo xisto-grauvaquico and the Lower Palaeozoic rocks is plane strain attributable to the main phase of deformation DV_1 .

The Douro Shear Belt, first recognised by Romano and Diggins (1974), and other, associated zones of ductile and brittle deformation are recognised along much of the fold belt discussed. The deformation in these zones of high strain is often multiple in type with ductile simple shear and brittle thrusting or faulting.

The later phases of Variscan deformation i.e. DV_2 and DV_3 only weakly folded Carboniferous sediments without the development of a cleavage. Considered related to these latter phases is the widespread development of ductile - brittle structures (Chapter 9).

There is an important set of northeast-southwest trending faults with dominantly sinistral movements which displace the main folds, prior to the intrusion of the Younger Granites.

1.8 METAMORPHISM

The metamorphism in north Portugal is divided into three types:

1. A low grade, regional metamorphism associated with the main Variscan deformation DV_1 .
2. A medium to high grade metamorphism associated with the intrusion of the Older Variscan Granites.
3. A contact metamorphism associated with the intrusion of the Younger Variscan Granites.

1. The Lower Palaeozoic and the Complexo xisto-grauvaquico have been regionally metamorphosed during the main Variscan deformation; the pelitic sediments comprising these formations now consist of low grade metamorphic mineral assemblages typically of muscovite, chlorite, quartz, \pm albite. In most of the pelitic rocks the phyllosilicate minerals are aligned with a dominantly planar orientation, often with a linear component, to form the S_1 regional cleavage. There is no evidence in these rocks of an earlier metamorphism, however, chlorite porphyroblasts grown during burial metamorphism are augened by the S_1 cleavage.

The quartzites and psammitic rocks have been recrystallised to varying degrees. In Penacova, the quartzites still show diagenetic features whereas in Serra do Marão

all detrital grains are completely or partially recrystallised.

2. Three separate, medium to high grade metamorphic zones are clearly spatially associated with the exposed Older Variscan Granites, (Fig. 1.9 B,C,D). Both the metamorphic zones and the granites have a Variscan trend i.e. a trend parallel to the main folds and regional cleavage, and on the larger scale of the major structural zonation. These metamorphic zones consist of sub-parallel isograds, increasing in grade from chlorite through biotite, andalusite-staurolite and sillimanite towards the granites. In addition kyanite, co-eval with staurolite and garnet, has been reported from Cavenais, near Viseu (Atherton et.al, 1974) which indicates the metamorphism, in part of the zone, was higher pressure than previously envisaged by Oen (1970). Garnets in zone B near Viana do Castelo indicate texturally that they grew syntectonically during the development of the main cleavage S_1 (Fig. 1.11 a). Syn-tectonic garnets are also contained in the Complexo xisto-grauvaquico in zone D near Vila Cova, in the northern area of Serra do Marão (Fig.1.10a). It is suggested here that this metamorphism occurred towards the end of the main deformation, quickly followed, as Oen (1970) has demonstrated, by the emplacement, to their relative level within the surrounding rocks, of the Older Variscan Granites. This accounts for the non-symmetrical nature of the zones and their discordance with the granites. Oen (op.cit.) points out that there is an overprinting of this metamorphism by sillimanite related to the final emplacement of the granites.

FIG. 1.9

Distribution of Older and Younger Variscan Granites
and associated plutonometamorphic zones in Northern
Portugal.

Older Granites Dotted areas

Younger Granites Shaded areas

Dotted lines mark the limit of metamorphic zones, A,B,C,D



(After Oen, 1970 Fig. 5)

FIG. 1.10

a. Syntectonic garnet porphyroblast in semipelitic schists, Complexo xisto-grauvaquico.

Curved quartz inclusion trails indicate a clockwise rotation of the garnet. Main S_1 cleavage E-W.

g garnet

q quartz

b biotite

m muscovite

Specimen no. M.35

Location. Kilometre post 153.8 on N 34 road , 15 km north of Campea, Serra do Marão.

b. Chiastolite porphyroblast overprinting the S_2 crenulation cleavage, NE-SW, S_1 cleavage E-W in slates of the Valongo Formation.

Specimen no. M202

Location. 10m west of junction between the Santa Justa and Valongo Formations , 70m west of the summit of Marão.

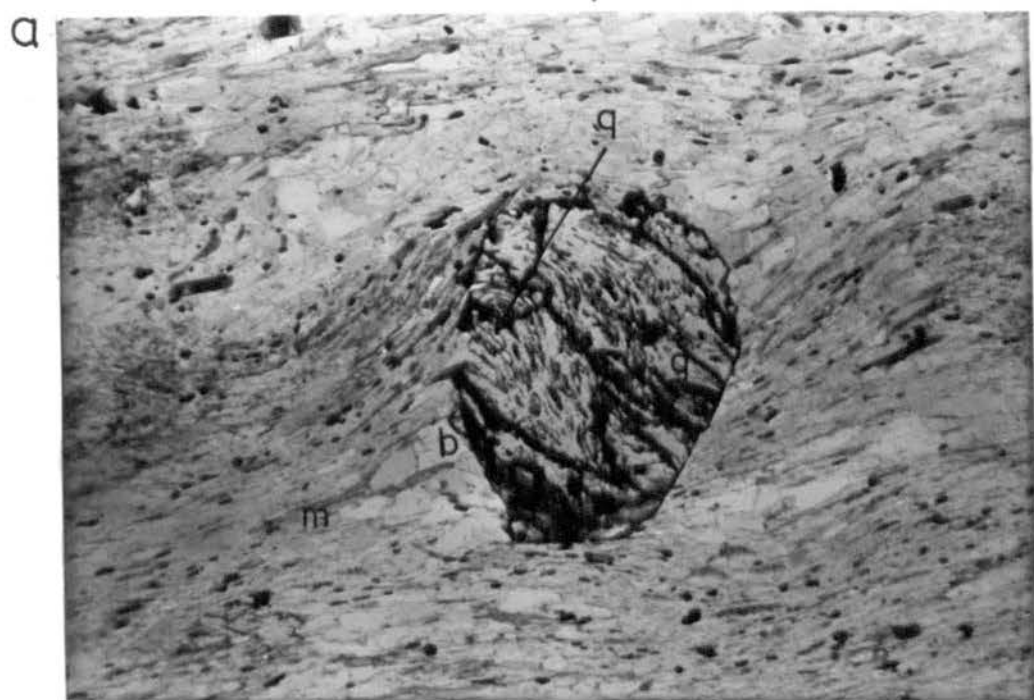


FIG. 1.11

a. Garnet and staurolite porphyroblasts in semi-pelitic schists, Complexo xisto-grauvaquico.

S_1 cleavage NW-SE crenulated by S_2 cleavage NE-SW.

X 5 $\frac{1}{2}$

Specimen no. C.11

Location. 50m from contact between Complexo xisto-grauvaquico and the Santa Justa Formation on coast, 1km west of Viana do Castelo.

b. Staurolite porphyroblast (dotted) aligned quartz inclusions. in semi-pelitic schists, Complexo xisto-grauvaquico.

X 10

b biotite

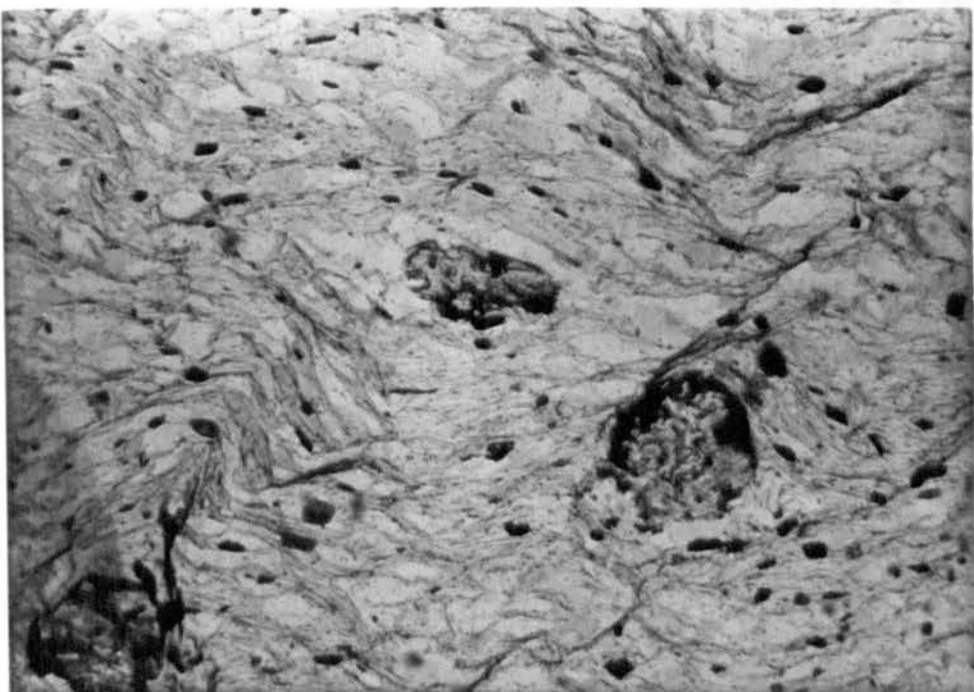
a albite

q quartz

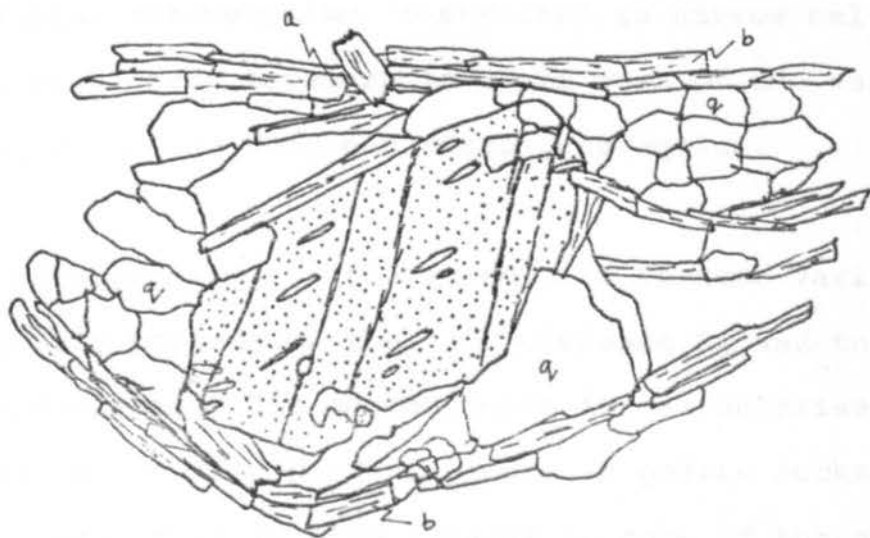
Specimen no. D51

Location. At Foz do Souza on N 108, 15km SE of Porto

a



b



In fact, in the River Douro area west of the Valongo Anticline, the Complexo xisto-grauvaquico contains high grade metamorphic assemblages with staurolite the dominant porphyroblast. The textural evidence indicates that the staurolites are possibly pre-tectonic, growing before the main Variscan cleavage S_1 (Fig. 1.11b). This metamorphism is believed to be the same as that to the west in a zone running between Oliveira de Azeneis and Albergaria a Velha (Fig. 1.9 Zone A). Similar metamorphic rocks occur in Tras-os-Montes (Ribeiro, 1974), however, the age of this metamorphism, to the west and east of the study area, and that west of the Valongo Anticline is not established. Oen (1970) has hinted that the rocks are possibly older than the Complexo xisto-grauvaquico and the metamorphism is pre-Variscan. This is contrary to a Variscan age proposed by Schermerhorn (1955). The metamorphism of the region has not been an important part of this thesis, however, from the evidence in thin section the present author supports the idea of a pre-Variscan metamorphism, restricted to narrow belts, and that the high grade metamorphic rocks west of the Valongo Anticline belong to the Complexo xisto-grauvaquico.

3. Contact metamorphism, in the aureoles of Younger Variscan Granites, clearly post-dates the cleavage, S_2 , and the earlier metamorphisms. The metamorphism is characterised by the growth of chiastolite porphyroblasts in pelitic rocks, (Fig. 1.10b). Cordierite is also present in some of the aureole rocks, often growing mimetically aligned in the main cleavage.

S E C T I O N B

This section describes the geology of the three major DV_1 folds in the fold belt. The section is divided into four chapters:

Chapter 2 covers the greater part of the Valongo Anticline, whilst the northern most extension of this structure exposed at Apulia and Viana do Castelo forms the subject of Chapter 3.

The geology of the Penacova and Marão Syndlines are described in Chapters 4 and 5 respectively.

THE VALONGO ANTCLINE BETWEEN VALONGO AND SATÃO

2.1 INTRODUCTION

In the first of the four areas examined (Fig. 1.1) five traverses, at approximately 6 to 10km. intervals, were taken across strike of the Valongo Anticline (Romano and Diggins, 1974) a kilometric Variscan DV₁ structure which folds Lower Devonian and older sediments (Fig. 2.1). A complementary parasitic syncline runs parallel to the axial trace of the anticline sharing a common sub-vertical limb. The axial traces of the two folds are continuous for 100km. from the coast at Apulia (Chapter 3) southeastwards to Castro Daire where they are truncated by a Younger Variscan Granite. A brief examination was carried out east of this granite where the syncline is exposed for a further 15km. southeastwards, where it is truncated by a granite of similar age near Satão.

This southeasternmost part of the area around Castro Daire has been described by Schermerhorn, (1956). Romano and Diggins (1974) have more recently re-examined the stratigraphy and structure around Valongo originally mapped by Delgado in 1908.

2.2 STRATIGRAPHY

1. COMPLEXO XISTO-GRAUVAQUICO

Rocks of the Complexo xisto-grauvaquico are

FIG. 2.1

Geology and traverses along the Valongo Anticline

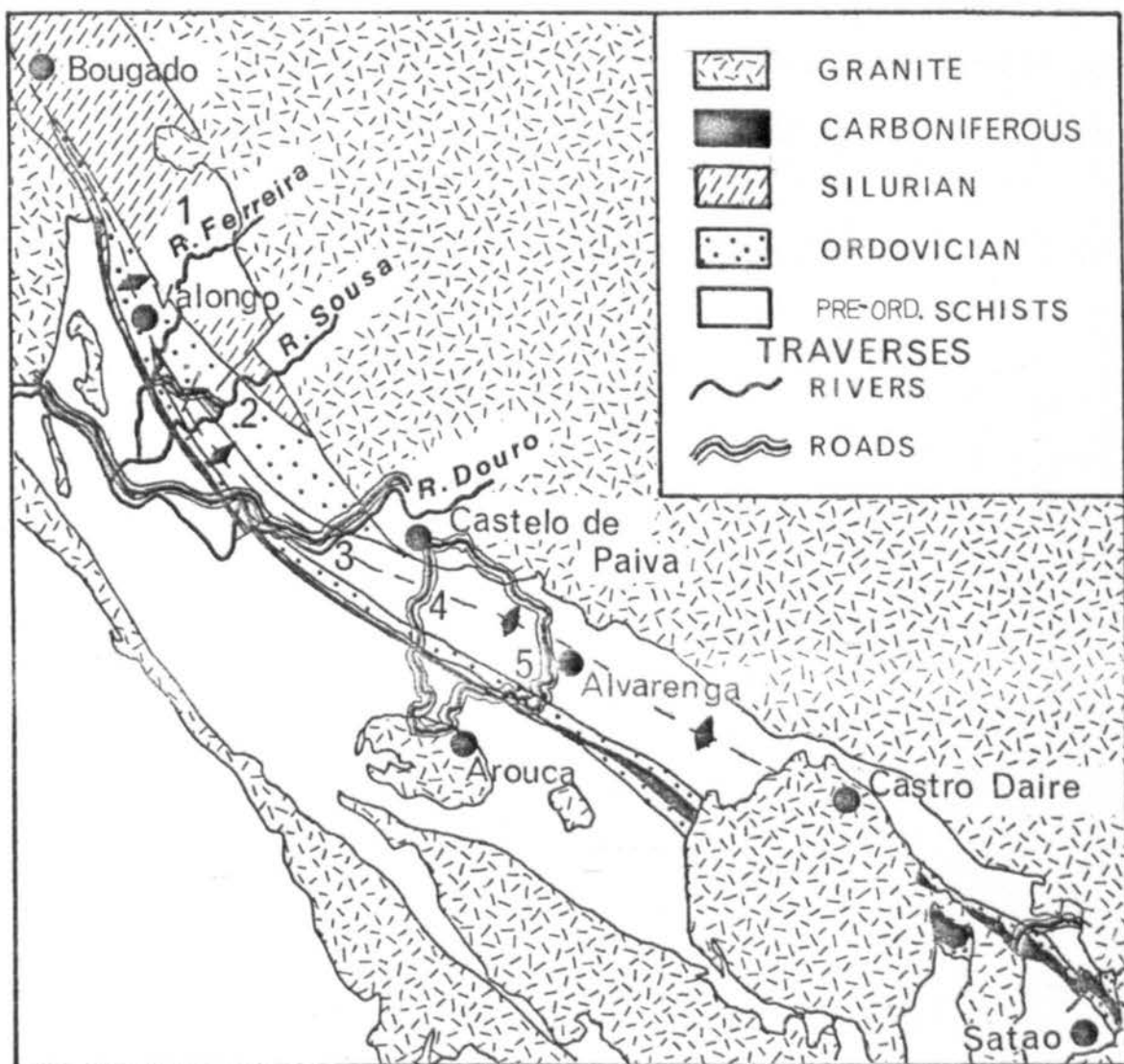


FIG. 2.2

The Ordovician straigraphy and the thickness variation
along the length of the Valongo Anticline.

FORMATION	THICKNESS IN METRES			
	VALONGO	R. DOURO	AROUCA	CASTRO DAIRE
SOBREDO	100	50	100	50
VALONGO	350	150	500	650
SANTA JUSTA	170	100	230	200

Castro Daire after Schermerhorn (1956)

Valongo after Romano & Diggins (1974)

predominantly fine-grained siltstones, slates and greywackes, and subordinate coarse-grained, highly veined, staurolite schists. Several horizons of quartz, and quartzite-pebble conglomerates repeatedly crop out within the succession.

2. ORDOVICIAN

The total deformed thickness of the Ordovician succession varies from 600m to 900m along the length of the structure, thinning generally but irregularly to the northwest. The base of the Santa Justa Formation Armorican Quartzite S.L. is exposed at several locations e.g. in the Rio Ferreira Valley on the western limb, where there is a slight angular unconformity with pelitic schists of the Complexo xisto-grauvaquico. The lower part of the formation consists of massive current bedded quartzites (Fig. 2.3a) interbedded with subordinate siltstones, conglomerates and pebbly quartzites. Quartz-pebble conglomerates are present in the basal beds for the whole length of the structure. However, the contact with beds of the Complexo xisto-grauvaquico is often tectonic and the sedimentary relationship between the two is obscured. The upper part of the formation is transitional with the massive quartzites and consists predominantly of interbedded quartzites and siltstones with ripple lamination (Fig. 2.3b), with shaly beds in the top few metres. The average bed thickness in the upper part of the formation is less than 0.5m, while quartzite beds in the lower ^{part} are commonly greater than 1m.

FIG. 2.3

a. Planar cross-bedding in a metre thick bed unit of quartzite , Santa Justa Formation.

Dark bands are slightly iron-rich laminae.

Location: Eastern limb of the Valongo Anticline, 1km east of Soboledo on the N108.

b. Ripple lamination in thin lenticular siltstones near the top of the Santa Justa Formation.

Location: 1km east of Aguiar de Sousa at junction between N319.2 and road east to Beloi, 20km ESE of Porto.

a



b



The whole formation contains abundant sedimentary structures particularly those resulting from soft sediment deformation, including slump folds, flame and water escape structures (Lowe, 1975) (Fig. 2.4b). Several horizons in the thin bedded quartzites are bioturbated by vertical (Skolithos) and horizontal burrows.

An Arenig age for the Santa Justa Formation is supported by the occurrence of *Cruziana rugosa* and *Cruziana furcifera* (Crimes, 1968; Seilacher, 1970) in quartzites in the top 200m of the Formation (Romano and Diggens, 1974).

The Valongo formation is characterised by blue-grey fossiliferous slates which commonly weather a rusty orange colour due to their high pyrite and magnetite content. The iron reaches a high concentration in the transitional facies between the underlying quartzites and siltstones of the Santa Justa Formation and the slates. Romano and Diggens (1974) place the top of the Santa Justa Formation (Armorican Quartzite S.l.) at the last quartzite bed in the slate succession. Rare, thin quartzites within the slates are the only bedding structures recognisable (Fig. 2.4a).

The Sobredo Formation at the top of the succession is less than 100 metres thick in the Valongo area and consists of pink sandstones and poorly consolidated pebbly greywackes.

FIG. 2.4

a. Sandy bed in slates near the base of the Valongo Formation.

n.b. S_1 cleavage is manifested as widely spaced fractures in the sandstone.

Location: At Quinta de Baixo, 3km southeast of Valongo.

b. Soft sediment water escape structure in thinly laminated siltstones near the top of the Valongo Formation

Location: 1km east of Aguiar de Sousa at junction between N319.2 and road east to Beloi, 20 km E.S.E. of Porto.

a



b

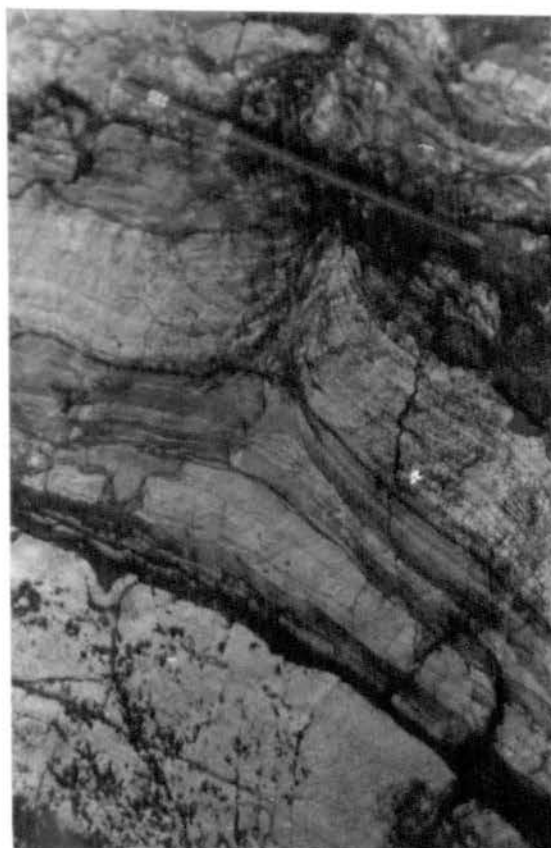


FIG. 2.5

a. F_2 microfolding of quartz vein and S_1 cleavage.

S_2 crenulation cleavage is axial planar to microfolds and approximately N-S in photomicrograph. S_1 approximately E-W, parallel to the vein.

Specimen no. 28V X20 †

Valongo Formation.

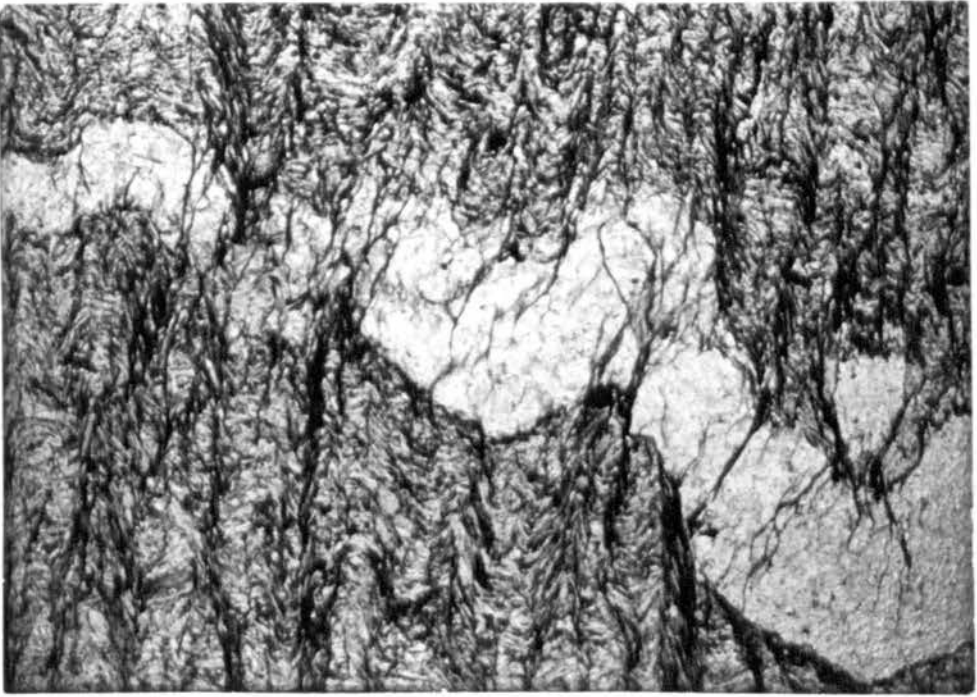
b. Localised development of S_2 crenulation cleavage in micaceous-rich laminae in slates.

S_1 grain alignment cleavage is parallel to bedding E-W in photomicrograph, see top.

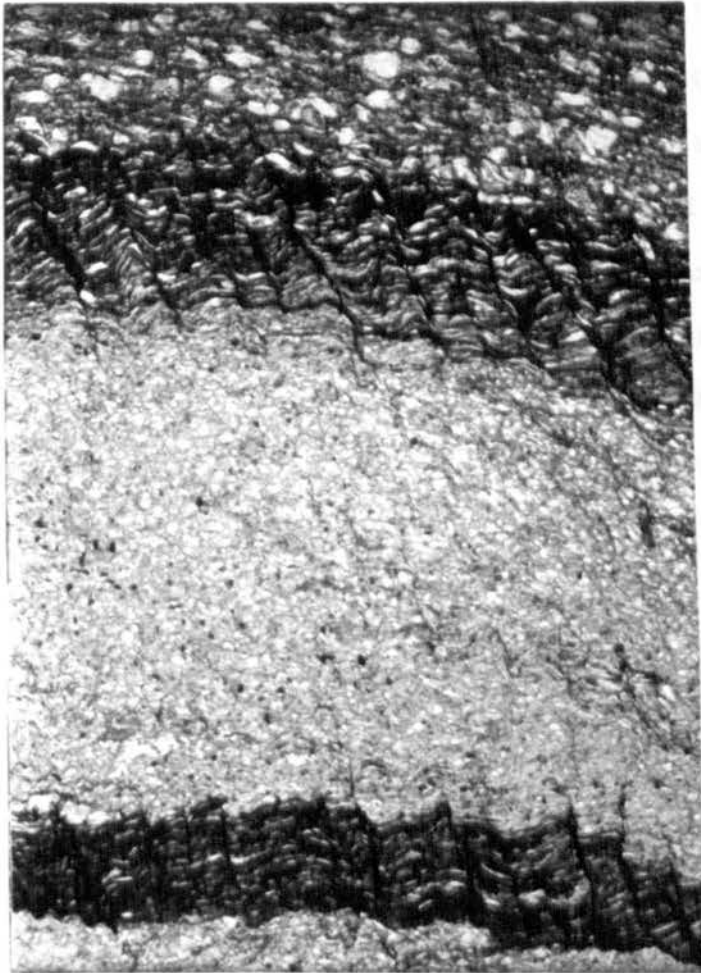
Specimen no. 27V X20 †

Valongo Formation.

a



b



The Silurian and Lower Devonian sediments are predominantly shales and slates with subordinate quartzites. Westphalian D. and Stephanian B-C sediments were deposited in limnic basins (Oen, 1970) and are exposed on the western limb of the Valongo Anticline. The sediments include polymictic conglomerates which lie unconformably on Lower Devonian 500m west of Acores, and on older sediments elsewhere and black shales containing plant fragments which outcrop 1.5km southeast of Covelo.

2.3 MAJOR STRUCTURE

Two different forms of evidence indicate that the sediments comprising the Complexo xisto-grauvaquico were folded during the Upper Cambrian. The first is an angular unconformity at the base of the Ordovician and the second is the variation in plunge of minor DV_1 fold axes around the basin and dome interference fold pattern in conglomerate beds in the Complexo xisto-grauvaquico (Fig 7.1). The pre-Variscan folds are large scale with no minor folds or associated cleavage.

The plunge variation of DV_1 fold axes in the Complexo xisto-grauvaquico cannot be the result of post DV_1 refolding since a similar dispersion would be expected in the Ordovician-Silurian-Lower Devonian rocks of the Valongo Anticline. Here the fold axes plunge consistently at low

FIG. 2.6

a. Elongate quartz grains in S_1 cleavage .

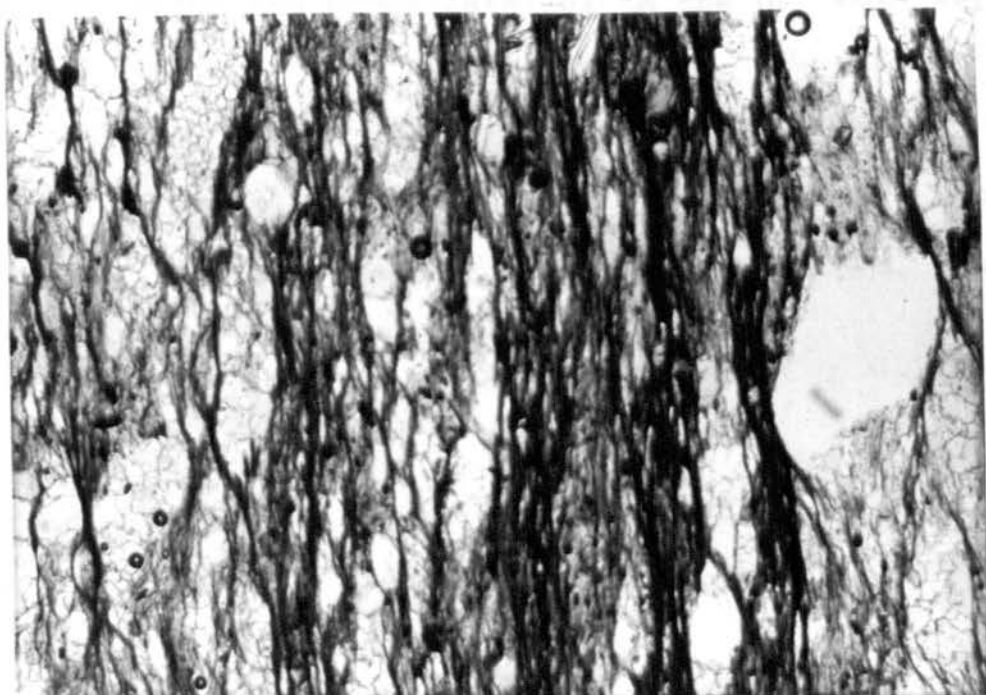
n.b. thin dark pressure solution seams (S_1' ?) , and
truncation of some grains.

Specimen no. D111. X10 \dagger

Santa Justa Formation

b. Same as a. in \dagger

a



b



angles to the northwest (Fig. 2.10a). The tight Variscan refolding of the Upper Cambrian folds has given rise to elongate basins and domes parallel to the DV_1 fold axial traces. Their geometry corresponds closely to a type D interference fold pattern (Ramsay, 1967 p.531). This pattern suggests the first fold axes were orthogonal and the axial planes were oblique to the Variscan plane of flattening (Fig. 7.18) .

The tight refolding by DV_1 caused the bedding and cleavage to be generally parallel, dipping vertically or steeply to the northeast (Figs. 2.8b, 2.9b). All linear structures i.e. fold axes, intersection lineations, and maximum elongation of pebbles plunge within the plane of the cleavage (Figs. 2.10b, 2.11b).

The outcrop pattern and bedding orientation of the Ordovician-Silurian-Lower Devonian sediments (Figs. 7.1, 2.8a) shows that they are folded into an asymmetric anticline, the Valongo Anticline (Romano and Diggens, 1974) and a symmetric syncline, the Oporto-Satão Syncline (Oen, 1970), which both plunge at a low angle (between 0° and 30°) to the north west. The anticline verges towards the south west with an axial plane dipping approximately 60° to the north east, whereas the syncline is upright with a vertical axial plane. The axial trace and western limb of the syncline is truncated by a major ductile-brittle movement zone, the Douro Shear Belt (Romano and Diggens, op.cit.) at Cabranca 4km east of Arouca (Fig. 7.1).

FIG. 2.8

Stereographic plots of poles to bedding , Valongo Anticline. .

a. For Ordovician and Silurian .

π pole to best fit great circle .

A.P.N. and A.P.S. axial planes for northern **and** southern areas of the fold respectively.

b. For Complexo xisto-grauvaquico.

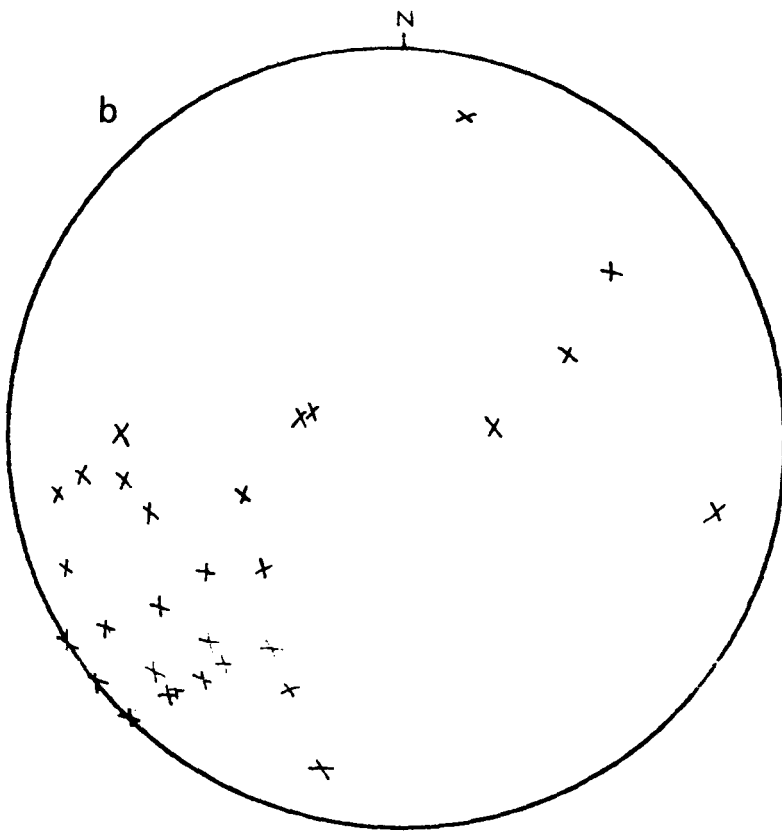
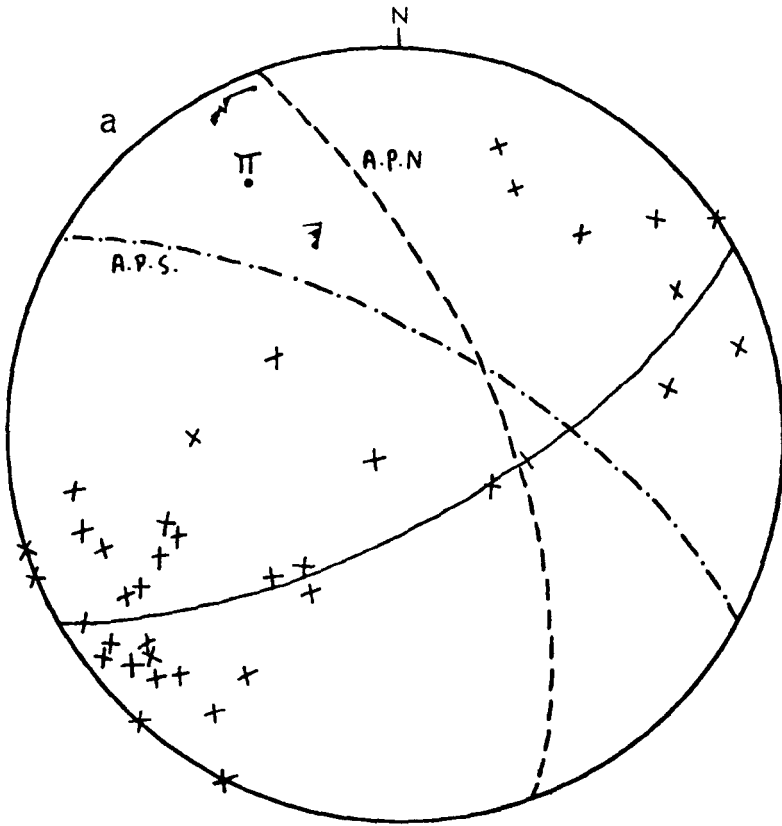


FIG. 2.9

Stereographic plots of poles to S_1 cleavage , Valongo Anticline.

a. For Ordovician and Silurian.

S_{1N} and S_{1S} are mean cleavage planes for the northern and southern areas of the fold respectively.

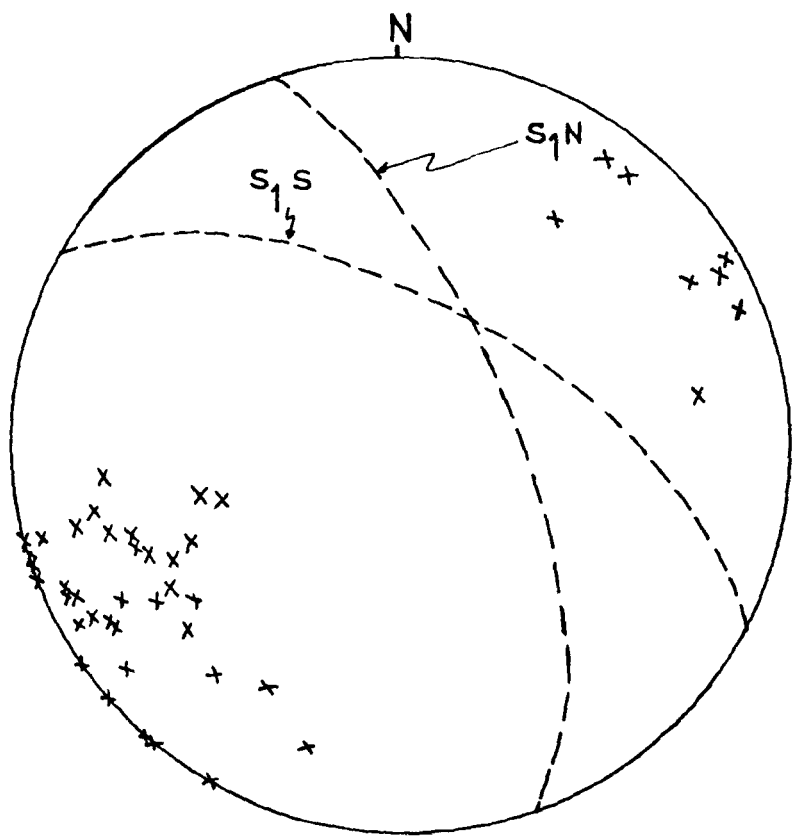
b. For Complexo xisto-grauvaquico.

S_1 is mean cleavage plane.

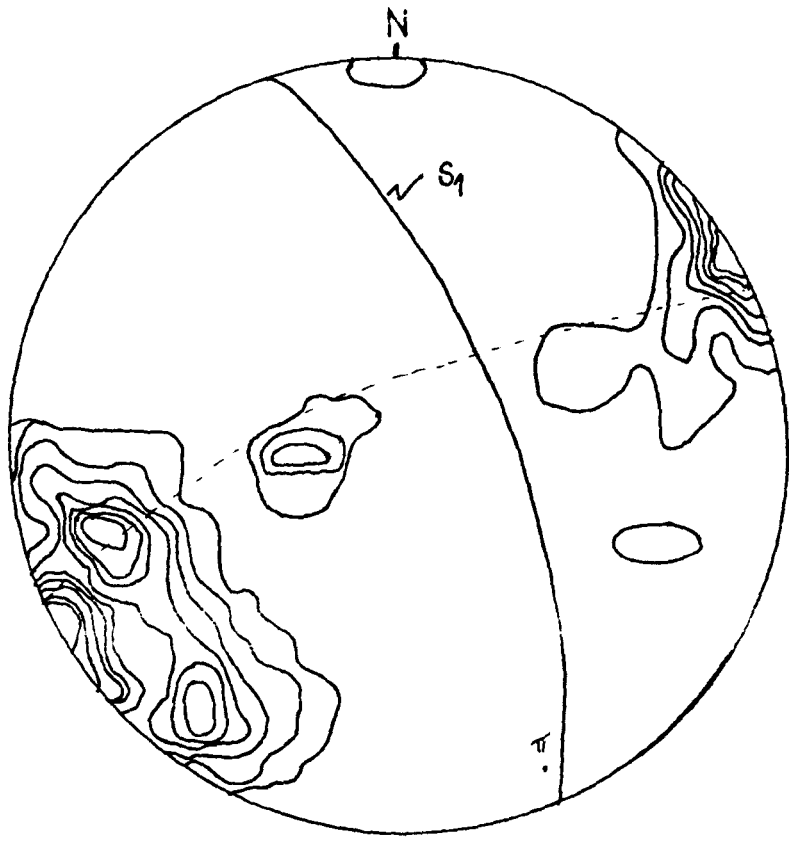
Contours are 0.5 to 7.5 in 1% intervals.

110 points

a



b



A minimum apparent wavelength of 6km was calculated for the combined folds (see Ramsay, 1967, p.354). The Armorican Quartzite effected a predominant control during the fold initiation and development behaving as a competent slab within the less competent medium of pelitic and semi-pelitic rocks of the Complexo xisto-grauvaquico and Valongo Formation (see also Chapter 5). Applying a simple buckling equation for layered viscous materials:

$$Wd = 2\pi t \sqrt{\frac{3\mu_1}{6\mu_2}} \quad (\text{Ramsay, 1967, p.375})$$

The Armorican Quartzite, for an average formation thickness of 200m (t) and a viscosity ratio between the quartzite and the pelitic rocks of 2.5 (ratio based on Menhert (1939)), a dominant wavelength (Wd) of approximately 1km is predicted for the development folds. This value is much less than the actual wavelength of folds in the Armorican Quartzite. There are several possible explanations for this:

1. The low internal strain within the Armorican Quartzite indicated by undistorted sedimentary structures and weak shape and mineral fabrics (see Chapter 8) could indicate the ductility ratio used was too low. This ratio will obviously vary with temperature and confining pressure.
2. Evidence from the internal strain state of minor fold structures in addition to the existence of undeformed

beds indicates internal buckling was accomplished predominantly by flexural-slip along bedding surfaces, with some flexural-flow (Fig. 2.17). Hence the Armorican Quartzite behaved as a competent multilayer involving internal deformation by slip, as opposed to deforming homogeneously as assumed in the equation. Further, the sequential development of folds during buckling may check the propagation of the first order buckles (Price, 1967; see also Section, 5.3,4).

3. The major buckles are non-sinusoidal and non-periodic which is not accounted for by the equation which assumes sinusoidal fold growth.

The axial traces of the major Variscan fold structures curve through an arc of 40° between Valongo (bearing 160°) and Arouca (bearing 120°) (Fig. 2.7); the origin of this arcuate form of the fold belt is considered to be primary and co-eval with the F_1 folding. (See Chapter 11).

2.4 MINOR STRUCTURES

1. CLEAVAGE

A primary or slaty cleavage, S_1 , is developed in all Lower Palaeozoic Sediments except in competent massively bedded quartzites. It is geometrically associated with the major and minor fold structures of DV_1 age (Figs. 7.1, 2.9, 2.10) and strikes parallel to the arc and the fold

FIG. 2.10

Stereographic plots of the plunge of F_1 minor fold axes,
Valongo Anticline.

a. For Ordovician

π pole to best fit great circle.

b. For Complexo xisto-grauvaquico.

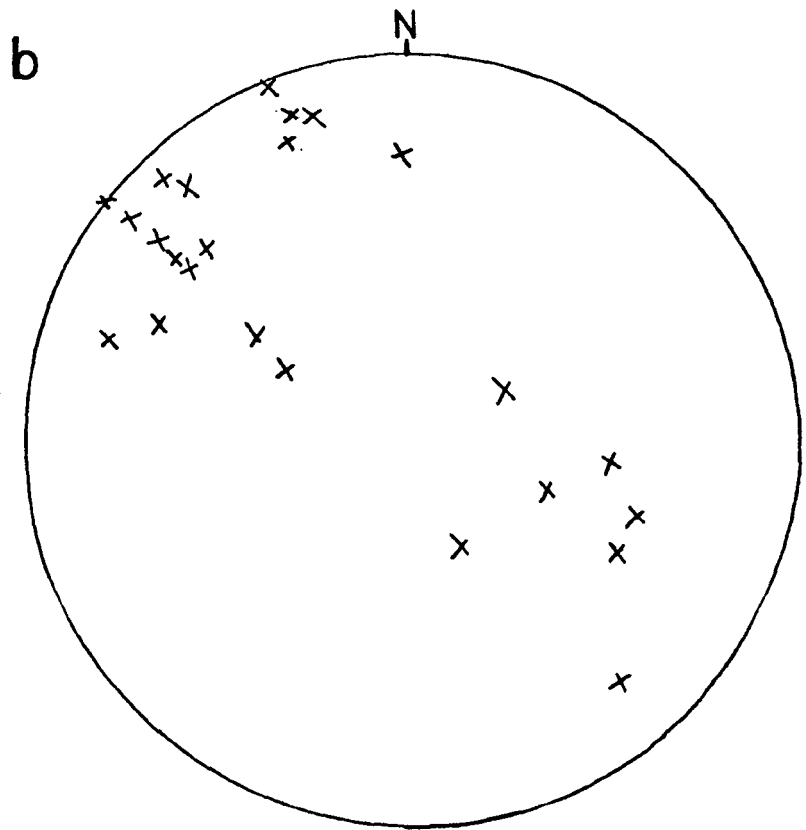
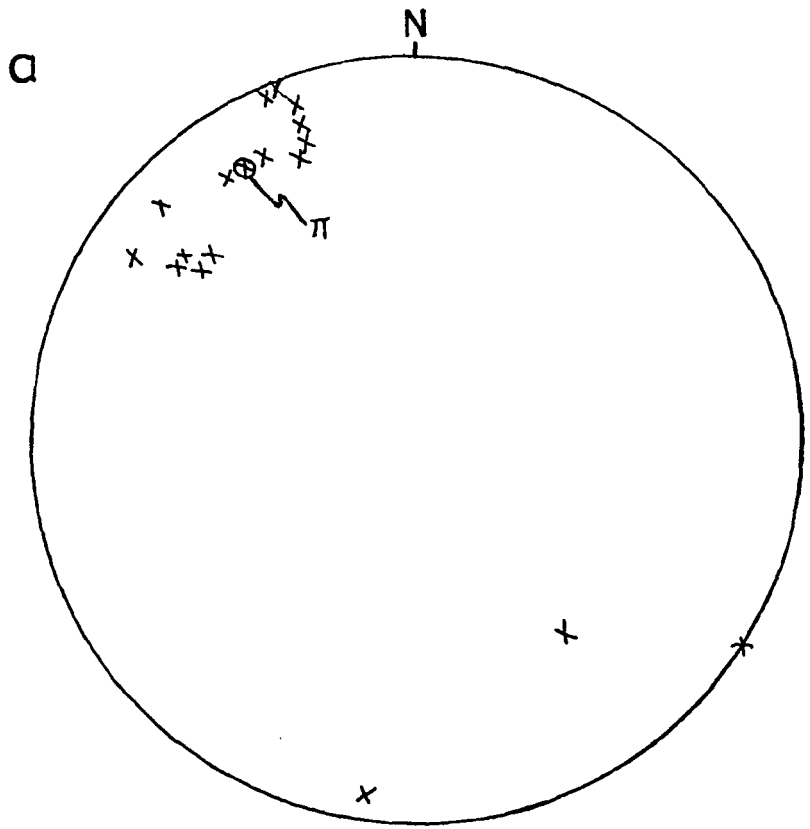
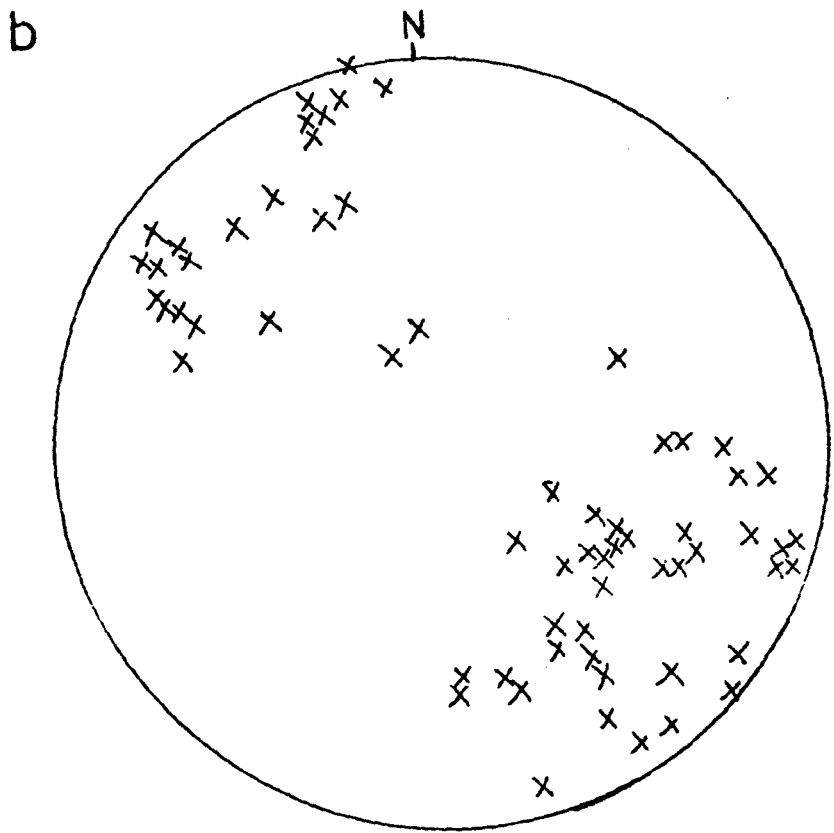
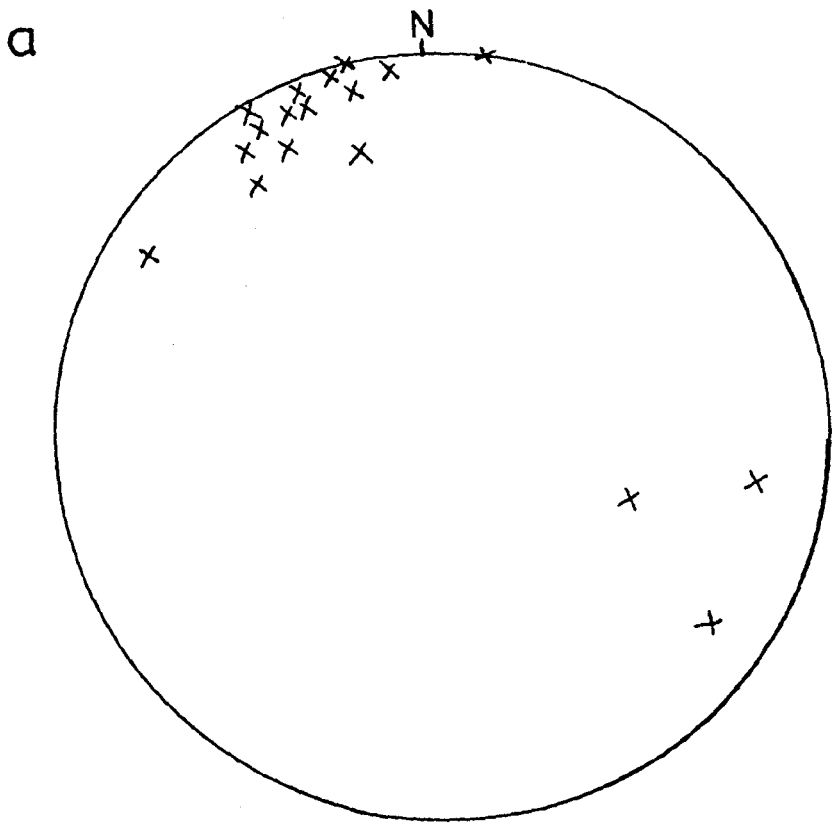


FIG. 2.11

Stereographic plots of the plunge of mineral lineations
and maximum elongation directions , Valongo Anticline.

a. For Ordovician

b. For Complexo xisto-grauvaquico.



axial traces.

The cleavage fans around the Valongo Anticline ^{and} dips between 45° southwest and vertical about the inclined axial plane (Fig. 2.9a).

The cleavage varies from a penetrative cleavage of aligned minerals in the pelitic sediments, which near the village of Valongo produces perfect homogeneous black slate, to a two component cleavage in the semi-pelitic and psammitic sediments. One component of this cleavage is a weak to strongly developed quartz grain alignment (S_1) parallel to muscovite, white mica and chlorite between the quartz grains. The other component is a spaced cleavage (S'_1) which comprises thin (1mm) sinuous anastomosing dark seams of concentrated micaceous minerals and opaques (Fig. 2.6a, b). These seams parallel the grain alignment although they commonly deflect around quartz grains which are frequently truncated (Fig. 2.6a). A pressure solution mechanism outlined for the S'_1 cleavage in Serra do Marão (Section 5.3) is proposed for the generation of the seams.

In Serra do Marão two similar cleavages S'_1 and S_1 or cleavage components are developed commonly parallel to each other but occasionally obliquely. In Marao the grain-alignment cleavage S_1 , crenulates the pressure-solution seams, but in the Valongo Anticline the two cleavages are sub-parallel and their time relationship is unclear.

The S_1 cleavage in the Complexo xisto-grauvaquico for the most part is parallel to bedding except around the hinges of DV_1 Variscan minor folds (Fig. 2.13a).

Bedding and cleavage in the Complexo xisto-grauvaquico are truncated on the western limb of the Valongo Anticline by the Douro Shear Belt (Romano and Diggins, 1974). Post- DV_2 ductile-brittle movements along the shear belt are indicated by strongly sheared S_2 cleavage in the Westphalian D sediments along traverse 4, near Arouca. The S_2 cleavage in the Carboniferous sediments is a pervasive cleavage approximately co-planar to the DV_1 cleavage developed in the older sediments. This co-planar nature suggests a co-axial tightening of the DV_1 major syncline in which the sediments were deposited. However a variable oriented, S_2 crenulation cleavage is sporadically developed in the Complexo xisto-grauvaquico and Ordovician-Silurian-Lower Devonian rocks (Fig. 2.5a). Only the pelitic and semi-pelitic rocks carry this cleavage which deforms the early grain alignment parallel to the bedding (Fig. 2.5b). The plunge of F_2 crenulations corresponds to the Π pole for the warped S_1 cleavage (Fig. 2.12a, b) to the southeast. On a mesoscopic scale S_2 is often manifested as widely spaced angular crenulations or kinks in pelitic slates in the Complexo xisto-grauvaquico (Fig. 2.14a).

FIG. 2.12

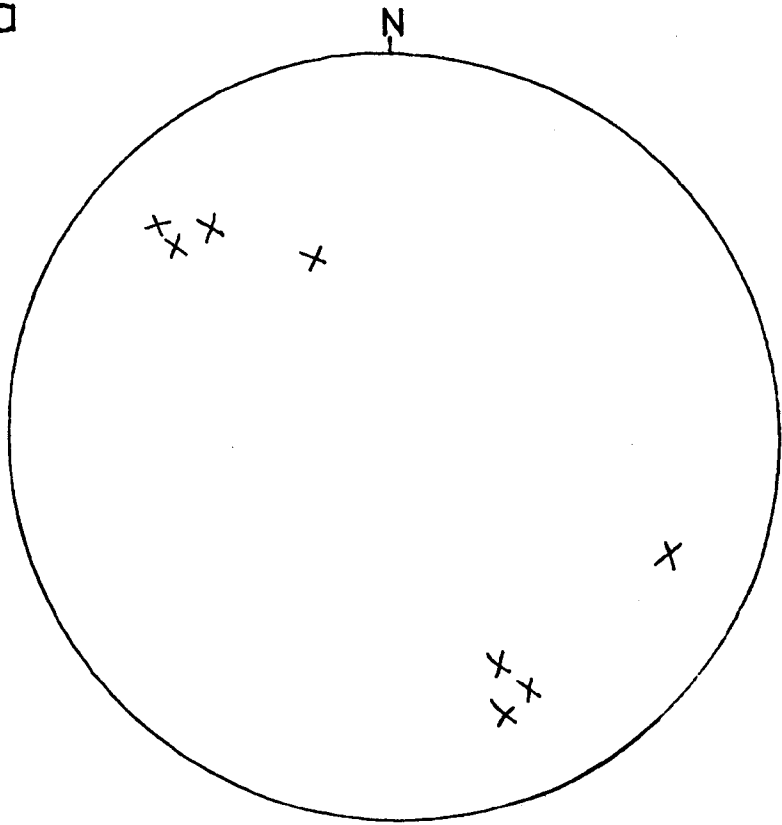
Stereographic plots of S_2 crenulation cleavage, Valongo Anticline.

a. Poles to cleavage planes.

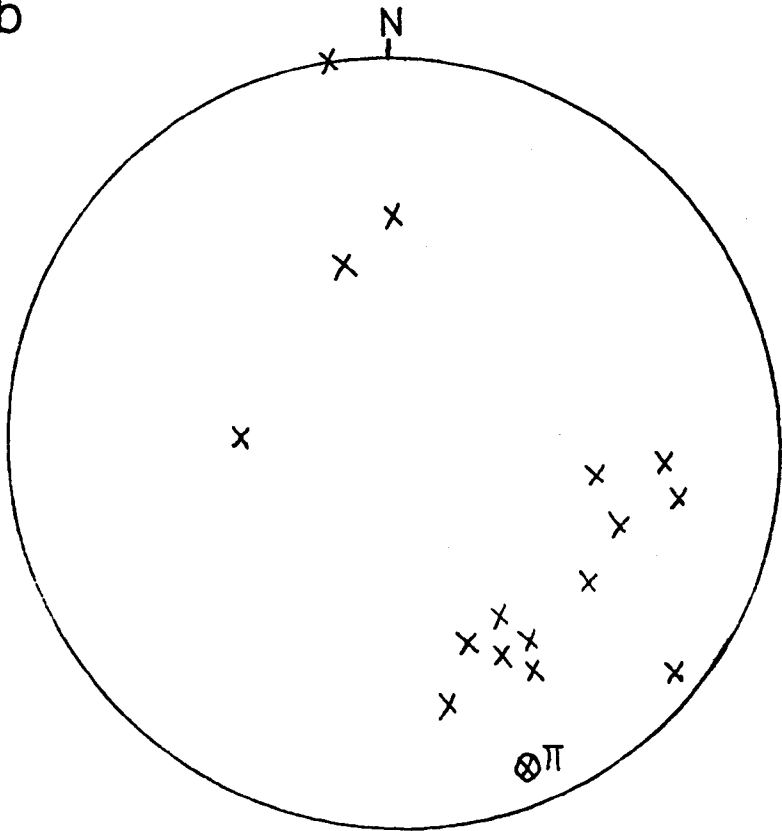
b. Plunge of microfolds

π pole to S_1 cleavage (from Fig. 2.9b).

a



b



2. MINOR FOLDS

Few F_1 minor folds have developed in the Complexo xisto-grauvaquico. In thinly bedded siltstones and mudstones Class 1C-2 folds predominate over more open Class 1B in occasional quartzite beds between 0.5 and 1m thick (Figs. 2.13a, 2.15a). Overtaken asymmetric 'S' folds indicate local vergence on the western limb of the Valongo Anticline (Fig. 2.13b).

In all cases a single, axial planar cleavage (S_1) is developed and folds fold only bedding, substantiating the absence of an early cleavage associated with the Upper Cambrian folding. However it is possible some of the minor folds are Upper Cambrian folds whose axes and axial planes have rotated into the plane of the S_1 cleavage during DV_1 .

In the Santa Justa Formation F_1 folds develop on all scales in bedded quartzites (Figs. 2.16a, b). Most folds are asymmetric and are congruous with the Valongo Anticline. Variation in bed thickness often results in disharmonic folds and décollement surfaces (Fig. 2.16a).

In bedded quartzites deformation of initially vertical burrows around the hinges of minor F_1 folds suggests that buckling was partly by flexural-flow, (Fig. 2.17a, b) while slip along the surfaces of beds

FIG. 2.13

F₁ minor folds in the Complexo xisto-grauvaquico.

a. Fold closure in bedded mudstones.

n.b. the steep S₁ axial planar cleavage

Location: 500m east of Gamarao de Cima on N326 , 5km
north of Arouca.

b. Asymmetric fold in siltstones and mudstones .

Location: 1.5km west of Reris on N225, 11km west of
Castro Daire.

a



b



FIG. 2.14

F_2 minor folds in the Valongo Anticline.

a. Angular folds folding S_1 cleavage in pelitic schists of the Complexo xisto-grauvaquico.

Location: North bank of the Rio Douro directly opposite the villiage Crestuma, 15km southeast of Porto.

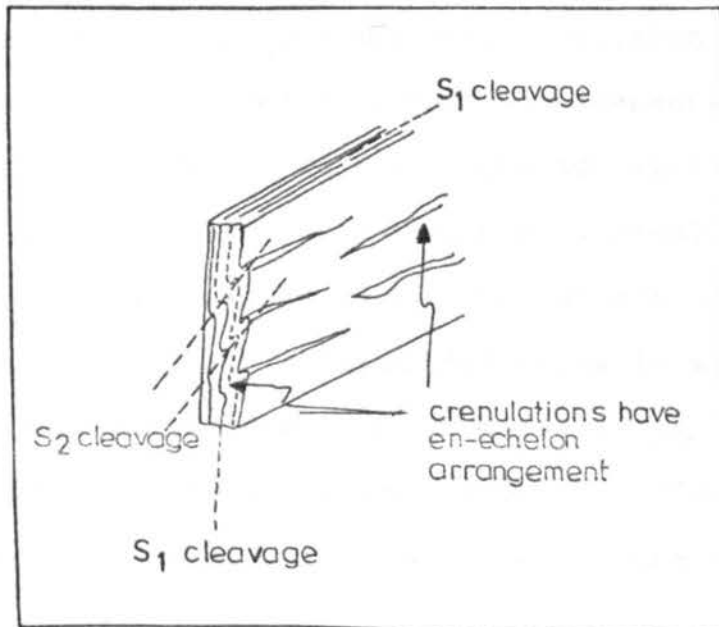
b. Microfolds in slates of the Valongo Formation.

Location: 1.2 km southeast of Campo, 4km east of Valongo on N15.3 to Recarei.

a



b



indicates a component of flexural-slip.

3. ELONGATION STRUCTURES

There is a variety of minor structures in the sediments of the Complexo xisto-grauvaquico and Ordovician which indicate sub-horizontal finite elongation during DV_1 (Fig. 2.7, 7.1).

Boudinage is common in the well layered quartzites of the Armorican Quartzite (Fig. 2.18a). Single beds are boudinaged with extension parallel to minor F_1 fold axes (Fig. 2.19b). A similar extension is indicated in the Complexo xisto-grauvaquico by boudinage in competent beds in siltstone-shale facies, often with vein quartz occupying the necking region (Fig. 2.18b). Early quartz veins also show boudinage and folding in the same deformation (Fig. 2.19a). Staurolite porphyroblasts are flattened in the S_1 cleavage and also develop quartz pressure-shadows indicating maximum elongation within the cleavage parallel to bedding/cleavage intersection lineation (Fig. 2.15b). On many cleavage surfaces in pelitic sediments a mineral lineation is developed which coincides with the maximum elongation direction determined from deformed fossils. Ellipsoidal spots in slates, shales and siltstones are also elongated parallel to a mineral lineation which coincides with the bedding cleavage intersections in the Ordovician rocks (see Chapter 6 for strain

FIG. 2.15

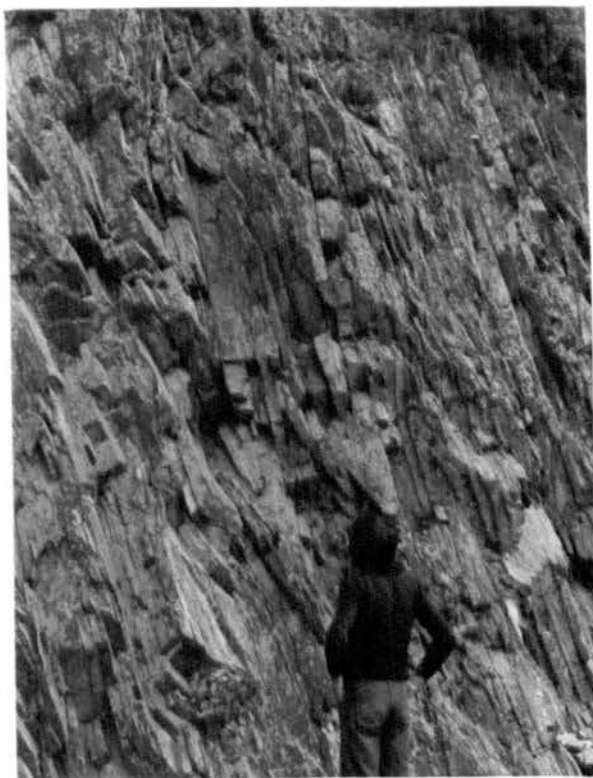
Tight F_1 folds in bedded siltstones in the Complexo xisto-grauvaquico.

Location: 1km northeast of Gamarao de Cima on N326, 6km north of Arouca.

b. Quartz pressure shadow fringes around the ends of staurolite porphyroblasts flattened in S_1 cleavage in pelitic schists of the Complexo xisto-grauvaquico.

Location : 2km south of Fos da Sousa, 15km southeast of Porto on N108.

a



b



FIG. 2.16

a. Disharmonic minor F_1 folds in bedded quartzites ,
Santa Justa Formation

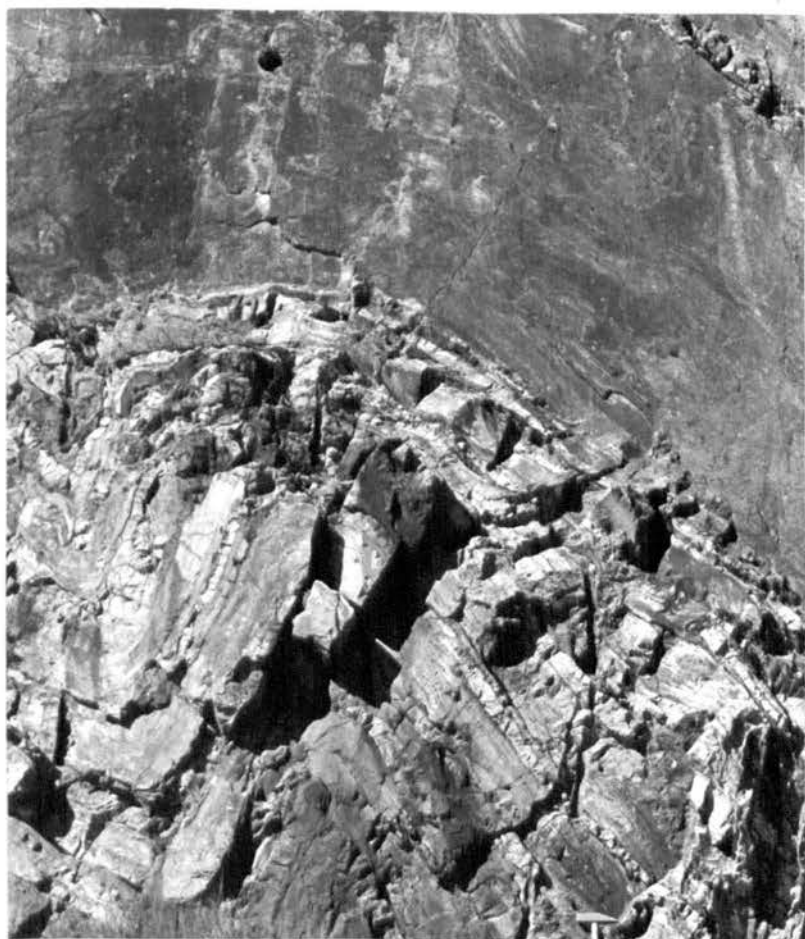
n.b. change in style of the hinge of the central fold
from angular to rounded along the axial trace towards
the thick quartzite bed, top.

Location: 500m east Cancelos, 10km east of Melres on
N108.

b. F_1 minor fold in bedded quartzites , Santa Justa
Formation.

Location : 2km north of Beloi on Rio Ferreira , 3km
south-southeast of Porto.

a



b

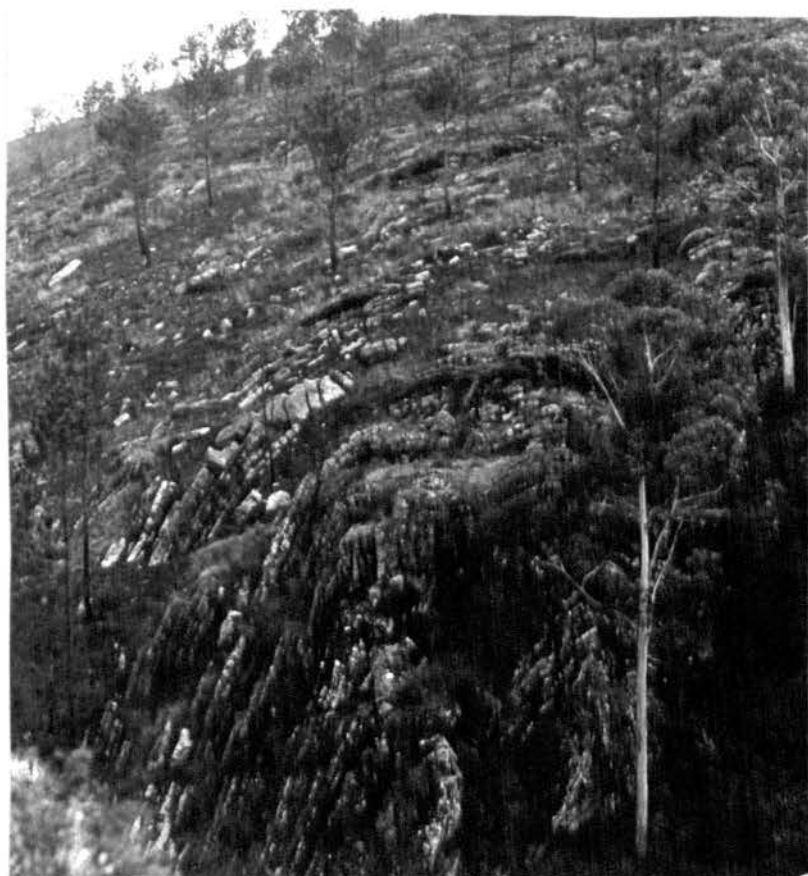


FIG. 2.17

a. Deformed burrows in the hinge zone of F_1 fold
in impure quartzites. True fold profile.

b. Increase in shear strain of the burrows away from
the hinge trace of fold in a.

Location : 1km east of Aguiar de Sousa, 8km southeast
of Valongo.

a



b

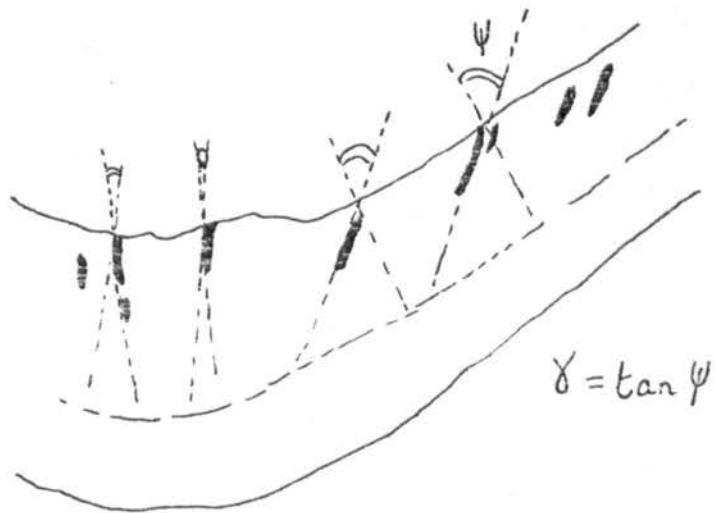


FIG. 2.18

a. Boudins in massively bedded quartzites, Santa Justa Formation.

Location: 500m east of Cancelos, 10 km east of Melres on N108.

b. Boudinage in competent quartzite beds in pelitic schists of the Complexo xisto-grauvaquico.

Location: On north bank of the Rio Douro , opposite the villiage of Crestuma, 15km southeast of Porto.

a



b



FIG. 2.19

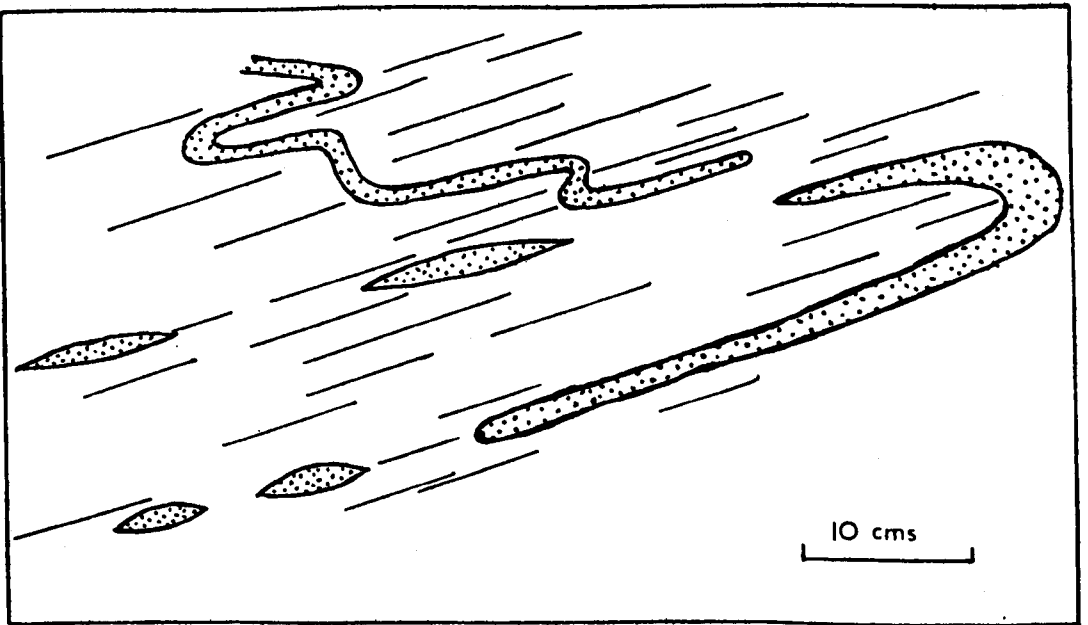
a. Folded and boudinaged quartz veins in pelitic schists of the Complexo xisto-grauvaquico.

Lines indicate trace of S_1 cleavage .

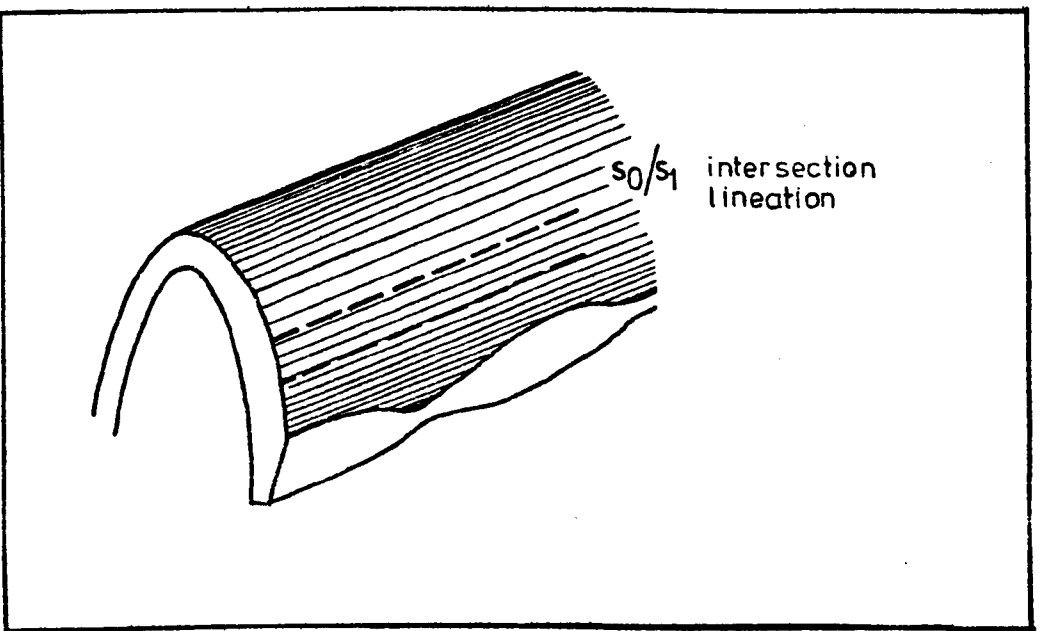
Location: 15km southeast of Porto.

b. Geometrical relationship between direction of boudinage, bedding and cleavage in F_1 folds in the Ordovician.

a



b



measurements). All these linear features indicate maximum elongation parallel to the DV_1 Variscan fold axes (c.f. Figs. 2.10a, and 2.11a). Deformed conglomerates in the Ordovician contain pebbles which are flattened in the main cleavage and elongate sub-parallel to the axis of the Valongo Anticline, plunging shallowly to the northwest. Deformed pebbles in the conglomerates of the Complexo xisto-grauvaquico are also aligned in the plane of the S_1 cleavage with their long axes plunging parallel to the cleavage/bedding intersection lineation and minor F_1 fold axes. Detailed strain analysis was carried out using deformed objects in the Ordovician and Complexo xisto-grauvaquico. This is described in Chapters 6 and 7 respectively.

2.5 SUMMARY

In this region of the Valongo Anticline an Upper Cambrian (pre-Variscan) deformation has folded metasediments of the Complexo xisto-grauvaquico consequently there ^{is} an angular unconformity at the base of the Ordovician.

The main Variscan deformation DV_1 folded Ordovician-Lower Devonian sediments into the Valongo Anticline, and refolded the Complexo xisto-gravaquico sediments into elongate basin and dome structures.

The minor DV_1 fold axes, mineral and S_1/S_0 intersections and elongation structures in the Ordovician

sediments are parallel and plunge at shallow angles to the northwest= indicating a maximum finite elongation parallel to the axis of the Valongo Anticline.

CHAPTER 3

THE COASTAL REGION AROUND APULIA AND VIANA DO CASTELO

3.1 INTRODUCTION

Rocks of the Complexo xisto-grauvaquico and Lower Ordovician are well exposed in this area along two restricted coastal sections at Apulia and Viana do Castelo, two fishing towns 40 Kms. and 65 Kms. north of Porto respectively (Fig.3.1).

These rocks are involved in a continuation of the Valongo Anticline system of folds to the southeast, however, the continuity of the structures is interrupted by 'Older' and 'Younger' Variscan Granites. The Complexo xisto-gravaquico sediments lie in a plutonometomorphic zone, an extension of Zone B (Fig.1.9) and contain staurolite and garnet. Many of the sediments have also been thermally metamorphosed during the emplacement of neighbouring 'Younger' Variscan Granites.

Romano (1974) has described the Lower Ordovician succession at Apulia which is the only definitive study carried out since its recording by Delgado (1908).

3.2 STRATIGRAPHY

1. APULIA

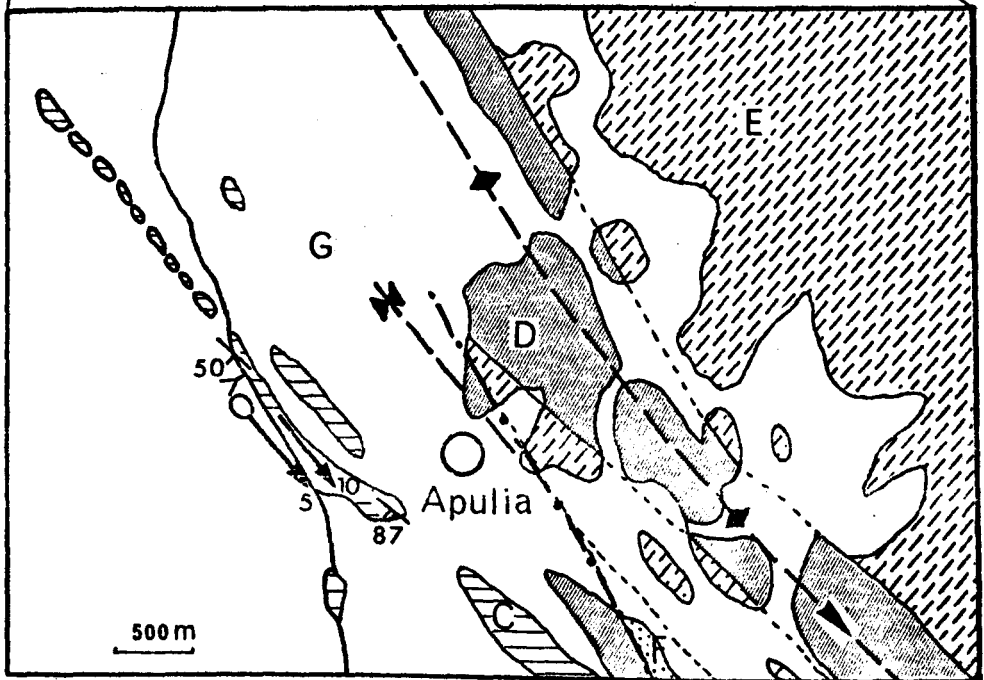
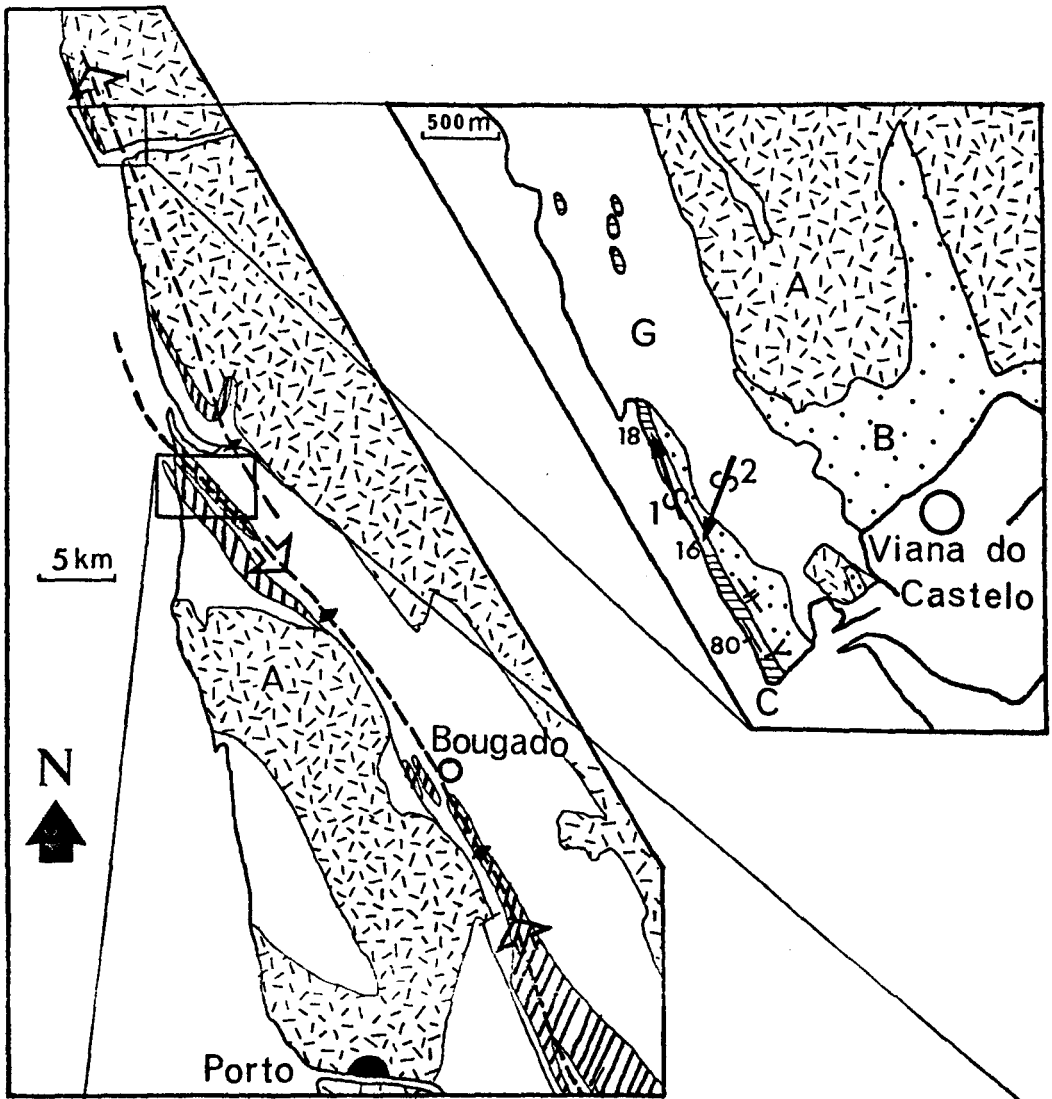
The American Quartzite (s.l.) is the only Ordovician formation exposed in an area which is largely covered by recent sand and gravel deposits. The minimum thickness of

FIG. 3.1

Location and geology of the areas around Viana do
Castelo and Apulia.

After Carta Geologica de Portugal. Sheet 51c 1:50,000.

- A granite
- B Complexo xisto-grauvaquico
- C Santa Justa Formation
- D Valongo and Sobreido Formations
- E Silurian



of this formation is 165m (Romano, 1974).

The lowest exposed beds are orthoconglomerates comprising angular to sub-rounded pebbles, up to 20 cms. in diameter, of vein quartz, quartzite and sandstone composition contained in a green chloritic sandstone matrix. The texture of the conglomerates ^{varies} from pebble-to matrix-supported showing coarse grading in what is generally a poorly sorted deposit (Fig.3.2a). The rest of the succession comprises inter-bedded quartzites, siltstones and mudstones with thin conglomerate beds in the first 30m. For a detailed log of the succession refer to Romano (1974). Animal burrows particularly Skolithos, are common throughout most of the succession, and these provide a good indication of the finite strain (Section 3.3). Sedimentary structures are abundant, including soft sediment deformation features such as ball and pillow structures and minor slump folds (Fig.3.3a.b.) as well as planar and large scale trough cross-bedding. The succession is divided into two distinct facies; the lower characteristic of a fluvial channel environment; the upper facies is more typical of a marine shelf environment (Romano, 1974). There are abundant sedimentary structures which show that the succession becomes younger towards the northeast to the core of a major syncline whose axis runs 500m east ^{of} Apulia village.

FIG. 3.2

a. Polymictic conglomerate at the base of the Santa Justa Formation.

Surface is approximately parallel to the plane of flattening. n.b. long axes of pebbles are sub-horizontal.

Apulia.

b. Conglomerate bed in quartzite.

Pebbles are flattened in a vertical plane. n.b. cleavage not manifested in quartzite.

Surface approximately Y,Z.

Apulia.

a



b



2. VIANO DO CASTELO

Three members comprising the Armorican Quartzite are exposed at low tide along the beach west of the town (Fig.3.1). The lowest member consists of thin interbedded siltstone and mudstones which yield Cruziana furcifera (Diggens pers. com). Massively bedded quartzites comprise the middle member, while interbedded slates and quartzites comprise the upper member of the formation. The base of the lower member is exposed at the contact with the Complexo xisto-grauvaquico which consist of predominantly pelitic schists intruded by acid pegmatites and tourmaline rich dykes, and subordinate psammites.

The contact between the Complexo xisto-grauvaquico and the Armorican Quartzite appears conformable where clearly exposed although minor folds of DV_2 age and a S_2 crenulation cleavage deform the contact and obscure the relationship. Recrystallisation and deformation of the sediments at Viana do Castelo may account for the absence of sedimentary structures. Chiastolite slates of the Valongo Formation are exposed at low tide further north along the coast.

3.3 STRUCTURES AT APULIA

The beds exposed along the beach section west of Apulia strike between 120° and 140° and dip at moderate to steep angles ($50^\circ - 80^\circ$) to the southwest (Fig.3.5a). They are situated on the overturned limb of a major syncline whose axial trace is truncated by a fault a few hundred metres east of the village (Fig.3.1). This syncline is a continuation of the Satão Syncline 10 Km. west of Castro

Daire. The axial trace of the Valongo Anticline to the east of this syncline is continuous from Valongo to Apulia (Fig.3.1), with a small outcrop of the Santa Justa Formation at Bougado. The steeply dipping regional cleavage (S_1) is developed in all the sediments except the massive quartzite beds of the Armorican Quartzite. The cleavage bedding intersection lineation plunges between horizontal and 40° to the southeast and steeply to the southwest (Fig.3.5a). The outcrop pattern within the region indicates the Valongo Anticline plunges southeasterly, implying a shallow plunge depression between Valongo and Apulia. The strike of the S_1 cleavage is fairly constant across and along the section ¹varying between 130° and 140° (Fig.3.5a). Pebbles in the basal conglomerate are flattened in the plane of the cleavage, oblique to the bedding which dips 50° southwest. The pebble long axes are aligned in a sub-horizontal orientation (plunge 5° to southeast) (Fig.3.2a).

A total of 30 pebble shapes was determined from polished sections, cut parallel to the plane of flattening, normal to the elongation direction, and normal to the first two planes. All the pebbles measured are quartzitic in composition and deformed roughly homogeneously with the chlorite quartzite matrix. The mean pebble shape: 1.75 (x): 1.00 (y): 0.64 (z) indicates a relatively low strain similar to that in the basal conglomerate outcropping in the Douro Valley (c.f. 1.64 (x): 1.00 (y): 0.70 (z) and 1.30 (x): 1.00 (y): 0.63 (z)).

FIG. 3.3

a.

Ball and pillow structure in laminated muddy siltstones,
Santa Justa Formation.

Apulia.

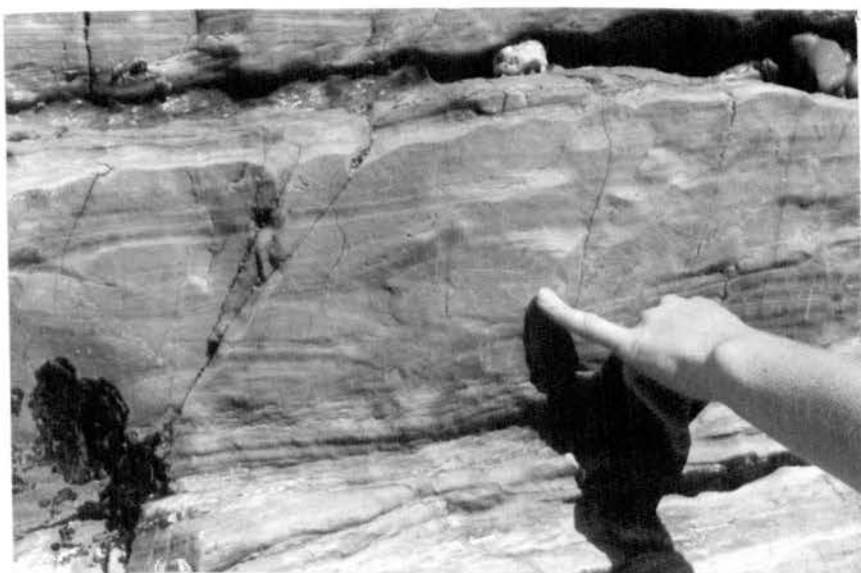
b. Slump folds in laminated siltstones.

Apulia.

a



b



The mean value obtained from measurements indicates the deformation approximates to plane strain (see Fig.6.1).

Deformed Skolithos

Abundant animal burrows, predominantly Skolithos (see Romano, (1974) for facies detail), are present in the quartzite and shaly rocks of the Santa Justa Formation. The deformation in these beds has been studied using the amount of distortion of Skolithos burrows.

Burrow Morphology

The burrows vary in diameter from 2 to 6 mm and in the least deformed beds (quartzites) have circular cross-sections. They are up to 25 mm in length and are generally straight and parallel sided.

In the least deformed beds the burrows are approximately at right angles to bedding. The burrows are filled with poorly sorted sediment comprising dominantly quartz with subordinate muscovite, sericite and opaque minerals. The impure host quartzite is generally finer grained, but similar in composition to the sediment in burrows; whereas in the shales the burrows are more quartz-rich compared to the micaceous host.

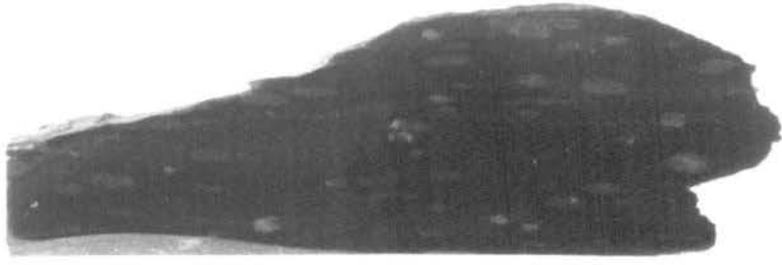
In detail, the main (S_1) cleavage wraps around the burrows illustrating their more competent behaviour during deformation. The internal structure of the burrows is annular

FIG. 3.4

a. Elliptical sections of burrows on a surface cut at right angles to the cleavage.

b. Detail of burrows in siltstones indicating truncation by pressure solution.

a

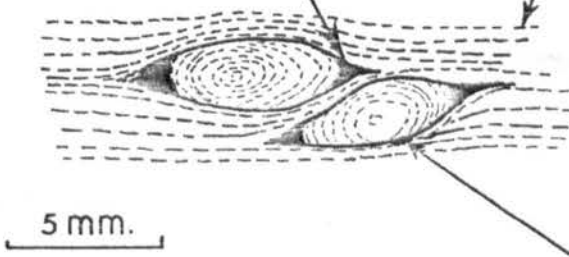


3cm.

b

quartz
pressure - shadow

S_1 cleavage
trace



5 mm.

truncation of
annular structure

but often truncated by the pressure solution cleavage with development of quartz pressure-shadows (Fig.3.4b). Occasionally, burrows are boudinaged along their lengths (Fig.3.6a) although, they more commonly deform homogeneously with a weak internal grain alignment parallel to the cleavage in the surrounding matrix.

Across and along the length of the exposed section of the overturned limb, the distortion of the burrows indicates an up-dip shear component for the deformation which has an overthrust movement towards the northeast. However, many deformed Skolithos and the deformed conglomerate have a strong horizontal shear component. The amount of shear strain was calculated for a number of beds although the strain across the limb is noticeably inhomogeneous, sometimes within a single bed. Strain studies using deformed burrows have been made by Wilkinson et.al. (1975) and McLeish (1971) although the magnitude of strain they describe is considerably greater.

The parameters measured in the rocks at Apulia are:

1. Angular shear strain from the minimum angle between the burrow and the bedding (ψ) (Fig.3.6b).
2. Shape of the elliptical true cross section through the burrow (major axis (a) and minor axis (b)) to show the amount of flattening.

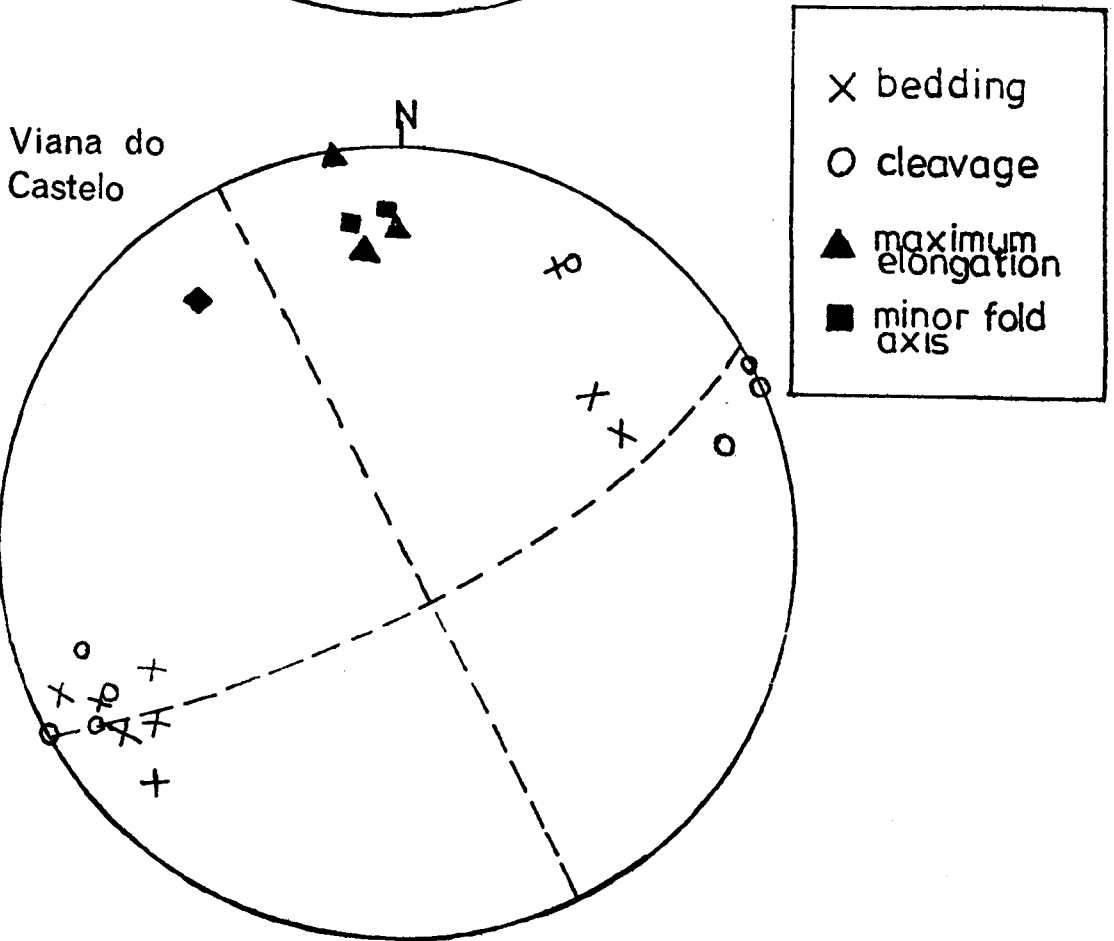
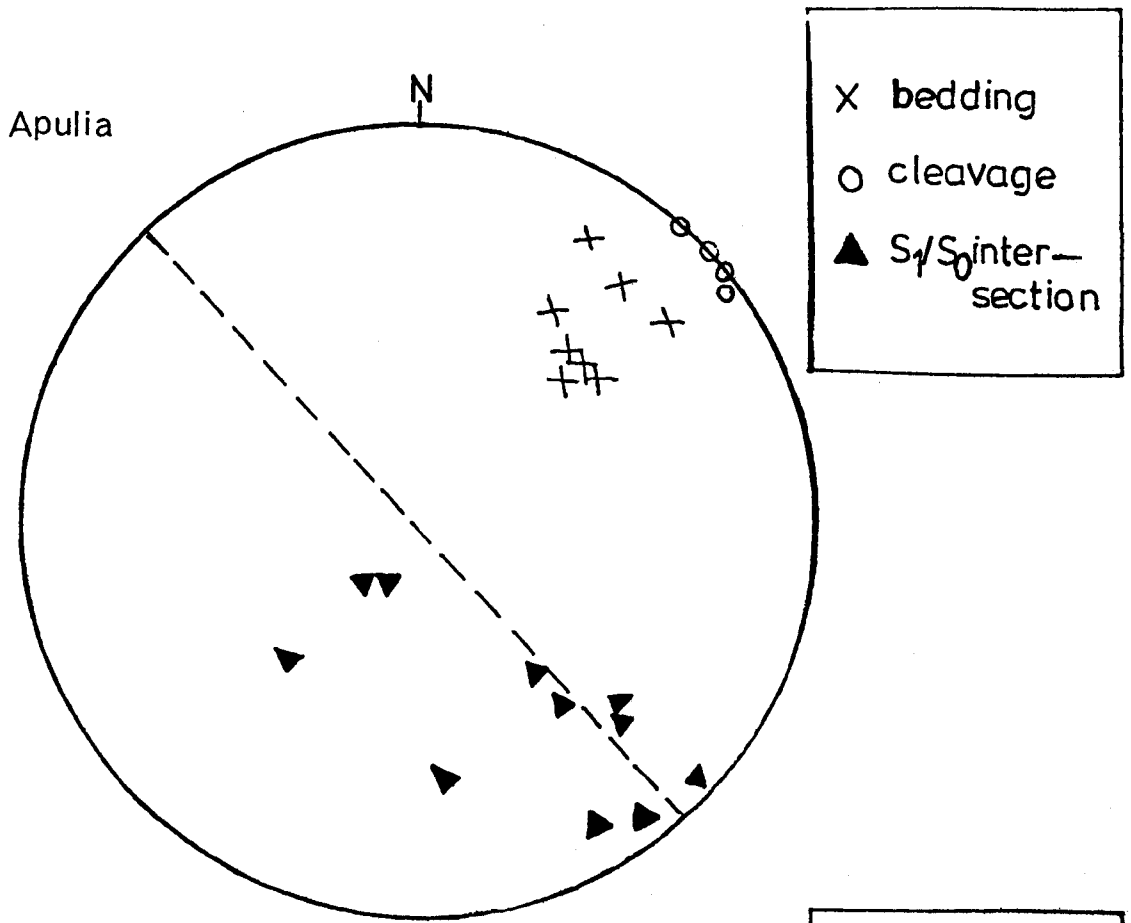
The strain in single deformed burrows investigated by measuring serial sections of two specimens taken at intervals of approximately 3mm (Fig.3.7) remains fairly constant

FIG. 3.5

Stereographic plots of bedding, cleavage and linear structures.

a. Apulia

b. Viana do Castelo.



along the length of burrow despite fluctuations in diameter. It was therefore considered accurate to measure any section through the rock at right angles to the burrows to obtain a mean cross-sectional shape.

As stated earlier, in shaly rocks the burrows do not deform homogeneously with the matrix rocks and represent only minimum values for the total flattening. In the quartzites the difference in ductility between the burrows and the matrix is very small, giving more representative whole rock flattening.

The cross-sections of 120 burrows were measured in three specimens (Fig.3.8), while average cross-sections were measured using fewer burrows per specimen in several others. The results can be summarized as follows:

Cross-section	a :- b varies from
of burrows in deformed	
quartzites	1.60 : 1.00 to 1.81 : 1.00
Cross-section	
of burrows in deformed	
pelites	3.03 : 1.00 to 4.30 : 1.00

The above results illustrate the variation in flattening in beds of different composition.

However, a measurement of the maximum shear strain of individual homogeneously deformed beds is possible using the amount of angular shear strain the burrows have

FIG. 3.6

a. Diagram of deformed burrows in muddy siltstones.
Deformation is by simple shear parallel to the bedding
planes.

Apulia.

b. Burrows deformed in muddy siltstones.

n.b. burrows undeformed or slightly deformed in beds
either side of the shear zone.

Apulia.

$$\gamma = \tan \psi$$

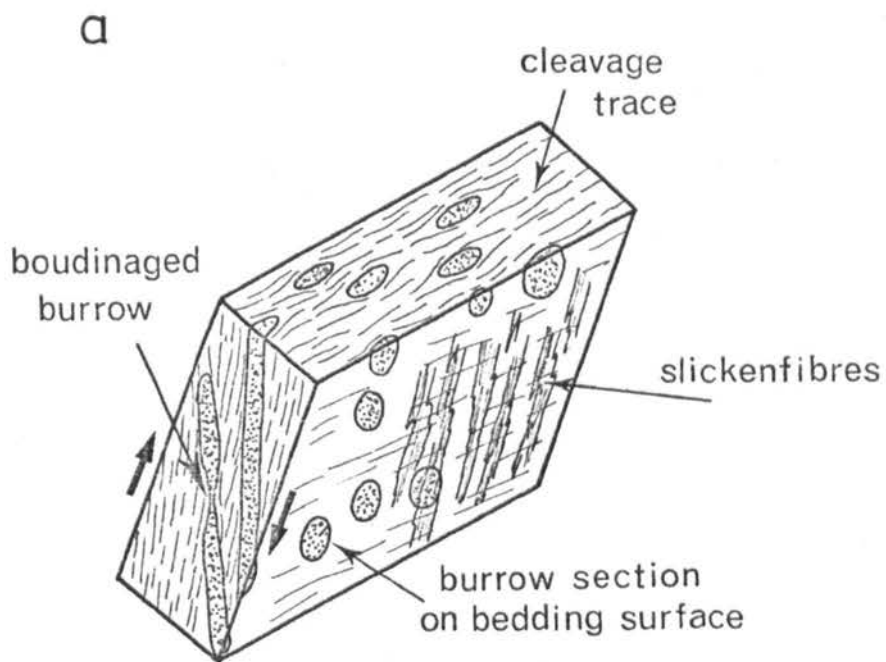


FIG. 3.7

Table showing the variation in diameter of the burrows
along their length.

Specimen 014

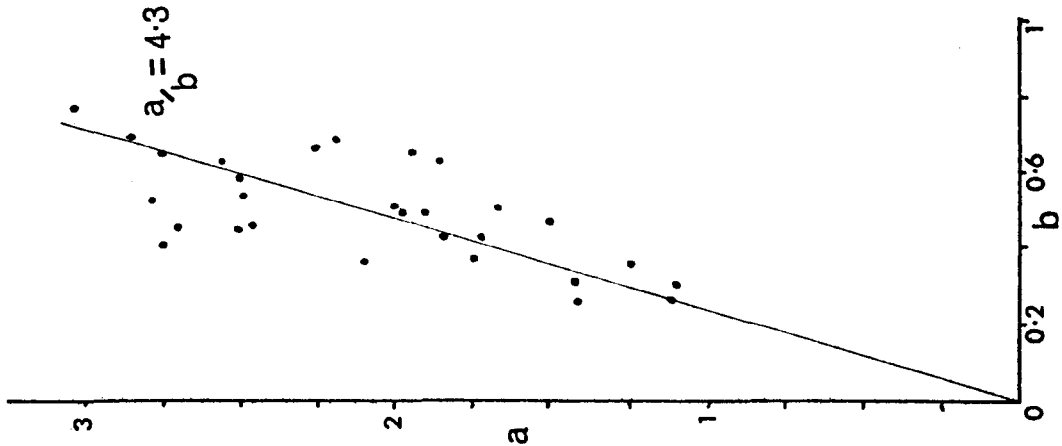
a	b	a/b		a	b	a/b
1.22	0.49	2.49		2.24	0.55	4.07
1.24	0.50	2.48		1.98	0.53	3.74
1.22	0.50	2.44		2.06	0.52	3.96
1.19	0.50	2.38		1.99	0.51	3.90
1.26	0.52	2.42		2.01	0.58	3.47
1.20	0.52	2.31		2.02	0.64	3.16
1.29	0.55	2.35		1.89	0.64	2.95
				2.16	0.67	3.22

Measurements of the principal axes a, b of the cross-sections of two burrows . The measurements were made at 3mm intervals from serial sections.

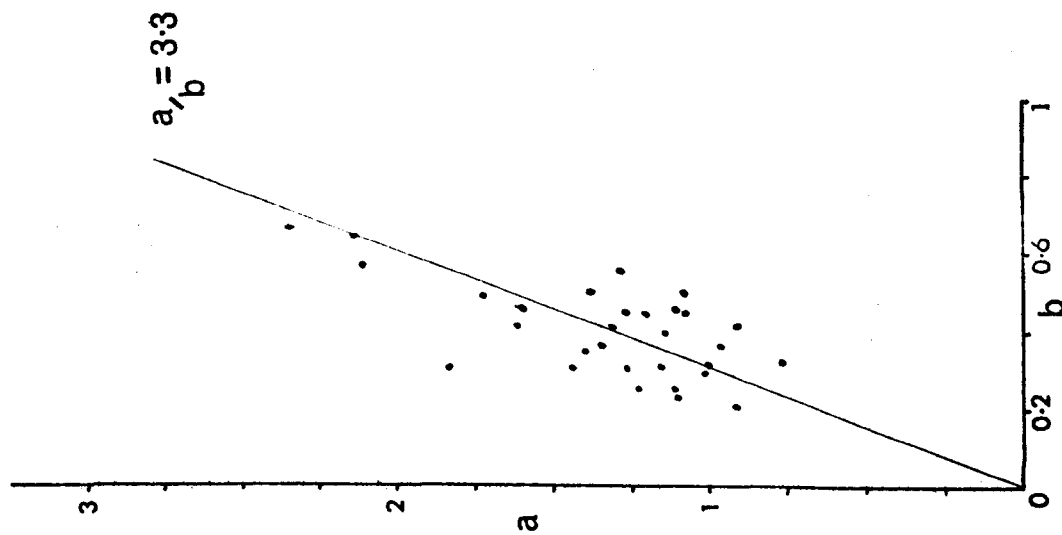
FIG. 3.8

Graphical solution of the strain ellipse for burrow sections deformed in shear zones.

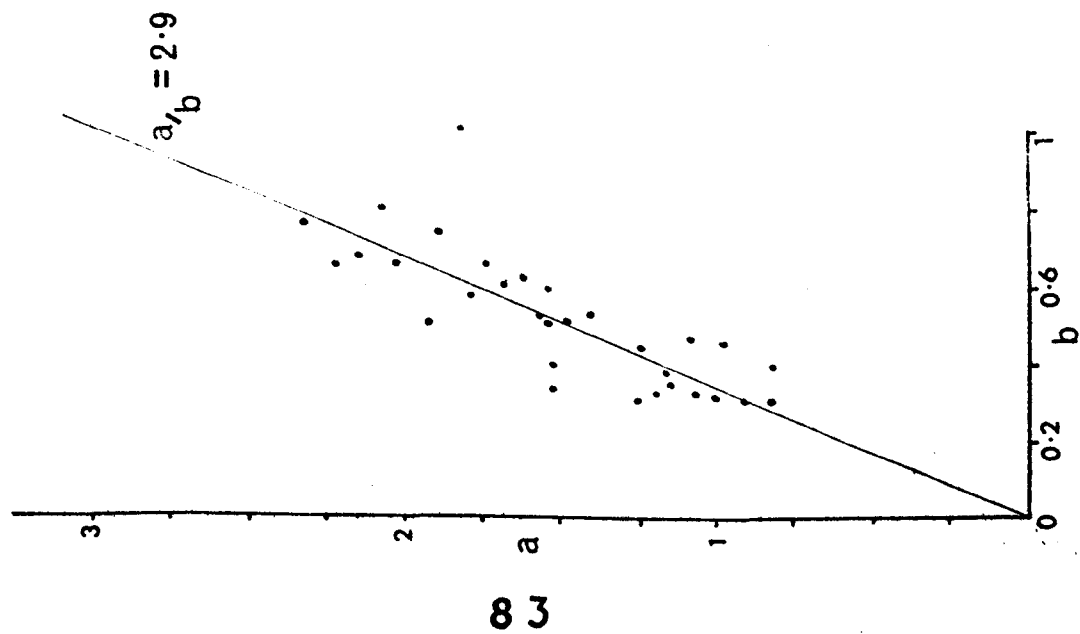
Sp. O15



Sp. O14



Sp. O13



experienced, as $\delta = \tan \psi$ (Ramsay, 1967, p.53) (Fig.3.6b).

The shear strain varies from 1.00 up to 2.90 calculated from 6 different beds of varying composition. The inhomogeneous nature of the deformation is generally bedding controlled with alternating high and low strain in adjacent beds with the shear planes parallel to the bedding surfaces. However, cleavage traces on bedding surfaces wrap around elliptical burrow cross-sections indicating there is a further pure shear flattening component to the deformation. Slickenfibres are common on many bedding surfaces, and indicate a similar direction of shearing to the distorted burrows.

Summary

A single cleavage^{related to shearing} dips steeper than the bedding on the overturned eastern limb of a major syncline. The pebbles in the thick conglomerate are flattened in a plane parallel to the cleavage and are elongated in a sub-horizontal orientation. The deformation is homogeneous on the scale of the conglomerate bed (approx.10m).

The quartzite and shale beds comprising the remainder of the succession have been inhomogeneously deformed by a simple shear mechanism with a variable shear direction between sub-horizontal with a dextral sense of movement, to up-dip within the plane of the bedding. The dominant shear direction is sub-vertical, with an overthrusting of beds to the northwest. This is incompatible with a flexural slip fold mechanism

for the syncline, and implies the simple shear overthrusting determined from the rotation of the burrows is post (DV_1) folding.

It is proposed therefore, that the zone of ductile movements in the area at Apulia represent a continuation of the Douro Shear Belt (Romano & Diggens, 1974) defined further to the south near Valongo. The age of these ductile movements is correlated with transcurrent ductile shearing at Viana do Castelo where the deformation clearly post-dates the growth of chlorite in the pelitic rocks, which is associated with the intrusion of the 'Older' Variscan Granites.

Late Variscan Structures

Post-cleavage ductile shear zones and kink bands form a conjugate set of planar, transcurrent movement structures which result from a N.E. to S.W. compression (Fig.3.9b).

One set of structures strikes 010 and consistently shows a dextral sense of displacement; the other set strikes 060 and shows a sinistral sense of displacement (Fig.3.9 b). Shearing occurs along narrow zones, less than 10cm. wide, which show ductile displacements of less than a metre. However, brittle shearing occurs either centrally or to one side of some zones, in the zone of maximum shear strain. The strain across these zones is best observed where they cut across the basal conglomerate and re-deform the flattened pebbles (Fig.3.9a). The zones in both orientations displace one

FIG. 3.9

a. Conjugate minor ductile shear zones redefining conglomerate pebbles, Santa Justa Formation.

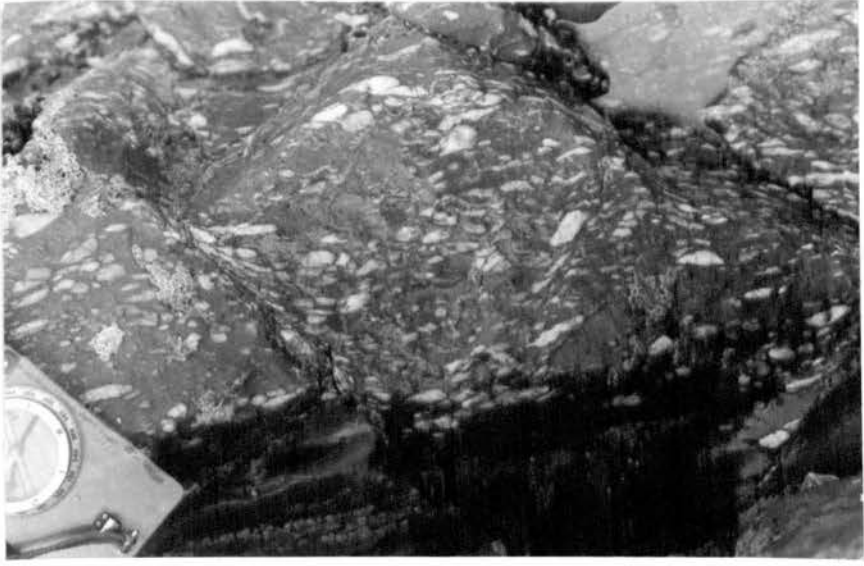
S_1 plane of flattening approximately E-W.

Apulia.

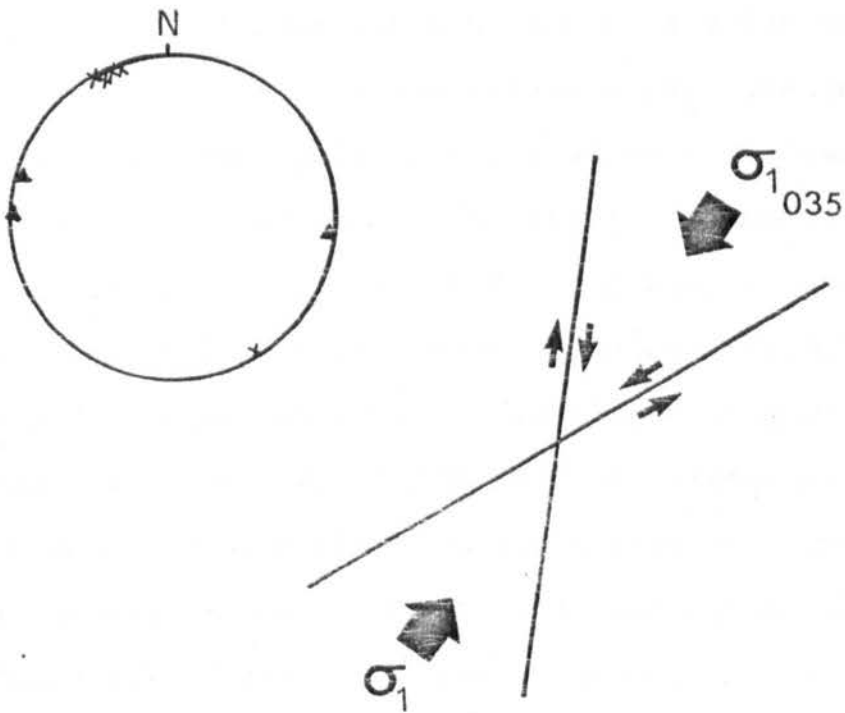
b. Compressive stress direction for conjugate shear zones.

Stereo plot of poles to shear zones.

a



b



another implying synchronous development.

The maximum compression direction σ_1 for the generation of these structures is 035° (i.e. bisector of the two sets) and corresponds to the principal compression direction for the major folds and ductile shear structures in the area, suggesting the stress system possibly remained constant for a major part of the Variscan deformation. However, these transcurrent structures indicate compressional stresses oblique to those for R. Douro and Arouca areas (see Chapter 9).

3.4 STRUCTURE AT VIANA DO CASTELO

Complexo xisto-grauvaquico and Ordovician sediments are exposed on the coast near Viana do Castelo. They have a regional strike approximately 150° and dip between 30° S.W. and 65° N.E. on the western limb of a major anticline (Fig. 3.1, 3.5b). A penetrative cleavage (S_1) has developed in the pelitic and semi-pelitic rocks of both successions and predates a second co-planar cleavage which is associated with transcurrent ductile shearing. The main cleavage developed is axial planar to the folded bedding (Fig. 3.5b). Tight symmetric minor buckles are developed in quartzites interbedded with pelites of the Complexo xisto-grauvaquico within a zone of ductile shearing and plunge parallel (18° to 350°) to the elongation direction resulting from the shearing (Fig. 3.5b). These folds may be either: 1) primary folds F_1 associated with the major F_1 anticline, which have been rotated and modified during the shearing so that their hinges

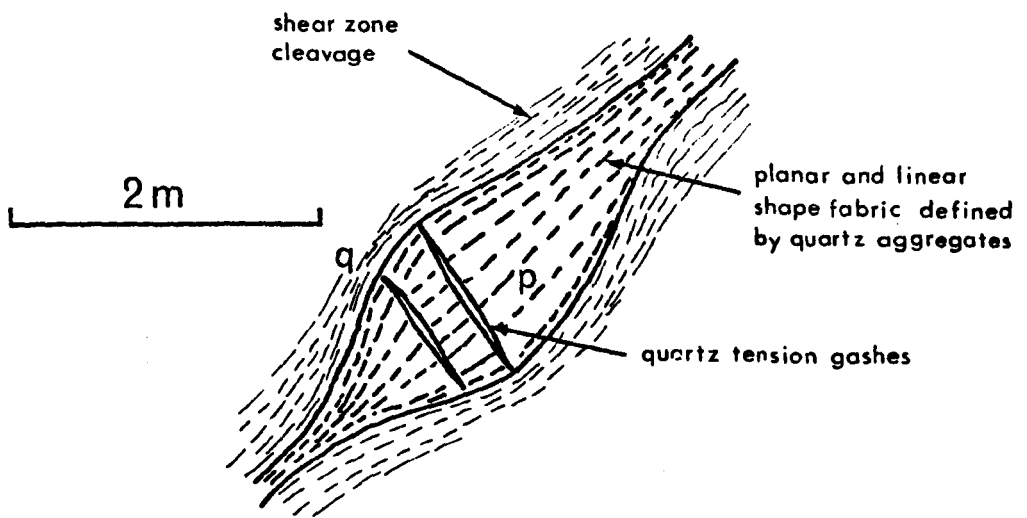
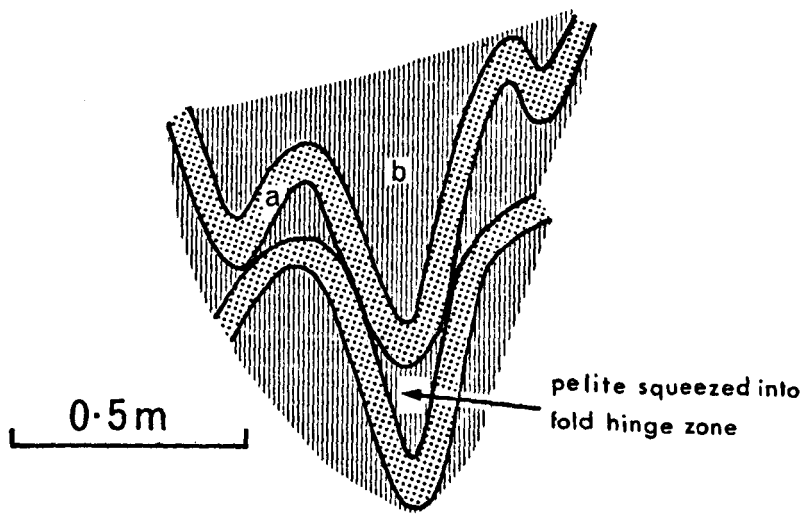
FIG. 3.10

a. F_1 minor folds in psammitic beds (a) in chiasmolite slates (b) of the Complexo xisto-grauvaquico.

Viana do Castelo.

b. Boudinaged tourmaline-quartz beds (p) in pelitic schists (q) of the Complexo xisto-grauvaquico.

Viana do Castelo.



have rotated parallel to the direction of maximum elongation ; 2) second phase folds produced by the ductile shearing; 3) or possibly pre-Variscan folds. The axial planar cleavage is an early cleavage co-axially modified by ductile shearing.

More open F1 folds, interlimb angles \hat{c} 90° , fold massive beds in the Armorican Quartzite. No cleavage is associated with these folds in the quartzite which exhibits recrystallisation. The folds plunge at a low angle to the north and are associated with a major anticline to the east.

Ductile Shear Zones

As already mentioned, two main cleavages are evident in these rocks; a late cleavage associated with ductile shearing develops parallel to the earlier regional S₁ cleavage. The pelitic and semi-pelitic rocks of both successions contain abundant chiasmolite porphyroblasts which have grown in the metamorphic zones around the intrusions of an 'Older' Variscan Granite (Oen, 1970) which is exposed less than a kilometre from the coast (Fig.3.1).

The chiasmolites vary greatly in size from microscopic up to 10cm. in length and 1.5cm. in diameter. This variation in size and density in proportion to the groundmass is controlled by the composition of the sediments producing a planar location fabric corresponding to bedding (Figs.3.11a, 3.12a). The chiasmolites are an important time marker for the deformation. A number of beds contain randomly orientated chiasmolites which both mesoscopically and in thin section

FIG. 3.11

a. Strongly deformed chiasolite porphyroblasts in
muddy siltstones , Santa Justa Formation.

Viana do Castelo.

b. X,Z and Y,Z sections of one specimen of deformed
chiasolite slate to illustrate the preferred orientation
of the porphyroblasts. .

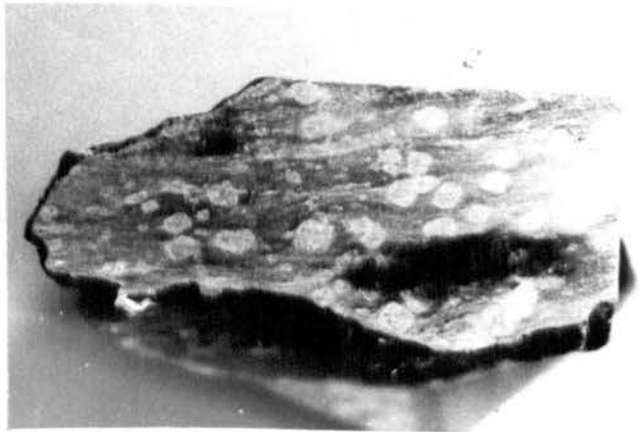
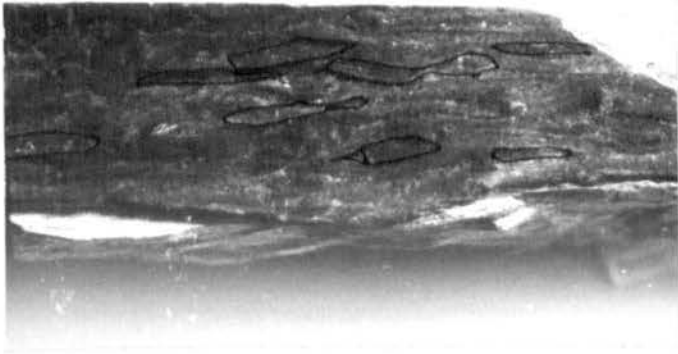
The chiasolites have been outlined for clarity.

Viana do Castelo.

a



b



clearly show a growth post-dating the S_1 cleavage which is preserved as planar inclusion trails of opaque minerals within the porphyroblasts. However, the succession contains a high density of narrow shear zones, commonly 1m to 2m wide, in which the chistolites undergo ductile deformation with the generation of a new cleavage parallel to S_1 . These sheared rocks develop a range of deformation fabrics defined by the chistolites (Fig.3.12). One end member, rarely developed, is a planar fabric with the chistolites randomly orientated within the plane of the compound cleavage (Fig.3.12b). Most fabrics also have a linear element with the long dimensions of chistolites aligned, to various degrees, within the cleavage plane (Fig.3.12c). The maximum elongation direction plunges 20° to 350° in which direction the chistolites are extremely attenuated and commonly boudinaged (Fig.3.11b). Competent beds composed of tourmaline and quartz, in the Complexo xisto-grauvaquico, are boudinaged and develop shape fabrics with a sub-horizontal maximum elongation direction which is sub-parallel to the maximum elongation direction of the mineral fabric developed in the chistolite schists..

Garnet and staurolite in semi-pelitic beds within shear zones contain inclusion trails of quartz which indicate a post S_1 growth similar to those examined in the Complexo xisto-grauvaquico east of Porto (Chapter 1).

The ductile shearing at Viana do Castelo is shown to be post- DV_1 folding. The major transcurrent movements in

FIG. 3.12

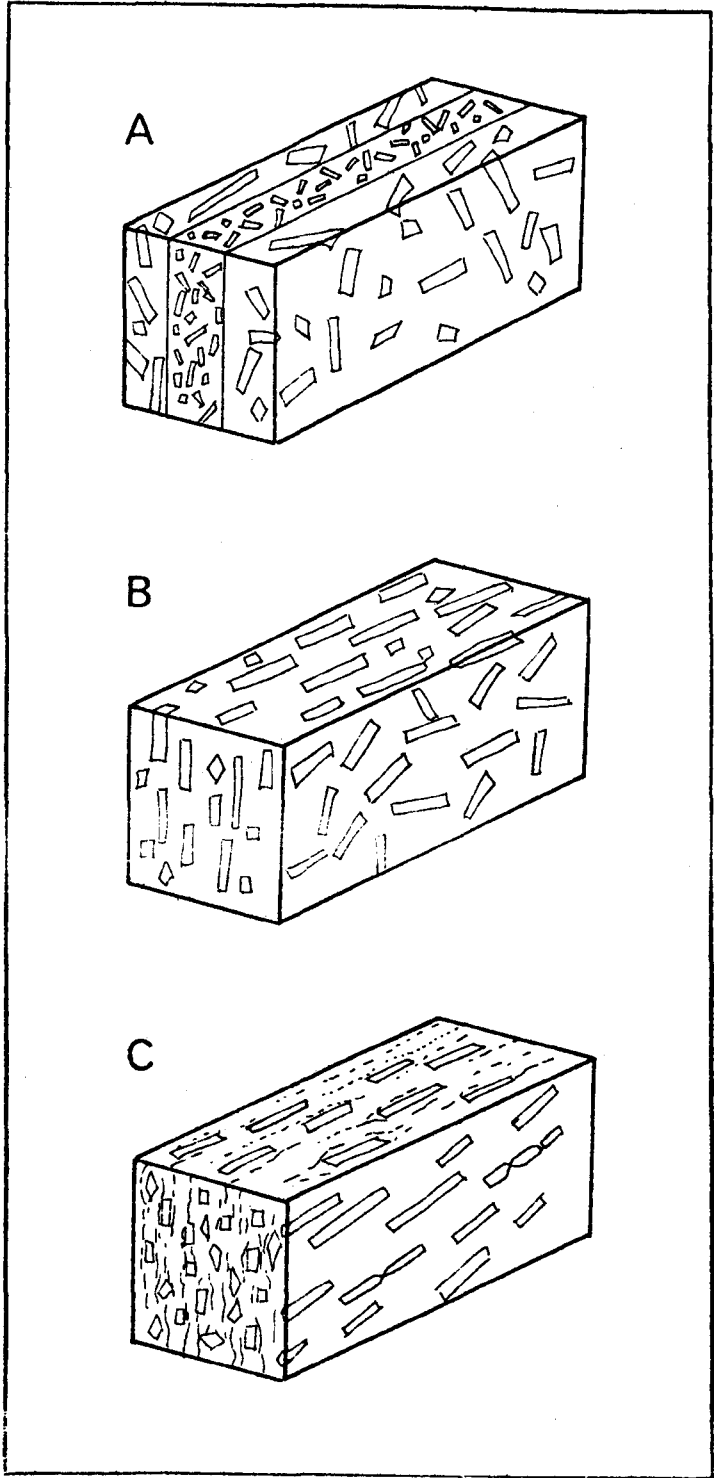
Diagram of the fabrics in chiasmolite slates and siltstones at Viana do Castelo.

A. Location mineral fabric defined by variation in size and density of porphyroblasts . In this case there is no preferred orientation of minerals.

B. Planar fabric with slight linear component.

C. Strong linear fabric .n.b. boudinaged crystals.

B and C are generally combined with a location fabric(A).



shear zones are tentatively correlated with the important phase of ductile shearing at Apulia, where the movements are overthrusting and transcurrent. It is proposed therefore, that the Duoro Shear Belt or an associated parallel belt extends to Viana do Castelo.

The increasing rotation and alignment of chiasmolites from planar to linear fabrics indicates an increase in simple shear strain (Escher & Watterson, 1974) assuming the porphyroblasts grew in a random orientation and not mimetically in the S_1 cleavage.

CHAPTER 4

THE PENACOVA SYNCLINE BETWEEN LUSO AND POIARES

4.1

INTRODUCTION

Complexo xisto-grauvaquico, Ordovician and Silurian sediments are folded into the Penacova Syncline, a major kilometric scale synclinal structure of DV₁ age whose axial trace trends between 130° and 150° approximately 25 km east of the city of Coimbra.

This chapter describes the stratigraphy and structure of the syncline between Luso, 20 km NNW of Coimbra, and Poiares, 15 km east of Coimbra, from observations from four across strike traverses and small well exposed areas (Fig. 4.1).

4.2

STRATIGRAPHY

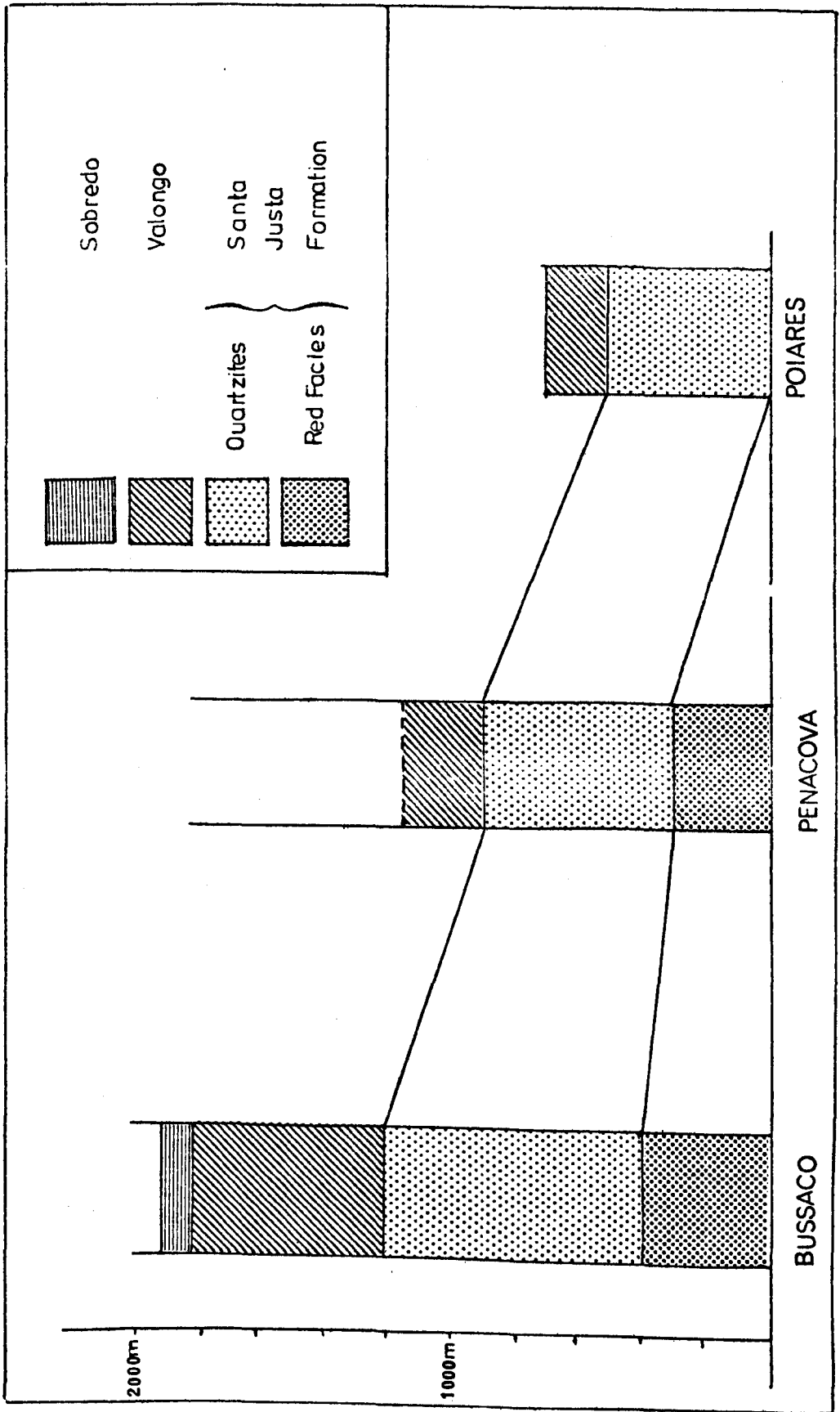
The oldest rocks in the area are well-bedded pelitic schists, siltstones and quartzites belonging to the Complexo xisto-grauvaquico. The pelitic schists have low grade metamorphic assemblages comprising chlorite, muscovite and quartz with subordinate opaque minerals. All these sediments lie in a narrow zone of low grade metamorphism between two belts of high grade metamorphism (see Fig. 1.9 zones A and B).

There are virtually complete sections through the Ordovician succession which forms the eastern limb of the syncline at Poiaras (section 1), Penacova (section 2) and Louredo (section 4). Summaries of these sections are presented in Fig. 4.2.

The stratigraphy of the Lower Palaeozoic successions between Luso and Penacova was first described by Delgado in 1908 with subsequent revision of the Ordovician in the area around Bussaco by Mitchell (1974) who introduced new formational names for the Middle and Upper Ordovician. However, the formational names adopted here are consistent with those used in the other areas described in this thesis adopted from Romano and Diggins (1974), (see Fig. 4.2 for comparison) i.e. Santa Justa Formation (Armorican Quartzite), Valongo Formation, Sobredo Formation.

Some details of the Ordovician stratigraphy are described. The base of the Santa Justa Formation is exposed both north and south of the Rio Mondego on the eastern limb of the Penacova Syncline, 2 km northeast of Penacova (see Fig. 4.1). On the south side of the river, at the base, a series of thin graded conglomerates, each unit being 4cm thick, are in probable faulted contact with schists of the Complexo xisto-grauvaquico which show brittle deformation. . The conglomerates contain pebbles of underlying shaly-schists, which are cleaved. On the north side of the river a similar conglomeratic sequence

FIG. 4.2. Sections through the Ordovician on the eastern limb of the Penacova Syncline



truncates cleaved and folded grey-green siltstones of the Complexo xisto-grauvaquico at an angular unconformity of 60°.

These basal conglomerates are the lowest members of a red facies of sediments, including marls, sandstones and conglomerates. This lowest facies is not exposed at section 1 or along the whole southwestern limb. The red colour is due to a hematite-rich matrix, which towards the top of this facies is secondary in origin i.e. late diagenetic, where the red colour is structurally and lithologically controlled.

The red facies passes transitionally into massively bedded white quartzite with individual bed units between 0.5 and 2m thick. Metre scale cross-bedding occurs in the upper 200m of this the most predominant facies of the formation.

Vertical burrows occur in the upper 20m of the basal red facies and the upper 30m of the massive white quartzite facies (see p. 22 for environmental interpretation).

The Valongo Formation consists of light-brown fossiliferous mudstones to shales, dark-blue slates (rarely fossiliferous), siltstones and thin quartzites. This formation passes up into siltstones, mudstones and volcanoclastic sediments of the Sobredo formation.

Very weathered dolerite sheets intrude the Sobredo Formation parallel to the axial trace of the syncline. A discontinuous lensoid, possibly boudinaged, bed of limestone, approximately 200m thick, outcrops near C. de S^{to} Amaro and at Poiares in the same stratigraphic position in the Sobredo Formation.

Silurian sediments outcrop in the core of the syncline north of Penacova along section 3 between Alagoa and S. Paulo (Fig. 4.1). They comprise thin interbedded shales and quartzites with subordinate quartzites than a metre

4.3

STRUCTURE

1. The Upper Cambrian Deformation

There is evidence of the Upper Cambrian deformation as far south as Penacova. There is a non-brecciated contact, and angular unconformity at the base of the Santa Justa Formation on the eastern limb of the Penacova Syncline on the north side of the Rio Mondego (Fig. 4.3).

Both north and south of the Rio Mondego on the eastern limb of the syncline the conglomerate at the base of the Santa Justa Formation contains sub-angular clasts of grey-green quartzitic schists which a slight fissility which pre-dates the main S_1 cleavage in the conglomerate

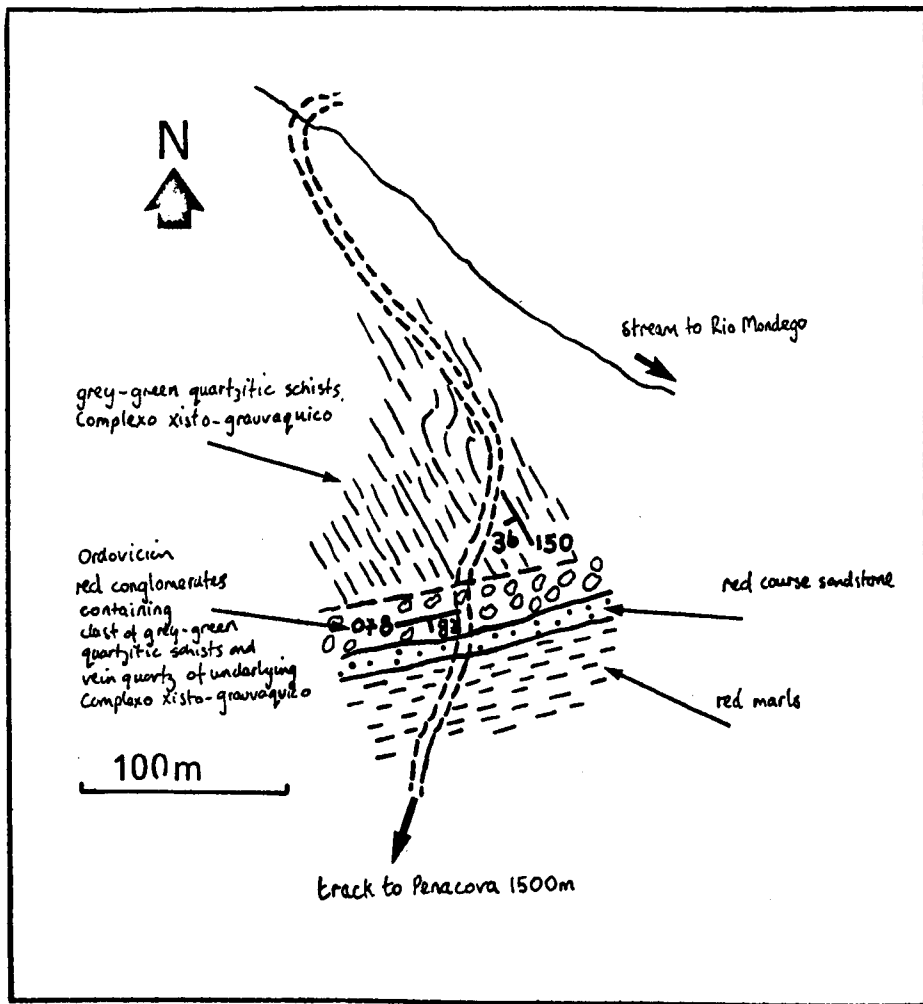


FIG.4.3. Diagram of the unconformity at the base of the Ordovician on the eastern limb of the Penacova Syncline within the Penacova Deformation Zone.

Location: On the track on the north side of the Rio Mondego, 1500m northeast of Penacova village.

matrix. These clasts are locally derived from the underlying Complexo xisto-grauvaquico.

Only one cleavage is normally visible in the sediments of the Complexo xisto-grauvaquico which in most cases is parallel to bedding. The age of this cleavage is considered to be Variscan DV1 as the crenulation cleavage which is rarely developed is Variscan DV2 in age being related to DV2 folds. Hence, the main cleavage in the Complexo xisto-grauvaquico has modified any mineral or shape fabric relating to an Upper Cambrian cleavage. No folds of Upper Cambrian age were recognised.

2. Morphology of the Penacova Syncline

Delgado (1908) first recognised the existence of a major synclinal structure mainly through the repetition of the Ordovician stratigraphy.

Regionally the syncline lies to the west of the axial zone of the Variscan Fold Belt as defined in the first chapter (p.3). The syncline is exposed for almost 40 km over which distance it displays a non-cylindrical geometry. It is an upright fold with a near vertical axial plane but varies in tightness along its length from an isoclinal fold at Penacova, where the eastern limb is slightly overturned, to a more open fold north-westwards and south-eastwards with a maximum interlimb angle of 80° at Bussaco (Fig. 4.1). The rarity of evidence for post-DV₁

refolding both in the absence of superposed folds and in the local development only of a weak S_2 crenulation cleavage, indicates this change in gross fold profile geometry along its axial trace is a primary feature implying inhomogeneous shortening.

The π poles for the bedding indicate there is also a slight fluctuation in the plunge of the major syncline which is not systematically related to tightness of the fold or the plunge of the minor DV1 folds (see stereograms on Fig. 4.1 and Fig. 4.4a, 4.4b).

A major fault striking approximately parallel to the axial trace of the syncline truncates the western limb, mainly the Santa Justa Formation, for much of the length of the fold. South of Penacova village near Carvoeira the fault repeats the Santa Justa and the lower part of the Valongo Formations in a parasitic syncline. Further north, near the village of Alagoa, the Valongo Formation is faulted against the Complex xisto-grauvaquico.

3. Cleavage and minor structures

A single cleavage, S_1 is associated with the Penacova Syncline. It is generally steeply inclined and axial planar to minor DV1 folds (Fig. 4.6a). It is developed in pelitic sediments only, while the competent rocks such as quartzites have undeformed diagenetic textures (see chapter 8). The internal deformation of the sediments in the

FIG. 4.4.

a. Stereographic plot of π poles to bedding for the sub-areas on each of the sections along the Penacova Syncline. The π pole to cleavage for Penacova indicates the axis of the cleavage fan.

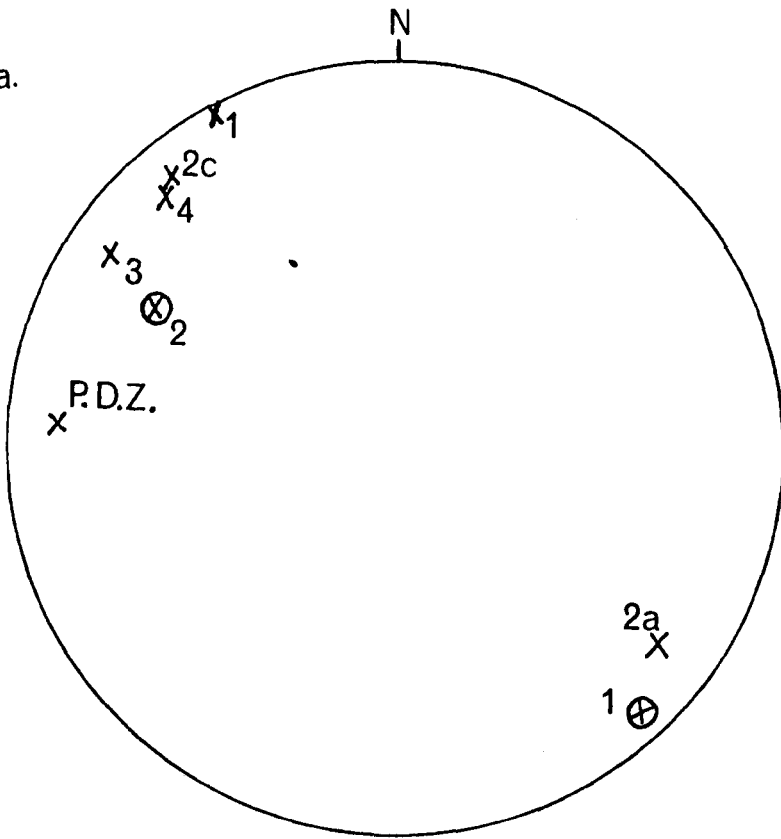
x = bedding , @ = cleavage, the annotations refer to the sections on Fig. 4.1.

P.D.Z. = Penacova Deformation Zone.

FIG. 4.4

b. Stereographic plot of F_1 fold axes and bedding/ S_1 cleavage intersection lineation.

a.



b.

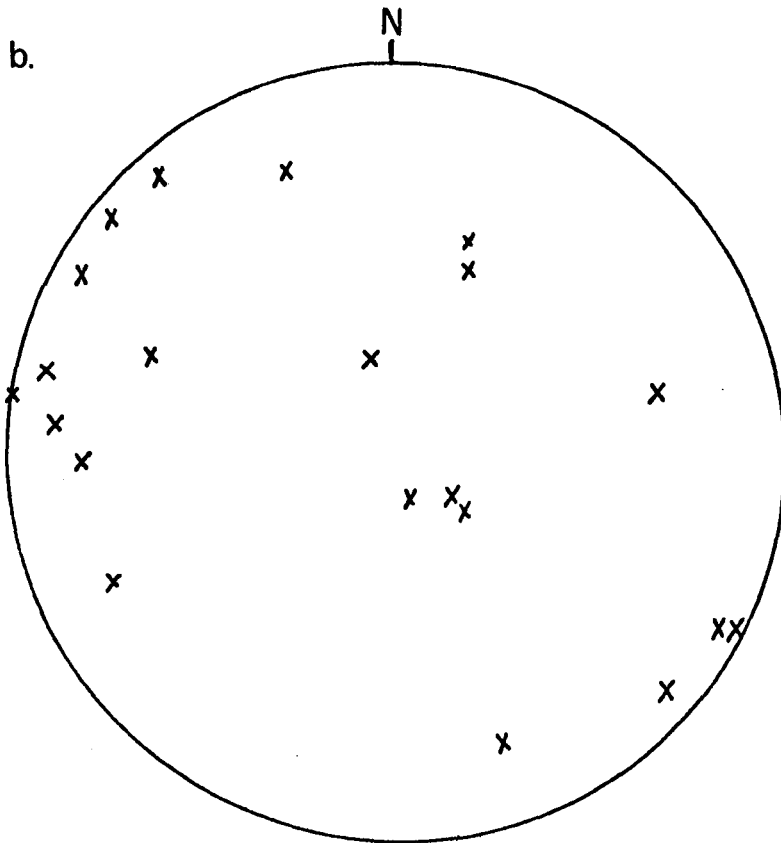
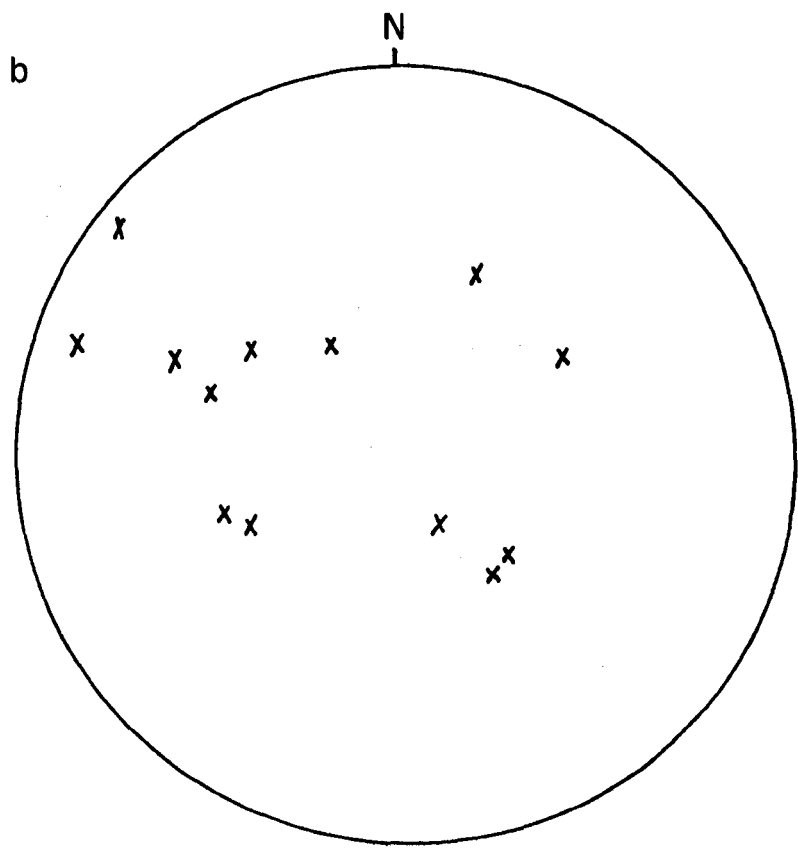
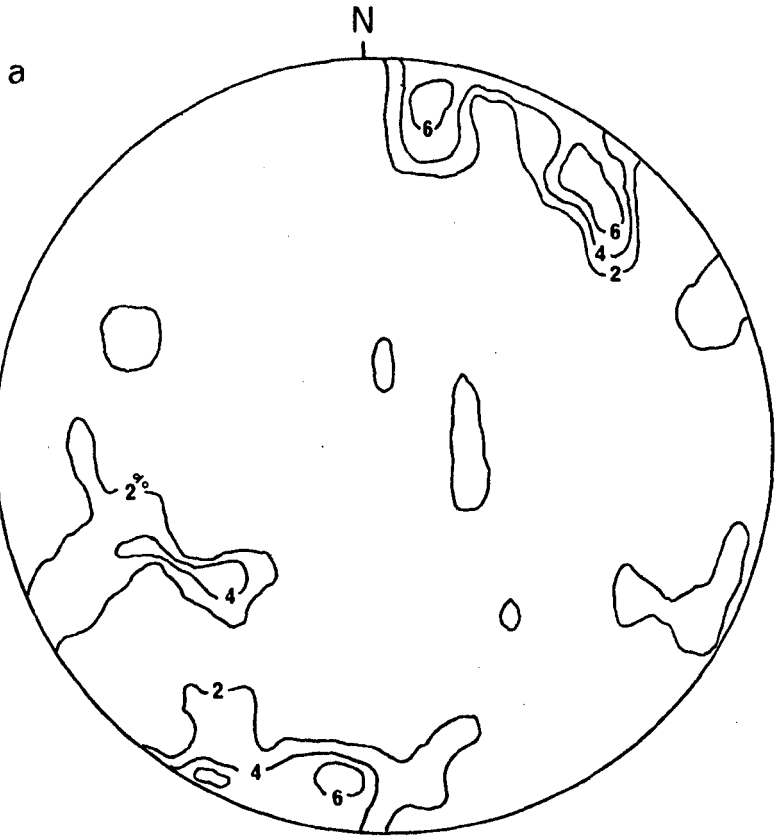


FIG. 4.5

a. Contoured stereographic plot of the S_1 cleavage for the sections along the Penacova Syncline including the Penacova Shear Zone.

FIG. 4.5.

b. Stereographic plot of F_2 fold axes.



Penacova Syncline is less than in the other major fold structures analysed. The cleavage developed in the shales and slates of the Valongo Formation is weak and most fossils are undeformed.

Minor folds, less than 5m wavelength, of DV_1 age (F_1) are occasionally developed in thin bedded quartzites, and interbedded quartzites and shales of the Ordovician and Silurian. Where a cleavage is developed it is axial planar to the folds (Fig. 4.6a).

Slickensides are common on the bedding surfaces of massive quartzites of the Santa Justa Formation especially on the eastern limb of the Penacova Syncline in the road cutting on the south bank of the Rio Mondego. Brecciated movement zones and single fault surfaces are also common in bedded quartzites (Fig. 4.6c).

Bedding plane slip or faulting along bedding surfaces has developed during the main folding, while occasionally these faults have propagated obliquely to bedding. A section on the southern side of the Rio Mondego (section 2a) through the lower part of the Santa Justa Formation shows tectonically truncated beds at a bedding plane fault (Fig. 4.7a). The geometry of these structures is considered to be essentially bedding plane faults propagating across beds as illustrated in Fig. 4.7b. Open symmetrical flexures in the same bedded sediments exposed in the cliff

FIG. 4.6. Minor structures in the Ordovician and Silurian sediments.

a. Sketch looking NNW a minor F_1 fold developed in a thin sandstone bed in cleaved shales of Silurian age. The fold is an asymmetric 'Z' fold parasitic on the eastern limb of the major syncline.

Location: 100m west of crossroads, 2km SE of Sazes do Lavao (section 3, Fig. 4.1).

b. Minor F_1 fold in bedded quartzites, Santa Justa Formation. The axial surface is inclined due to open refolding by F_2 folds. Chlorite occurs on bedding surfaces which have developed slickensides due to flexural slip buckling.

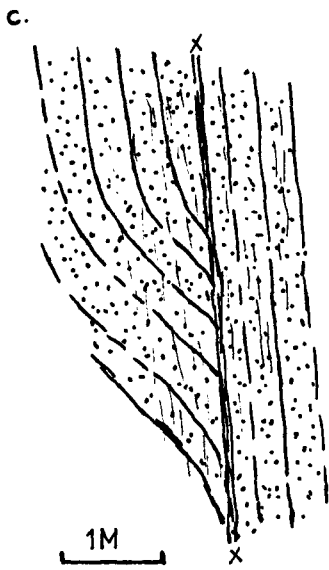
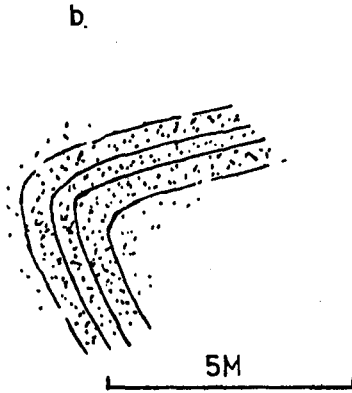
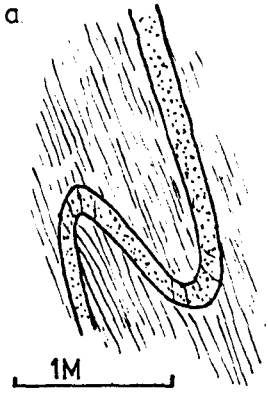
Location: 1 km NE of crossroads, 2 km SE of Sazes do Lavao (section 3, Fig. 4.1).

c. Steeply dipping brecciated movement zone in bedded quartzites of the Santa Justa Formation. A weak cleavage is developed parallel to the zone.

Location: 200m S. of kilometre post 238 on road S. of Rio Mondego NE of Penacova.

d. Tight, minor F_1 fold in bedded quartzites of the Santa Justa Formation. The axial surface of the fold has been reorientated to the shallow dip due to movements of the Penacova Deformation Zone.

Location: 500m SSW. of Penacova on the upper road to Cheira.



on the opposite of the river are thought to be folds generated by such faults where they step across bedding (Fig. 4.7c).

The large thickness of the Santa Justa Formation on the eastern limb of the syncline is partly explained by the repetition of beds by the faulting described above.

4. DV₁ Strain

The internal strain in these folded sediments is considerably lower than in the two other major DV₁ folds described.

Weakly deformed reduction spots (Fig. 4.8) are present in the red marls in the lower 30m of the Santa Justa Formation on the eastern limb of the syncline (see

Fig. 4.2). These spots are the only strain markers within the sediments which indicate they have any significant internal strain. In thin section, the marls contain weakly aligned detrital micas which give rise to a planar mineral fabric parallel to the XY plane of the deformed spots (Fig. 4.8). The angular detrital quartz clasts show little evidence of pressure solution at their boundaries or plastic deformation.

The mean strain ellipsoid calculated from polished surfaces cut parallel to the principal planes of the spot

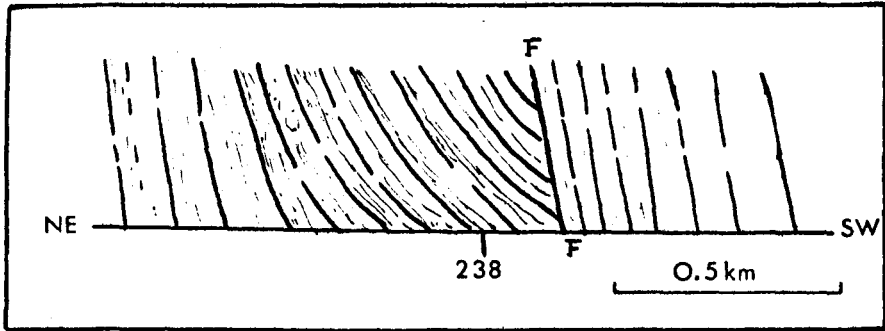
FIG. 4.7.

a. A roadside section showing the trace of a bedding surface-fault **F-F** and the true dip traces of bedding units either side. The fault brings folded and fault truncated beds into contact with undeformed bedding as suggested in the model illustrated below(b). Location: At 238 kilometre post on the southern side of the Rio Mondego, E. of Penacova, in the Santa Justa Formation. See also Fig. 4.6.c.

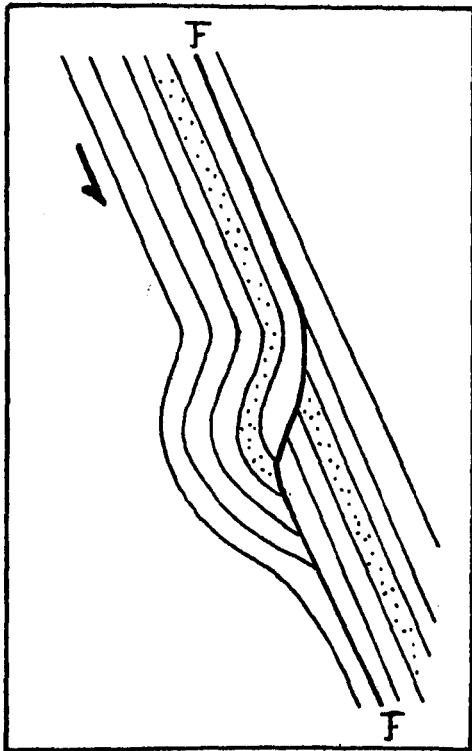
b. Diagram to illustrate how a bedding surface-fault cuts through bedding units and gives rise to folds, based on a model by Dahlstrom (1970).

c. Symmetric flexural folds in beds along strike from those in the road section above (a), exposed in cliff section on the north bank of the Rio Mondego. These folds are considered to develop by faulting as illustrated in b.

a



b



c

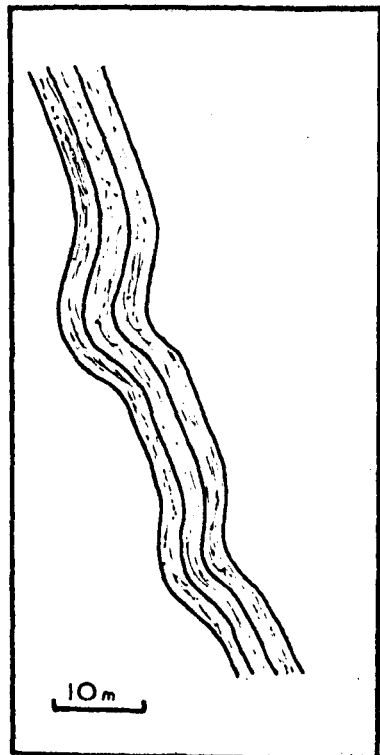


FIG. 4.8

a. Enlarged prints of polished surfaces of marls with reduction spots from the Santa Justa Formation. The surfaces are cut parallel to the principal planes of the spot ellipsoid i.e. XY, YZ, ZX.

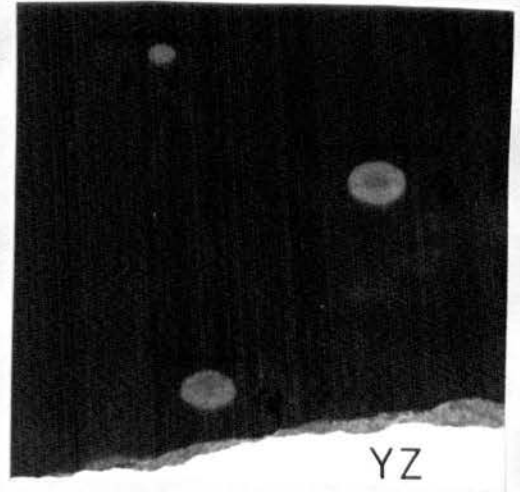
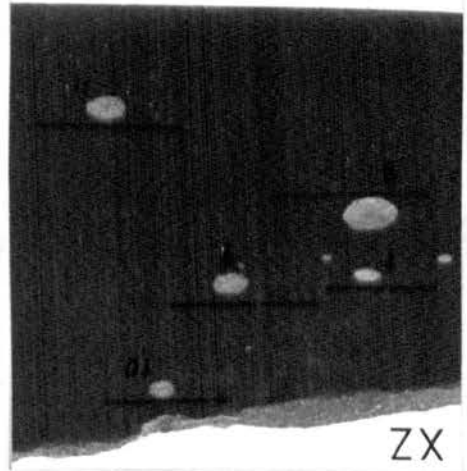
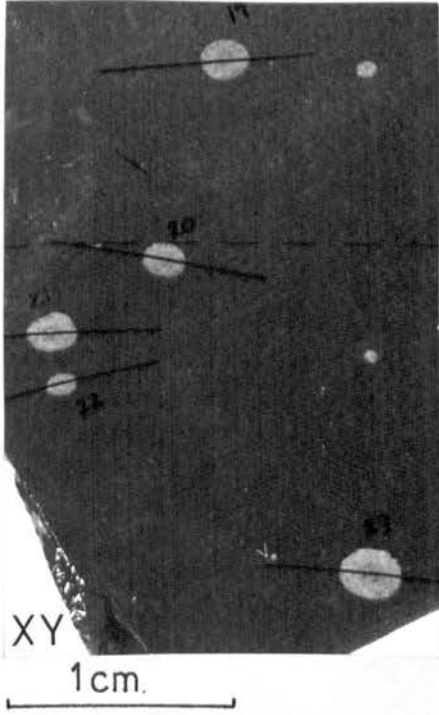
Location: 20m above the base of the Santa Justa Formation on the eastern limb of the Penacova Syncline, 150m NE. of kilometre post 238 on the road S. of the Rio Mondego (section 2a, Fig. 4.1).

b. Photomicrograph of a reduction spot showing its concentric colour structure. Note the cleavage defined by the weak alignment of micas in a plane containing the long axis of the spot. Also note the isotropic fabric of the undeformed, angular quartz grains.

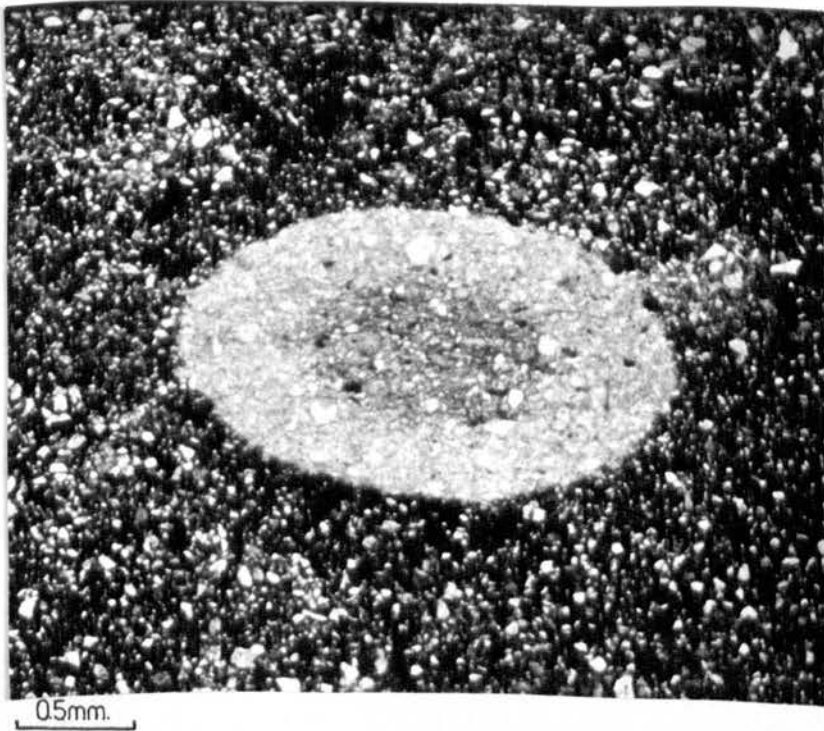
Same location as 4.8.a.

Specimen no. P2.

a.



b.



ellipsoids is X:Y:Z, 1.30 : 1.00 : 0.79. The maximum elongation direction is 15° to 315° indicating a weak extension, at least locally, sub-parallel to the axis of the major fold.

In the cleaved pelitic rocks also, a low degree of flattening is indicated by virtually undeformed brachiopods and trilobites.

Commonly occurring narrow zones of brecciation (Fig. 4.6c), minor faults, and steeply plunging slickenstriae on sub-vertical bedding surfaces in the quartzites of the Santa Justa Formation indicate that the internal deformation accomplished within the competent formation during folding was by movement on narrow zones, in particular bedding plane slip, with little or no internal ductile deformation of the beds.

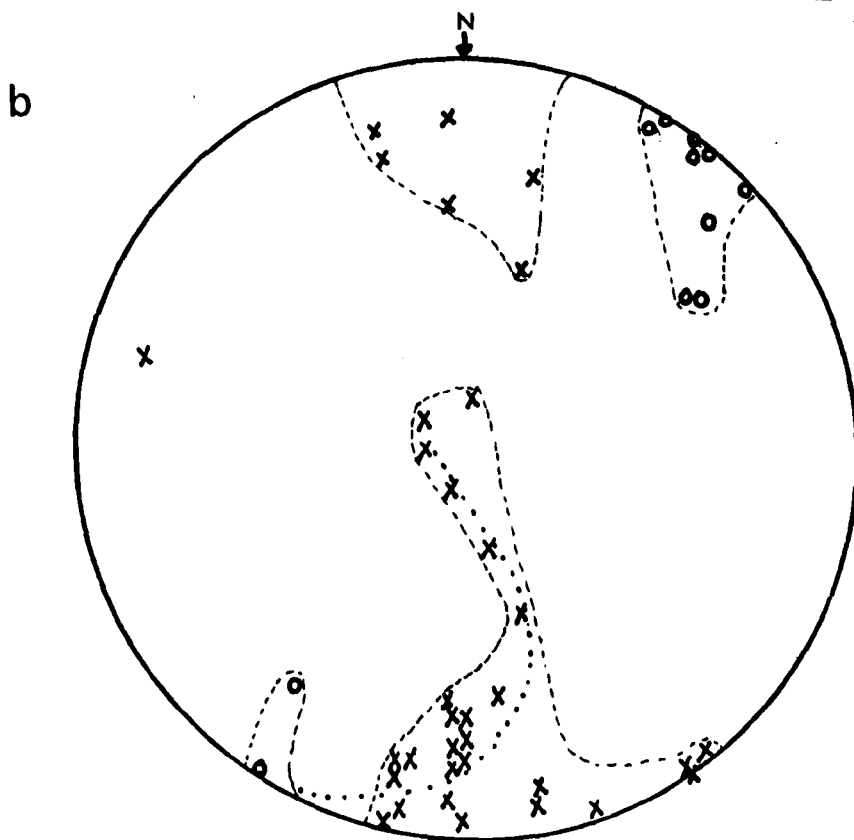
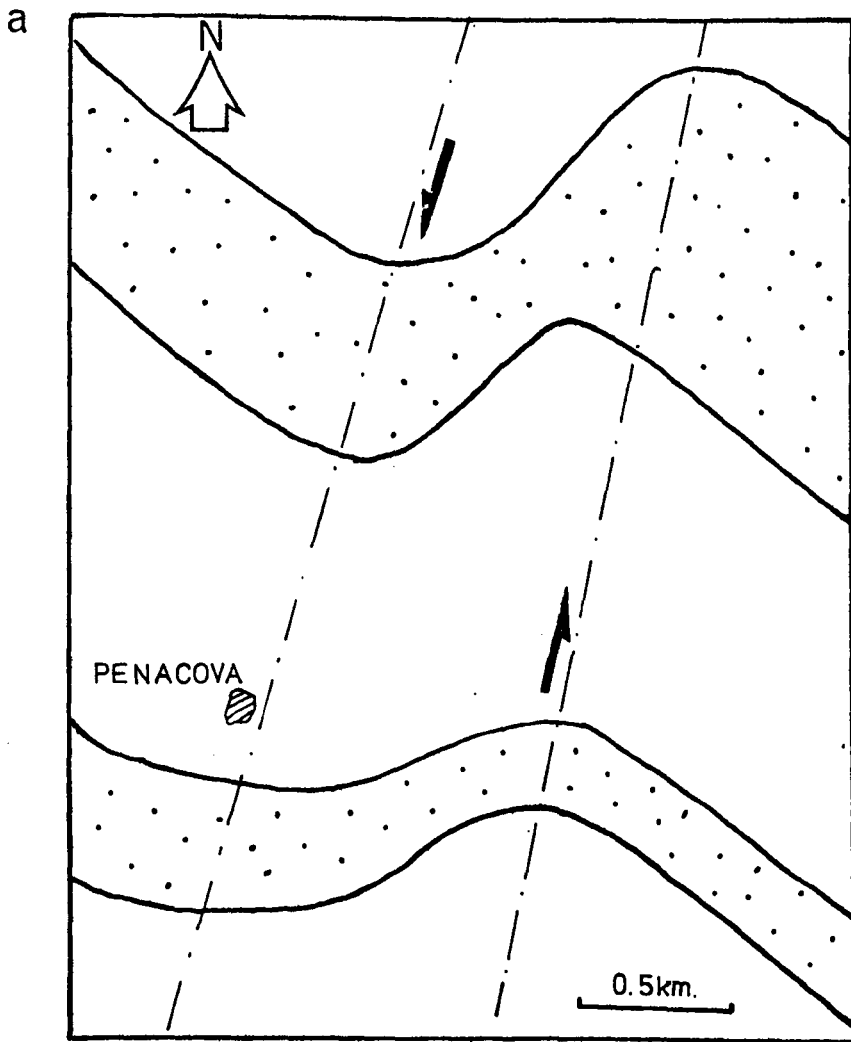
5. The Penacova Deformation Zone

A deformation zone, trending 020° , displaces the Penacova Syncline at Penacova. The zone is approximately 1 km wide, narrowing slightly northwards, with a horizontal sinistral displacement of the synclinal axial trace of 1.2 km (Fig. 4.9a). The effects of the deformation are: 1. Bedding becomes progressively reorientated from a strike 120° outside the zone i.e. the main strike of the beds in the limbs of the fold, to an extreme of 030° in the centre of the zone, while the dip of the beds

FIG. 4.9.

a. A plan section of the Penacova Deformation Zone indicating the limits of deformation and the horizontal displacement of the Santa Justa Formation (dotted) for each limb of the syncline.

b. Stereographic plot of the poles to bedding inside (x), and outside(o) the Penacova Deformation Zone. The dotted line shows the locus of a single plane progressively rotated into the zone.



becomes horizontal from subvertical (Fig. 4.9b).

2. The F_1 fold axial planes and the S_1 cleavage are reorientated in the zone in a similar way to the bedding.

This reorientation of the beds and minor structures within the zone is not accompanied by the development of any new cleavage. The geometry of the reorientated bedding indicates that the movement direction in the zone is inclined with an upth eastern block and a sinistralhorizontal component.

The age of the deformation is later than DV_2 and is possibly related to the ductile-brittle structures of late Variscan age described in Chapter 9.

4.4

SUMMARY

The Penacova Syncline is a tight non-cylindrical fold with an interlimb distance (i.e. minimum wavelength) of between 2 and 3 km, whose geometry is largely controlled by the competent quartite series of the Santa Justa Formation (the Armorican Quartzite).

The folded sediments, except quartzites, have developed a weak cleavage although fossils indicate their internal strain is low. Evidence indicates that during the buckling process which produced the major syncline much of the deformation

and accommodation has been by movement on bedding surfaces and steep faults and deformation zones.

5.1 Introduction

The third major fold investigated in the Variscan Fold Belt is the Marão Syncline; a DV_1 structure which folds Complexo xisto-grauvaquico, Ordovician and Silurian sediments.

The fold lies to the east of the axial zone of the Variscan Fold Belt (see section 1.1) where the regional cleavage dips to the S.W. Only the eastern limb of the syncline is exposed for much of the outcrop, so that the attitude of the axial plane is indeterminable except at the southern extremity of the fold where it is near vertical. The N.E. vergence depicted on earlier maps for the Serra do Marão region indicates the vergence of minor folds parasitic on the eastern limb of the syncline. (Carta Tectonica de Portugal, 1972).

The eastern limb of the syncline is exposed for approximately 25km, with the central exposures in the Serra do Marão, a mountain range with a highest point of 1415m. The resistant quartzites (Armorican Quartzite) of the Santa Justa Formation form the highest part of the range which lies 100km east of Porto and is traversed by the N15 road between Amarante and Vila Real. (Fig. 5.1).

The central area of the Serra do Marão was mapped in

detail and is serviced by two mine tracks and several cart tracks which provide the best exposures. A section was traversed across the northern end of the syncline near Pardelhas where the eastern limb dips approximately 45° S.W. A further section was traversed at Mesão Frio, 10km south of the central Marão area, where the eastern limb is sub-vertical (Fig.5.2b).

5.2 Stratigraphy and Lithologies

1. The Complexo xisto-grauvaquico

In the central area and to the south at Mesao Frio the Complexo xisto grauvaquico succession comprises low grade metamorphosed pelitic and semi-pelitic schists. These metasediments have, however, yielded Lingulid brachiopods (Teixeira^{et.al.} 1964) which is supportive evidence that the succession is, in part, Cambrian in age.

In the north, east of Pardelhas, the Complexo xisto-grauvaquico lies in a high grade metamorphic belt, Zone D (see Fig. 1.1), to the south-west of an undeformed, two-mica granite belonging to the suite of Older Variscan Granites of Upper Westphalian age (Priem et. al., 1970). The schists near the contact of the granite, seen 1km due east of Pardelhas in the main road cutting, contain undeformed granitic dykes, off shoots from the main granite, which cross-cut the main regional schistosity (S_1).

The higher grade schists are dominantly coarse-grained pelites composed of biotite, garnet, muscovite, \pm chlorite,

and quartz (Fig. 1.10a). These schists become coarsely spotted (Spec. M34, M35) within 50m of the granite contact.

Towards the contact with the basal Ordovician the schists become dominantly psammites with occasional beds of quartzite. The bedding dipping between 30 and 60 S.W., in the pelitic schists is difficult to distinguish due to the coarse schistosity which is developed. As well as being aligned with a planar orientation in the main schistosity, the minerals are often aligned to produce a linear fabric which plunges 34° to 215° parallel to the DV_1 fold axes of the main syncline.

2. The Ordovician

In the road section near Padelhas, the base of the Santa Justa Formation consists of a fine-grained, variable packstone to wackestone conglomerate resting concordantly on the Complexo xisto-grauvaquico. Here the main cleavage is parallel to the contact, and the bedding in the conglomerate and the schists below. The pebbles comprising the conglomerate are dominantly vein quartz, well rounded and up to 5cms in diameter. The conglomerate is approximately 2m thick at Padelhas, and is overlain by a series of well-bedded grey to brown quartzites of a maximum bed thickness of 0.5m. Towards the top of the Armorican Quartzite the quartzites contain abundant magnetite and iron silicates of sedimentary origin (Priem 1962). It is noteworthy to mention that this iron-rich horizon is recognised in the Ordovician stratigraphy

FIG. 5.2

a. Location of traverse and geology of the area around Paredelhas , northern Marao. East limb of the M̃arao Syncline.

b. Cross-section showing dip of the limb of the syncline from the enveloping surface of minor second order folds.

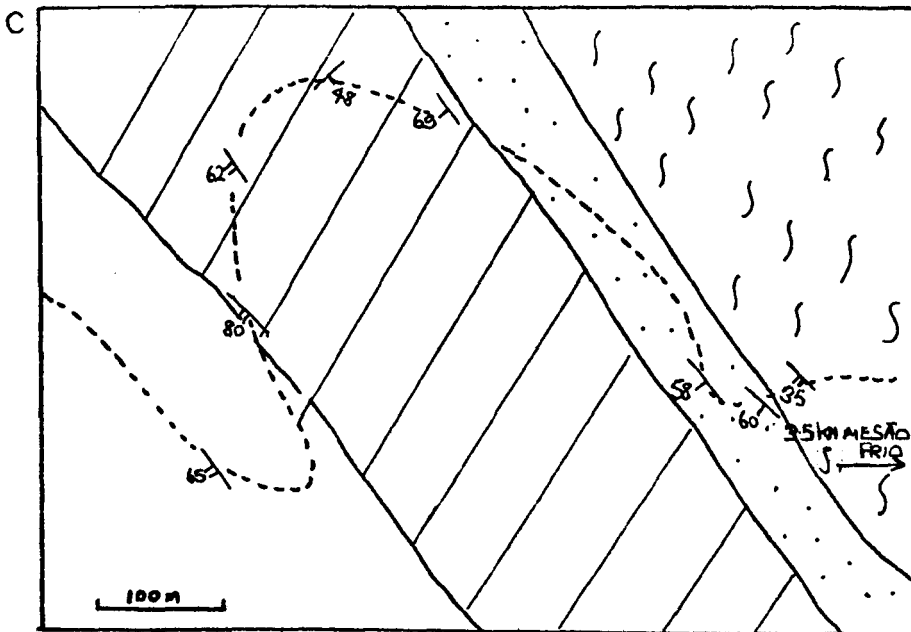
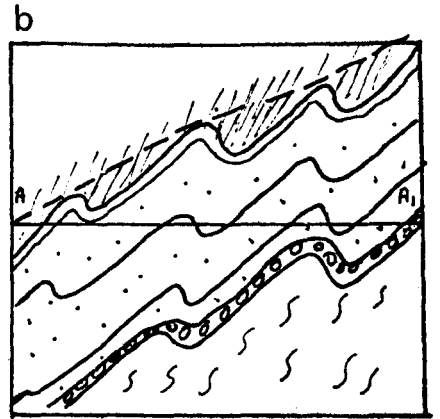
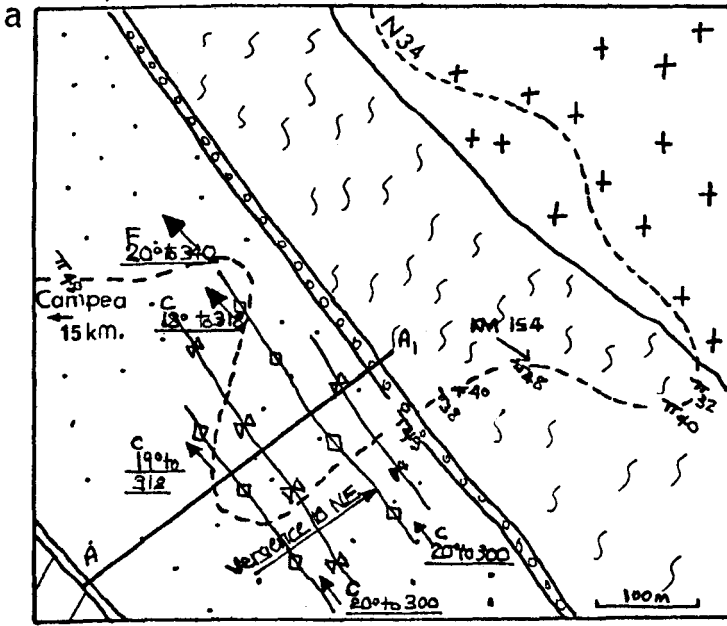
c. Location of traverse and geology of the area around Mesão Frio, southern Marão. East limb near Mesão Frio.

+ Granite

§ Complexo xisto-grauvaquico

•• Basal conglomerate } Santa Justa Formation
∴ Quartzites }

// Slates Valongo Formation



throughout the Variscan Fold Belt at north Portugal.

The quartzites (Armorican Quartzite) of the Santa Justa Formation pass up into a thick succession of blue-grey slates of the Valongo Formation.

The approximate thicknesses of the Ordovician formations folded by the Marão Syncline are presented in Fig. 5.3 .

In the central area of Serra do Marão the base of the Santa Justa Formation consists of an unusually thick sequence of conglomerates and grits. The conglomerate is folded and faulted but its thickness is estimated at 100-120m. It is extremely variable in composition, both laterally and vertically, ranging from a fine or coarse pebble-supported quartzite conglomerate to a matrix supported mudflake conglomerate. There is no regular vertical change in grain size, which varies greatly on a small scale (Fig. 5.4a). Excepting the lowermost facies of the conglomerate, it is well bedded with occasional flame structures and graded beds.

In the exposures along the mine track, 1.5km northwest of the summit of Marão (Fig. 5.1), the lowermost facies of the conglomerate the Marão Conglomerate, estimated at 50m thick, is faulted against the Complexo xisto-grauvaquico and the upper, iron-rich, quartzites

FIG. 5.3

Variation in thickness of the Ordovician sediments
along the eastern limb of the Marão Syncline .

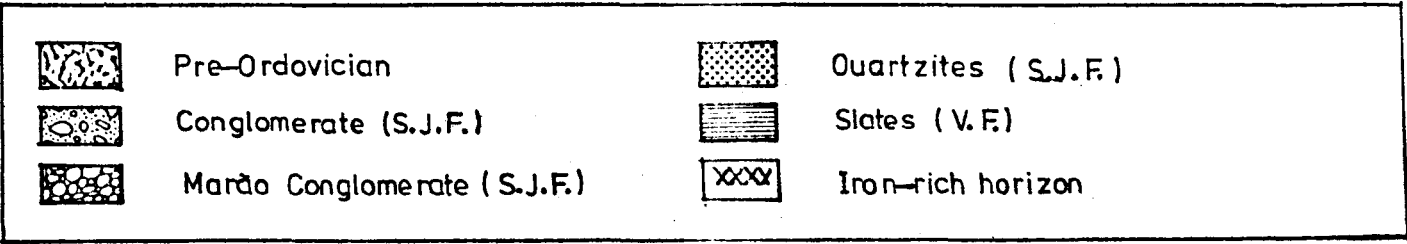
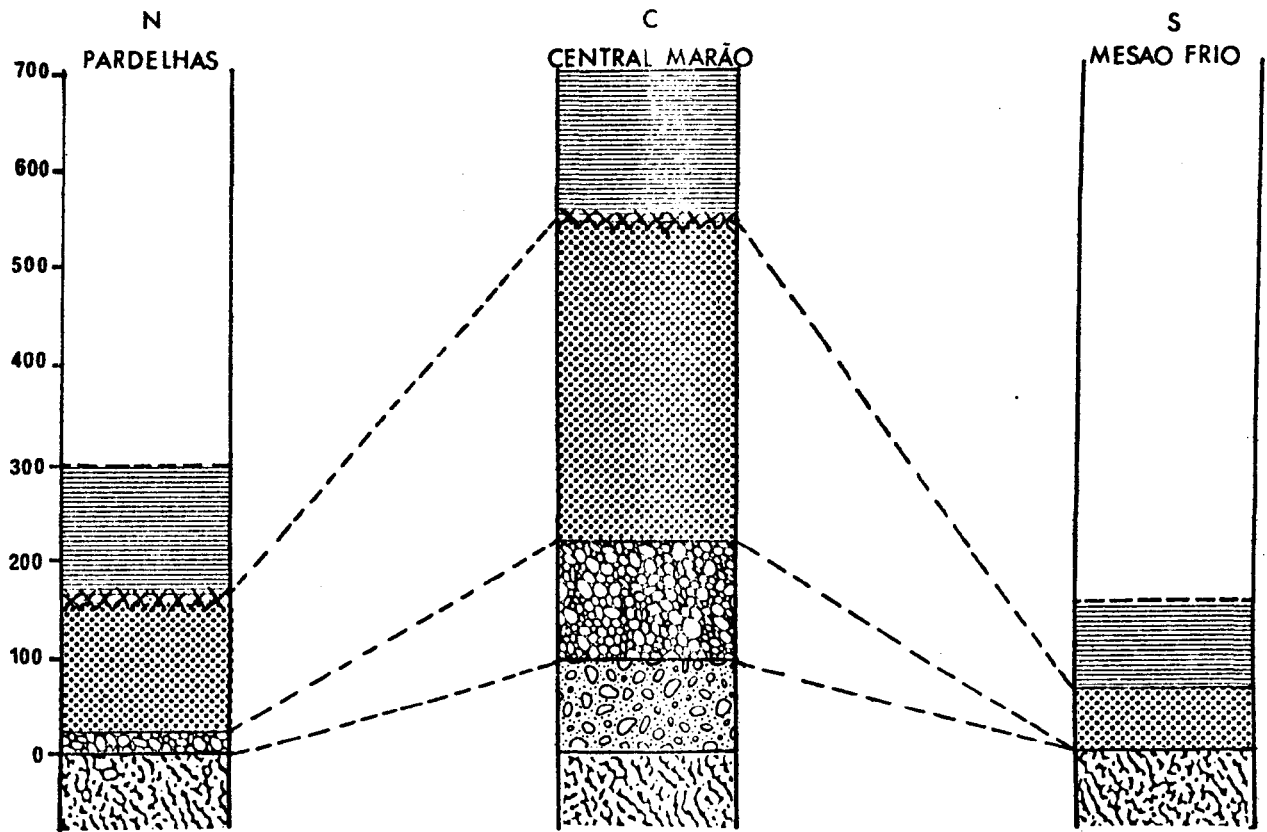


FIG. 5.4

Marão Conglomerate at the base of the Santa Justa Formation

a. Characteristic section of the conglomerate illustrating the variation in size and composition of the pebbles.

Cleavage S_1 sub-vertical.

b. Rare bedding in the conglomerate.

Location : Mine track 1500m north of the summit of Marão.

a



b



of the Armorican Quartzite. This part of the conglomerate is relatively homogenous, unbedded and consists of numerous pebble types, dominantly of psammite, semi-pelite and subordinate vein quartz (Fig. 5.5) which are either matrix or pebble supported. The pebbles are poorly sorted in type and size, with individual boulders reaching up to 50cm diameter. Other exposures of the conglomerate within 2km to the N.W. show that it has been faulted and thrust into slices (Fig. 5.19). The exposed base of this lowest conglomerate is always tectonic. A more detailed description of the Marão Conglomerate is given in section 5.3.5.

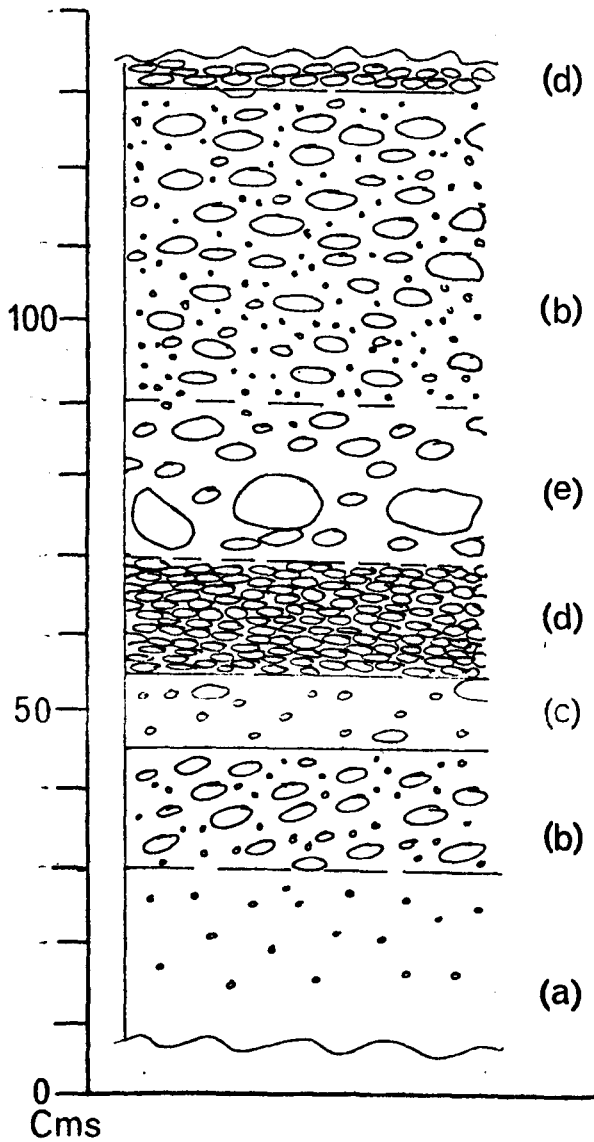
Overlying the conglomerate facies is a sequence of 400m thick ^{of} massive bedded and thin planar cross-bedded grey quartzites and psammites (Fig. 5.6a). These sediments are recrystallised with low grade metamorphic mineral assemblages of quartz, muscovite, chlorite + biotite and opaques. Towards the top of the formation the quartzites pass up into interbedded bioturbated siltstones and mudstones (Fig. 5.6b).

At the top of the Santa Justa Formation and the lowest 5 metres of the Valongo Formation the sediments contain iron silicates (Priem, 1962). The Valongo Formation comprises a monotonous sequence of blue-grey slates of unknown original thickness. In the aureole of a Younger Variscan Granite body to the S.W. of the Serra do Marao the slates contain chiastolite porphyroblasts and

FIG. 5.5

Log of typical section in the conglomerate sequence
above the Marão Conglomerate.

Location: Track to summit of Marão, 100m due west of the
summit of Freitas.



(d) - repeated D unit

bimodal matrix supported
 (b) - pebble sizes @ 5cms and 1cm small rounded quartz 'beads' in the matrix

Quartzite pebbles matrix
 (e) - supported and large vein quartz pebbles up to 10cms

packstone layer of
 (d) - quartzite pebbles - near unimodal

(c) - few pebbles in muddy siltstone

(b) - repeated B unit

(a) - pebble free band

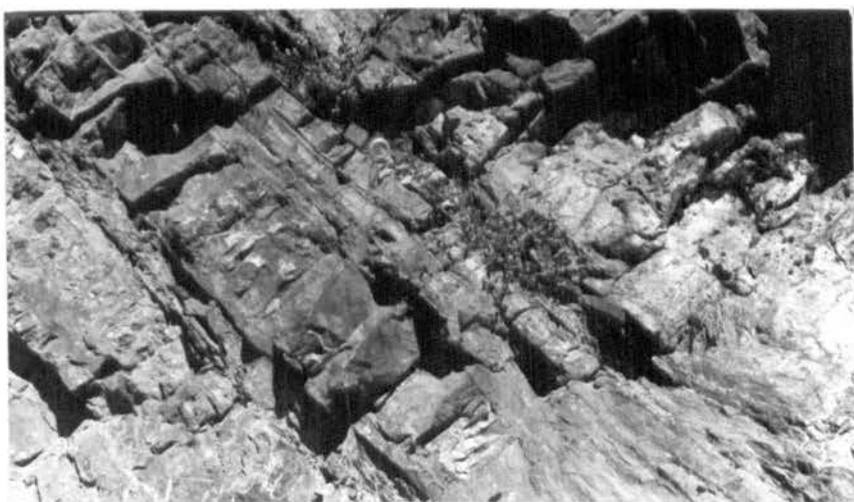
FIG. 5.6

a. Iron-rich bedded quartzites ,Santa Justa Formation.

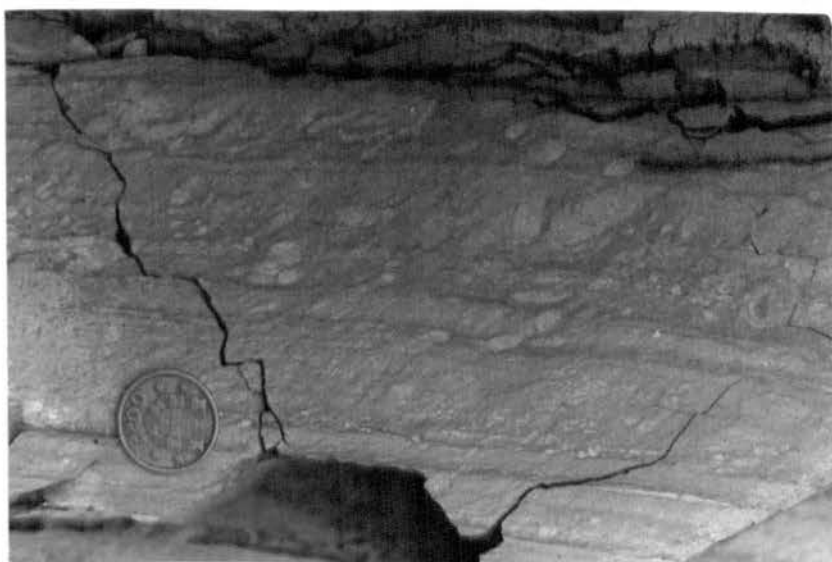
Location: Mine track 1400m north of the summit of Marao.

b. S_1 cleavage in bioturbated mudstones , Santa Justa
Formation.

a



b



sericite pseudomorphing cordierite.

At Mesão Frio the Ordovician succession is much thinner (Fig. 5.3). There is no basal conglomerate, whilst 5m of massive bedded quartzite overlies schist of the Complexo xisto-grauvaquico. Above the quartzite is 20m of thin bedded quartzites, of bed thickness less than 0.5m, with micaceous partings. These pass up into 40m of thinly interbedded siltstones and shales, bioturbated in some horizons, completing the Santa Justa Formation.

Typically the Valongo Formation at Mesão Frio comprises blue-grey slates. No fossils are preserved in the Valongo Formation in this region due to the higher grade of metamorphism in comparison to Valongo and Penacova.

5.3 Structure

1. Major structure of the Marão Syncline

The Marão Syncline is a major first order fold of DV₁ age. The axial trace of the fold is for the most part indefinable, however the overall trend of the well exposed eastern limb is N.N.W. The fold is non-cylindrical but plunges consistently between 0°-20° to 300°.

The syncline is truncated to the north, south and west by syn-, and post-tectonic Older and Younger Variscan Granites, leaving, for the most part, only the eastern

limb exposed (Fig. 5.1). Near Tarouca, 10km south of Lamego a small inlier of the steeply inclined western limb is enclosed in granite, suggesting that the fold is near upright at its southern extremity. At Mesão Frio the eastern limb is sub-vertical, opening northwards in central Marão to an average limb dip of 30° W.S.W., i.e. the dip of the enveloping surface of the second order folds. Further northwards at Pardelhas the limb dip is steeper at 45° W.S.W. It is considered that this change in the profile geometry of the major fold is largely the result of the control of the thick sequence of quartzites and psammities, the Armorican Quartzite, behaving as a competent layer during buckling, i.e. a more open fold with a large wavelength develops in the central area of Marão where the Armorican Quartzite is thickest. This is based on the theory that the dominant wavelength produced by buckling is a function of the layer thickness and the viscosity contrast between the matrix and the imbedded layer (Biot, 1961).

2. Minor Folds

The eastern limb of the syncline is folded by three orders of minor folds of DV_1 age: The wavelengths of these folds are as follows:

Second order folds	0.5 to 2km
Third order folds	25m to 100m
Fourth order folds	less than 5m

Stereographic plots of the poles to folded bedding and S_1 cleavage for the Marão Syncline are presented in Figs. 5.8, 5.9, 5.10. The π poles to bedding and the fold axes of all minor folds plunge shallowly between 0° and 20° to the N.W. between 280 and 310 . (Fig. 5.11a) within the plane of the S_1 cleavage.

The second order folds are steeply inclined, verging to the N.W. The projected enveloping surface, i.e. the limb of the syncline (first order fold) dips 30° S.W. (see section on Fig. 5.1). These folds have rounded to angular hinge zones and sometimes develop as multiple hinge, or box folds (Fig. 5.7a, b).

The third order folds developed on the limbs of second order folds (Fig. 5.7a,b) are asymmetric with their axial planes dipping S.W.

Fourth order folds are developed on the limbs of third order folds and locally verge to the N.E. or S.W. with 'Z' and 'S' profiles (looking N.W.).

The folds vary between gentle and close (Fleuty, 1964) in the central area of Marão but are tight in the Pardelhas area. They are most commonly parallel folds (Class 1b, Ramsay, 1967), maintaining a constant orthogonal thickness around their hinge zones indicating buckling was probably by a flexural slip mechanism.

FIG. 5.7

a. Typical multiple hinge ,second order F_1 fold in bedded quartzites , Santa Justa Formation.

Looking northwest from the summit of Marão.

b. Second order F_1 folds with a vergence to the northeast.

Looking northwest , 2km north of summit of Marão.

a



b



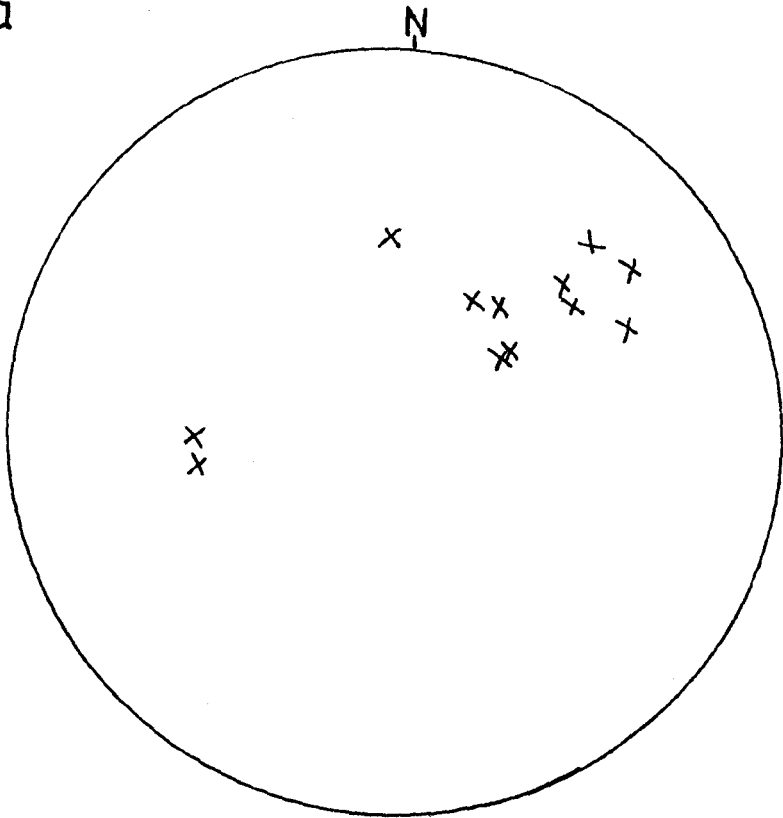
FIG. 5.8

Stereographic plots of structures at Pardelhas, north
Marão.

a. Poles to bedding and plunge F_1 minor fold axes.

b. Poles to S_1 cleavage.

a



b

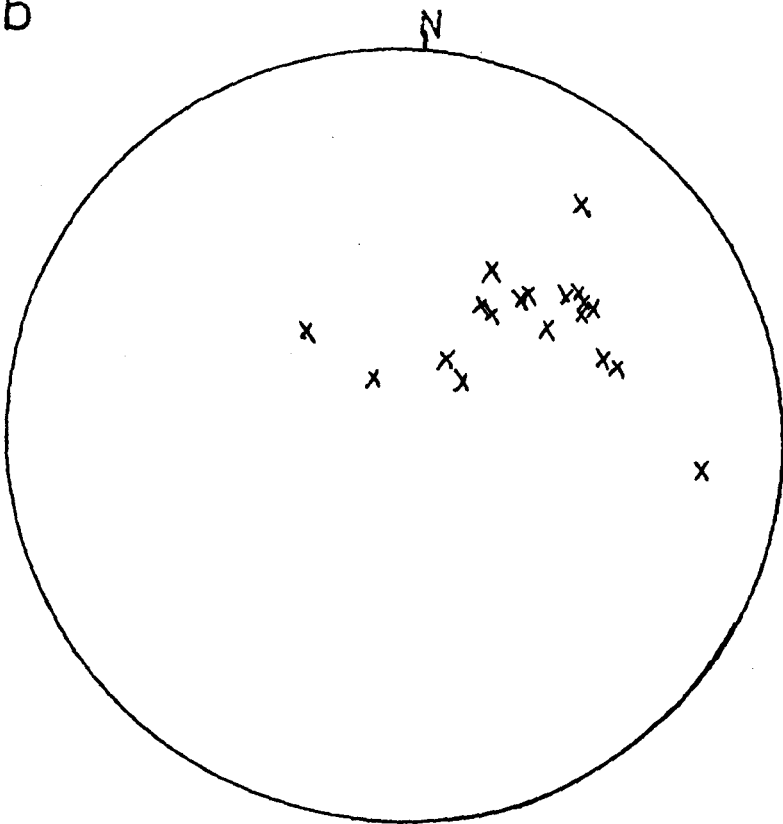


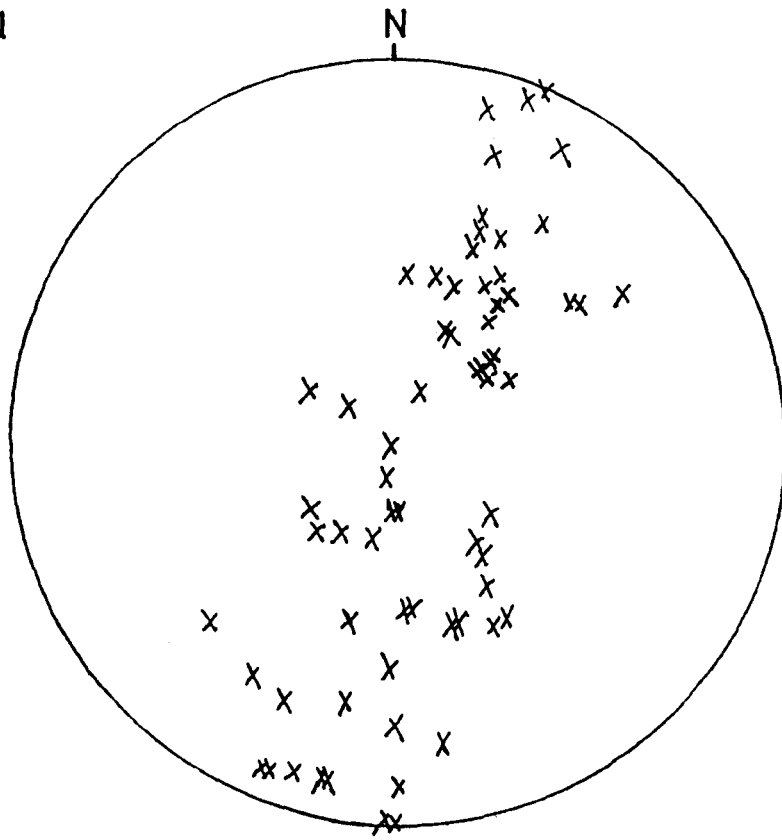
FIG. 5.9

Stereographic plots of structures in Central Marão.

a. Poles to bedding

b. Poles to S_1 cleavage.

a



b

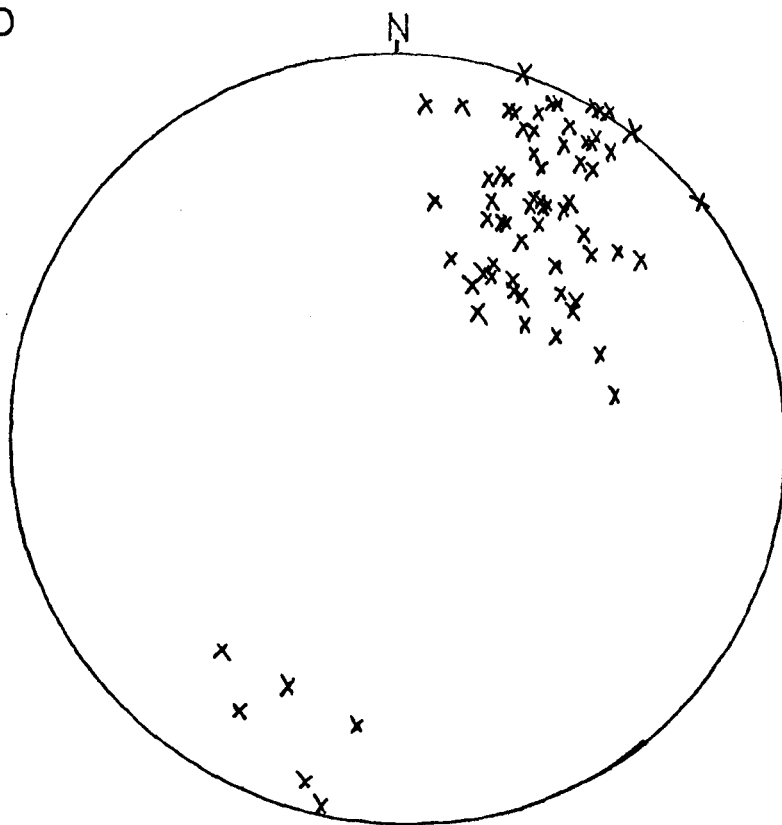


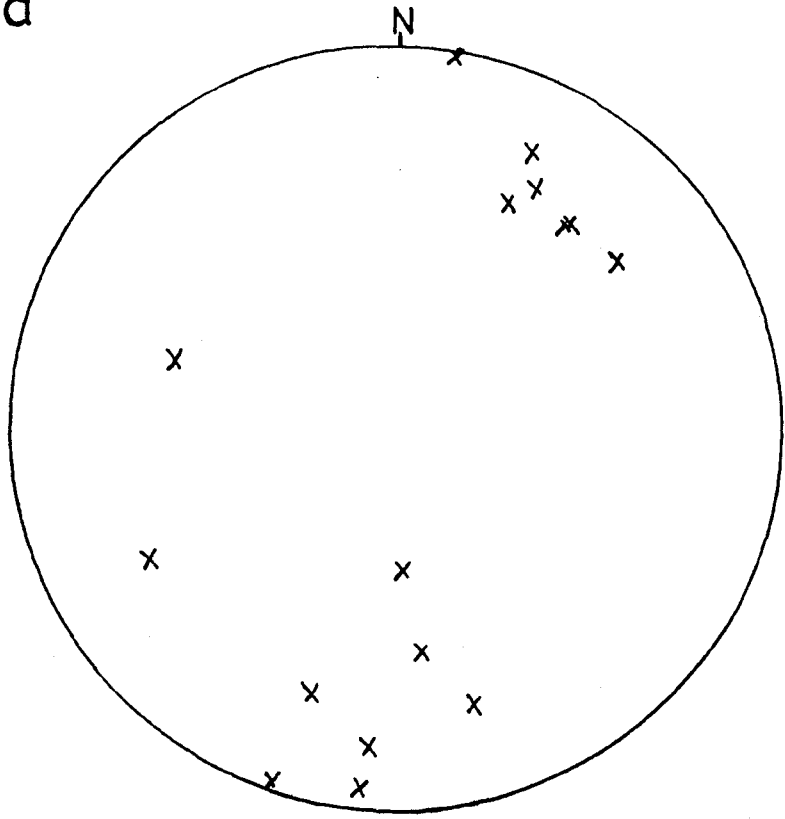
FIG. 5.10

Stereographic plots of structures at Mesão Frio.

a. Poles to bedding

b. Poles to S_1 cleavage.

a



b

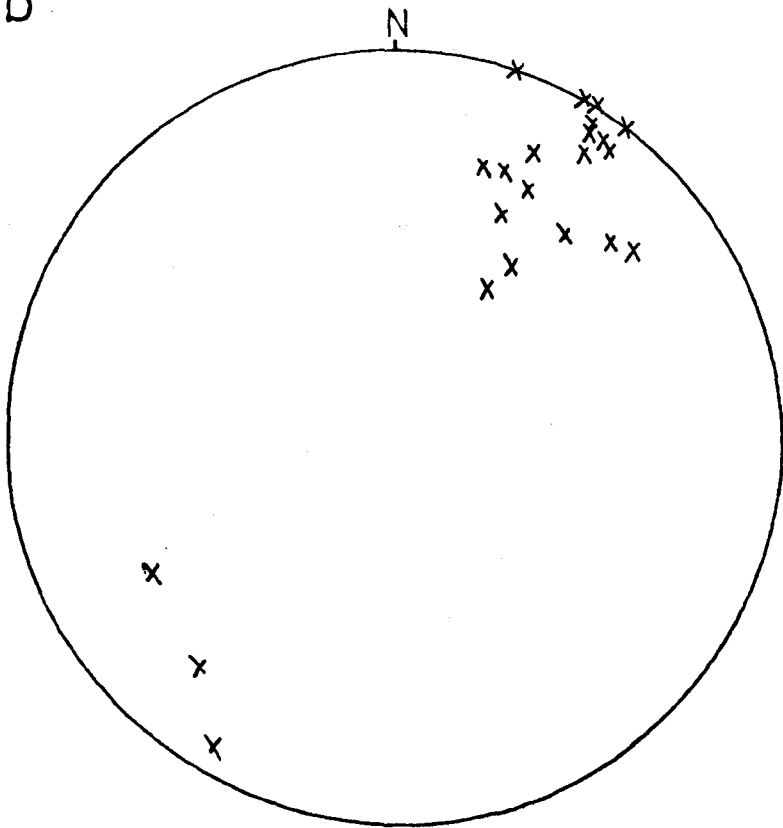


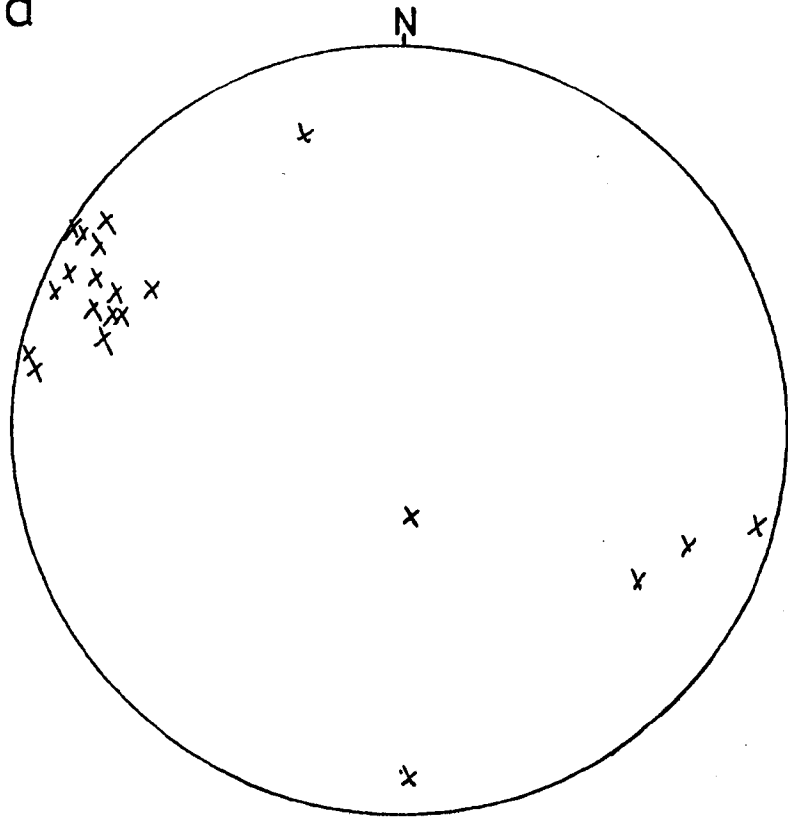
FIG. 5.11

Stereographic plots of structures in Central Marão.

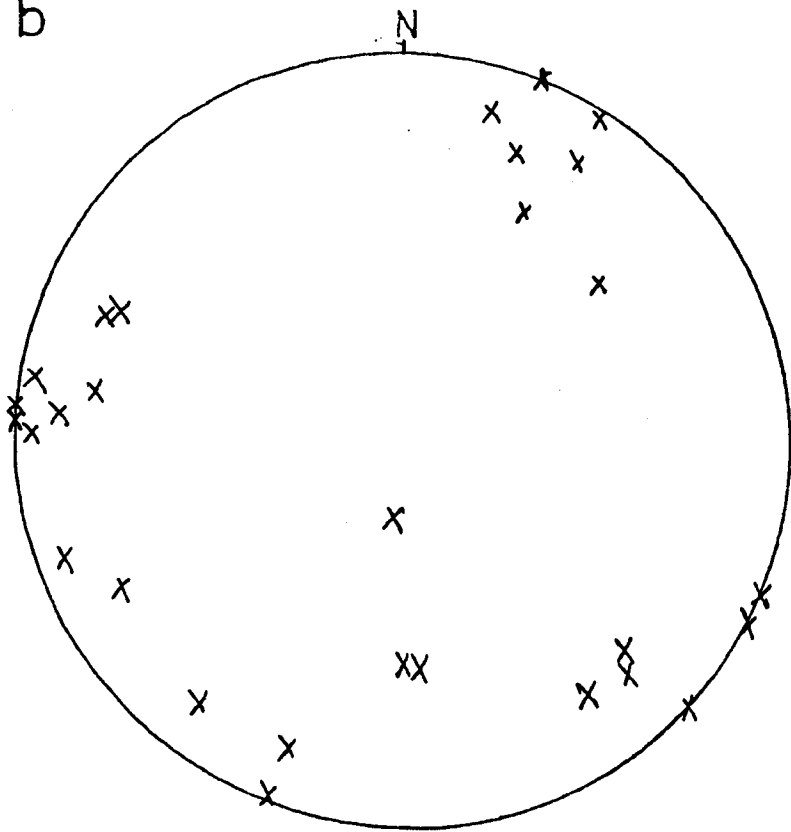
a. Plunge of F_1 minor fold axes •
and elongation direction χ

b. Poles to S_2 cleavage •
and plunge of F_2 microfolds χ

a



b



Cleavage is folded by rare N-S trending F_2 folds of less than 1m wavelength which develop in the slates of the Valongo Formation. These minor folds have a vertical axial planar crenulation cleavage in the hinge region of the open major F_2 syncline between Fragas da Erminda and Seixinhos S.S.E. of Marão summit.

3. Cleavage Development

Two cleavages are developed in this region which are both temporally and geometrically related to the DV_1 folds. The two cleavages are recognised by their morphology and relative age to each other. The earlier cleavage is referred to by the symbol S_1' and the latter S_1 .

The S_1' cleavage

The S_1' cleavage is best developed in the psammites and quartzites of the Santa Justa Formation (i.e. the Armorican Quartzite). It has a constant ESE strike and displays an axial planar convergent cleavage fan around the hinges of second, third and fourth order minor folds (Fig. 5.12a, b).

The morphology of the cleavage is very distinctive where it is developed in the quartz-rich sediments. It is a spaced pressure solution cleavage (Fig. 5.13a) consisting of dark-coloured seams, less than 1mm wide which are zones of dominantly platy minerals including biotite, muscovite, chlorite and sericite, and tourmaline and opaque minerals,

FIG. 5.12

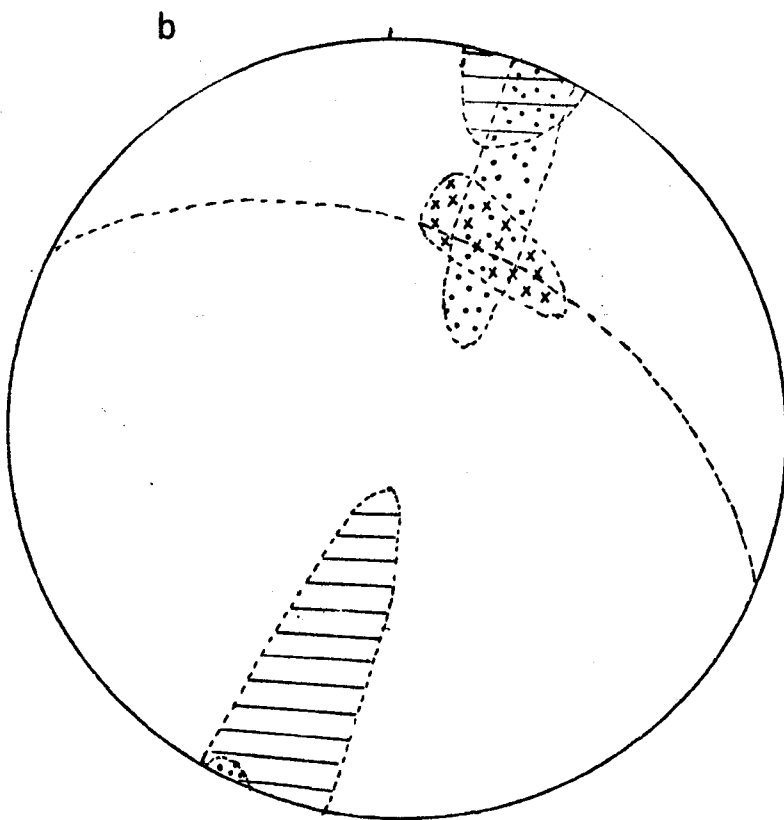
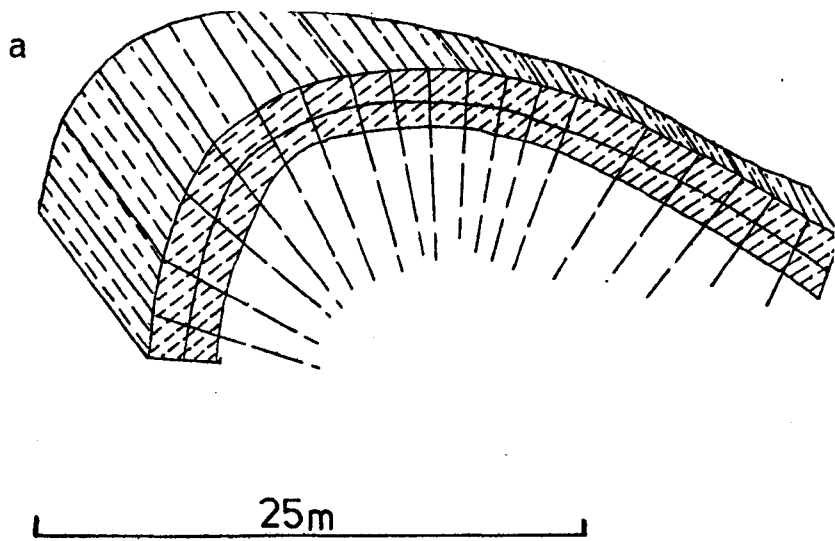
a.

Sketch of third order minor F_1 fold closure reconstructed from field measurements . Illustrates the relationship between bedding and the two cleavages S'_1 and S_1 .

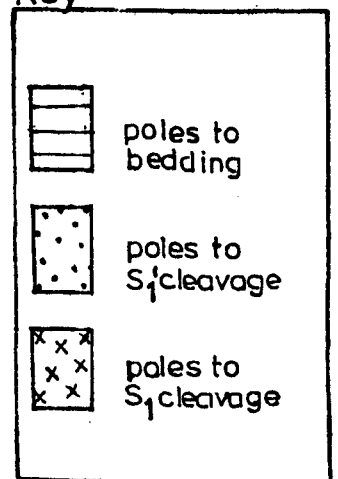
S'_1 solid line ; S_1 dashed line.

b. Stereographic plot of bedding and cleavages S'_1 and S_1 for the fold in a.

Great circle is axial plane.



Key



with subordinate quartz. The quartz is generally much smaller than that found in the matrix, and is in the form of thin elongate grains which together with the platy minerals are aligned with their long dimensions parallel to the plane of the seam (Fig. 5.14a, b).

These seams separate thicker lithons of original host psammite or quartzite (Fig. 5.13a). The psammites are composed of between 60% and 80% quartz with subordinate amounts of the above listed platy minerals, tourmaline and opaque minerals all of which are evenly disseminated throughout the lithons.

The spacing of the seams increases with increasing quartz content and ranges between 0.1cm and 1cm (Fig. 5.13a and 5.16b). Also the seams commonly anastomose or are en-échelon in two dimensions (Fig. 5.13a).

The mechanism by which the S_1' cleavage developed is largely pressure solution (Elliot, 1973; Beach, 1974) involving the whole or partial dissolution of quartz grains during compression and the transfer of this dissolved quartz along selected planes or seams. The composition of the seam and lithon material are compared in two specimens (Fig. 5.13b). Clearly the composition of the seams reflect a depletion in quartz and an increase in less soluble minerals with respect to the psammitic material in the lithons. For each specimen the volume ratio of seam to lithon material was calculated and addition of

FIG. 5.13

a. S_1^1 spaced pressure solution cleavage in impure quartzites.

Central Marão

b. Histogram comparing the compositions of the S_1^1 pressure solution seams with the lithon.

a



b

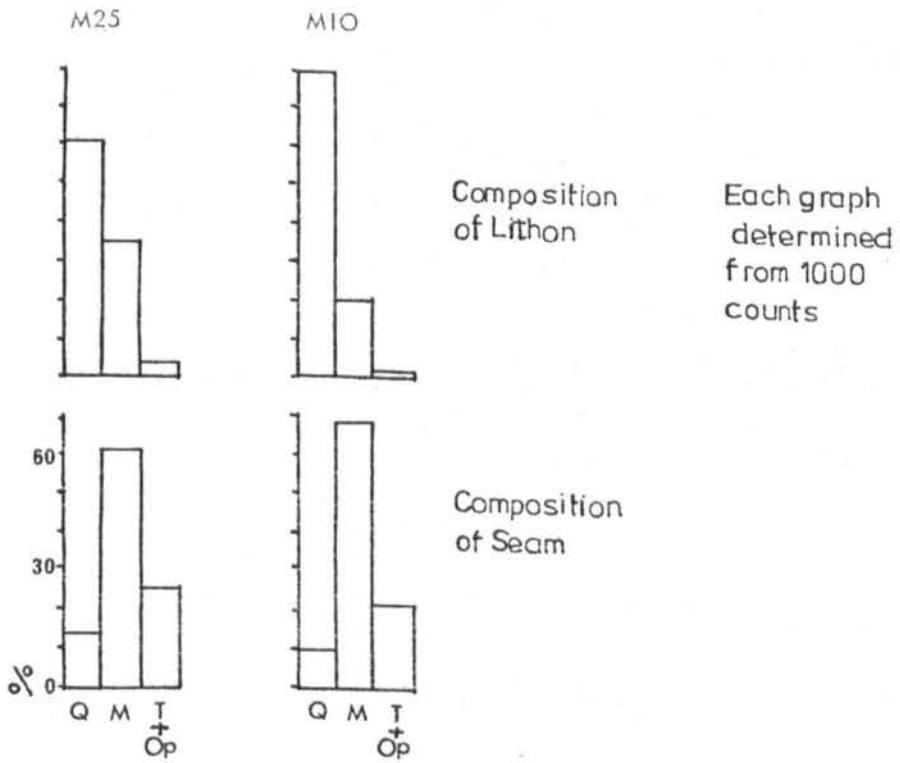


FIG. 5.14

a. S_1' pressure solution seams ,NW-SE, oblique to S_1 grain alignment cleavage , approximately E-W.

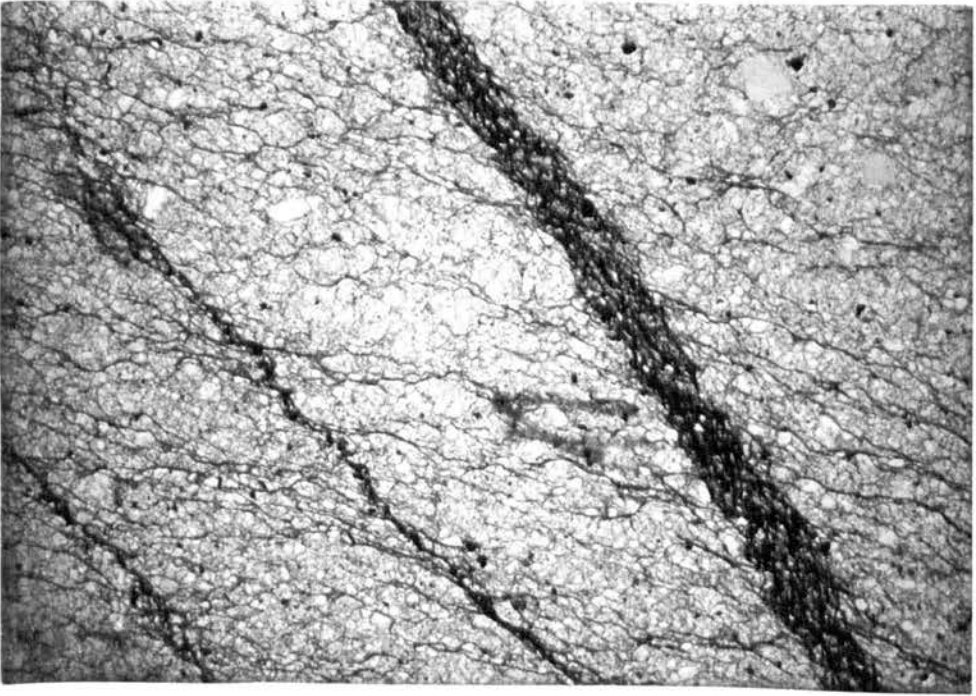
Specimen no. M25 X50 †

Central Marão.

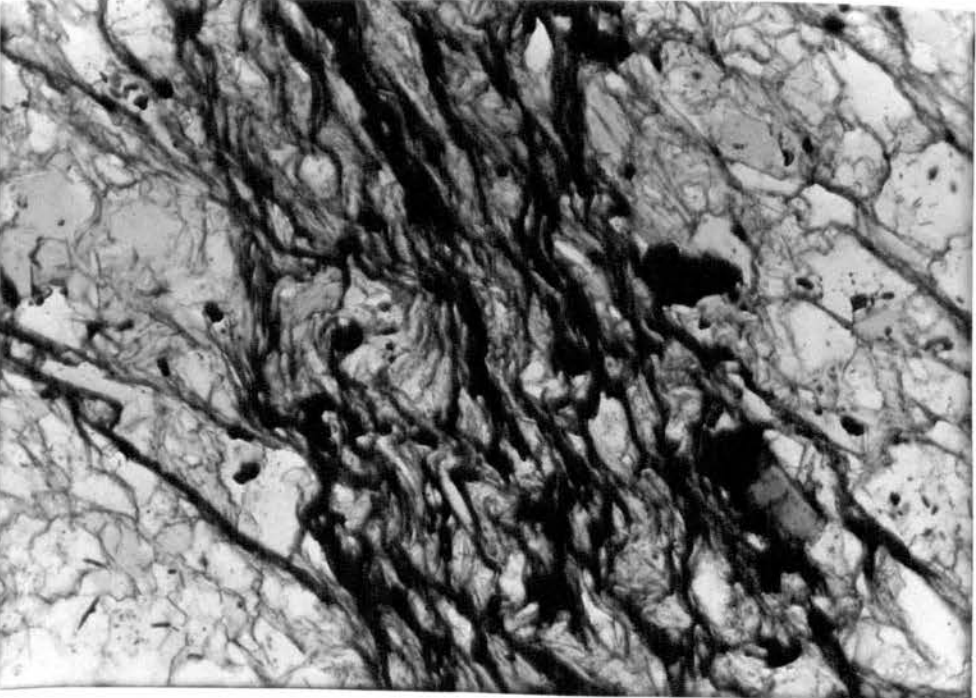
b. Detail of S_1' pressure solution seam , approximately N-S, . Muscovite and chlorite parallel to the seam boundary are crenulated by S_1 , NW-SE.

Specimen M25 X80 †

a



b



seam widths. This combined with the calculated loss of volume of quartz from the seam by comparing the quartz contents of seam and lithons for each specimen produced figures of 7.7% (M10) and 9.8% (M25) shortening along a layer. This calculation assumes that the quartz in solution has migrated out of the system, in this case a single bed.

During deformation quartz in solution will diffuse, probably via grain boundaries, towards areas of least stress and can redeposit itself in voids, such as synformational vein cavities (Beach, 1974) or as overgrowths in local pressure shadow areas around grains. However, it is difficult to detect whether the change in shape of the quartz grains in the lithons is a result of additional quartz which had diffused from neighbouring seams.

The pelitic sediments of the Complejo xistograuvaquico and Ordovician have developed only one cleavage S_1 , a pervasive grain alignment cleavage. This cleavage is considered to have initiated at the same time as S'_1 in the psammitic sediments, and continued to develop throughout DV_1 .

The S_1 cleavage

The S_1 cleavage has a consistent ESE strike, parallel to S'_1 and such that the intersection of bedding, S'_1 and S_1 is a line parallel to the plunge of the minor fold axes

FIG. 5.15

a. S_1' pressure solution seams parallel to S_1 grain alignment cleavage.

X60 †

Central Marão

b. Chiastolite porphyroblasts and S_2 crenulation cleavage.

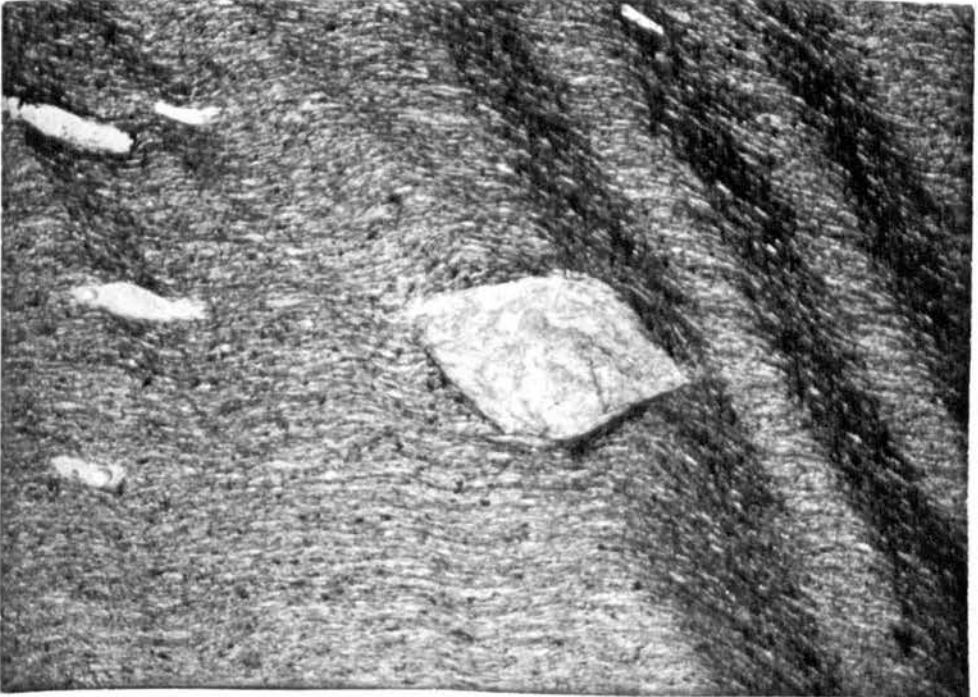
X50 †

Valongo Formation , Central Marão.

a



b



(Fig. 5.12a). The S_1 cleavage dips between 50° and 89° to the southwest (Figs. 5.8b, 5.9b, 5.10b). Tight minor folds, particularly those at Pardelhas, have an almost axial planar S_1 cleavage but more commonly this cleavage lies oblique to axial planes (Fig. 5.12a).

In detail the S_1 is a pervasive cleavage with a strong planar mineral and shape fabric and occasionally with a linear element which is parallel to the plunge of the DV_1 fold axes (Figs. 5.16a, 5.14a, b). There is an incipient development^{of} dark pressure solution seams parallel to the S_1 grain alignment (Fig. 5.14a). However, pressure solution is not as an important mechanism in the formation of S_1 . In the psammitic rocks S_1 results largely from plastic deformation with the development of intra-grain deformation bands (see chapter 8).

The S_1 shape fabric occurs on all scales from flattened boulders in the basal Ordovician conglomerate to single quartz crystals in the quartzites.

In psammitic rocks where the S_1 cleavage is oblique to S_1' , the grain alignment fabric clearly crenulates the S_1' mineral alignment in the seams (Fig. 5.14b). The implications of establishing the later age of development of the S_1 cleavage are discussed later in this chapter under 5.3.4.

FIG. 5.16

a. Hand specimen quartzite with $S_1^!$ pressure solution cleavage, E-W, oblique to strong shape fabric, S_1 cleavage, NW-SE.

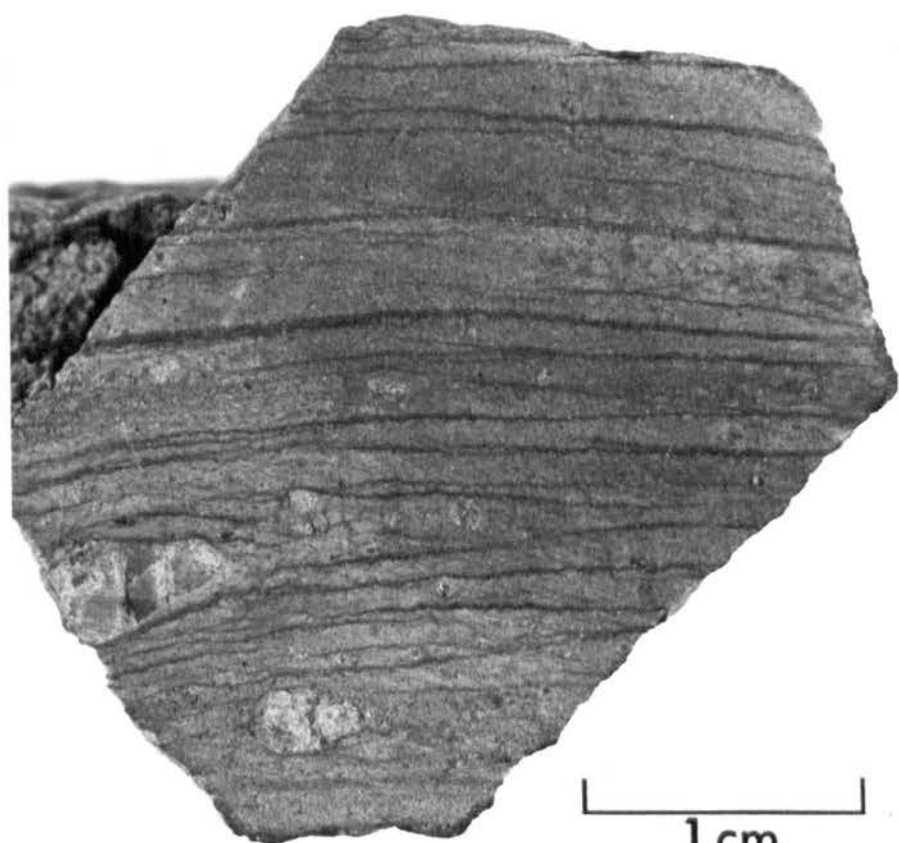
Central Marão.

b. Polished section of quartzite showing $S_1^!$ pressure solution cleavage parallel to S_1 .

a



b



The S₂ crenulation cleavage

A crenulation cleavage S₂ is developed axial planar to rare F₂ minor folds which fold the S₁ cleavage. The S₂ is only locally developed, mainly in the slates of the Valongo Formation. In thin section the crenulations post-date the growth of chiasmolite (Fig. 5.15b) in the thermal aureole of a Younger Variscan Granite. This suggests the age of the open second folding and S₂ crenulation cleavage in the Serra do Marão is as late as Permian.

4. Evolution of the D₁ structures

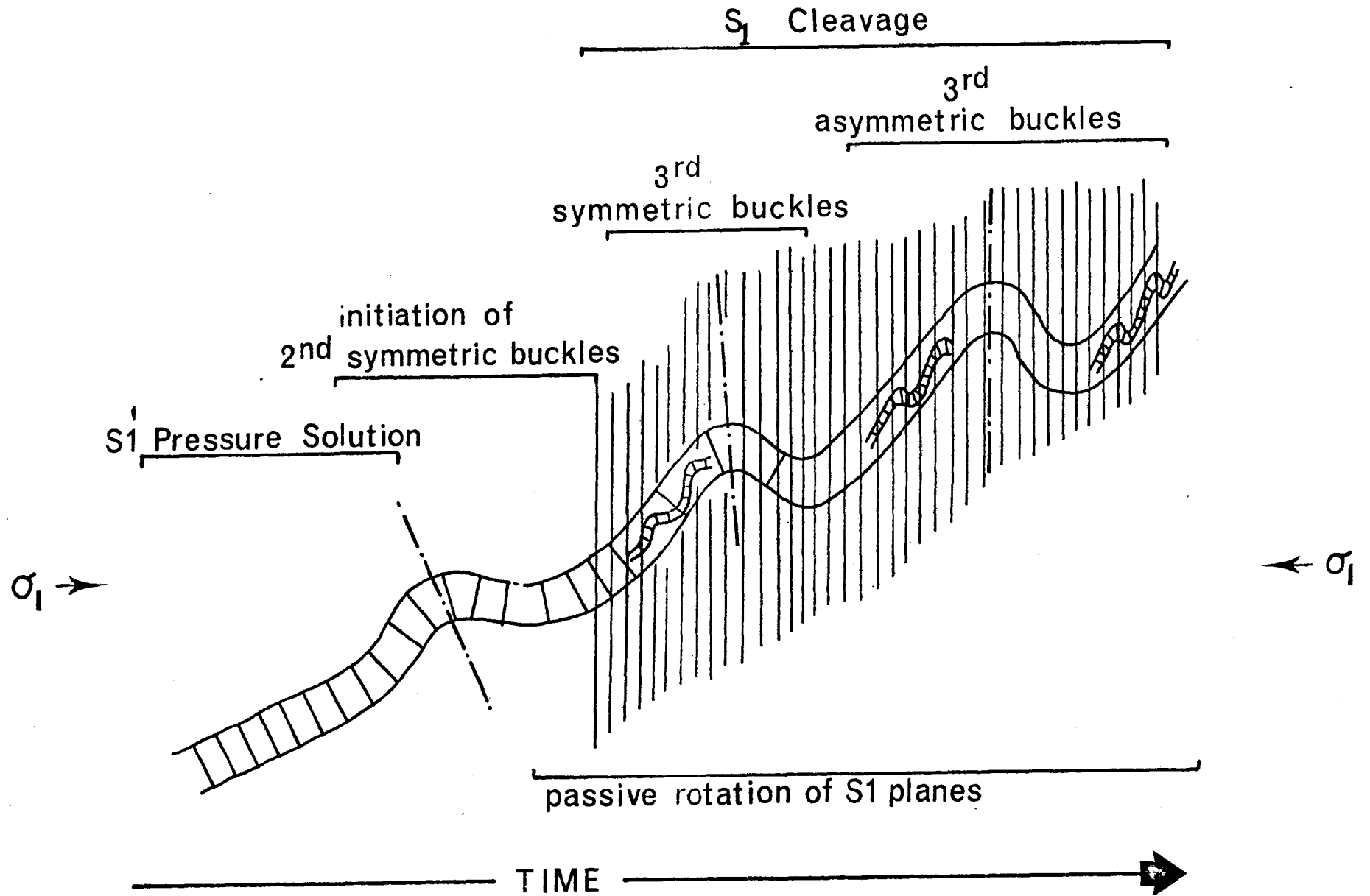
The following is an explanation of the development of the fold and cleavage relationships described in the last section. A summary of the evolution with time is schematically represented in Fig. 5.17.

The S₁ⁱ cleavage was initiated very early in the fold history, possibly before the onset of buckling, resulting from layer parallel compression. The S₁ⁱ planar seams initiated, and remained active sites for pressure solution during the early development of all the orders of minor folds; but they have rotated during buckling which produced a convergent fanning geometry in the hinge zones of minor folds.

There was a change in physical conditions during the development of the buckles which gave rise to a change in deformation mechanism with respect to cleavage development;

FIG. 5.17

Schematic representation of the development of F_1 folds ,
 S'_1 cleavage and S_1 cleavage with time.



i.e. the initiation of plastic deformation of grains and cessation of pressure solution. The change from the one cleavage type to the other is possibly due to an increase in the strain rate or increased depth of burial.

As stated earlier, wavelength of the folds comprising the Marão Syncline is governed largely by the thickness of the layers being buckled, from the generally accepted buckling theories, such that the Armorican Quartzite has behaved as a competent multilayered slab between the less competent pelitic sediments of the Valongo Formation and Complexo xisto-grauvaquico. The total thickness of the slab relates to the first order fold with descending thickness of layers, comprising compound to single bedded units, relating to the other orders of folds.

It is suggested that the minor folds on the eastern limb of the syncline developed sequentially due to buckles locking up at particular critical interlimb angles (Price, 1967) i.e. sequentially in descending order of wavelength.

The main compression direction during folding is, from the cleavage orientation over the area, sub-horizontal to slightly inclined. Minor folds initiating on the limb of the syncline were therefore in beds inclined to the maximum compressive stress direction e.g. second order folds on the inclined limb of the first order syncline after it began to lock up.

From theoretical work by Treagus (1973) buckles developing in layers inclined to the maximum principal stress have initially symmetrical profiles. The effective compressive stress for this condition is approximately parallel to the layer boundary in a system with a moderate viscosity ratio (Treagus, op.cit) (Fig. 5.18b, c). Price (1967) suggested that it is the resolved shear stress acting parallel to the layer boundary that determines the geometry of the resulting buckle (Fig. 5.18a) i.e. a symmetric buckle. Symmetric buckles of small wavelengths (4th order) are common, as would be expected if they are the last to develop on the inclined limbs of second and third order folds. The S_1 cleavage is non-axial planar in these folds.

As all orders of buckles develop they become progressively more asymmetric and overturned to the NE such that their axial planes rotate towards the plane of the S_1 cleavage. The folds at Pardelhas show the most advanced development being strongly asymmetric with a near axial planar S_1 cleavage.

Two cleavages which are also related to one episode of folding, and with similar morphologies to S'_1 and S_1 are developed in Upper Dalradian sandstones and slates of the Birn am district, Scotland (Harris et. al. 1976). These cleavages are considered by the authors to be broadly coeval, with the grain alignment cleavage passing into the spaced cleavage, but unlike in the M̄rao Syncline it does

FIG. 5.18

a. Shear stress τ acting parallel to layer from oblique maximum compression σ' .

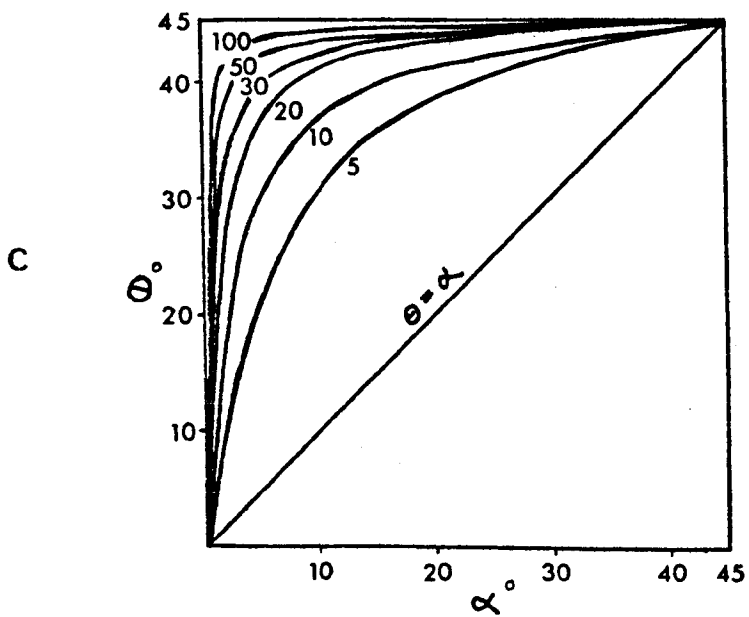
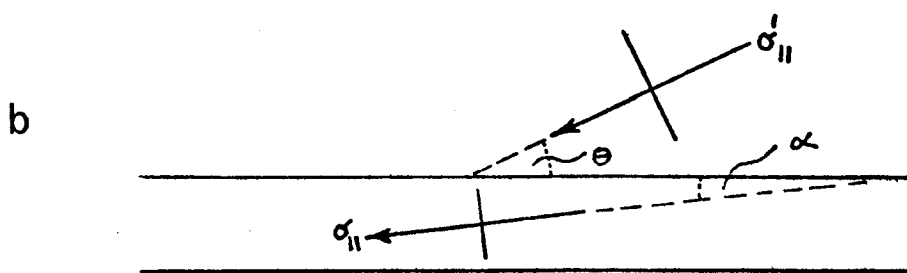
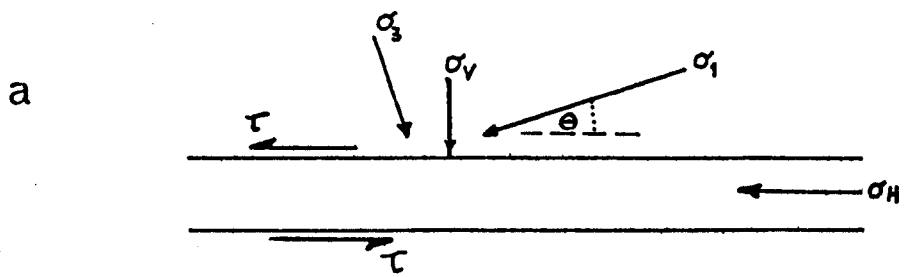
After Price, 1970.

b. Principal compressive stress, σ_{11} , is approximately parallel to the layer i.e. α very small, for oblique principal stress, at angle Θ to layer, in a system with a moderate viscosity ratio.

After Treagus, 1973

c. Graph of angle α for changing angles of Θ for case b. above for different viscosity ratios (numbers). For systems of moderate viscosity ratio (> 50) the principal stresses in the layer are approximately parallel to the layer boundary.

After Treagus, 1973.



not crenulate it.

5. Pebble deformation and cleavage development in the Marão Conglomerate

At the base of the Ordovician conglomerate facies 1km north of the summit of Marão outcrops a restricted deposit of homogeneous unbedded conglomerate approximately 100m thick. The conglomerate resembles deposits which have been described as ancient mudflows (Schermerhorn et. al. 1963), having an original muddy matrix with a range of chaotic unsorted clasts. The deposit extends for only 2km and thins both north and south of the main section traversed by a mine track (Fig 5.1). The original geometry of the deposit is distorted by the main folding, thrusting and faulting, hence it is difficult to reconstruct.

The matrix of the conglomerate is pelitic to semi-pelitic, consisting of quartz, muscovite, chlorite, biotite and opaque minerals. The quartz content is less than 20%.

The conglomerate is deformed, developing a compound S_1' and S_1 cleavage such that the pressure solution seams are parallel to the strong grain alignment fabric in the lithons (Fig. 5.20b). The spacing of the seams varies from 0.1 to 1cm (Fig 5.20a).

The clasts of pebble to boulder size are flattened

FIG. 5.19

Map showing the extent of the Marão Conglomerate.

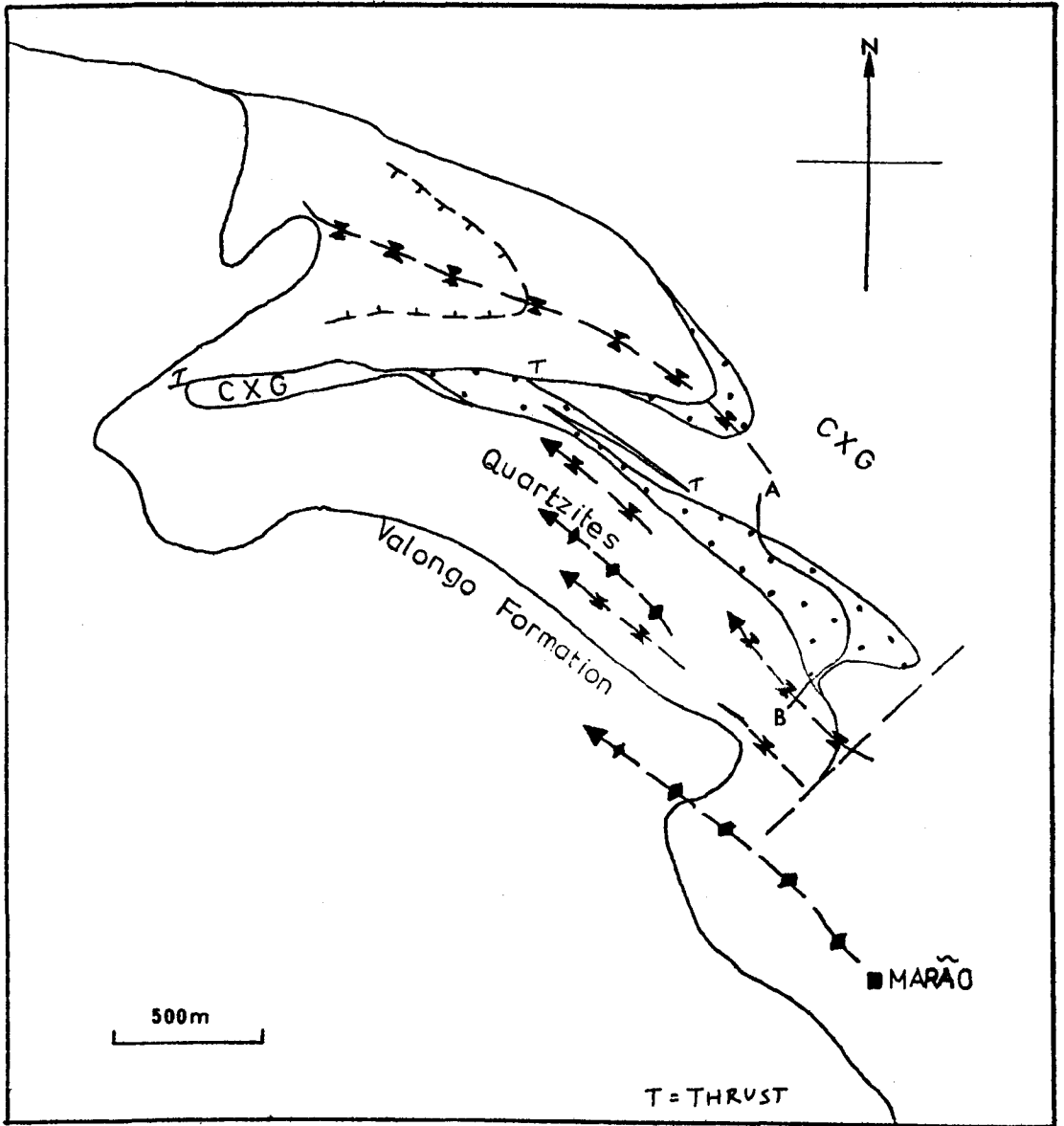


FIG. 5.20

a. Polished section of Marão Conglomerate cut parallel to XZ.

b. S'_1 and S_1 cleavages parallel in the conglomerate.

a



b



and stretched in the plane of the compound cleavage with their long axes plunging between 10° and 12° to 300° parallel to the plunge of the minor DV_1 fold axes. The mean strain ellipsoid calculated from measurements of deformed pebbles on surfaces cut parallel to the planes containing two principal axes, is 2.65 : 1.00 : 0.5 for X : Y : Z. The deformation of the matrix was calculated by measuring the spacing and orientation of the pebble centres following the method outlined by Ramsay (1967, pp 195-197) for pressure solution (Fig. 5.21). Adopting the method to calculate the strain in conglomerates one must assume that the pebbles were originally randomly distributed. The strain obtained is a minimum strain for the matrix of 3.9 : 1.0 for X : Z which is less than the strain obtained from the deformed pebbles. The low strain may be explained by effects associated with pebbles in contact with one another.

Cleavage development in the pebbles

A spaced pressure solution cleavage S'_1 is developed within deformed psammitic pebbles and boulders in the conglomerate (Fig. 5.22a, b). The seams pass into the pebbles where they are refracted or pass straight through. The pebbles also possess an internal planar mineral fabric (i.e. S_1) which is parallel to the plane of flattening (Fig. 5.23b). Competent vein quartz pebbles deflect both cleavages around their surfaces (Fig. 5.22c). The sense of

and stretched in the plane of the compound cleavage with their long axes plunging between 10° and 12° to 300° parallel to the plunge of the minor DV_1 fold axes. The mean strain ellipsoid calculated from measurements of deformed pebbles on surfaces cut parallel to the planes containing two principal axes, is 2.65 : 1.00 : 0.5 for X : Y : Z. The deformation of the matrix was calculated by measuring the spacing and orientation of the pebble centres following the method outlined by Ramsay (1967, pp 195-197) for pressure solution (Fig. 5.21). Adopting the method to calculate the strain in conglomerates one must assume that the pebbles were originally randomly distributed. The strain obtained is a minimum strain for the matrix of 3.9 : 1.0 for X : Z which is less than the strain obtained from the deformed pebbles. The low strain may be explained by effects associated with pebbles in contact with one another.

Cleavage development in the pebbles

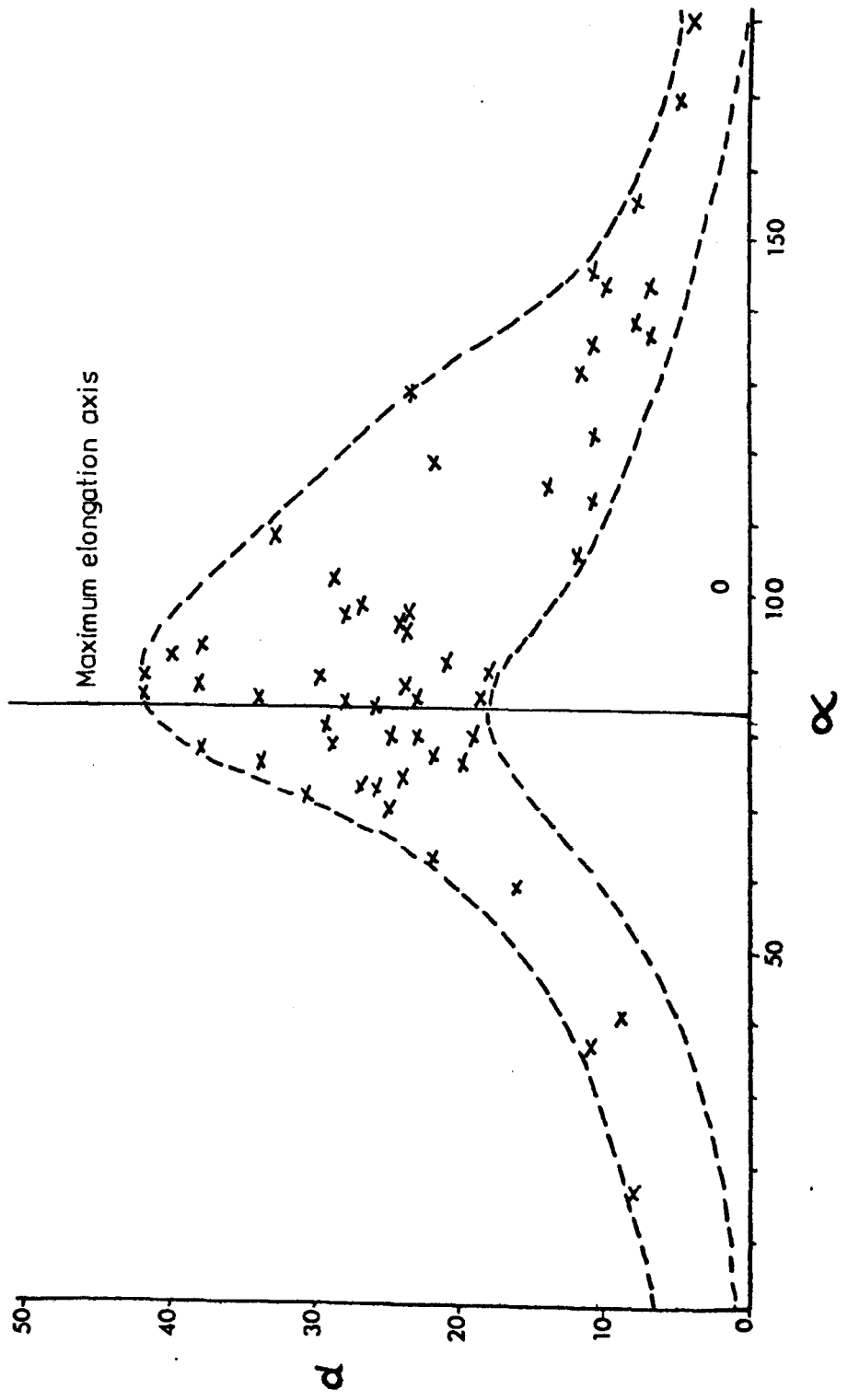
A spaced pressure solution cleavage S'_1 is developed within deformed psammitic pebbles and boulders in the conglomerate (Fig. 5.22a, b). The seams pass into the pebbles where they are refracted or pass straight through. The pebbles also possess an internal planar mineral fabric (i.e. S_1) which is parallel to the plane of flattening (Fig. 5.23b). Competent vein quartz pebbles deflect both cleavages around their surfaces (Fig. 5.22c). The sense of

FIG.5.21

Estimate of 2D strain in conglomerate matrix by
centre to centre method (Ramsay, 1967, p195)

d = distance between pebble centres

α = angle between the line joining the centres of
neighbouring pebbles and datum.



refraction of the cleavage seams through psammitic pebbles is biased towards clockwise, but in many cases the cleavage passes straight through (Fig. 5.23a). Some pebbles appear pulled apart along the plane of the refracted cleavage seams (Fig. 5.24a).

The pebbles, aligned and internally deformed, must have behaved as semi-rigid (psammitic) and rigid (vein quartz) bodies within the less competent matrix (pelitic) during the formation of the compound cleavage. The occurrence of refracted and non-refracted cleavage seams in the pebbles indicates the conglomerate deformation may have followed one of two possible courses.

The less favoured interpretation is that pressure solution cleavage seams developed within the pebbles which were subsequently rotated in a rigid manner and then flattened, whilst the seams remained active sites of pressure solution. The result after 30% shortening from pure shear deformation for pebbles originally at various orientations is shown in Fig. 5.25. Alternatively during the early stages of deformation the pebbles may have deformed internally.

Pure shear experiments with semi-rigid bodies (representing psammitic pebbles) showed that in a less competent

matrix they deform internally by pure shear only in the exceptional case when originally aligned in the plane of flattening, otherwise in other orientations they deform by simple shear due to a shear couple set up during

FIG. 5.22

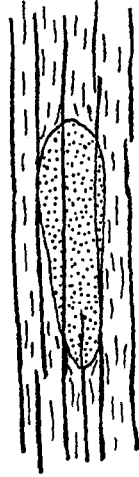
Relationship between S'_1 and S_1 cleavages and pebbles in the Marão Conglomerate.

a. Cleavage seams S'_1 extend undeflected through psammitic pebbles.

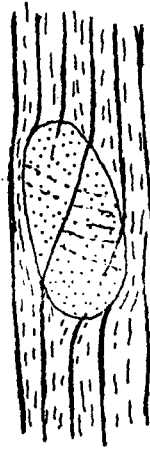
b. Cleavage seams S'_1 are refracted through psammitic pebbles.

c. Cleavages S'_1 and S_1 are deflected around vein quartz pebbles.

a



b



c

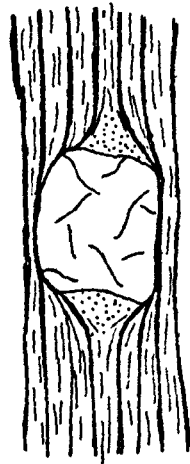


FIG. 5.23

a. Histogram to show the percentage of the S_1' cleavage orientations in psammitic pebbles.

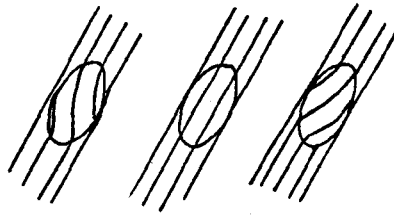
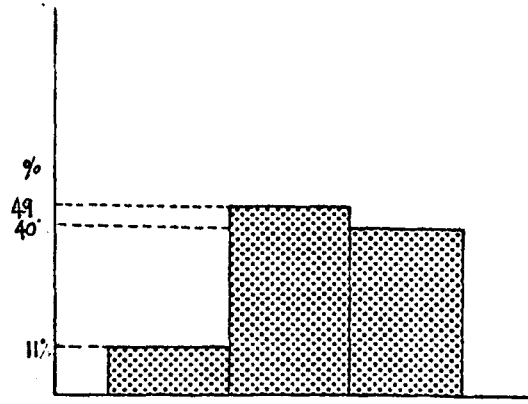
100 pebbles noted

b. Drawing from thin section of cleavage seams S_1' refracting through a psammitic pebble (shaded).

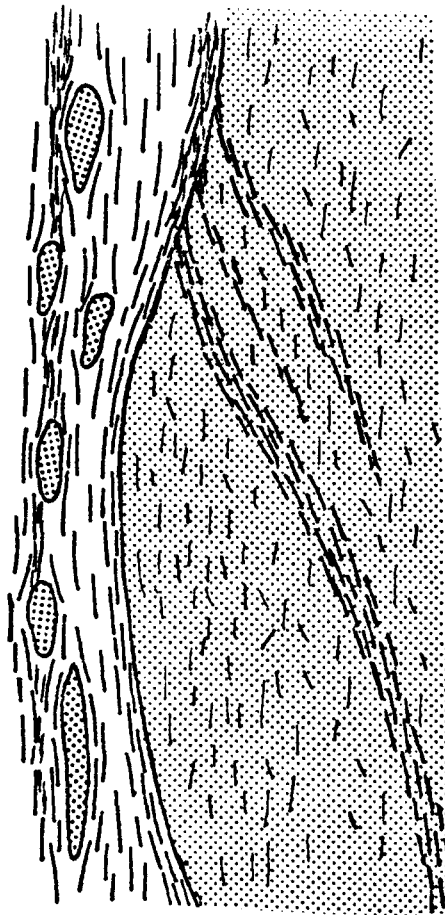
S_1 alignment of micas in pebble is parallel to the XY plane of the pebble and the S_1 cleavage in the matrix

Specimen no. M214b X20.

a



b



their rotation (Fig. 5.26) towards the plane of flattening. The amount of deformation depends upon their shape, orientation, viscosity contrast and amount of deformation. Investigations into deformation and rotation of bodies have been carried out by O'Driscoll (1964). Applying this to the pebbles, the developed cleavage is parallel to X, Y, plane of the strain ellipsoid within the pebbles which refracts in a direction and amount depending upon the orientation of the pebble. Pebbles will continue to rotate towards the flattening plane in the matrix so that eventually most are aligned in that plane.

However, sigmoidally-shaped pebbles and the bias for clockwise refraction of cleavage through pebbles indicates that the deformation had a clockwise simple shear component. The sigmoidal pebbles develop by the migration and deposition of quartz in the local pressure shadow areas at the ends of the pebbles during rotation (compare Figs. 5.24b and 5.27).

It is concluded that : (a) the deformation in the conglomerate is a combination of pure and simple shear and (b) the cleavage seams in the psammitic pebbles indicate that they behaved as semi-rigid bodies during the deformation.

5.4 Summary

The fold structures comprising the Marão Syncline are largely the result of buckling of a competent, multilayered

FIG. 5.24

a. Pebble separated by semi-pelitic matrix in the Marão Conglomerate.

b. Sigmoidal-shaped quartzite pebble in Marão Conglomerate.

S_1 cleavage is approximately N-S.

a



b

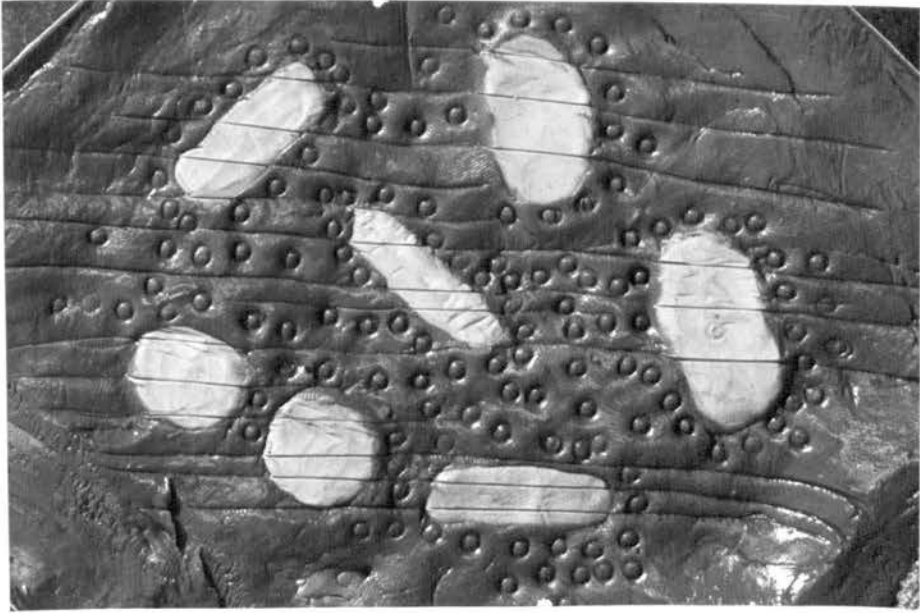


FIG. 5.25

Experimental pure shear deformation of semi-rigid inclusions (representing pebbles) in a less viscous matrix.

n.b. the cleavage trace and the amount of rotation of the pebbles.

1. UNDEFORMED



2. 30% SHORTENING

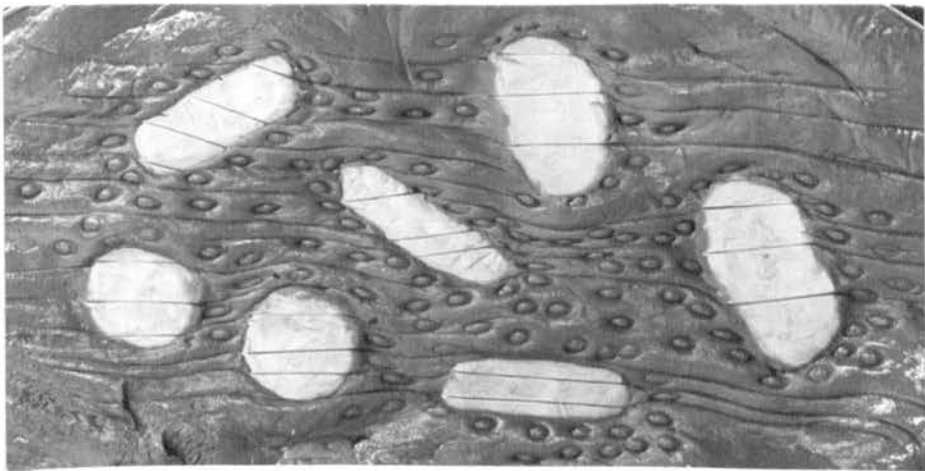


FIG. 5.26

Diagram drawn from experiments of pure shear deformation of semi-rigid inclusions in a less viscous matrix.

n.b. the direction of rotation is governed by their original orientation.

n.b. the orientation of the strain ellipse within the inclusions and that the strain is lower than in the matrix.

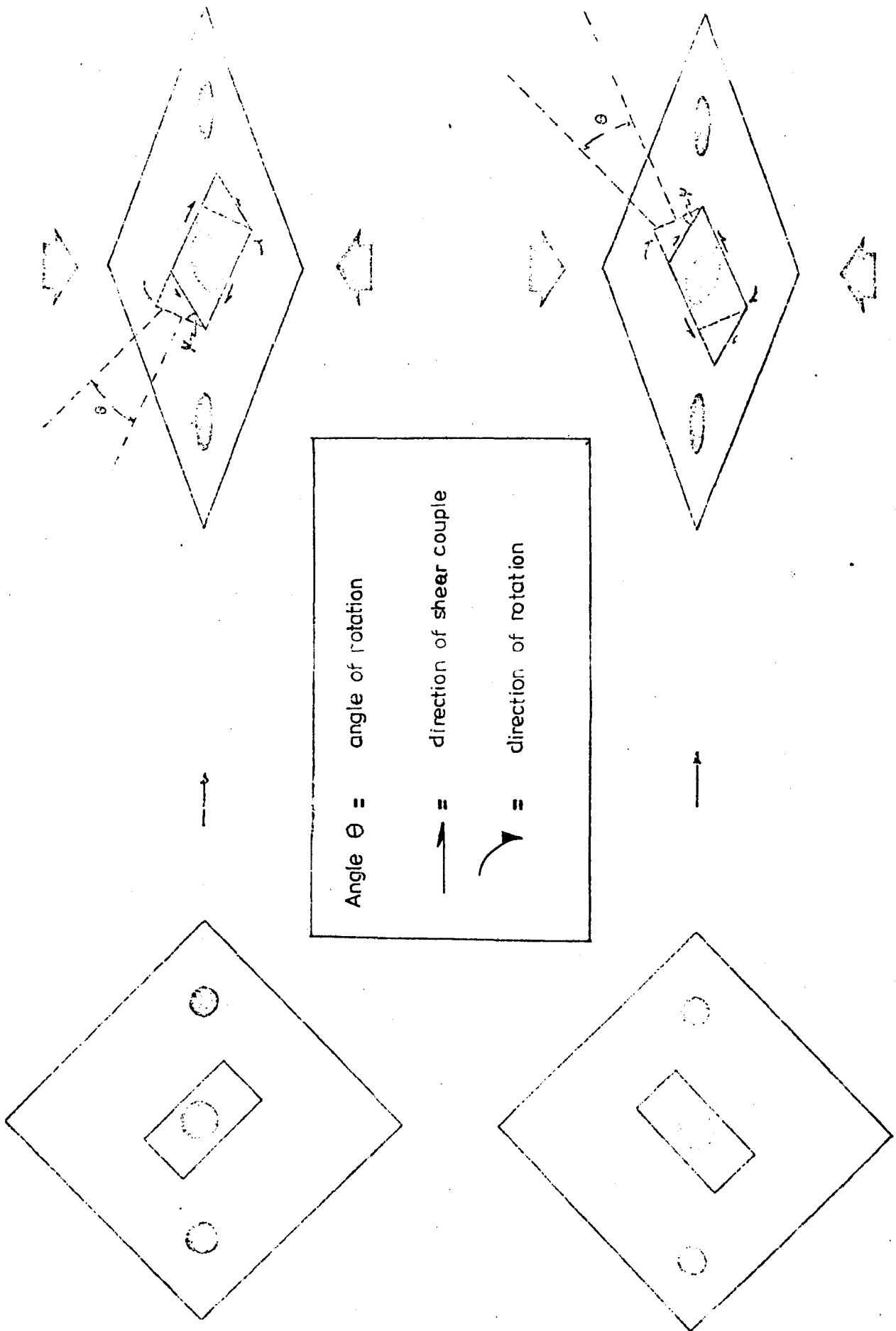
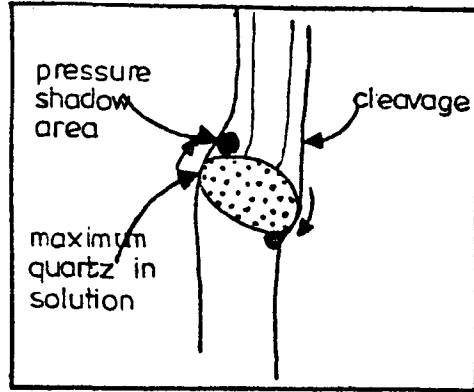


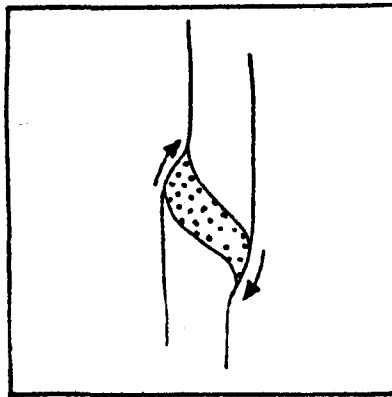
FIG. 5.27

Model for the development from a to c of quartz tails in quartzite and psammitic pebbles during their rotation by deformation.

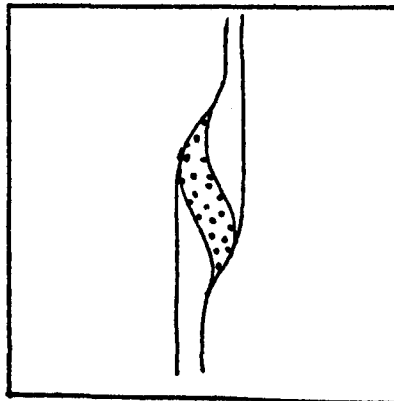
a



b



c



slab, the Armorican Quartzite. This gave rise to four orders of folds which developed sequentially, initially as symmetric buckles which progressively tightened, increasing in asymmetry such that their axial planes rotated towards the plane of the S_1 cleavage.

Two different cleavages, both associated with DV_1 , are developed in the same quartz-rich lithologies. The first cleavage S'_1 is a spaced pressure solution type initiating during or before the onset of buckling, whilst the second S_1 , a pervasive grain alignment cleavage post-dates S'_1 in the psammitic rocks. As the buckles tighten, S_1 changes progressively from strongly non-axial planar to an almost axial planar cleavage.

S E C T I O N C

This section describes the strain and three other important aspects of the deformation of the rocks comprising the fold belt.

FINITE STRAIN IN THE ORDOVICIAN ROCKS

Only one cleavage, S_1 , is developed ubiquitously in the Ordovician sediments in north Portugal. S_1 is geometrically associated with F_1 folds, generally parallel to their axial planes and temporally related to buckling, as demonstrated by relationships in the Marão Syncline (Chapter 5). This cleavage is a manifestation of the main ductile deformation and finite strain in the Ordovician sediments; an S_2 crenulation cleavage is only locally developed, slightly modifying the S_1 fabrics, and represents a low internal strain. An 'early' DV_1 cleavage, S'_1 , is developed in the psammitic rocks of the Marão Syncline but little penetrative ductile strain is associated with it (see Chapter 5).

Deformed objects, including conglomerate pebbles, ellipsoidal spots and concretions, and various body fossils are flattened and extended within the plane of the S_1 cleavage in Ordovician sediments. Finite strains have been calculated from these objects for the three major DV_1 folds.

There were two main objects in obtaining finite strains for the Ordovician rocks:

1. To analyse the variation, or non-variation of the finite strain within each fold and between the folds in relation

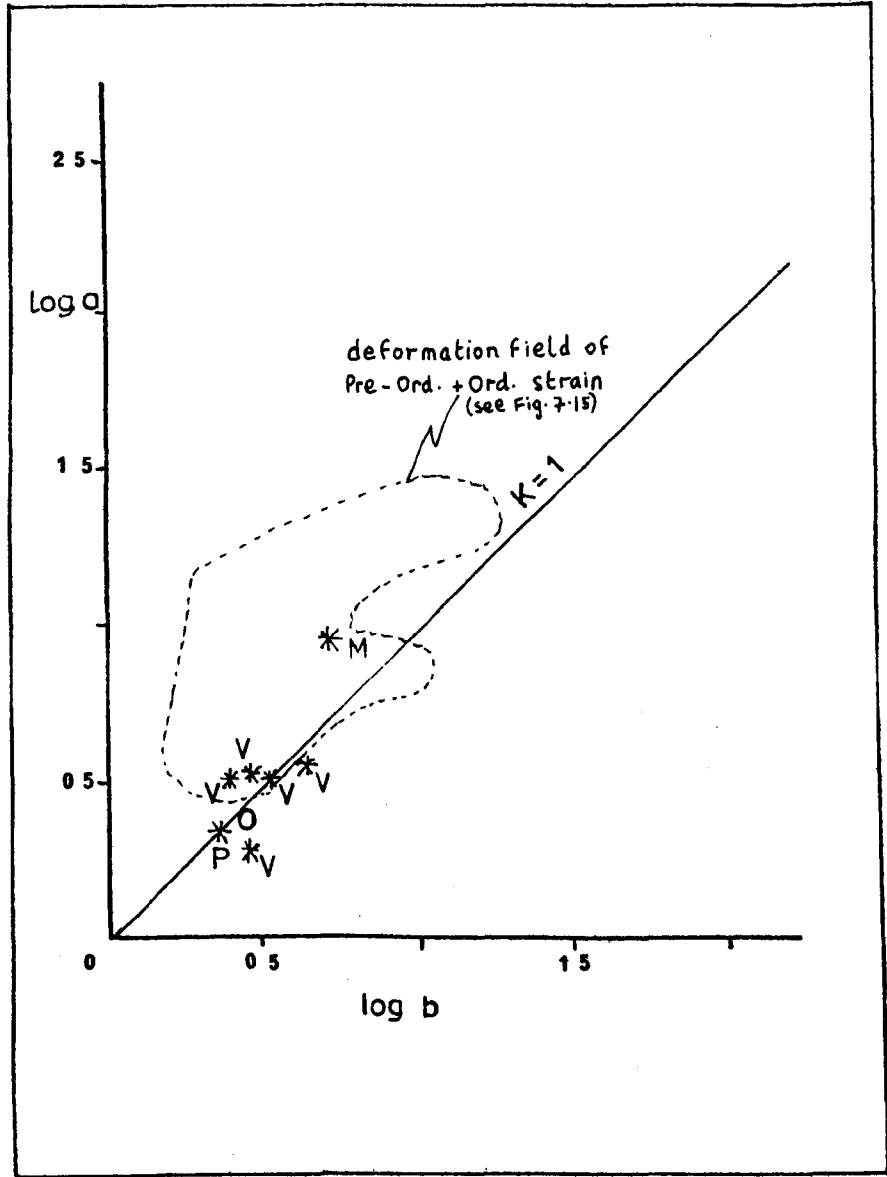
FIG. 6.1

Flinn Plot of finite strain in the Ordovician from deformed conglomerates and spots.

M = Marão Syncline

V = Valongo Anticline

P = Penacova Syncline



to their geometry.

2. To compare the finite strain in the Ordovician rocks (i.e. Variscan strain) with that in the Complexo xistograuvaquico to establish the nature of the pre-Variscan strain.

Finite strain determination for the Ordovician from the different deformed objects is described.

6.1 Conglomerates

Conglomeratic horizons occur near, or at the base of the Santa Justa Formation in all three of the major folds (see the respective chapters in section B for details of the lithologies). The conglomerates used as strain markers comprise quartz or quartzite pebbles in a quartzitic matrix, except in the Marão Syncline where the matrix is semi-pelitic to pelitic.

Polished surfaces of orientated specimens were prepared parallel to the principal planes of the strain ellipsoid. This was done by cutting the first plane parallel to the cleavage (X Y) and determining the maximum extension direction in that plane, and cutting the other two planes orthogonally to the first, one containing the X axis, the other the Y axis. For fine grained conglomerates measurements of the pebble ellipses were made from enlarged photographs taken of each surface (Fig. 6.2b). The

FIG. 6.2

a. Concentrically structured spots in siltstones.

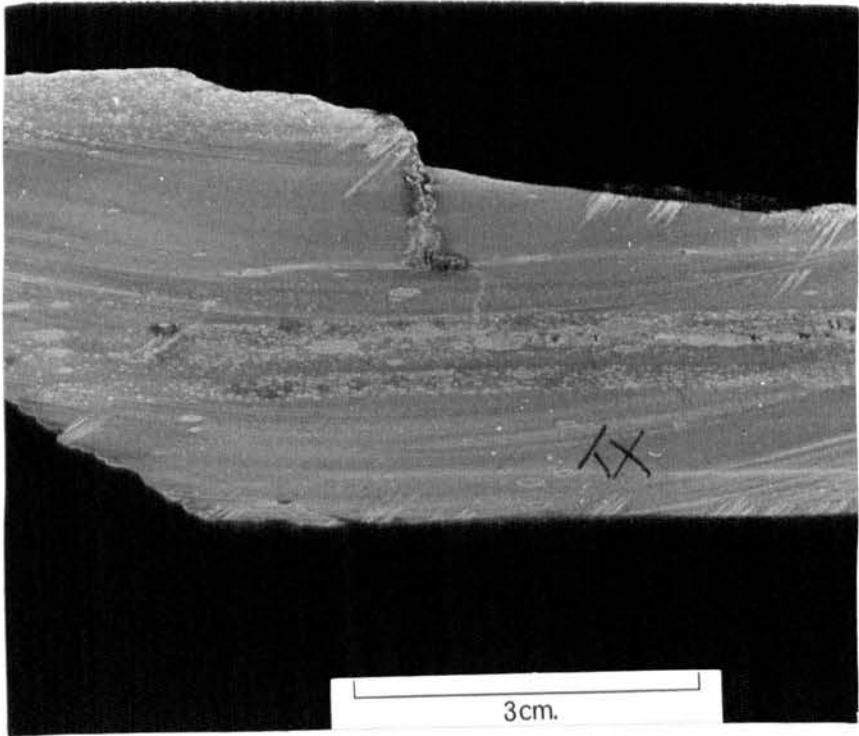
Location : 1km west of Melres.

b. Polished surface of Ordovician conglomerate

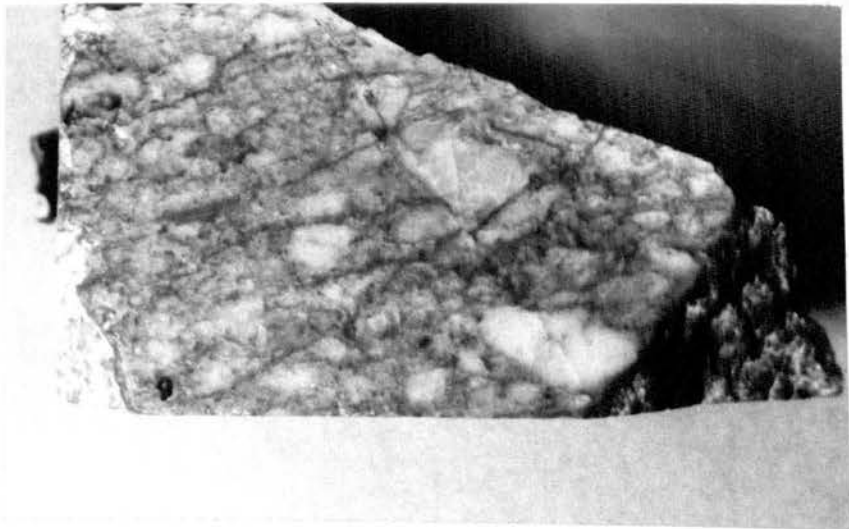
X1.5

Location : 1.5 km south of Mo on the N224, 10km
north-northwest of Arouca.

a



b



similarity in composition between the pebbles and the matrix, and in turn between the composition of these conglomerates and those in the Complexo xisto-grauvaquico increases the accuracy of the strain determinations and makes the comparison of strain between areas realistic. The problems and errors involved using pebbles for strain determinations are discussed in the next chapter (7).

Apart from in the Penacova Syncline, where conglomerates are undeformed, the pebbles in the Ordovician conglomerates are strongly aligned and flattened in the cleavage S_1 , and their long axes plunge at shallow angles (less than 20°) approximately parallel to neighbouring F_1 minor fold axes or bedding/cleavage intersection lineations (see Figs. 2.10a; 2.11a; 3.5b; 5.11a).

The finite strains as represented on a Flinn plot (Flinn, 1962) in Fig. 6.1 approach the plane strain type (i.e. $K = 1$, (Flinn, op.cit.)), excepting those in the Marão Syncline which are slightly constrictional (i.e. $K > 1$). Also the magnitude of strain is low within the deformation field defined by the finite strains determined in the Complexo xisto-grauvaquico. The strains in the conglomerates in the Penacova Syncline are too small to determine and are not represented in the plot.

6.2 Ellipsoidal Spots

Deformed spots occur rarely in slates, siltstones and

marls of the Ordovician. In the Valongo Formation 5 km NNW of Valongo, slates contain ellipsoidal quartz-rich objects which are possibly of organic origin (Fig.6.3).

They are confined to thin lenses, less than 20cm long and 5cm thick, parallel to bedding, and deform less than the matrix. The cleavage wraps around the spots and quartz-rich tails have developed in pressure shadows at their ends (Fig. 6.3). The dimensions of these spots were measured from enlarged photographs of polished surfaces which were cut parallel to the principal planes of the strain ellipsoid. These spots indicate strain symmetry and minimum finite strain in the slates.

Concentrically zoned reduction spots occurring in siltstones in the Santa Justa Formation 2 km west of Melres, deform homogeneously with the matrix (Fig. 6.2). The strain was measured in these spots from polished specimens.

Red marls in the Santa Justa Formation in the Penacova Syncline also contain reduction spots which deform homogeneously with the matrix providing maximum finite strains. Details of these spots are outlined in chapter 4.

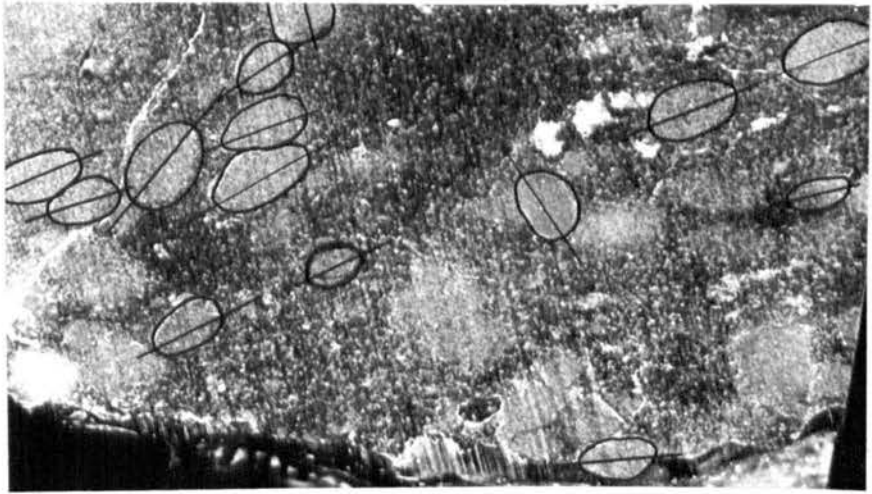
The finite strains determined from the spots described above approximate, like those from the conglomerates, to plane strain (Fig. 6.1). Also, the plunge of the long axes of the spots is parallel to the bedding/cleavage intersection lineation.

FIG. 6.3

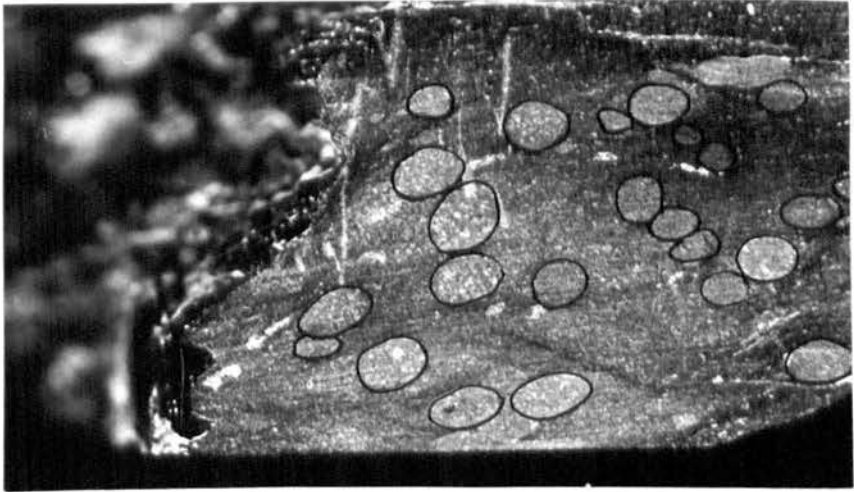
Polished specimens of slates containing deformed spots. The spots are slightly more quartz rich than the slate.

Specimen no. 24V

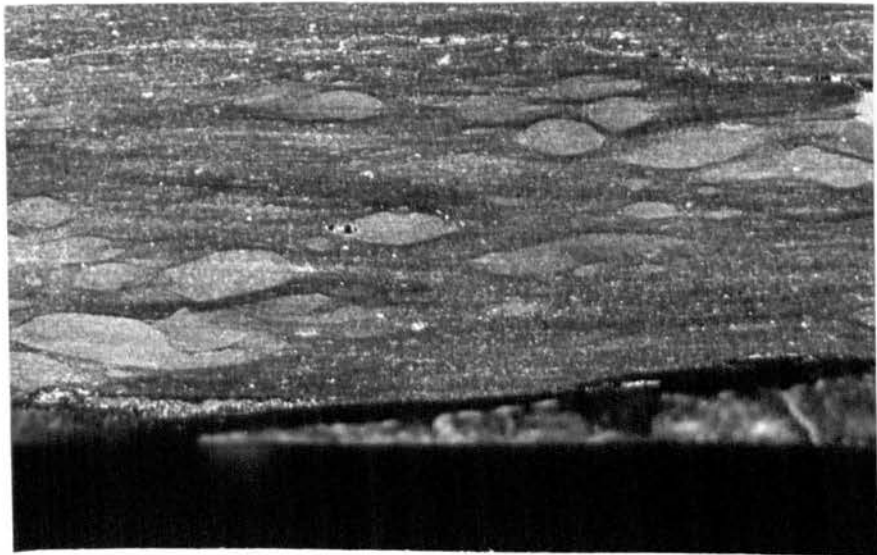
Location: Slate quarry at Quinta da Abelheira,
2km north of Valongo.



XY



YZ



XZ

2cm.

3. Fossils

Several horizons within the slates and shales of the Valongo Formation contain an abundant, well preserved fauna, including trilobites, brachiopods, nautiloids and graptolites (Delgado, 1908; Curtis, 1961; Romano, 1976; Romano & Diggens, 1974). Except in Penacova, these fossils are deformed in the plane of the cleavage (Fig. 6.5a, b). The fossils are the same composition and deform homogeneously with the matrix.

The restricted preservation of these fossils on cleavage planes, only provides a value for the two dimensional strain of the XY plane of the strain ellipsoid (Fig. 6.4).

Specimens of trilobites and brachiopods whose forms originally possessed a bilateral symmetry or a right angle e.g. the axis and thoracic segments of a trilobite, were used to calculate the strain ellipse by measuring the amount of angular shear strain of lines originally at right angles.

This was possible using either single fossils and the maximum elongation direction (a stretching direction) or two fossils by constructing a Mohr diagram (Ramsay, 1967 pp. 233-243). A method described by Wellman (1962) was also used for clusters of brachiopods. It was clear from this last method that the X direction of the strain ellipse for the XY plane (cleavage) is parallel^{to} a mineral lineation,

FIG. 6.4

Table of strain ellipses for XY plane of the strain ellipsoid determined from deformed fossils.

LOCATION	X	Y
VALONGO	1.80	1.00
"	2.85	1.00
"	3.28	1.00
"	1.85	1.00
COVELO	1.20	1.00
BELOI	1.60	1.00
"	1.30	1.00
"	1.70	1.00

FIG. 6.5

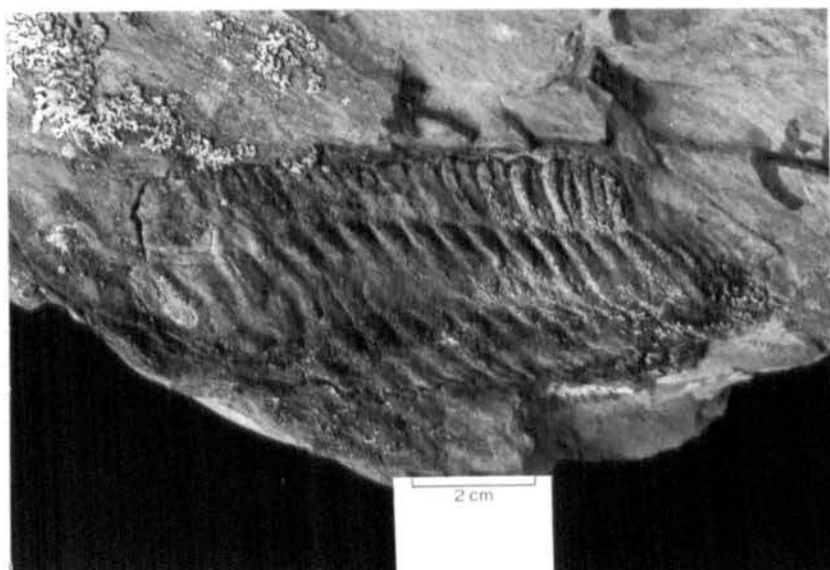
Deformed body fossils in slates of the Valongo
Formation.

Fossils are lying in the plane of the S_1 cleavage.

n.b. angular shear strain of the axis of the trilobite
approximately 40° .

X direction in slate containing brachiopod E-W.

d



b



which is the bedding/cleavage intersection. Hence, the maximum elongation direction in the slates is parallel to the minor F_1 fold axes. The plunge of the X axis determined from distorted fossils is shallow (less than 20°) (Fig. 2.11a).

The amount of elongation within the cleavage is variable (Fig. 6.4) but consistently in the direction of the minor fold axes. This variation is partly due to the compositional differences between the slates, but as the z axis of the strain ellipsoid could not be determined, further explanation of the variation is speculative. Wood (1971) has demonstrated the heterogeneous nature of the strain across the Cambrian Slate Belt, North Wales where the X axis is vertical to sub-vertical, normal to the fold axes. However, the orientation of the X axis in slates of the Valongo Formation implies sub-horizontal stretching parallel to the fold axes.

4. Summary

Several important statements can be made about the strain in the Ordovician sediments.

- a. A single phase of ductile deformation, DV_1 , gives rise to the S_1 cleavage, a planar-linear mineral and shape fabric defined by aligned micas and quartz grains, deformed pebbles, spots and fossils.
- b. The maximum elongation direction within the cleavage

plunges at a shallow angle, parallel to the minor F_1 fold axes. Boudinaged quartzite beds also support this sub-horizontal stretching (see Fig. 2.19b).

c. The symmetry of the three dimensional finite strain is approximately plane strain ($K=1$) (Fig. 6.1).

d. The magnitude of the strain is, except in the Marão Syncline, less than that in the Complexo xisto-grauvaquico (see Chapter 7).

e. The strain expressed in terms of percentage extension shows a general increase across the fold belt from Penacova in the southwest to Marão in the northeast (Fig. 6.6). The amount of extension is inhomogeneous along ^{the} length of the Valongo Anticline (Fig. 6.6).

f. For the three major DV_1 folds the finite strain determined from deformed objects in the Ordovician sediments does not reflect the amount of crustal shortening indicated by the tightness of the major folds e.g. low strains in the Penacova Syncline which is isoclinal. The geometry of the folds, however, is greatly controlled by the Armorican Quartzite (see section 5.3) and the folding mechanism is largely flexural slip involving little or no internal deformation of beds, especially in the limb regions. The strain determined in the slates and shales largely represents the accommodation of the low ductility rocks to the folding of the Armorican Quartzite.

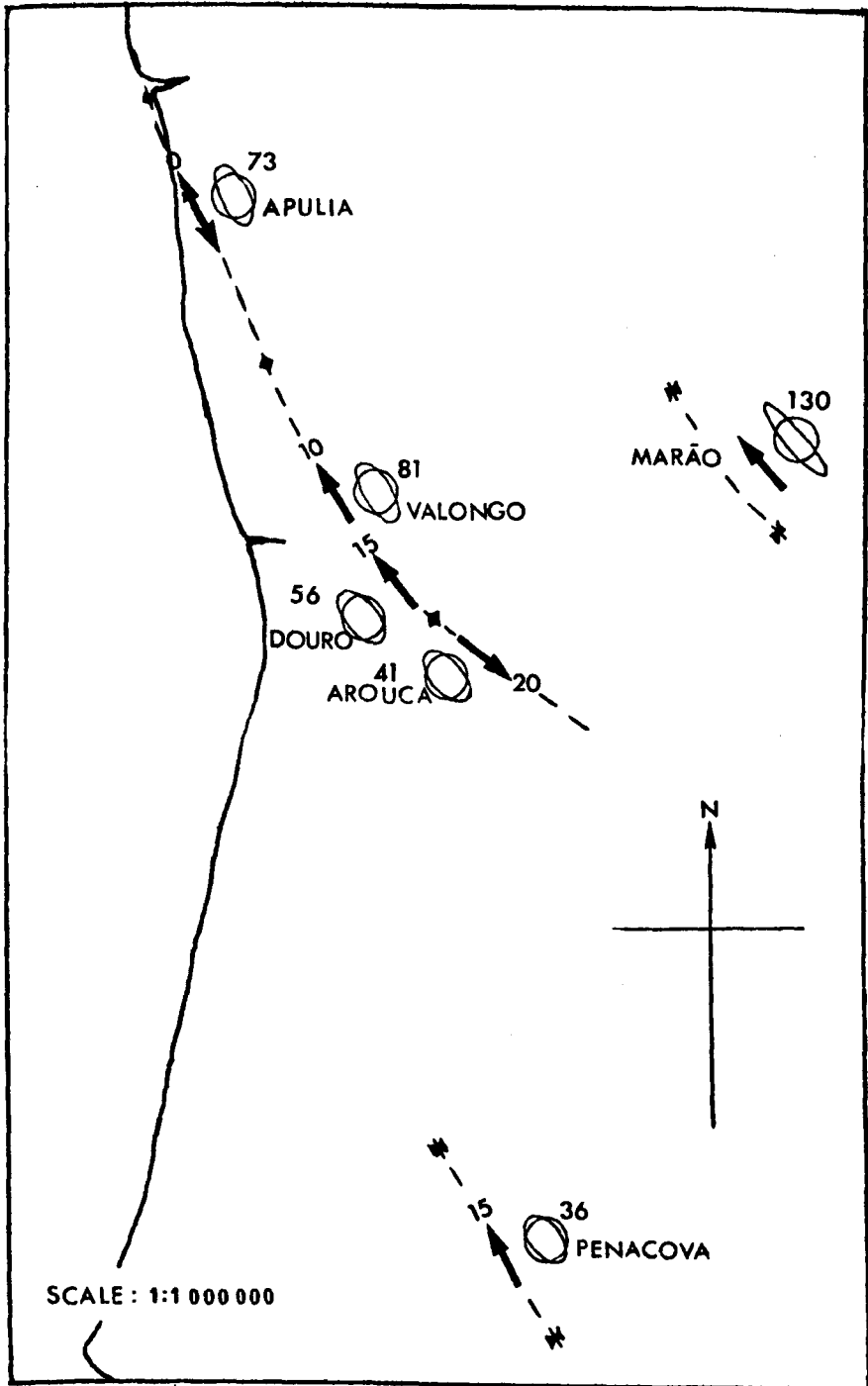
FIG. 6.6

Variscan finite strain , DV_1 , in Ordovician rocks for the fold belt in Northern Portugal.

Arrows indicate the average plunge of the maximum elongation direction (X).

Ellipses are XZ ellipses of the strain ellipsoid .

% extension in the X direction indicated by numbers.



STRAIN IN THE COMPLEXO XISTO-GRAUVAQUICO

7.1 INTRODUCTION

One of the main aims of this thesis is to investigate in detail the deformation of the sediments in order to establish the relationship between the major tectonic structures, DV_1 , and the strain distribution in the central zone of the Iberian Arc (Fig. 1.3). This should contribute to the further understanding of the Iberian Arc structure as a whole.

Ordovician rocks contain a variety of 'good' strain markers, e.g. fossils, spots and conglomerates, a pre-requisite for any regional strain analysis. The Complexo xisto-grauvaquico of the region contain extensive conglomerate horizons in the region of the Valongo Anticline (Fig. 7.1), and apart from rare occurrences of spots these are the only strain markers. Similar conglomerates are documented over a wider area of the Complexo xisto-grauvaquico from Varzielle, 70 km. southeast of Porto, to Carminha, 80 km. northwest of Porto and eastwards to Vila Real (Teixeira, 1954).

The conglomerates analysed display a variety of shape fabrics which result from ductile deformation, pressure solution and brittle fracturing of initially non-spherical pebbles.

Deformed pebbles have been used extensively in the study of

shape fabrics and finite strain (Ofte-dahl, 1948; Fairbairn, 1949; Brace, 1955; Flinn, 1956; Hossack, 1968; Gay, 1969)

and each type of conglomerate presents an individual set of problems in defining the strain ellipsoid. The main features of the conglomerates in the region of the Valongo Anticline are described in the next section (7.2) as a background to their use as strain markers.

7.2 THE CONGLOMERATES IN THE COMPLEXO XISTO-GRAUVAQUICO

1. SEDIMENTARY FEATURES

The conglomerates are interbedded with phyllites and schists with individual beds of between 10 cm. and 5 m. thick (Fig. 7.2a). Most conglomerate beds are graded, with sharp contacts top and bottom, but the direction of younging is difficult to determine due to frequent reversals in the grading of pebbles within beds. A strong flattening renders the recognition of sedimentary structures difficult, although possible load casts were noted at one location (Fig. 7.3a).

2. TECTONIC FEATURES

A pervasive steeply dipping cleavage ($> 70^{\circ}$ N.W) is developed in the Complexo xisto-grauvaquico (see Fig. 2.9b). This is a slaty cleavage of Variscan age DV_1 ; it is the earliest tectonic fabric recognised and is locally crenulated by S_2 (Fig. 7.4b). Conglomerate pebbles are aligned within the plane of this cleavage (S_1) which occasionally refracts through the generally steeply inclined bedding. Small shear

FIG. 7.2

a. Deformed quartzite pebbles in conglomerate of the Complexo xisto-grauvaquico.

Surface of outcrop is approximately XZ n.b. the steep plunge of the X axis.

Plane of flattening and bedding are parallel.

Location : 500m east of Lixa, 20km southeast of Porto on N108.

b. Pebble supported ,quartzite conglomerate , plane of flattening N-S.

Surface is approximately YZ.

Location : 500m south of Mo, 15km north of Arouca.

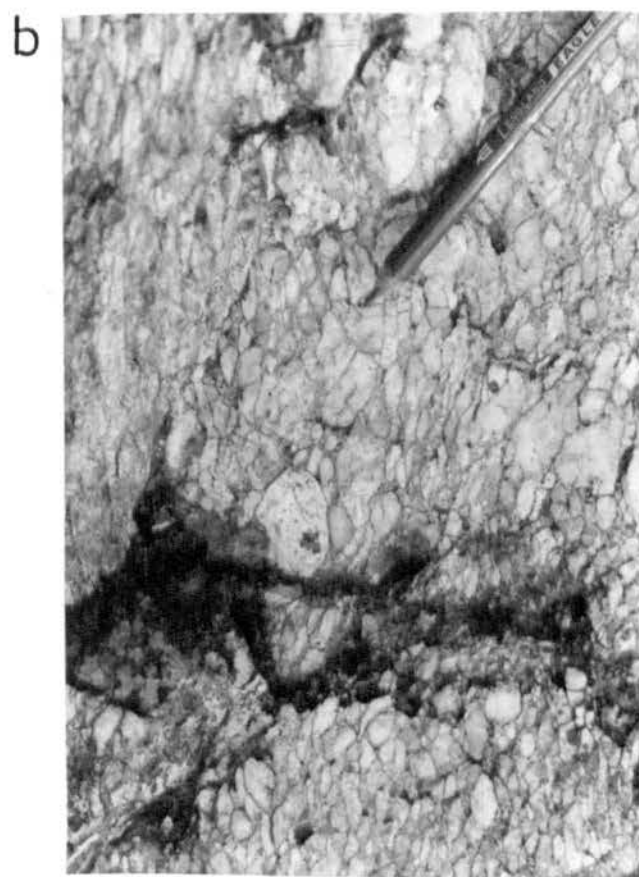


FIG. 7.3

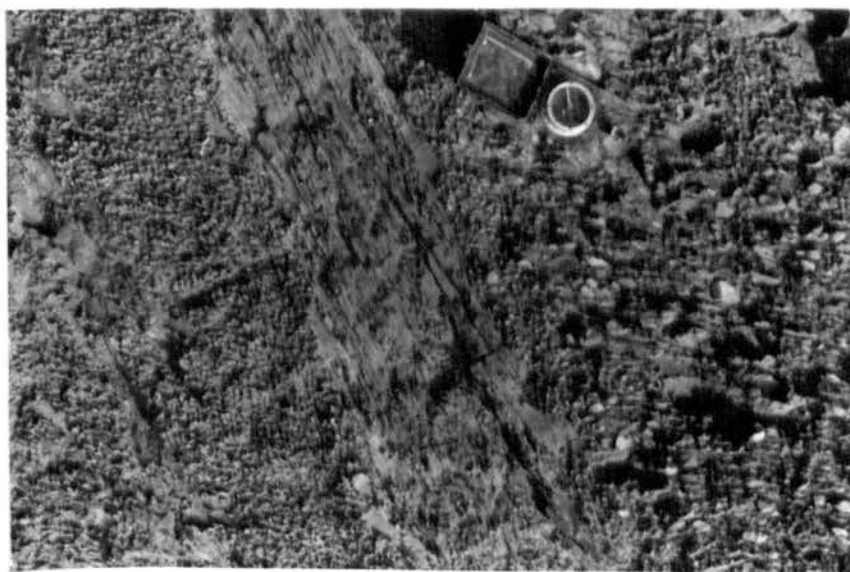
. Deformed conglomerate redformed by high angle shear zone, Complexo xisto-grauvaquico.

b. Detail of above (a).

a



b



zones, less than a metre in width, deform this cleavage and the associated pebble fabrics (Fig. 7.3a). This deformation is considered to be related to movements the Douro Shear Belt of probable Post - DV₂ age (see section 2.4).

3. COMPOSITION OF THE CONGLOMERATES

The composition of the conglomerate pebbles is relatively mature and homogeneous throughout the region. The pebbles are of two types, vein quartz and quartzite (Fig. 7.2b), although pebbles of chert, siltstone, slate and schist form up to 5% of the composition.

The pebbles are generally well-rounded and cemented by fine-grained psammite, of dominantly quartz and subordinate mica (0% - 10%) (Fig. 7.5a). Counts from a selection of conglomerates show the percentage of matrix varies between 15% and 50% i.e. most conglomerates are pebble supported.

The conglomerates are considered to have been deposited as slide conglomerates in deep water within a basin (Schermerhorn 1955).

Vein Quartz Pebbles

Vein quartz pebbles vary in size from 0.5 cm. to 10 cm. in diameter and are of translucent quartz, sometimes as single crystals. One mechanism by which these pebbles deform is the ductile - brittle development of extinction and

FIG. 7.4

a. Extension structures common in the Complexo xisto-grauvaquico, Valongo Anticline.

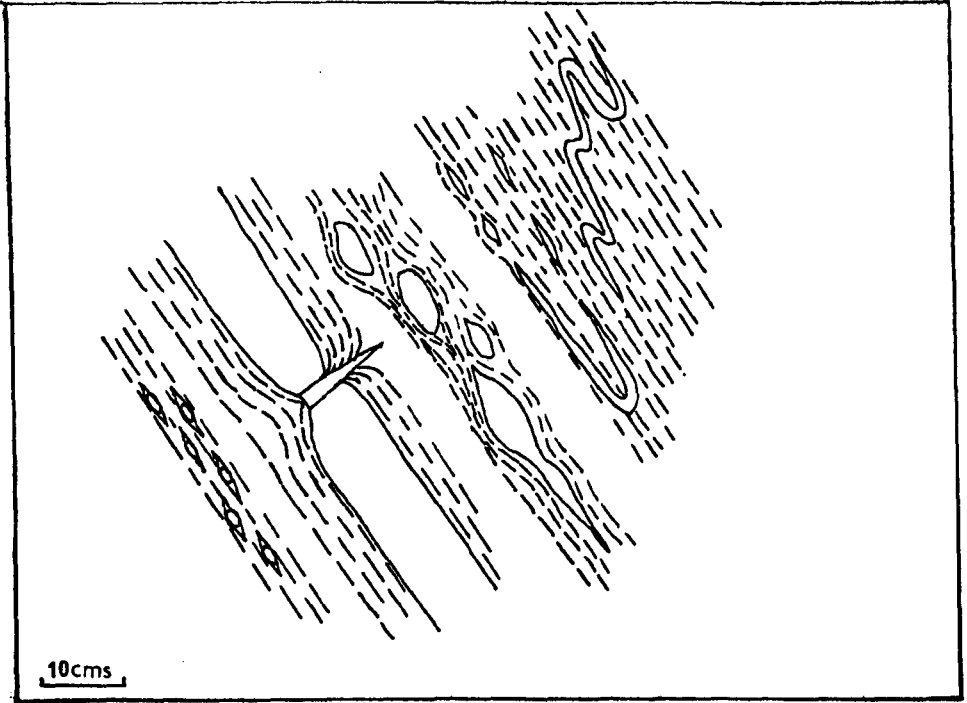
Left to right, staurolite porphyroblasts with quartz tails, boudinaged competent beds, boudinaged quartz vein, folded and boudinaged thin veins.

Location of examples of these structures : road section N108 north of the Rio Douro between Foz do Sousa and Seblido

b. Field sketch of S_2 crenulation cleavage cross-cutting the plane of flattening of the pebbles, S_1 , largely unaffected by their shape.

Location : 2km east of Lixa, 20km southeast of Porto.

a



b

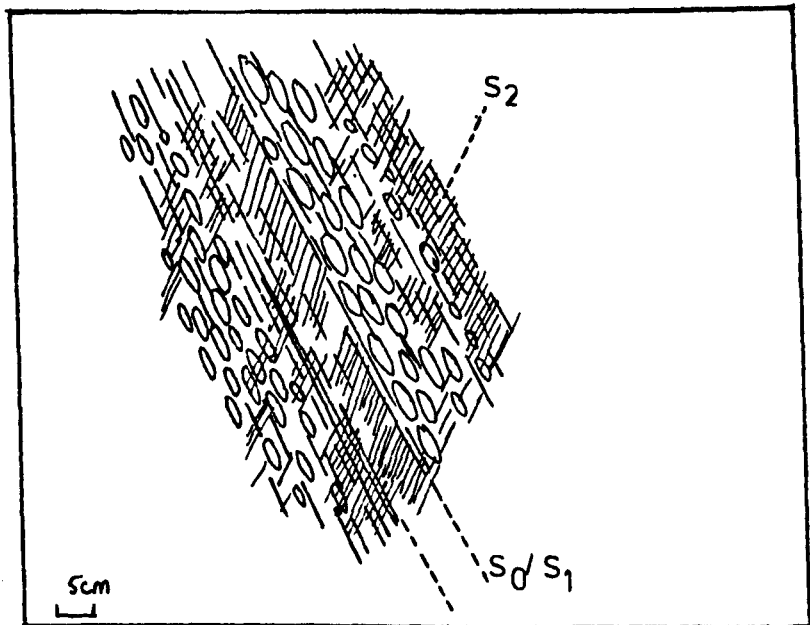


FIG. 7.5

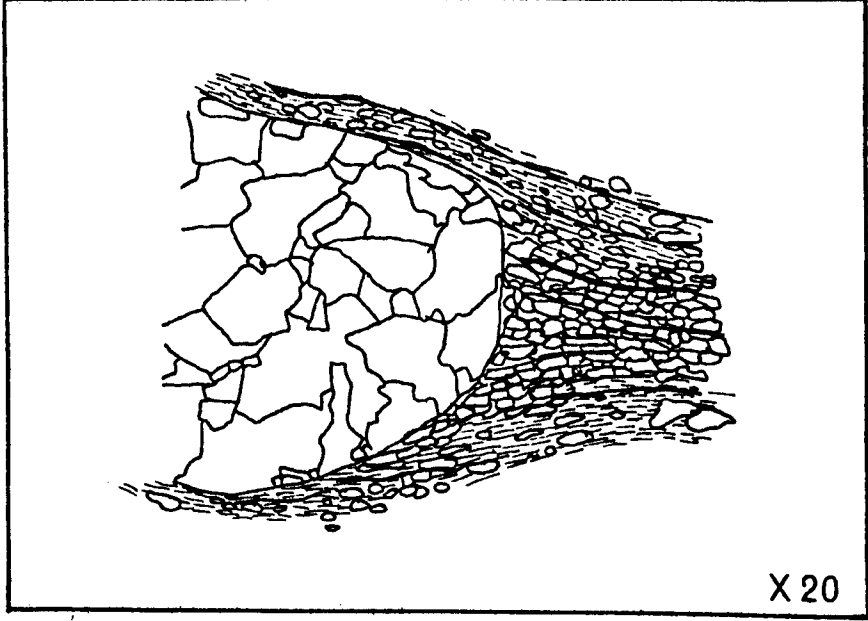
a. Drawing from thin section of quartz texture around the end of a pebble. Quartz is concentrated in pressure shadow area.

Specimen no. D97 X20.

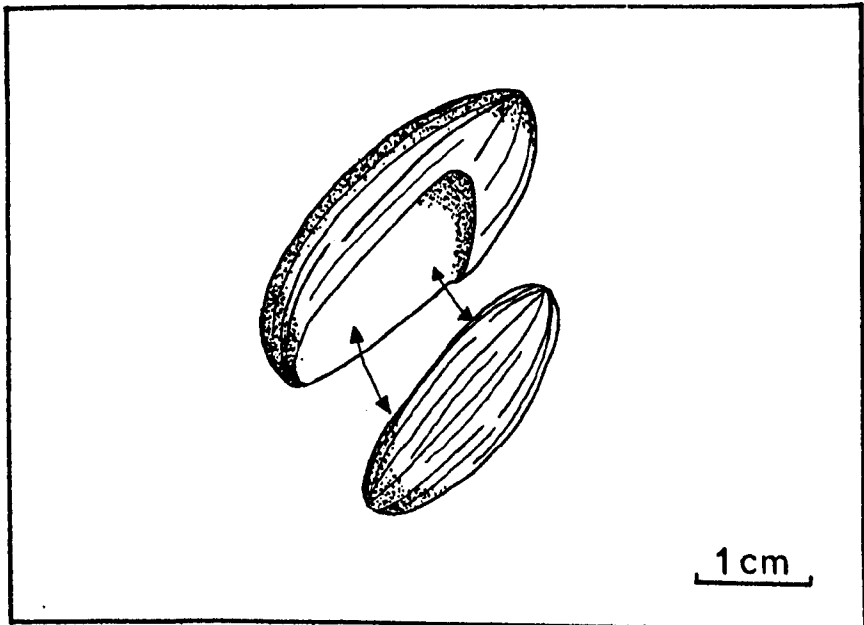
b. Example of planar pit in three dimensions .

Specimen no. AR2

a



b



deformation bands (Vernon, 1977 p.175) (see Figs. 8.3b and 8.7). Mapping these bands (in 2D) in pebbles in thin section indicates they develop at moderately high angles to the plane of flattening (Fig. 7.6) by slip on (0001) and [0001] (Vernon op.cit.).

The quartzite pebbles generally comprise quartz and up to 20% of mica, muscovite and sericite, and opaque minerals. These pebbles have a white as opposed to translucent appearance in the field. They are deformed and sometimes have an internal preferred orientation of the quartz. The grain boundaries within a typically deformed pebble were mapped by tracing a projection of a thin section through a microfilm documentor (Fig. 7.7a, b). The sections are parallel to principal planes in the pebbles and the polygonal texture clearly shows only a weak dimensional orientation of quartz grains. Other authors report textures with strongly developed grain fabrics which reflect the symmetry and shape of the pebble (Brace, 1955; Flinn, 1956; Goy , 1969). However, there is an alignment of muscovite within the pebbles, which suggests that the quartz fabric has been annealed. The C - axes of quartz grains plotted for the pebble in Fig. 7.7 to ascertain whether any optical fabric in the pebbles exists (Fig. 7.8). The pattern of C - axes indicate a weak orientation in two planes intersecting in Y and symmetrically disposed about X and Z. This pattern is possibly a weak fabric due to ductile deformation of the pebble or the remnants of a fabric after annealing. Strong C - axis

FIG. 7.6

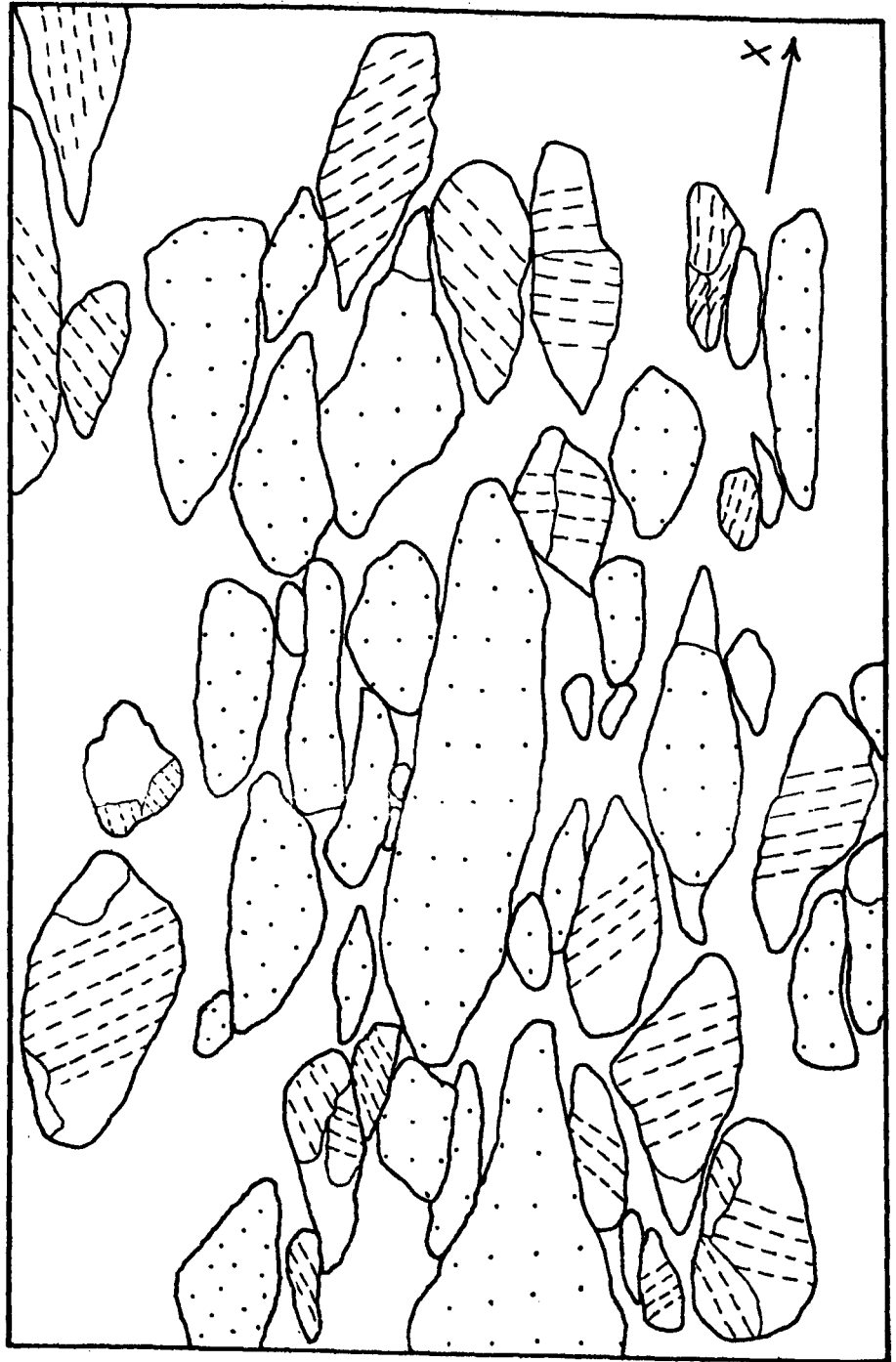
Orientation of deformation bands developed in single quartz-crystal pebbles in microconglomerate.

Thin section traced from projected image on a micro-film reader.

Dashed lines represent deformation bands, dotted pebbles comprising several grains.

Section XZ

Specimen no. D117 X6.5

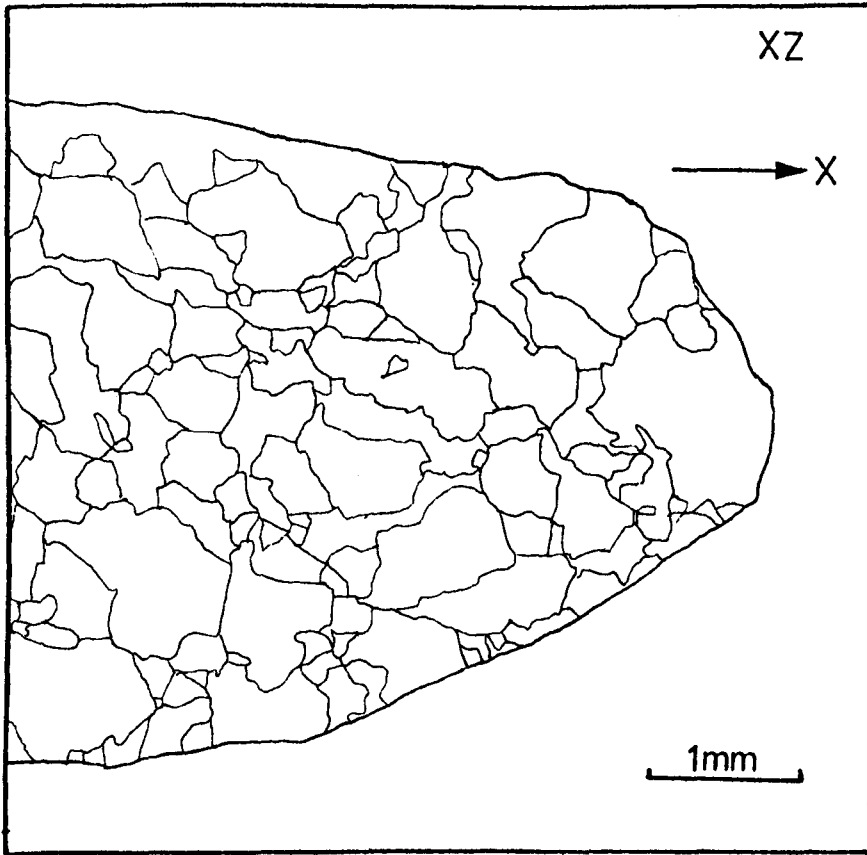


5mm

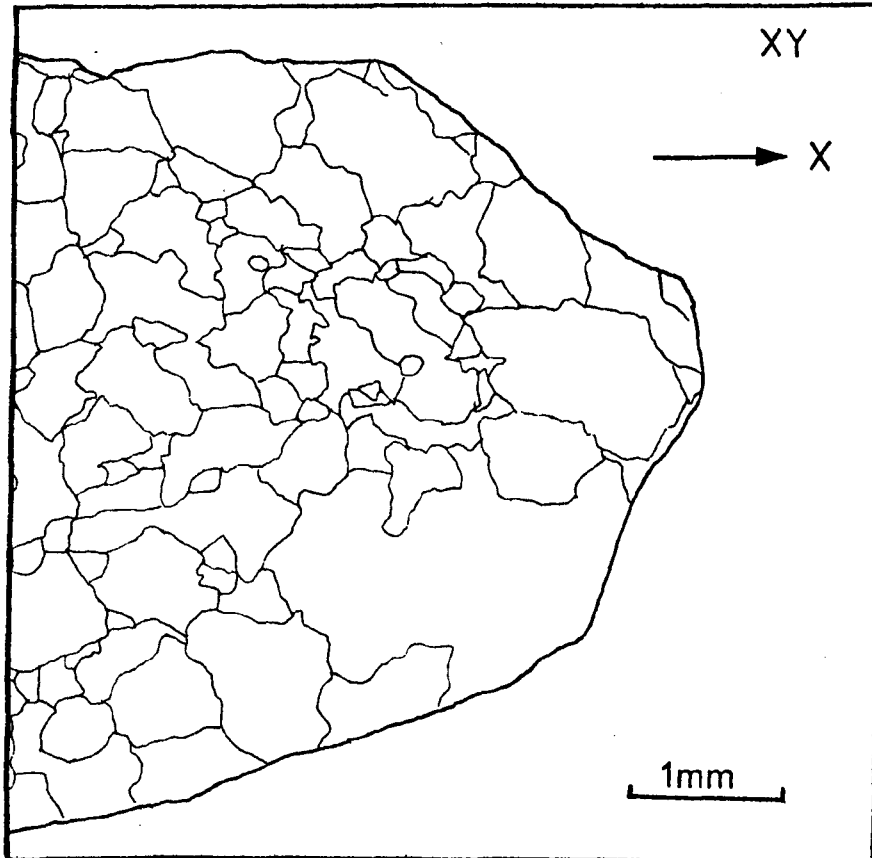
FIG. 7.7

Tracing from projected thin section of strongly flattened pebbles to show the lack of preferred orientation of quartz.

a



b



girdles in the plane normal to x have been reported from other deformed pebbles (Strand, 1944; Flinn, 1956). Some pebbles show elongation in the direction of their long axes by quartz filled extension fractures (Fig. 7.9a). The amount of extension is only between 2% and 3% and this post dates the ductile flattening of the pebbles. They do not form conjugate sets as may result from a compressional type stress (Ramsay, 1964) but rather an extensional type after the main ductile deformation.

7.3 ANALYSIS OF STRAIN USING THE DEFORMED CONGLOMERATES

1. METHODS OF MEASUREMENT

Strain measurements were made at 22 locations in the region of the Valongo Anticline. The shapes and orientations of pebbles were measured directly in the field where the pebbles could be removed from deeply weathered matrix. This was carried out using calipers to record the three axial lengths of each pebble and the orientations of the axis (X). A minimum of thirty pebbles were measured (see Hossack, 1968) from each location. At most locations orientated specimens were collected for measurement in the laboratory either because the pebbles are too small to measure accurately in the field (e.g. Fig. 9b), or pebbles are well cemented or highly fractured, making them difficult to remove from the conglomerate. The mean orientation of the long axes of the pebbles was recorded in the field. Pebble ellipses were measured either directly, or from enlarged photographs of polished surfaces cut parallel to the principal planes.

FIG. 7.8

Stereographic plot of C - axes of quartz in a quartzite pebble.

X,Y,Z correspond to the principal axes of the pebble.

Contours at 1% intervals from 1%.

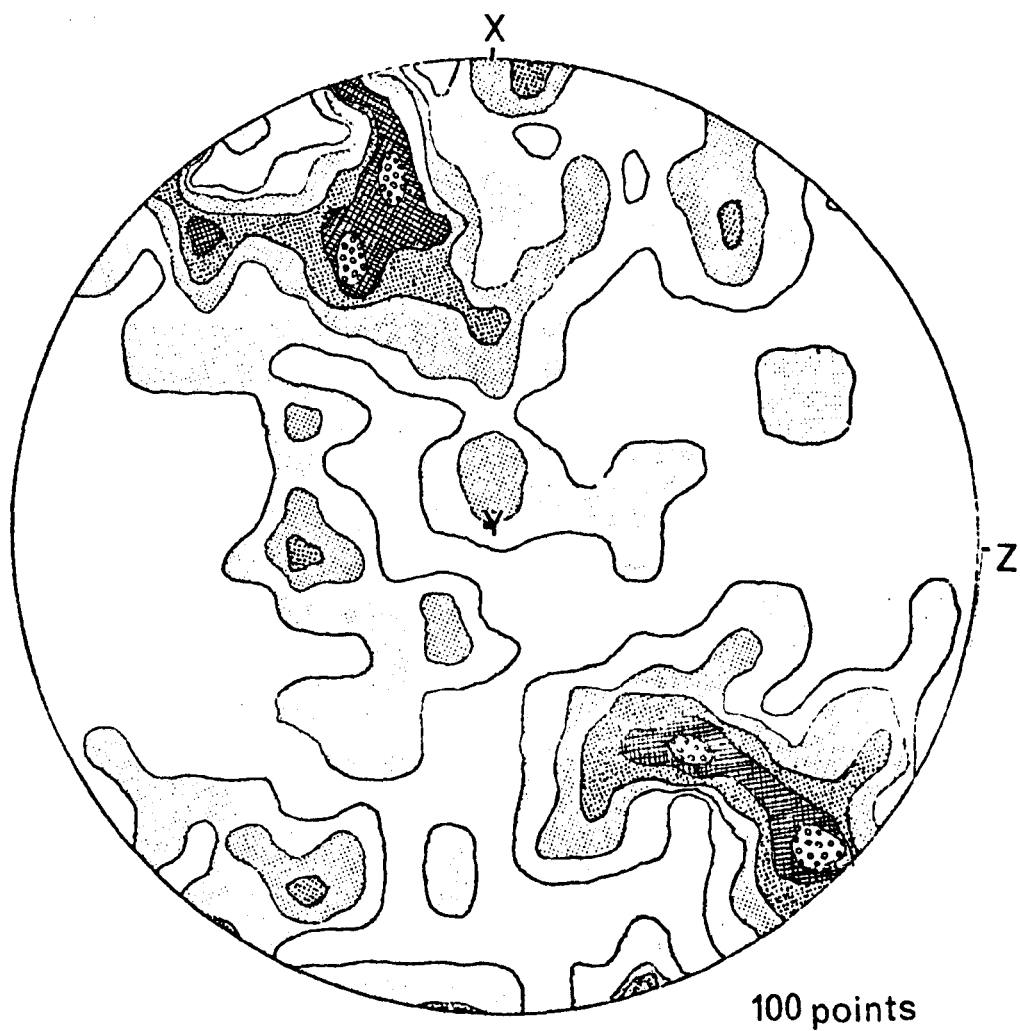


FIG. 7.9

a. Extension fractures in pebbles .

Fractures are filled with quartz and do not extend into the matrix.

Rose diagram of the orientation of fractures with pebble axes Z north and X east-west. Total 24 fractures
Specimen A52

Alvarenga.

b. Polished surface of pebbles in a microconglomerate.

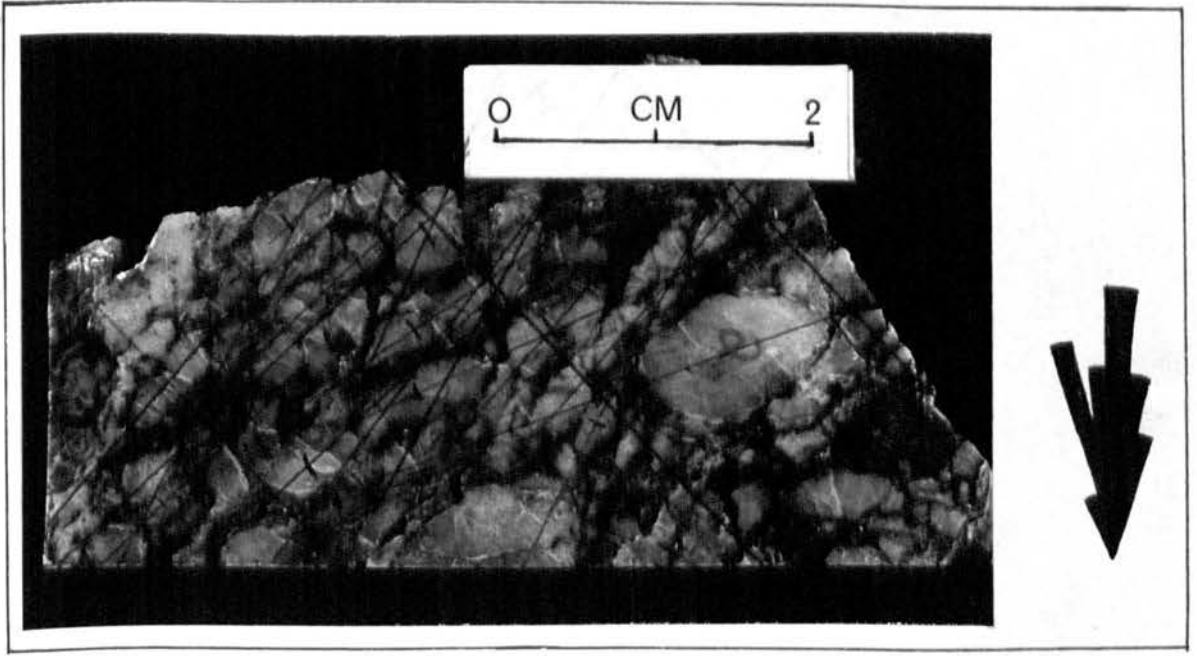
Some pebbles are outlined .

Surface XY.

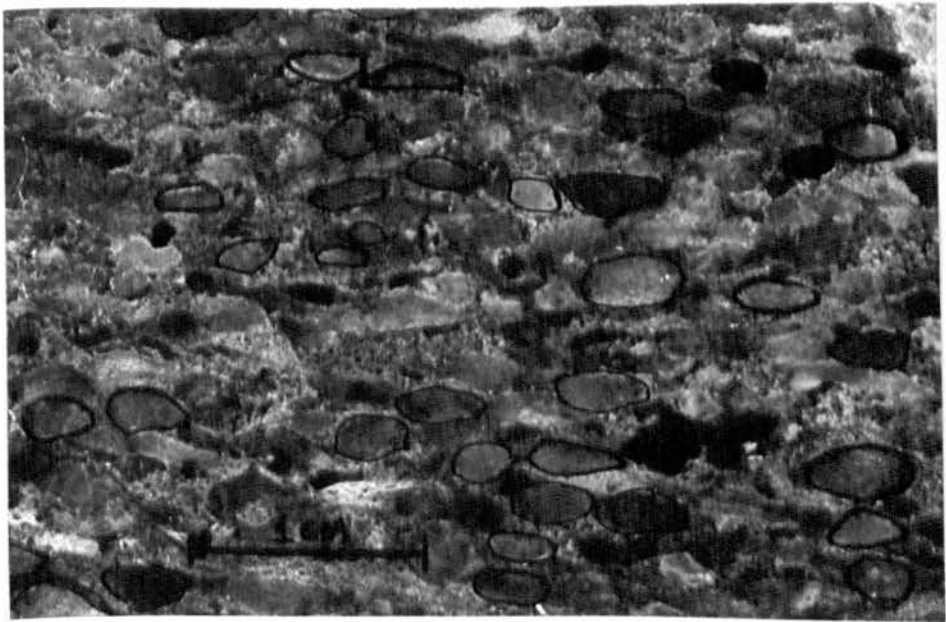
Specimen no. A50

Alvarenga.

a



b



These were cut by first determining and cutting either the plane of flattening or the plane normal to the long axis and determining the other axes or planes from this.

The mean pebble ellipsoid was calculated simply from the ratio of the ellipses (XY, XZ, Y,Z). In specimens where the long axes is more difficult to determine, measurements of ellipse ratios were made from three random cuts and the mean pebble ellipsoid was computed based upon the method devised by Ramsay (1967, p.142) using the parameters in Fig. 7.10.

Possible errors may arise from difficulty in defining the lengths of pebbles, where quartz rich tails develop, and in approximating the pebbles to true ellipsoids.

2. PEBBLES AND THE STRAIN ELLIPSOID

Several variables affect the finite strain recorded by deformed pebbles in these conglomerates.

a) PEBBLE COMPOSITION AND GRAIN SIZE

The homogeneous composition of the conglomerates makes them very suitable as strain markers as the pebbles and matrix deform with a low ductility contrast. Hence, strains from conglomerates throughout the region may be compared.

In conglomerates with a fine-grained quartz matrix, or matrix with a large percentage of mica (>10%) the cleavage

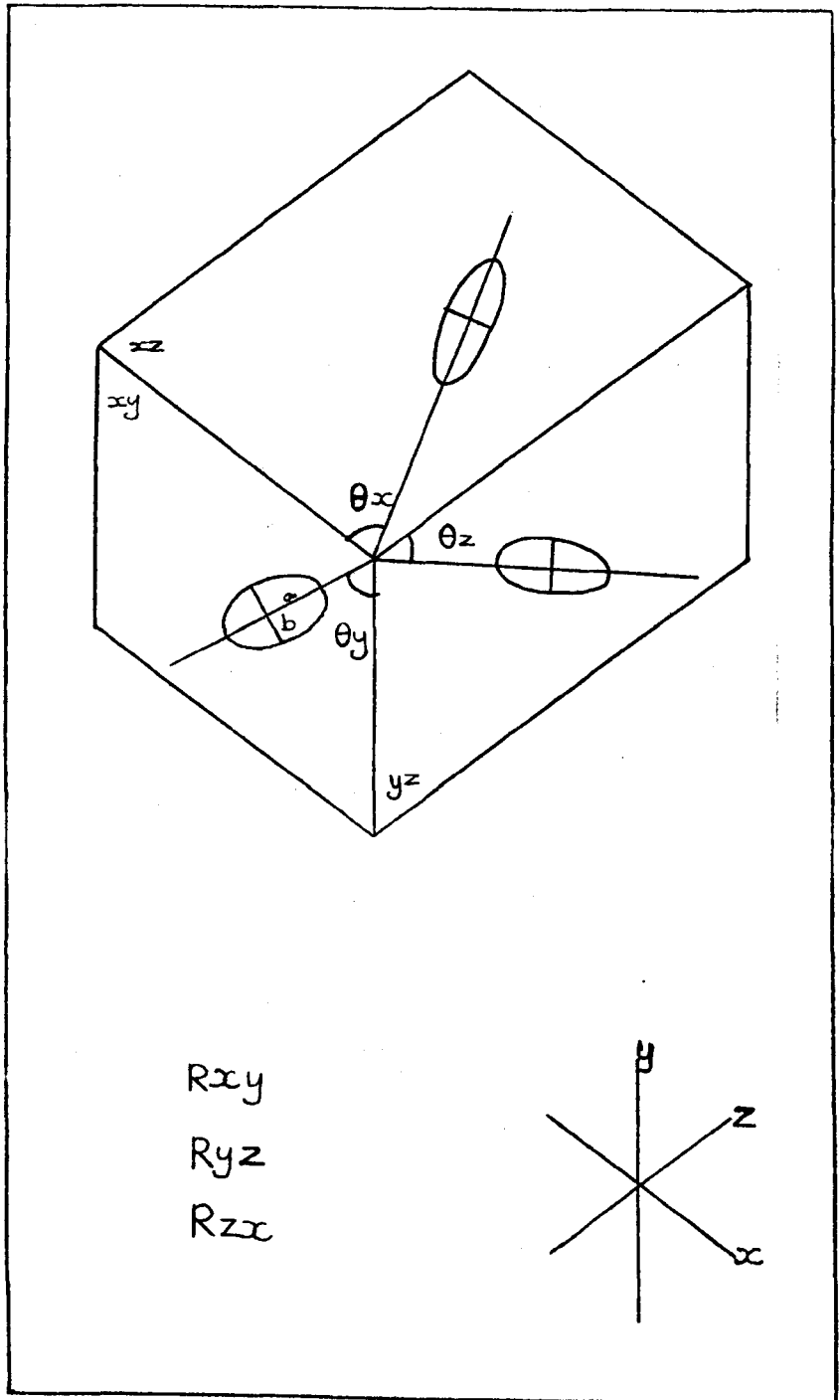
FIG. 7.10

Diagram to show the parameters used to compute the three dimensional strain in conglomerates where pebbles were measured on three orthogonal surfaces oblique to the principal planes of the strain ellipsoid (after Ramsay , 1967)

a, b are major and minor axes of the pebble ellipses.

x, y, z are the angles the long axes of the ellipses and the axes of the specimen.

$R_{x,y}, R_{y,z}, R_{z,x}$ are the rotations in the computation



wraps around pebbles indicating a ductility contrast; pressure shadows around the ends of pebbles have increased quartz content (Fig. 7.5a). Large single crystal vein quartz pebbles were not included in the measurements as they tend to behave very competently with little recrystallisation due to low total grain boundary surface area.

Pebbles are commonly pitted (Keunen, 1942; Ramsay, 1967 p.227) developing compromise planes by pressure solution (Fig. 7.5b); however, no correlation appears to exist between pebble shape or strain and size in pebble supported conglomerates (Fig. 7.11).

b) PRE-TECTONIC FABRIC

The effect of strain on sedimentary fabrics has been investigated by Dunnet and Siddons (1971) based upon the R_f/ϕ technique (Dunnet, 1969). To identify an original sedimentary fabric the technique relies upon bedding and cleavage being oblique (Dunnet and Siddons, 1971 p.316); however, in the conglomerates of the Complejo xisto-grauvaquico these two planes are nearly always parallel such that the long axes of the pebbles lie within the plane of both the bedding and cleavage. The symmetry of the scatter on R_f/ϕ diagram of a conglomerate (Fig. 7.12) illustrates the bedding and cleavage control of the finite strain. The finite strain calculated by this method (R_s) agrees closely with that derived from the mean pebble shapes i.e. 2.54:1.00:.71 (mean); 2.5:1.00:0.6 (R_f/ϕ).

FIG. 7.11

Plot of pebble shapes and their relative volumes.

Numbers 1 to 30 are pebbles of increasing volume.

Area outlined indicates a slight predominance of

larger pebbles with lower strains.

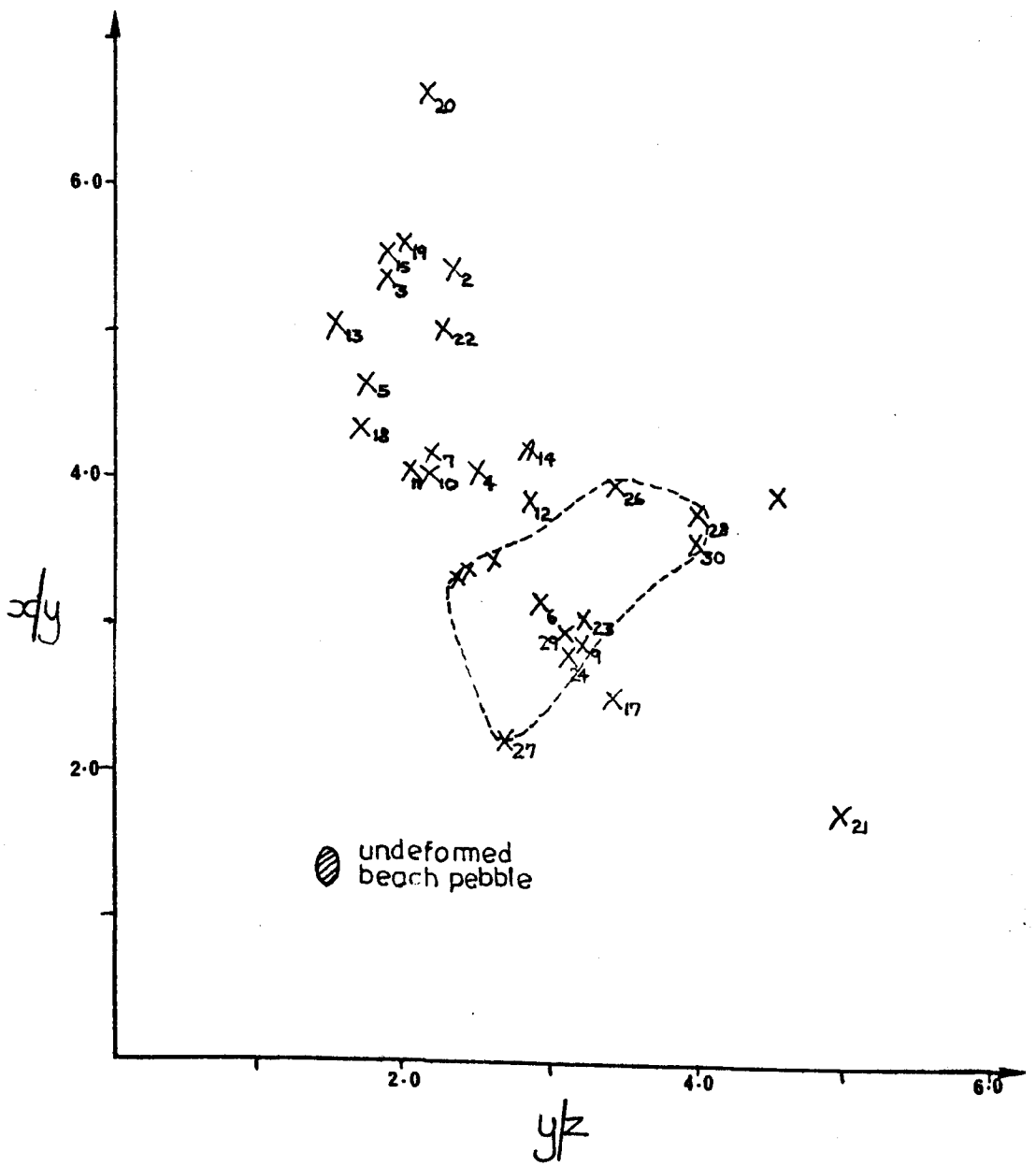
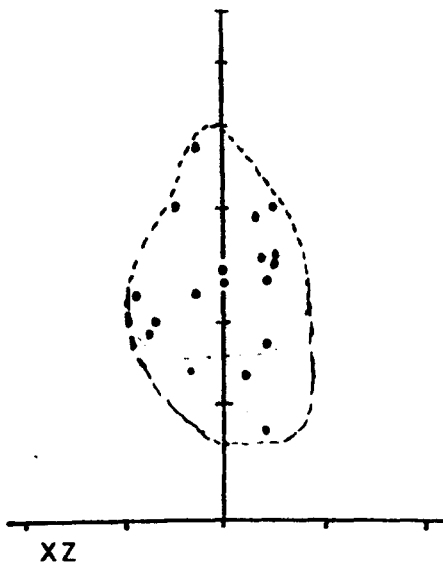
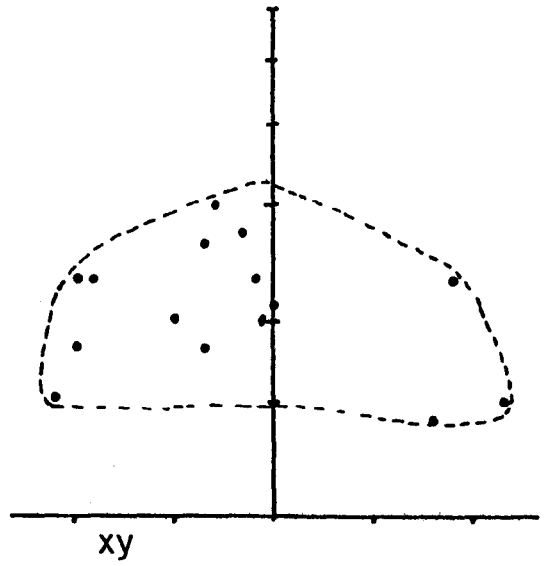
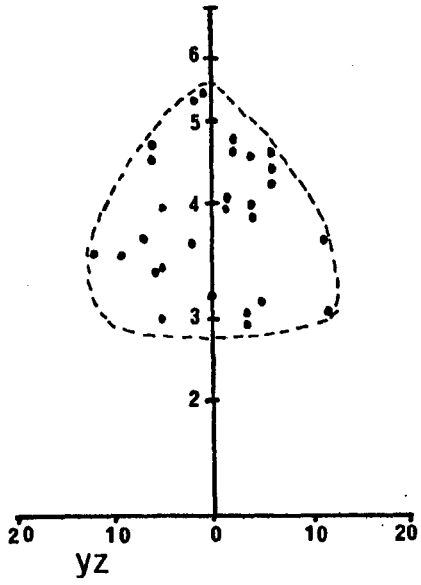


FIG. 7.12

Rf / ϕ plot of specimen A52



Experimental work by Gay and Fripp (1976) suggests for X:Y:Z, that significant flattening deformation may occur during lithification of conglomerates. Sedimentary fabrics are commonly recorded in undeformed conglomerates (Krumbein, 1939; Glenne et al. 1957; Ramsay, 1963) and it is likely that the pebble supported conglomerates of the Complexo xisto-grauvaquico also possessed a sedimentary fabric which contributed to the finite strain. It is demonstrated in section 7.5 that a significant pre-Variscan fabric was present in the conglomerates.

c) ROTATION OF PEBBLES DURING DEFORMATION

In conglomerates where a viscosity contrast exists, as in many of these conglomerates, pebbles will experience rigid body rotation during deformation (Jeffery, 1922). The precise path depends upon the shape and orientation of the pebble, the viscosity contrast and deformation mechanism. Rarely is any evidence of the rotations in natural deformation available (Ramsay, 1964)

Subtraction

of the DV_1 strain from the finite strain in the conglomerates indicates a pre- DV_1 fabric with pebbles aligned normal to the axes of early folds (U. Cambrian age, see section 7.5).

d) POLYPHASE DEFORMATION

There is evidence in the region of the Valongo Anticline that the Complexo xisto-grauvaquico was folded during an upper Cambrian folding phase D_U (see section 2.3). Only large

scale folds (F_0), wavelengths greater than 0.5 km., which have been refolded during the main Variscan deformation, DV_1 , are in evidence. Minor folds are rare and no cleavage is associated with the Upper Cambrian folding. The DV_1 deformation produced a penetrative cleavage, S_1 , and strain in the Complexo xisto-grauvaquico and Ordovician - Lower Devonian sediments.

Subtraction of the Variscan ductile strain from the conglomerates (see section 7.5) indicates that prior to deformation (DV_1) the pebbles possessed a bedding - parallel, planar - linear fabric. This early fabric is possibly sedimentary in part although it resulted largely from rigid rotation of the pebbles during the development of the Upper Cambrian folds (see section 7.5). The Upper Cambrian folds are large scale and develop in well layered rocks suitable for folding by a flexural slip mechanism. In support, large scale folds of the same age in the Complexo xisto-grauvaquico to the northwest, at Tras-os-Montes have box fold geometries (Ribeiro, 1974) which were most likely formed by flexural-slip or a mechanism involving no or low strain within beds. There is also no cleavage associated with the folds in Tras-os-Montes (Ribeiro, op.cit.).

7.4 REPRESENTATION AND DESCRIPTION OF THE STRAIN

The mean pebble shape was calculated from the measurements of at least 30 pebbles, or elliptical sections of pebbles for each location. For one specimen the mean pebble shape

strains represent strain increments deformation paths can be constructed (Hossack, 1968).

The Flinn Plot of Log_a versus Log_b where $\text{log}_a = \epsilon_1 - \epsilon_2$ and $\text{log}_b = \epsilon_2 - \epsilon_3$ is presented in Fig. 7.15. Because of low ductility contrast between the pebbles and the matrix and the similarity between conglomerates over the area the strains derived are considered to be approximate whole rock strains which can be meaningfully compared with each other. The finite strain and deformation field for each location is represented in Fig. 7.1.

The strain is inhomogeneous, varying in magnitude between 1.65 : 1.00 : 0.66 and 3.99 : 1.00 : 0.36 (X,Y,Z), and in symmetry between plane strain (K=1) and constrictional strain (K = 3.37). The finite strain determined from deformed concentrically structured spots in slates (Fig. 7.16) is also represented on the Flinn Plot. (Fig. 7.15). The mean shape of an undeformed beach pebble (Flinn, 1956) is also plotted for comparison to deformed pebbles.

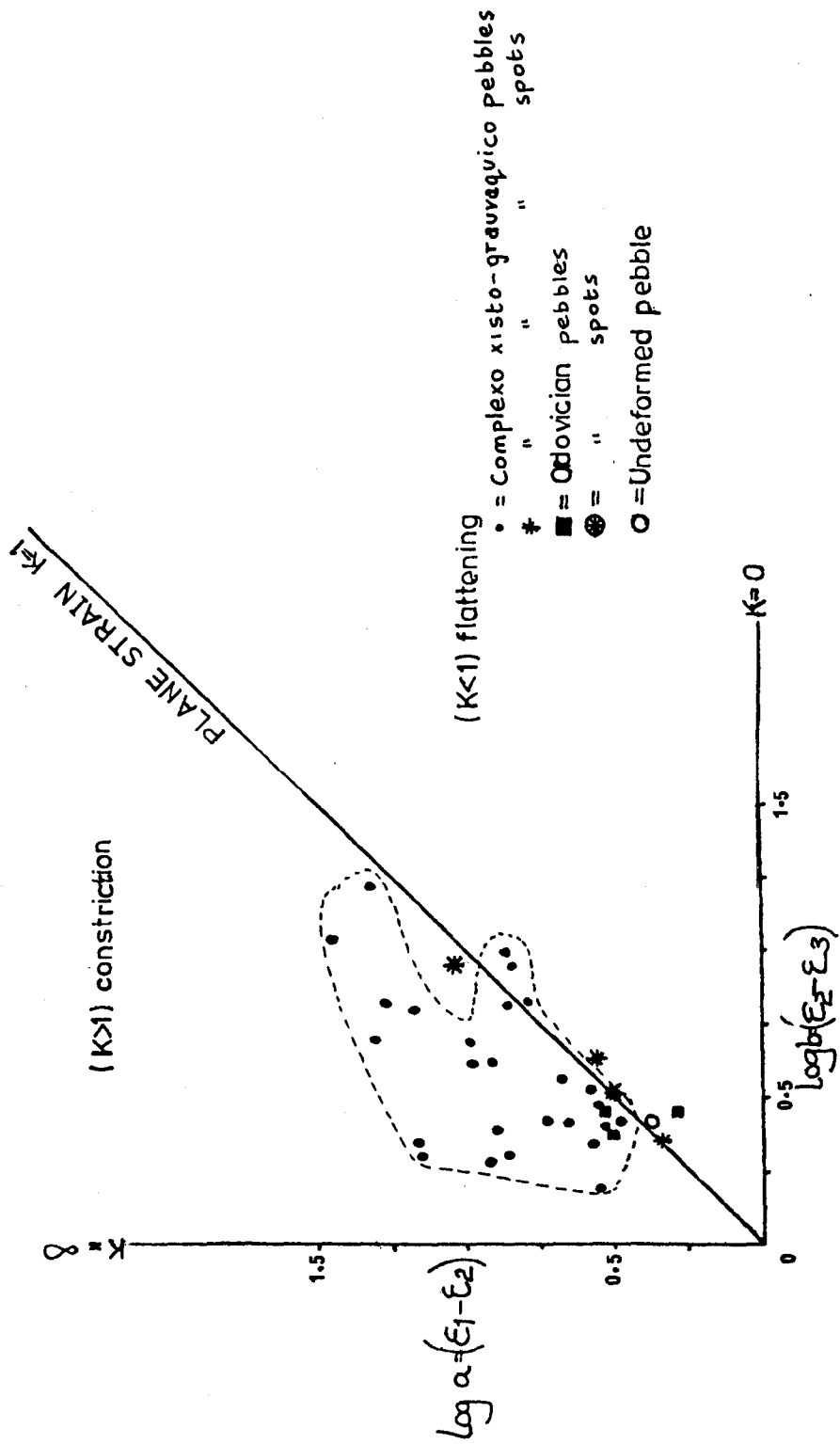
Several statements can be made about the finite strain in the conglomerates of the Complexo xisto-grauvaquico.

a) The magnitude of the strain is generally greater than the strain recorded from the Ordovician rocks in the same region compare Fig. 7.15 with Fig. 6.1. The greater strain indicated by deformed spots in the Complexo xisto-grauvaquico than deformed spots in the Ordovician substantiates this (see Fig. 7.15).

FIG. 7.15

Flinn Plot of finite strain for deformed conglomerates.

Expressed in natural strain.



b) The finite strain is inhomogeneous across the region, but the plane of maximum flattening of the pebbles is consistently parallel to the S_1 cleavage.

c) The maximum elongation direction plunges northwest ($300^\circ - 350^\circ$), southeast and east ($95^\circ - 170^\circ$) at angles between 0° and 70° (Fig. 7.17a) sub-parallel to the S_1 cleavage/bedding intersection lineation (Fig. 7.17b).

The variation in the azimuth of the plunge direction is largely due to the arcuate trend of the DV_1 Variscan structures along the Valongo Anticline. The maximum elongation direction in the deformed spots also plunges parallel to the S_1 /bedding intersection lineation (Fig. 7.16).

d) The finite strains almost all lie in the field of constriction (Flinn, 1962), some close to plane strain.

7.5 INTERPRETATION OF THE STRAIN

It has been established in Chapter 6 that the finite strain associated with the DV_1 deformation approximates to plane strain ($K = 1$) with a shallow plunging (less than 20° N.W) maximum elongation direction parallel to the S_1 cleavage/bedding intersection lineation and F_1 minor fold axes.

The greater magnitude of the strain, the common constrictional shape fabrics, and variable plunge of the maximum elongation direction in the Complexo xisto-grauvaquico

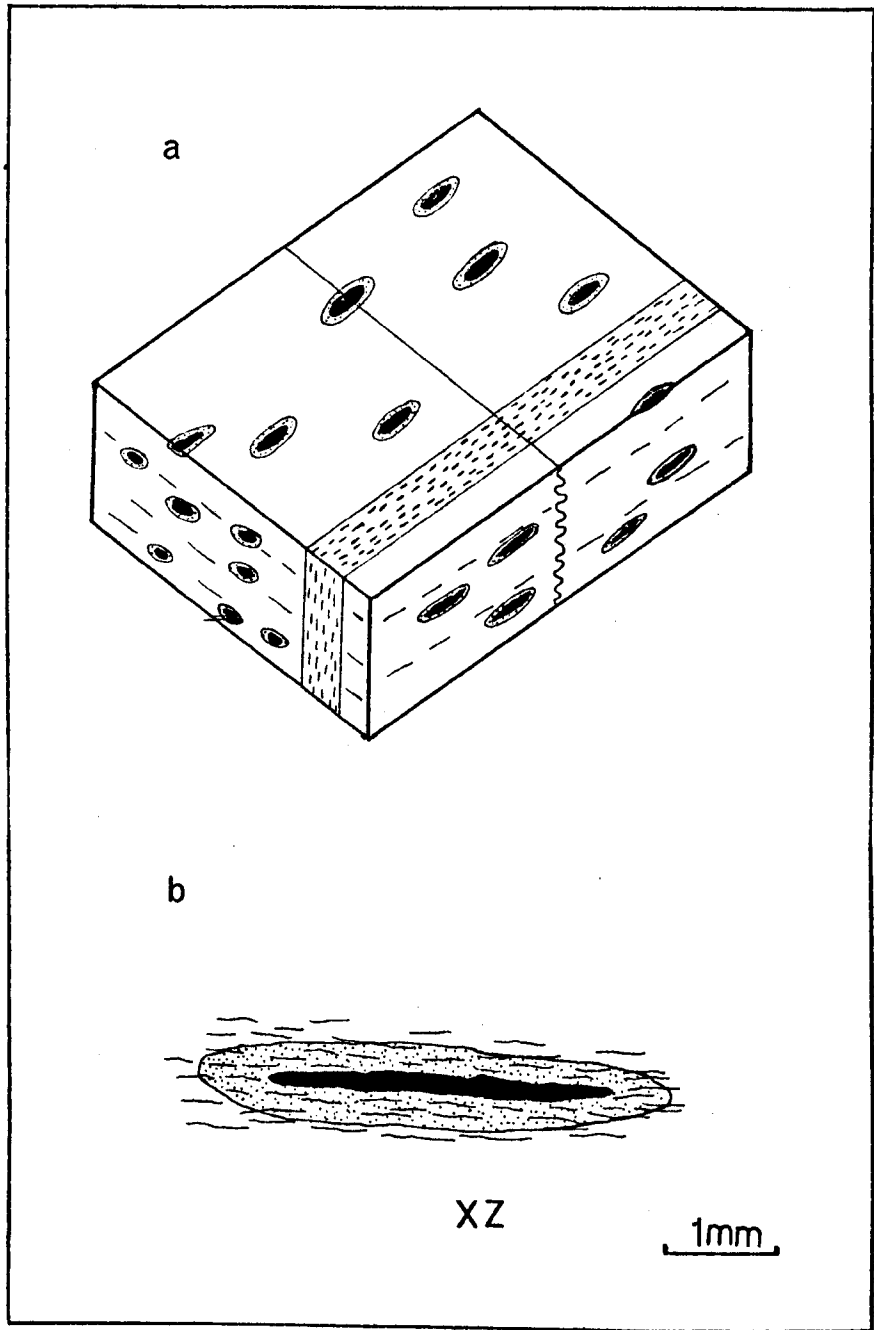
FIG.7.16

a. Geometry of deformed spots in relation to bedding and the S_1 cleavage in mudstones, Complexo xistograuvaquico.

Location: Cancelos villiage on north bank of the Rio Douro , 28km southeast of Porto.

b. Detail of spot structure in a, above.

XZ section showing elongate iron-rich core and surrounding halo.



indicate a significant pre-Variscan shape fabric of the pebbles.

The plunge of the F_1 folds (Fig. 2.10b) and S_1 cleavage/bedding intersection lineation (Fig. 7.17b) is largely controlled by the orientation of bedding after the Upper Cambrian folding (Fig. 7.18). The present basin and dome pattern of bedding indicates a tight refolding or cross-folding by F_1 folds. In areas of low DV_1 deformation in the Tra-os-Montes area folds of Upper Cambrian age in the Complexo xisto-grauvaquico have E-W to NE-SW axial planes and shallow plunging axes (Ribeiro, 1974), although the tight refolding makes it difficult to know the precise original orientation of the early folds in the region around the Valongo Anticline. The likely refolding system is shown in figure 7.18.

The plunge of the maximum elongation direction of the pebbles is controlled by this refolding of the bedding and implies a pre-Variscan shape fabric which is planar or planar-linear parallel to bedding.

1. SUBTRACTION OF THE DV_1 VARISCAN STRAIN

A technique described by Elliot (1970) for determining initial elliptical shapes from finite strains has been employed here to subtract the Variscan strain from the finite strain in the Complexo xisto-grauvaquico to establish the nature of the pebble fabric after the Upper Cambrian folding and to determine how that fabric evolved.

FIG. 7.17

Stereographic plots of linear structures in the
Complexo xisto-grauvaquico.

a. Plunge of the maximum elongation direction in
conglomerates.

▲ DOURO ● COVELO ■ AROUCA
✦ ORDOVICIAN ○ OTHERS IN VALONGO ANTICLINE

b. Plunge of fold axes, F_1 , and cleavage, S_1 , /bedding
intersection lineation.

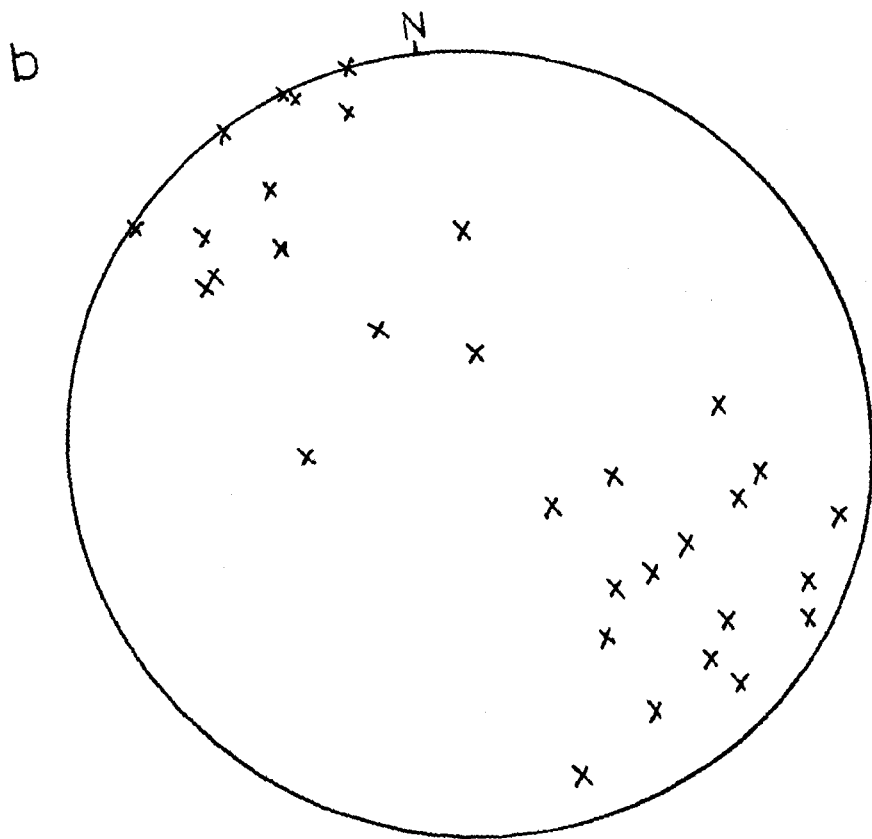
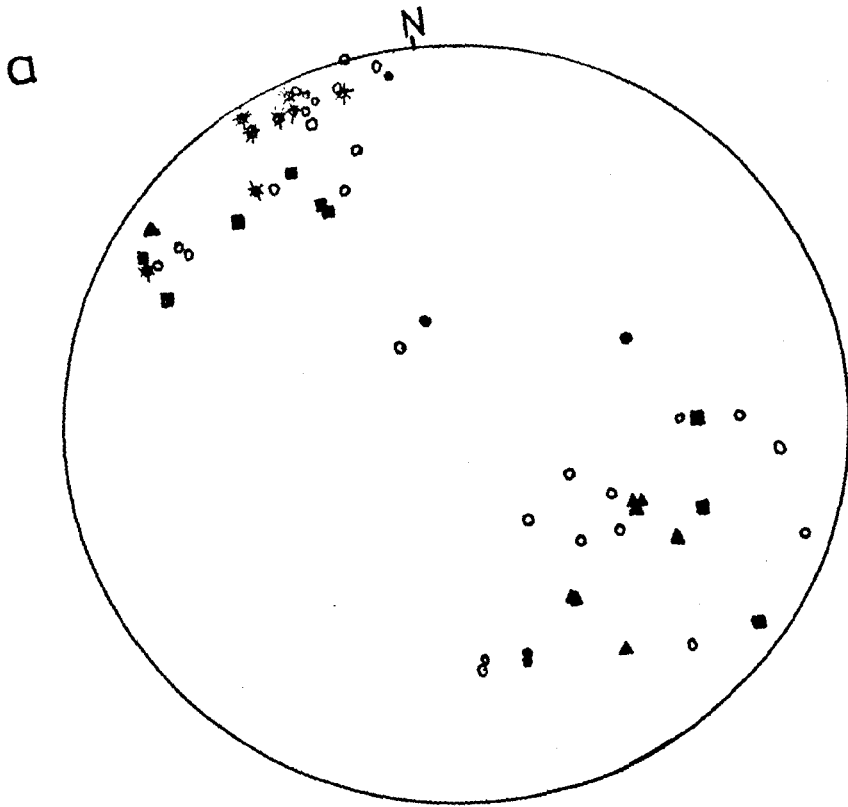


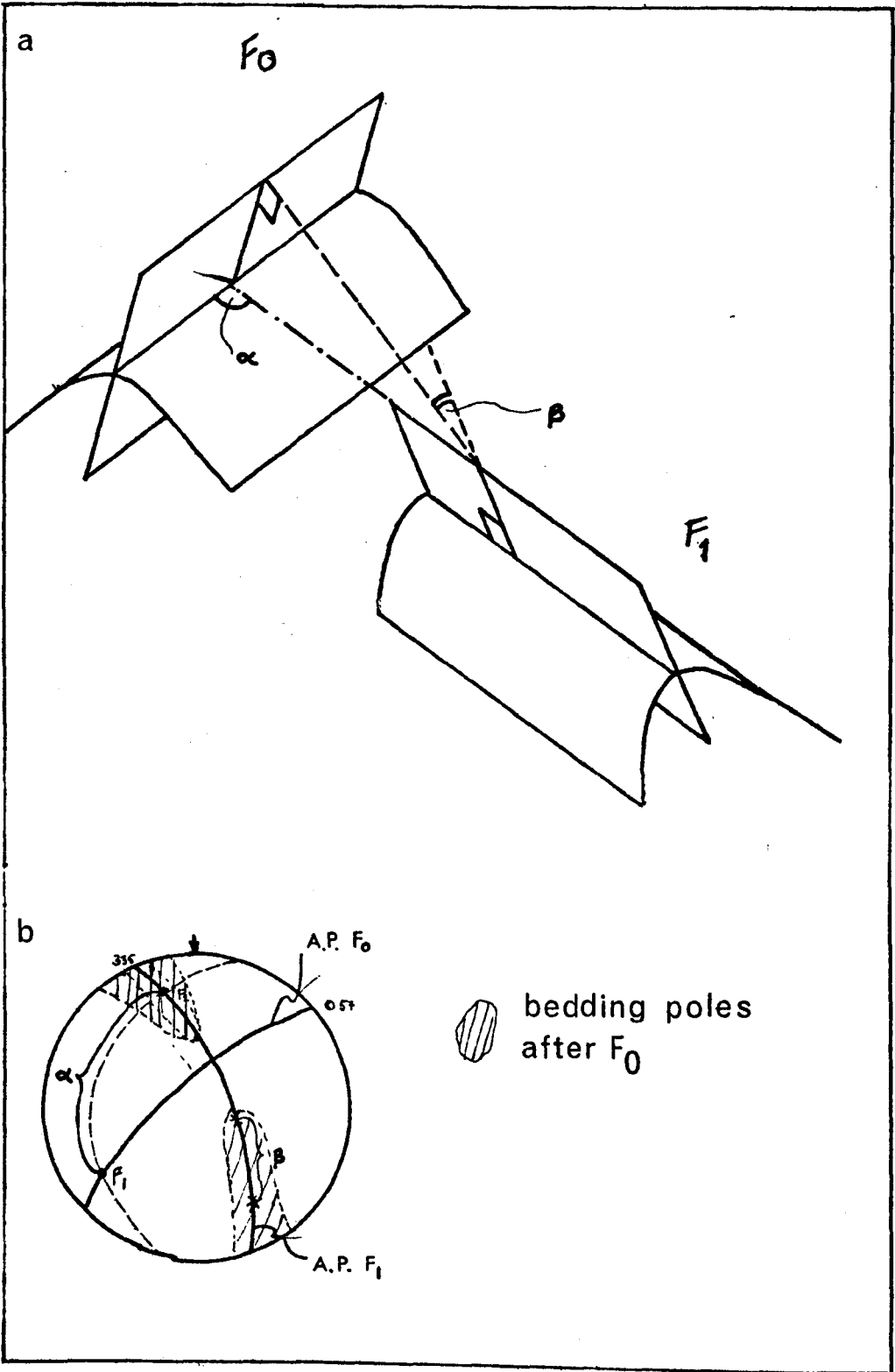
FIG.7.18

a. Diagrammatic representation of the refolding in the Complexo xisto-grauvaquico.

F₀ Upper Cambrian folds

F₁ Variscan folds.

b. Stereographic plot of a. above.



The Variscan strain (DV_1) in the Valongo Anticline region is relatively homogeneous and for the purposes of subtraction it is approximated to an average plane strain 1.63 (X) : 1.00 (Y) : 0.61 (Z). The X, Y strain ellipse for DV_1 with horizontal X axis is subtracted from the X, Y finite strain ellipse, with a variable plunge of X, for the combined Upper Cambrian and DV_1 deformations (Fig. 7.19a). The result of the subtraction gives the orientation and value for an elliptical section of the initial pebble which may or may not coincide with the principal plane X Y as the third dimension is not considered.

For the shape factor grid the pre-Variscan and resultant strain ellipses for X Y are expressed in terms of ξ_1 , ξ_s , and ξ_f respectively, where:

$$\xi = \frac{1}{2} \ln \left(\frac{X}{Y} \right);$$

the orientation of the x axes are θ_i , θ_s and θ_f (Elliot, 1970).

Firstly, the orientation of the X axes (θ_f) and finite strain (ξ_f) for the conglomerates, as measured, shows a broad increase in strain with increasing plunge of the X axis (Fig. 7.21a). With subtraction of the Variscan strain (ξ_s), with constant horizontal X direction ($\theta_s = 0$). the pre-Variscan pebble fabric (i , θ_i) indicates a more random distribution but still high pebble axial ratios for steep plunges (Fig. 7.21b).

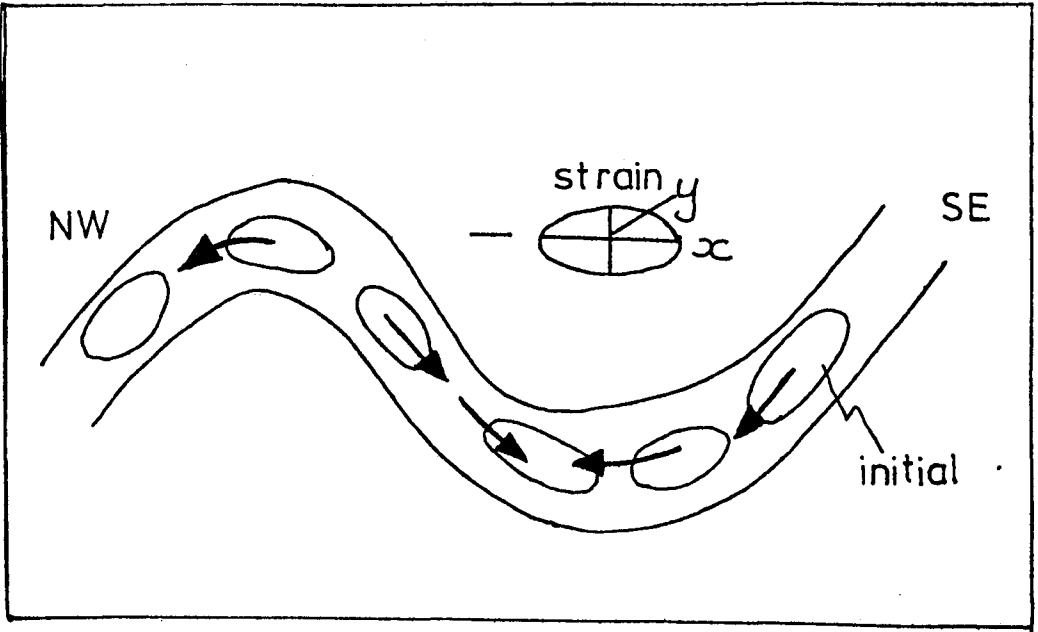
FIG. 7.19

a. Simplified section to show the the initial pebble ellipses prior to DV_1 .

Strain ellipse for Variscan deformation , DV_1 , is shown XY.

b. Parameters used in graphical plot for subtracting the Variscan strain (after Elliot, 1970).

a



b

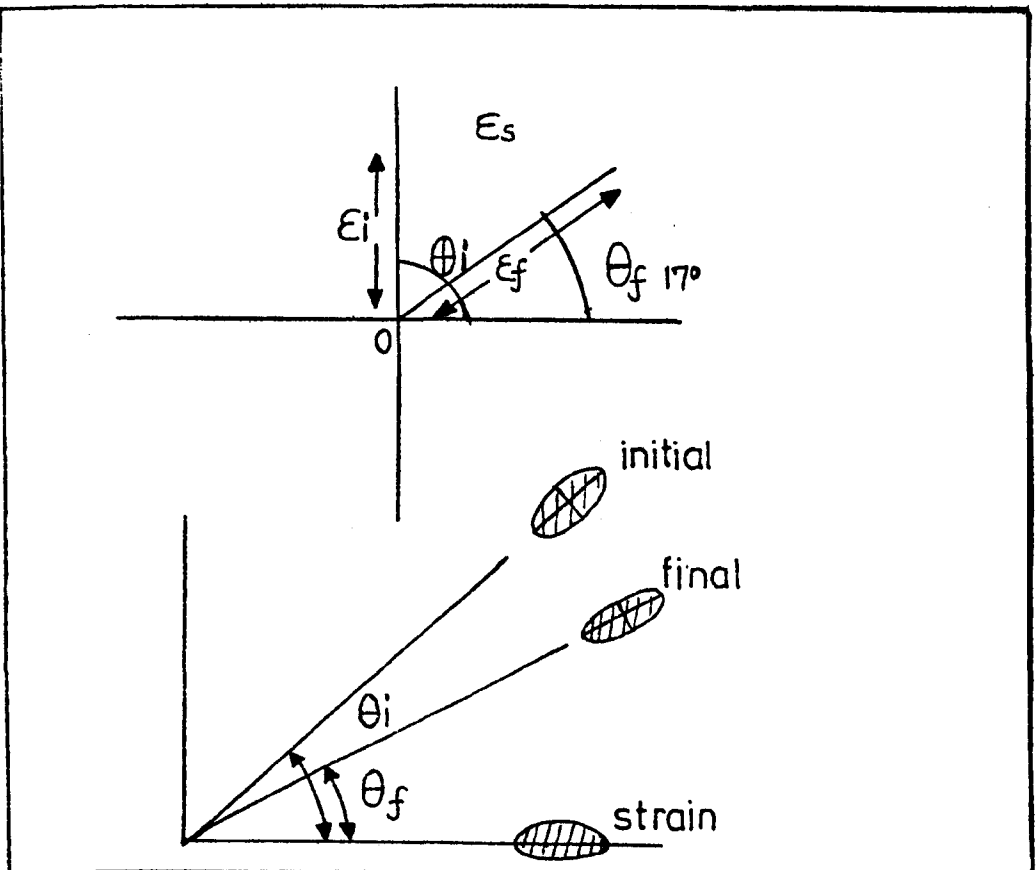


FIG. 7.20

Table of strain values

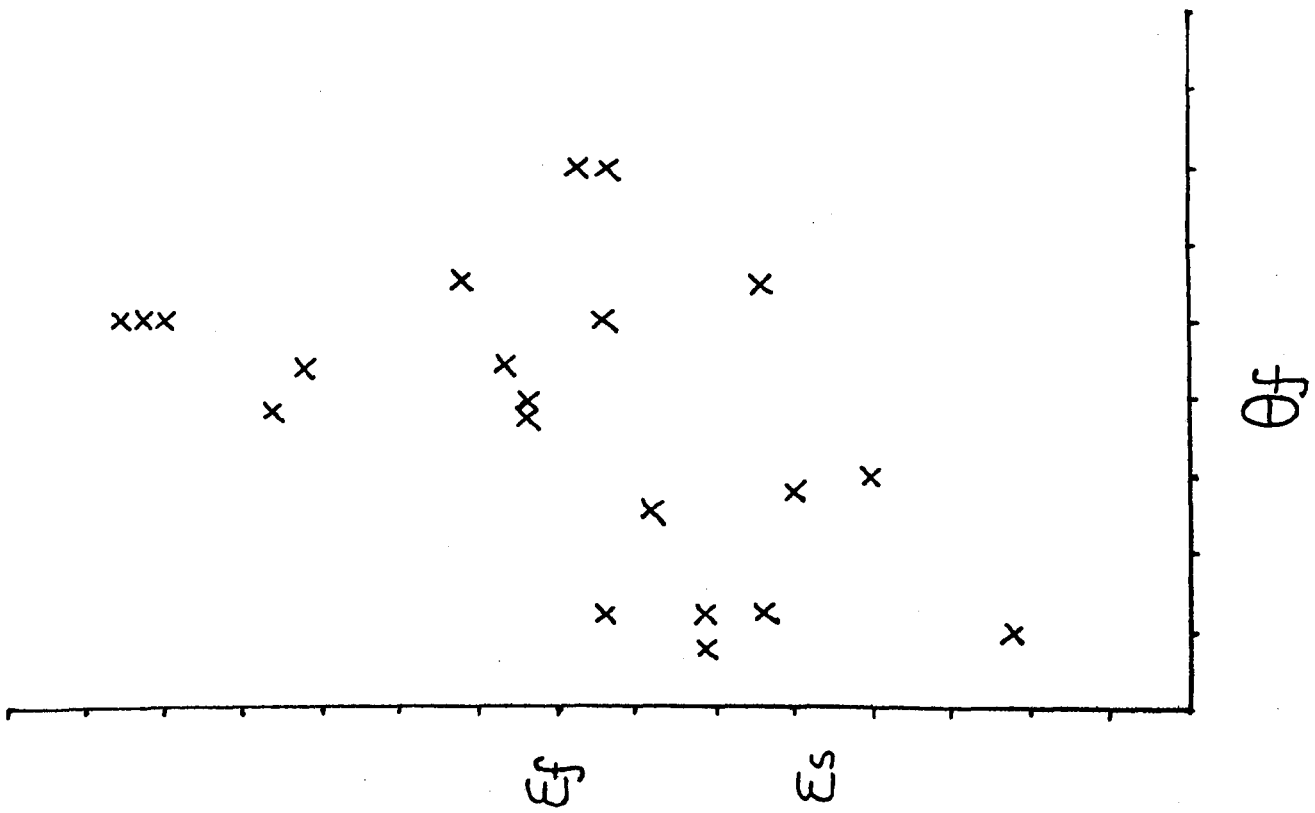
SPECIMEN NUMBER	ϵ_f	θ_f	ϵ_i	θ_i
D63	0.58	38	0.56	53.5
D64	0.20	30	0.22	63
D69	0.68	50	0.73	60
D69A	0.66	50	0.71	60
D70	0.64	50	0.70	60
D81	0.11	10	0.12	82
D92A	0.42	38	0.43	55
D93	0.307	8	0.11	25
D92B	0.39	38	0.43	57
D96	0.39	70	0.57	79
D97	0.37	50	0.46	66.5
D115	0.37	12	0.20	27
D116	0.25	24	0.14	56
D117	0.34	25	0.24	48
A50	0.24	35	0.27	62
A52	0.47	22	0.36	37
AR1	0.58	35	0.57	50
AR2	0.44	35	0.41	53
DL1(A)	0.28	46	0.37	67
DL2(B)	0.40	40	0.48	58
A49	0.49	40	0.44	56
DA(O)	0.33	10	0.10	27

FIG. 7.21

a. Graphical plot of final pebble ellipsoids ξ_f / θ_f

b. Graphical plot of pre-Variscan pebble ellipsoids

ξ_i / θ_i



Based upon the subtraction model the large and constrictional type finite strains in the deformed pebbles at many locations support the existence of some earlier fabric prior to the Variscan deformation. Constrictional strains from single deformations are known but they are the result of special conditions of high strain or below thrust planes (Flinn, 1956; Hossack, 1968).

It is difficult to suggest a significant early ductile deformation of the pebbles due to the absence of an Upper Cambrian age cleavage, which implies that the early fabric developed by rigid rotation during folding, possibly enhanced by a planar compactional fabric.

The large axial ratios of the elliptical sections of the initial pebbles (E_i) may imply that the model is too simplified and that the superimposition of the Variscan strain was much more complex (see Ghosh, 1974 for experimental work), with inhomogeneous Variscan strain in the Complexo xisto-grauvaquico. Although these initial pebble ratios ($X;Y$) are higher in a few cases than for undeformed pebbles (Flinn, 1956), it is considered that they correspond to $X Z$ or near $X Z$ elliptical sections. Hence, the steeply plunging (X) high finite strains are due to superimposition of the Variscan strain upon pebbles strongly aligned within the plane of the bedding in the limbs of the Upper Cambrian folds with their X axes normal to the fold axes and Z axes near normal to bedding (Fig. 7.22a). The lower strains tend to

be less steeply plunging and it is envisaged that a fold mechanism of flexural slip, with some flexural flow, has orientated the pebbles during the development of the Upper Cambrian folds with alignment increasing normal to the fold axes (Fig. 7.22a).

Ghosh and Ramberg (1976) state that there is a likely re-orientation of rigid inclusions parallel to X during simple shear and parallelism to X increases if the pebbles are closely spaced (Ghosh and Sengupta, 1973).

Although the bulk strain for the Variscan deformation (DV_1) is essentially plane strain, with a sub-vertical plane of flattening and horizontal elongations (Fig. 7.22b), oblique flexural-slip and flexural-flow were almost certainly important deformation mechanisms during F_1 folding of inclined anisotropic beds of the Complexo xisto-grauvaquico (Fig. 7.22c) (Ramsay, 1967 p.396). This would result in steep plunges of the X direction of the finite strain ellipsoid sub-parallel to the axes in the limbs of F_1 folds.

2. THEORETICAL SUPERIMPOSED STRAINS

The variation in finite strain resulting from the superimposition of a constant plane strain (DV_1) on undeformed pebbles orientated in 6 co-axial positions related to the plane strain is investigated.

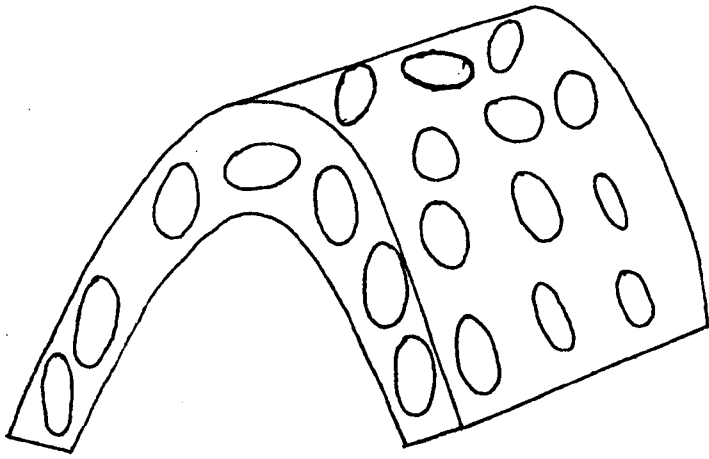
The undeformed pebble shape and Variscan strain are both

FIG. 7.22

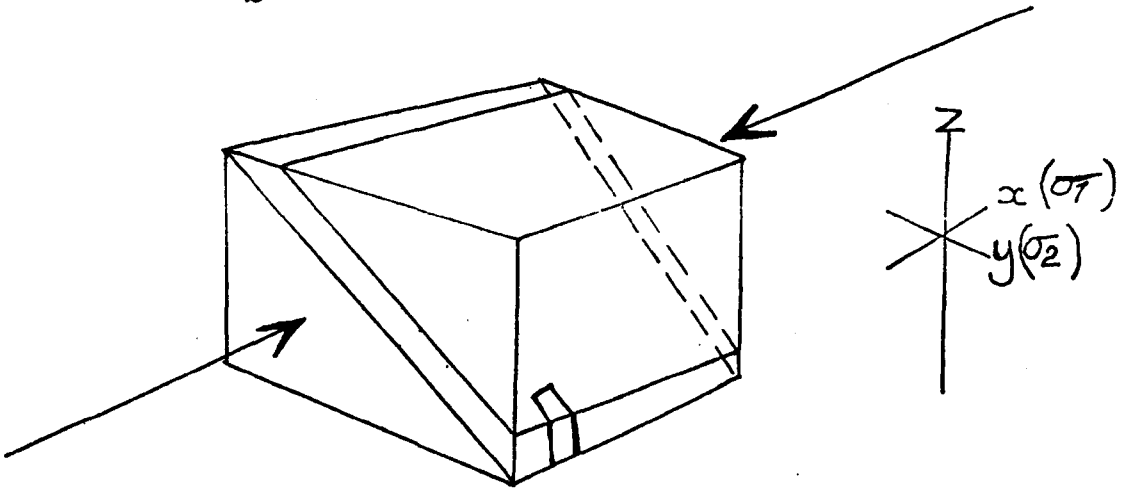
a. Diagram of pebble orientations after Upper Cambrian folding around F_0 fold.

b. & c. Oblique flexural-slip folding after Ramsay, 1967, p396.

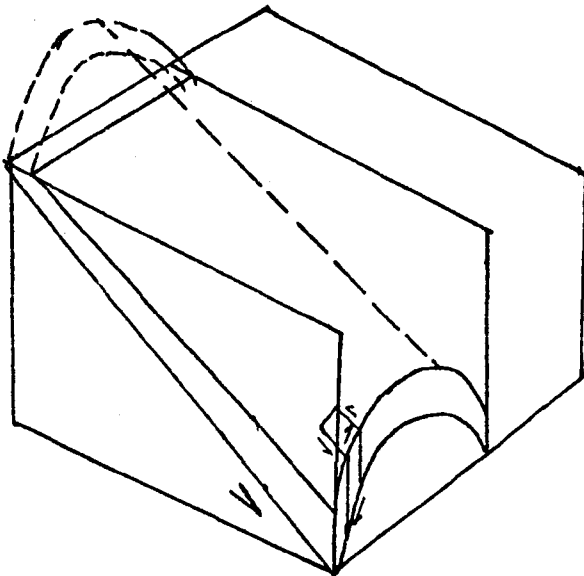
a



b



c



expressed in terms of natural strain parameters (see section 7.5.1) i.e. ξ_x , ξ_y and ξ_z for each ellipsoid. These ellipsoids can be added simply, to obtain the resultant ellipsoid. The undeformed pebble parameters were taken as:

Undeformed pebble $\xi_{ox} = 0.4$, $\xi_{oy} = 0$, $\xi_{oz} = 0.4$;
the Variscan Strain $\xi_{sx} = 0.5$, $\xi_{sy} = 0$, $\xi_{sz} = 0.5$.

(ξ_s average strain calculated from field measurements).

The six cases are presented in figure 7.23. A synoptic representation of the resultant ellipsoids is presented in figure 7.24 with the finite strain field for the deformed conglomerates. The majority of the finite strain measurements lie in the area between (1) and (2) supporting the hypothesis that the pre-Variscan fabric in the conglomerates was a planar-linear one, with the X direction normal to the Upper Cambrian folds within or near the plane of the later S_1 plane of flattening.

The inhomogeneity of the finite strain is due to the non-coaxial superimposition of the Variscan strain upon pebbles with different orientations. Passive rotation of early fabrics within the bedding during F_1 folding will cause migration from one case to another i.e. (1) to (5) for extreme orientations.

FIG. 7.23

Table of co-axial superimposed strains representing
the Pebble shapes for Upper Cambrian O the Variscan
strain T and the final pebble shapes F .

End column shows the six co-axial cases plotted on
Flinn Plot.

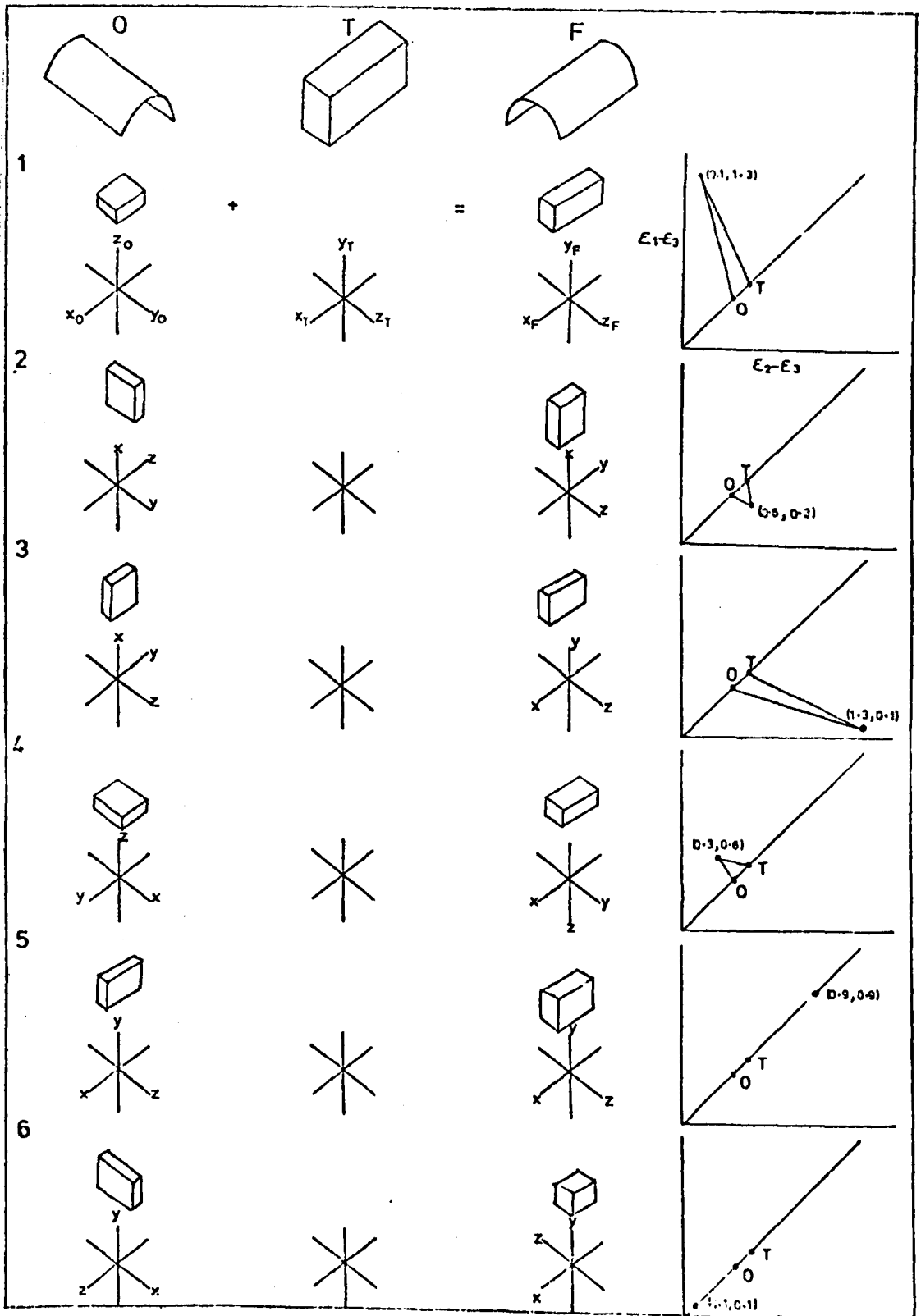
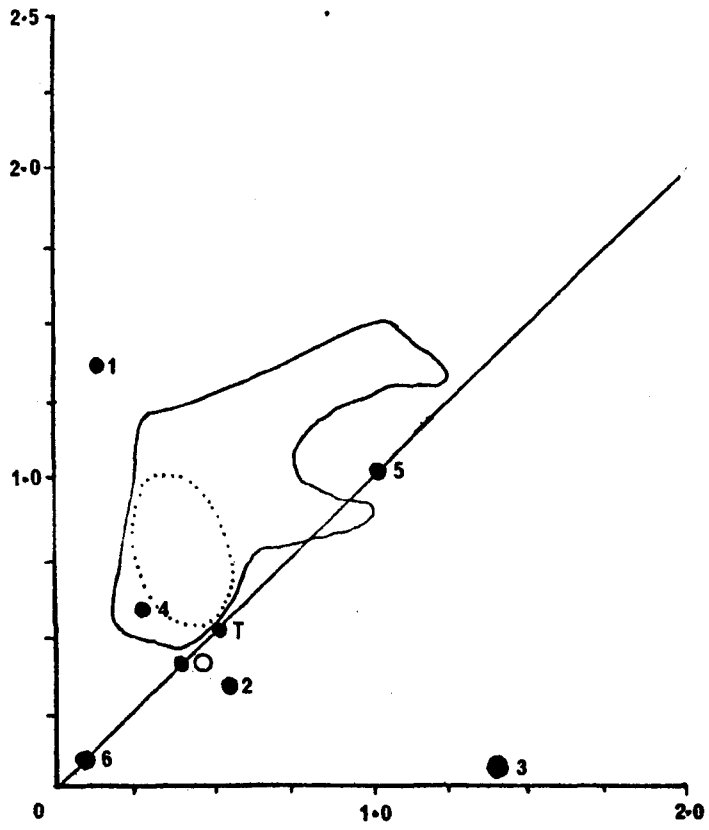


FIG. 7.24

Synoptic plot of the six co-axial cases of the super-imposed strain , using derived values .

The deformation field of final pebble strains is shown by the solid line.

Dotted line encloses the high concentration of pebble strains.



7.6 SUMMARY

The following statements summarise the deformation of the conglomerates in the Complexo xisto-grauvaquico.

1. The finite strain in the conglomerates is inhomogeneous across the region of the Valongo Anticline.
2. The finite strains vary between strong constrictional types ($K = 3.37$) and plane strain with the maximum plane of flattening (X Y) parallel to the S_1 cleavage.
3. The plunge of the maximum elongation direction is steep to shallow, sub-parallel to plunging F_1 fold axes and cleavage S_1 /bedding intersection lineations within the plane of S_1 cleavage.
4. Finite strain increases with increasing plunge of the maximum elongation direction.
5. It is demonstrated that the finite strain in the pebbles results from superimposition of a Variscan ductile deformation on a pre-existing shape fabric.
6. From strain analysis using deformed objects in the Ordovician rocks (see Chapter 6) the Variscan component of the strain is ductile and approximates to plane strain. The plunge of the maximum elongation direction is sub-horizontal to 20° N.W. parallel to the F_1 fold axes and lies within the

S₁ cleavage. Subtractions of this strain from the finite strain in Complejo xisto-grauvaquico conglomerates show that the long axes of the pebbles were previously aligned approximately in the plane of the bedding and normal to the Upper Cambrian fold axes.

7. Theoretical models of strain superimposition support the existence of this early pebble fabric.

8. The pre-Variscan fabric in the conglomerates is considered to have resulted from the rigid rotation of pebbles during folding by flexural-slip/flexural flow in Upper Cambrian times.

THE DEVELOPMENT OF TEXTURES IN THE ORDOVICIAN QUARTZITES

Massive quartzites of the Santa Justa Formation (Armorican Quartzite S.1) are an important component of the three major DV_1 folds studied in the fold belt. The microtextures of these quartzites are described and the degree of deformation they indicate is discussed.

8.1 GENERAL FEATURES OF THE QUARTZITES

There are a number of important features of the quartzites which influence the development of the textures observed.

1. The quartzites examined are massive, with bed thicknesses exceeding 0.5m, relatively homogeneous in composition and of consistent grain size i.e. medium sand (0.25 - 0.5 mm) (Pettijohn et.al. 1973 p.71).
2. The quartzites are commonly composed of 100% silica, i.e. orthoquartzites (silica cemented quartz grains) but often contain subordinate amounts of detrital and metamorphic minerals e.g. sericite, muscovite, tourmaline. The subordinate minerals may facilitate recrystallisation, especially by pressure solution.
3. The quartzites were collected from the steep limbs of folds, where cleavage is parallel to bedding and outside locally anomalously strained hinge zones.

4. A mesoscopic cleavage or shape fabric is not always present.

5. The quartzites are within areas of low grade regional, and in some cases thermal metamorphism.

Comparable quartzites of the same age in the Variscan Fold Belt of Spain and Brittany are little deformed. (Ries, 1974).

8.2 UNDEFORMED QUARTZITES OF THE PENACOVA SYNCLINE

The massive quartzites at Penacova contain undeformed fossil burrows and do not possess a cleavage. In thin section original detrital grains are easily identified under plane polarised light by the dusty coatings around their surfaces (Fig.8.1b). They are cemented by silica which is in optical continuity with the host grains (Fig.8.1a). There is no evidence of any pressure solution at grain boundaries or in the cement and all grains are optically strain-free. The texture is homogeneous within beds and there is little or no preferred orientation of the grains (Fig.8.2a).

8.3 DEFORMATION TEXTURES OF THE QUARTZITES OF THE VALONGO ANTICLINE

A variety of deformation textures are developed in the quartzites along the Valongo Anticline. In all the quartzites the grains show some indication of internal deformation or strain.

FIG. 8.1

Undeformed orthoquartzite

a. Quartz cement in optical continuity with detrital
quartz grains X12 †

Specimen no. P40

Penacova

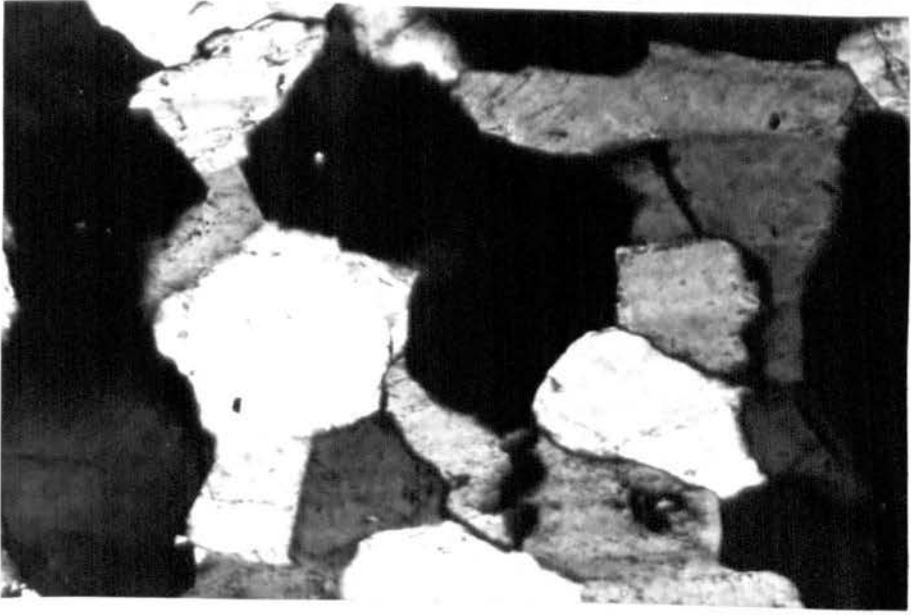
b.

Rounded detrital grain boundaries in specimen above.

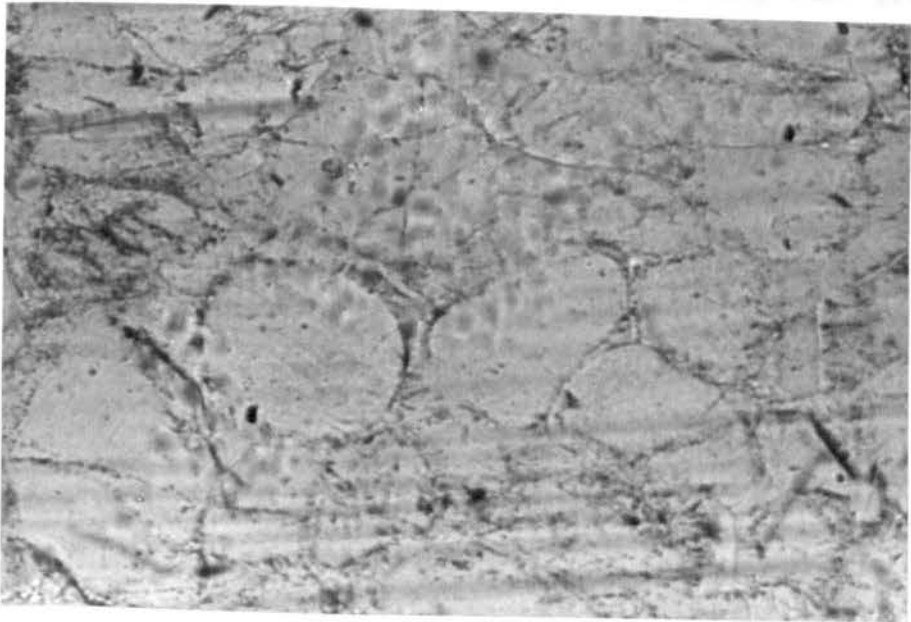
X12

†

a



b



In the least deformed quartzites detrital grains are still distinguishable but most of the grain boundaries are corrugated or stylolitic in along incipient cleavage planes due to pressure solution (Fig.8.2b). More prominent stylolitic planes or seams commonly develop at approximately 5 mm intervals producing a more prominent cleavage with a weak preferred orientation of the quartz. More commonly mortar textures are developed with extensive recrystallisation and the formation of small grains ($\approx 0.02\text{mm}$) around the boundaries of detrital grains (Fig.8.3a). There are several possible explanations for the evolution of this texture e.g. ductile or brittle cataclasis (see Fellows, 1943; Vernon, 1976 pp 178-179). However, in the same quartzites fractures and thin deformation bands tend to develop within large detrital grains and consist of small sub-grains. These zones are breaking up large grains and recrystallising sub-grains; both processes leading to a grain size reduction or cataclastic effect. A weak preferred orientation of the detrital grains has evolved in some of these quartzites with dominantly mortar textures.

Quartz with lobate or sutured grain boundaries is the second texture to develop (Fig.8.4a). These grain boundaries develop partly due to the grains recrystallising into smaller new grains possibly by grain boundary sliding during creep deformation or grain boundary migration during syntectonic recrystallisation (Vernon, 1976 p.181). Most

FIG. 8.2

a. General undeformed texture of the orthoquartzites
at Penacova.

X5 †

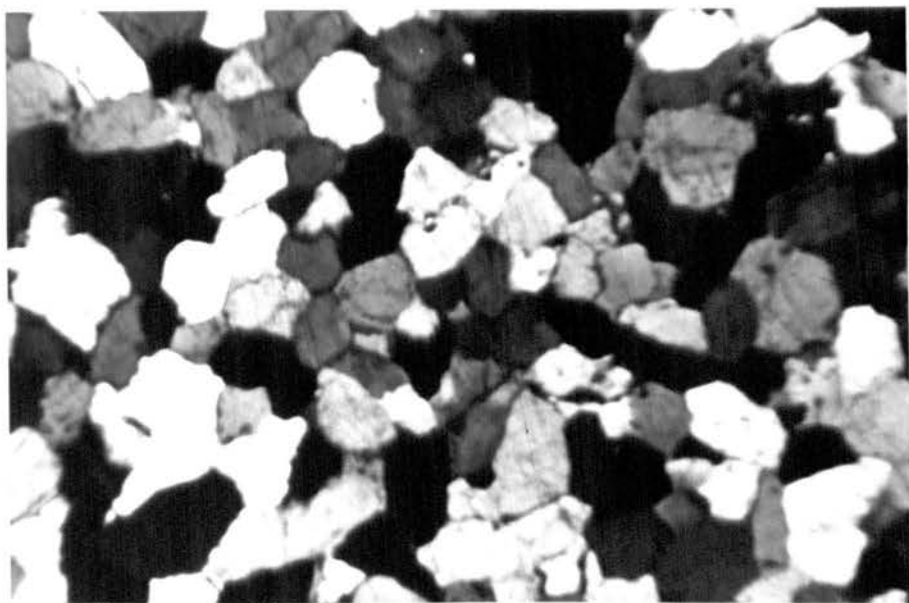
b. Stylolitic grain boundaries in weakly deformed
quartzite

X45 †

Specimen no. D121A

Arouca

a



b

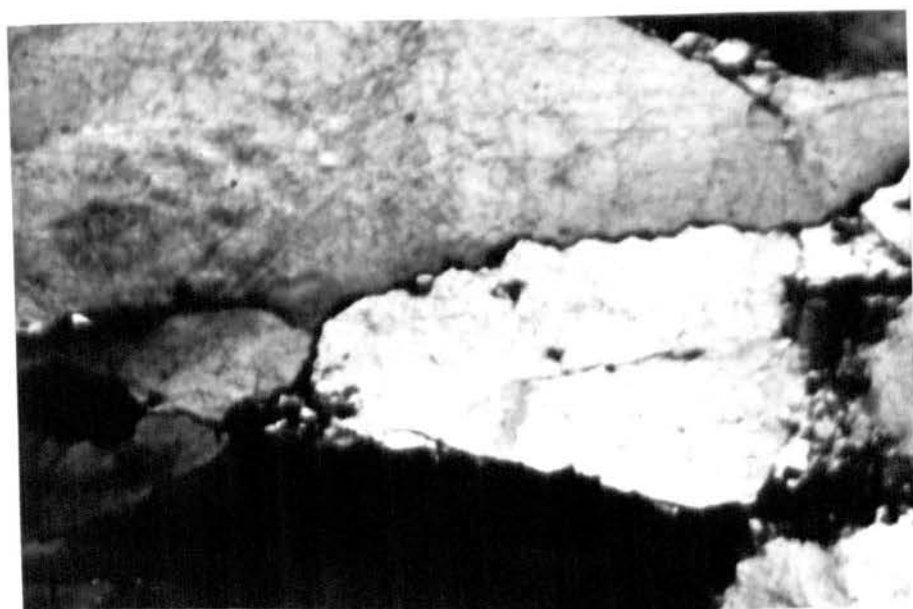


FIG. 8.3

a. Mortar texture in deformed quartzite,

Large detrital grains broken down into small new grains around and within grains.

X40 ~~†~~

Specimen no. D111

Pias, Valongo Anticline.

b. Detail of boundary of deformation band in quartz grain.

Lower half of photo is part of the detrital grain

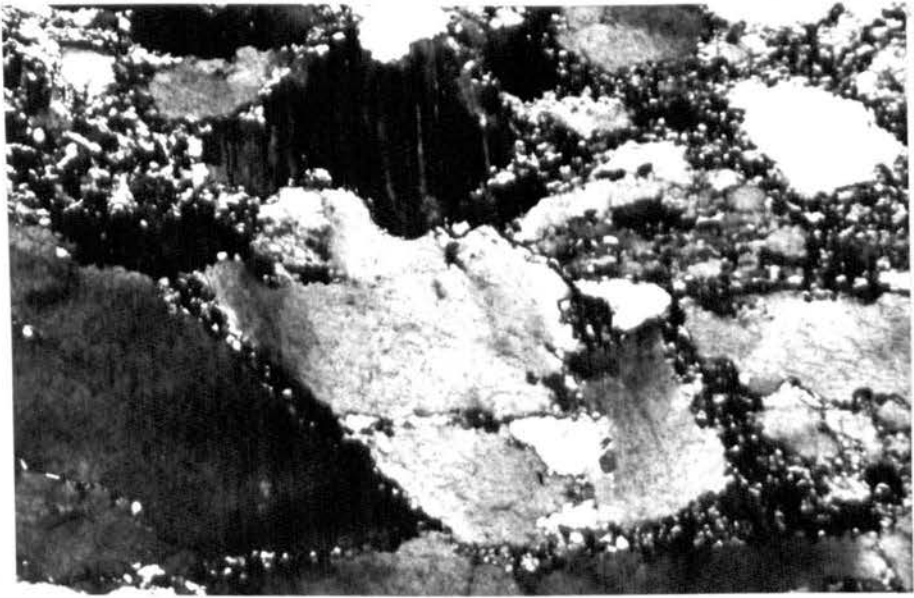
Top half of photo is strained detrital grain formed into strained sub-grains in deformation band.

New strain-free grains on boundary of deformation band.

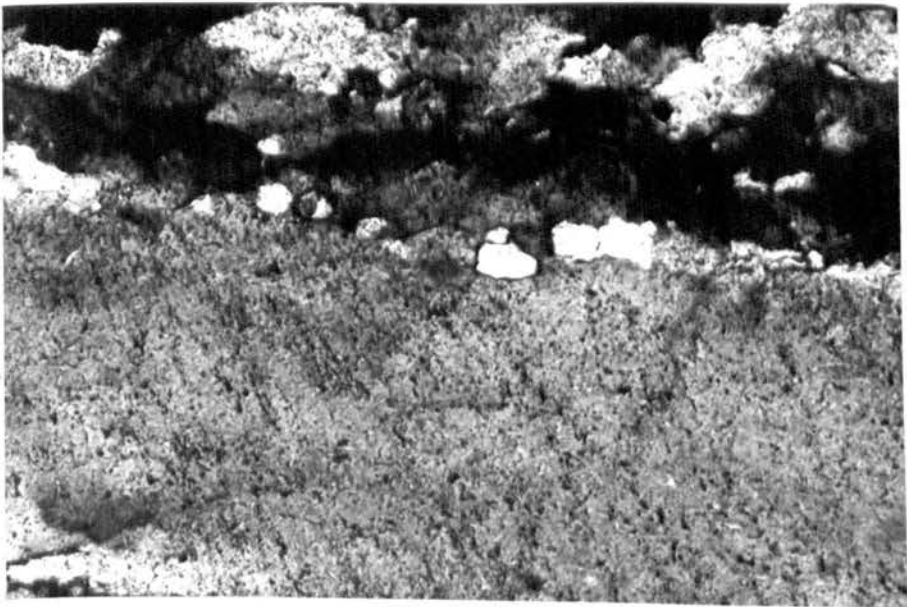
X150 ~~†~~

Acres, Valongo Anticline

a



b



grains in these quartzites are sutured all round indicating that the texture is unlikely to be the result of pressure solution which tends to be restricted to parallel planes. A weak to strong preferred orientation is developed in these quartzites.

In similar quartzites with slightly increased deformation highly strained grains have developed deformation bands (Vernon, op.cit. p.175) typical of low temperature and relatively fast strain rates.

In detail these bands are narrow shear zones deforming the grain from boundary to boundary with up to 0.2 mm displacement (Fig.8.6a). Other bands of similar width (0.5mm) develop parallel to each other within single grains, parallel to (0001) but many only show undulose extinction (see Fig. 8.7a) with little apparent displacement.

Within the zones or bands the host grain is recrystallised into sub-grains which are elongate parallel to the bands or shearing direction (Figs.8.3b; 8.7b). These sub-grains are themselves strained and show an overall undulose extinction pattern similar to the non-displacement bands in the same grain. At the sharp boundaries of the bands new, small sharply banded, optically strain-free grains result from recovery (Vernon, op.cit. p.166).

These shear zones result in reducing the grain size of the quartzites.

FIG. 8.4

a. Sutured and lobate grain boundaries in quartzite.

n.b. small sub-grains at some grain boundaries.

X36 ✱

Specimen no. D123

Arouca.

b. Pressure solution seams , E-W, in impure quartzite.

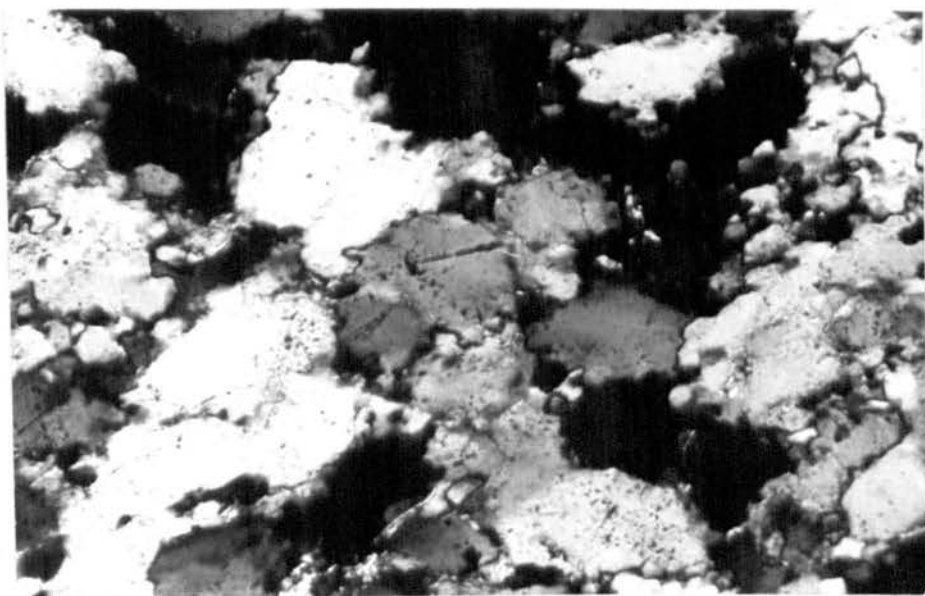
n.b. Some grains have planar truncated boundaries

X36 ✱

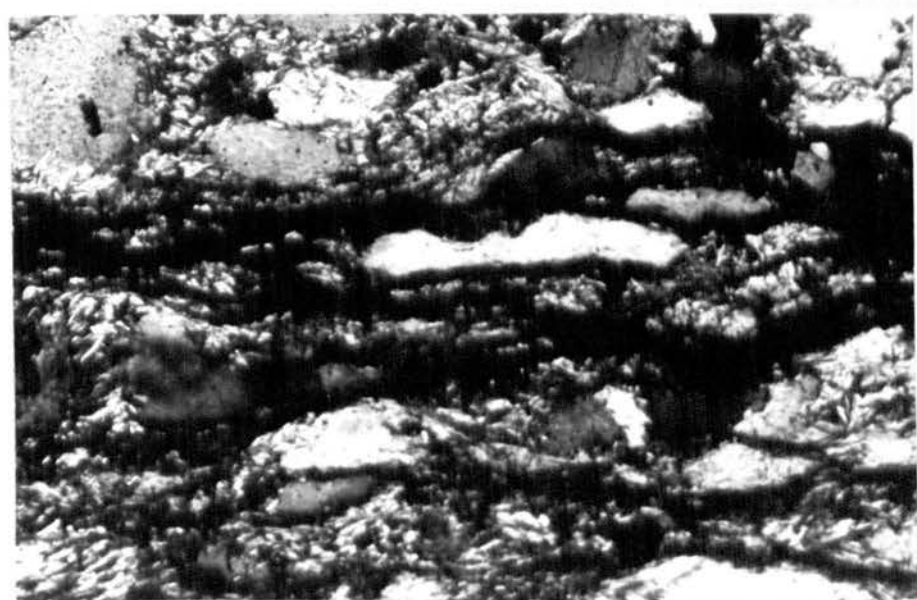
Specimen D111

Pias , Valongo Anticline

a



b



Another texture associated with quartzites in the same region which contain subordinate micas is a well developed pressure solution cleavage. On the east limb of the Valongo Anticline near the summit of the Pias the quartzites develop a cleavage which in detail consists of thin pressure solution seams of concentrated micas. Unstrained grains are truncated by the seams and attain very elongate shapes and consequently a strong preferred orientation or mineral fabric (Fig.8.4b).

The most deformed textures are rare developments of ribbon quartz in narrow zones of deformation (less than 1 mm) in similar specimens of quartzite to those examined (Fig.8.6a). These zones are very localised and do not reflect the overall state of deformation.

8.4 DEFORMATIONAL AND ANNEALED TEXTURES IN QUARTZITES OF THE MARÃO SYNCLINE

The quartzites in Marão have strong shape fabrics and early pressure solution seams (see Fig.5.16a). However, most of the textures in this area result largely from a post-tectonic recrystallisation or annealing which has greatly modified the early S_1 grain fabric.

Single grains in the least annealed rocks have a preserved preferred orientation with serrated and lobate grain boundaries (Fig.8.5b).

FIG. 8.5

Variation in general grain boundary form in the Ordovician quartzite.

Traced from projected thin sections.

a. Undeformed angular grains , Penacova.

X13

b. Elongate grains with preferred orientation and pressure solution , stylolitic grain boundaries, Arouca

X9

c. Serrated and lobate grain boundaries with preferred orientation of grains. Marao.

X13

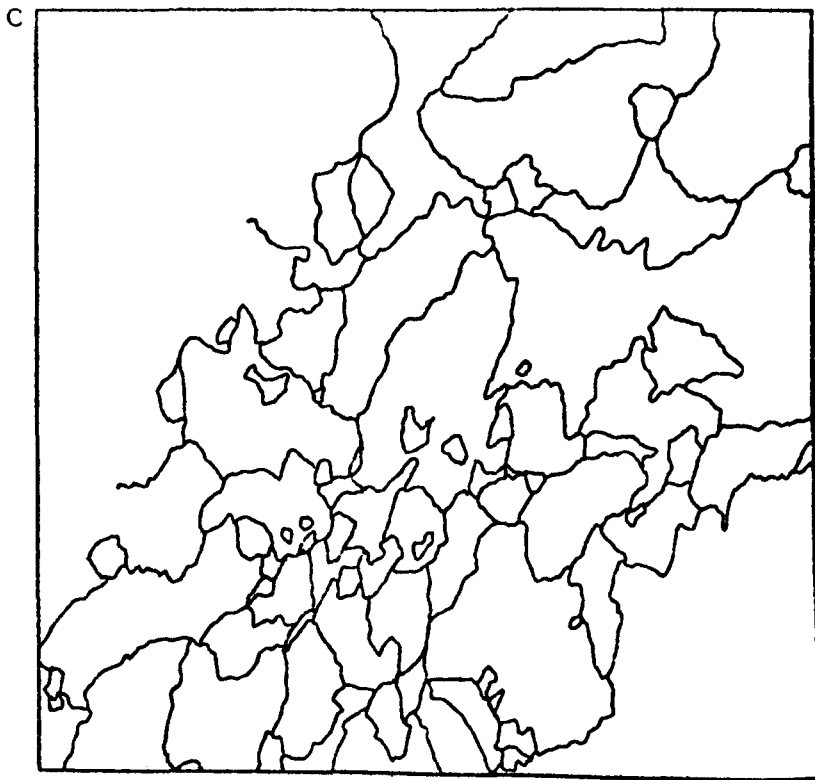
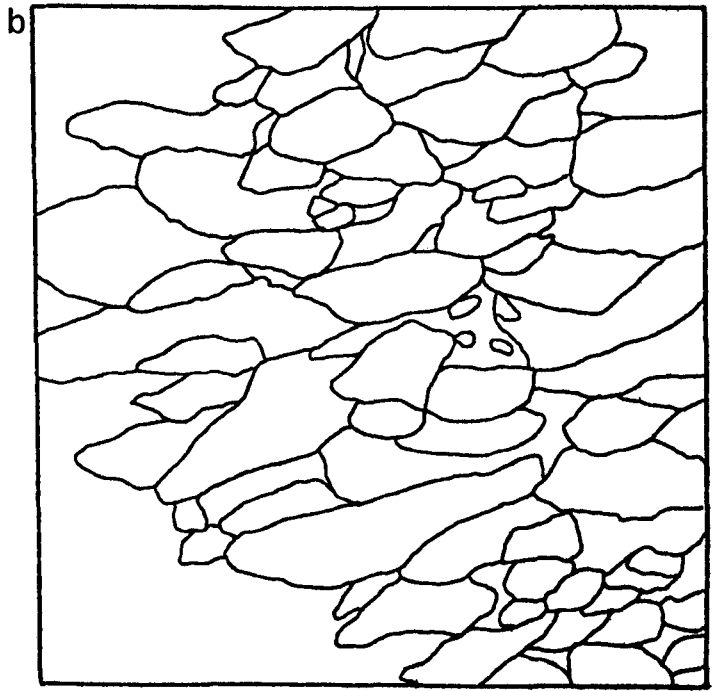
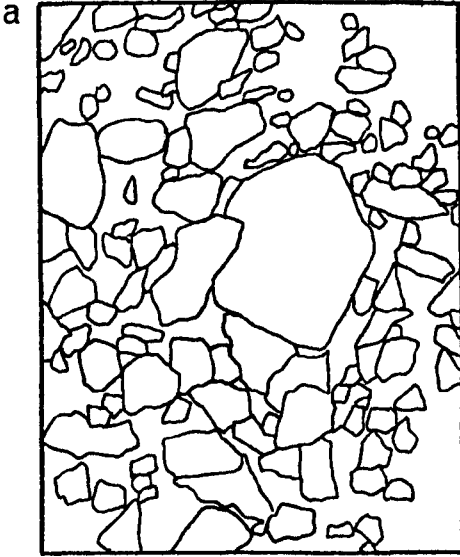


FIG. 8.6

a. Ribbon quartz in high strain zones between large grains.

X50 ~~†~~

Specimen no. D121A,

Arouca.

b. Partially annealed texture with S_1 preserved in in the alignment of muscovite and sericite , NW-SE

X 10 ~~†~~

Specimen M207

Marao.

a



b

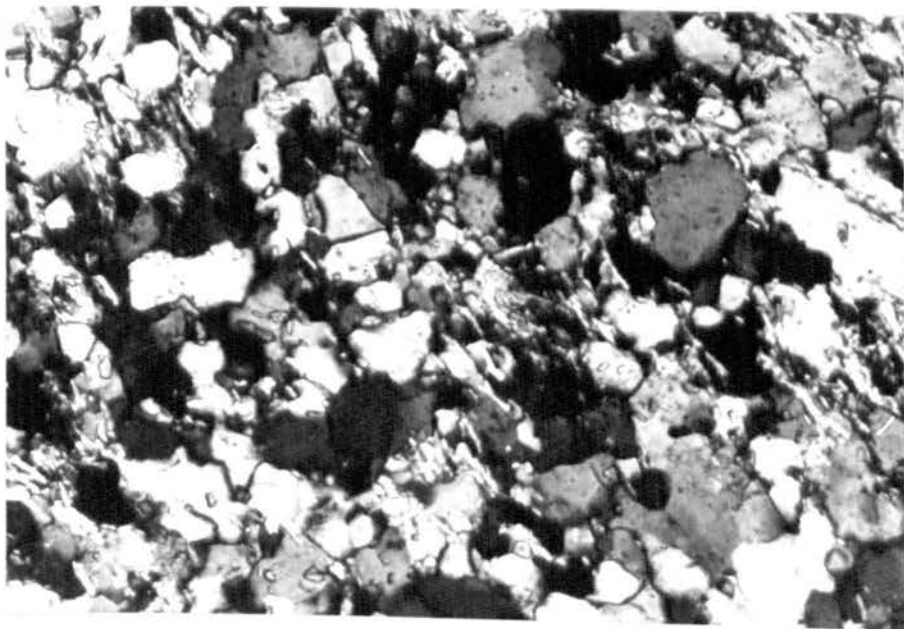


FIG. 8.7

a. Deformation band in single quartz grain.

Drawn from projected thin section.

X100

Specimen D101.

Acres , Valongo Anticline.

b. Detail of deformation band (photomicrograph 8.3b)
area shown in the above figure.

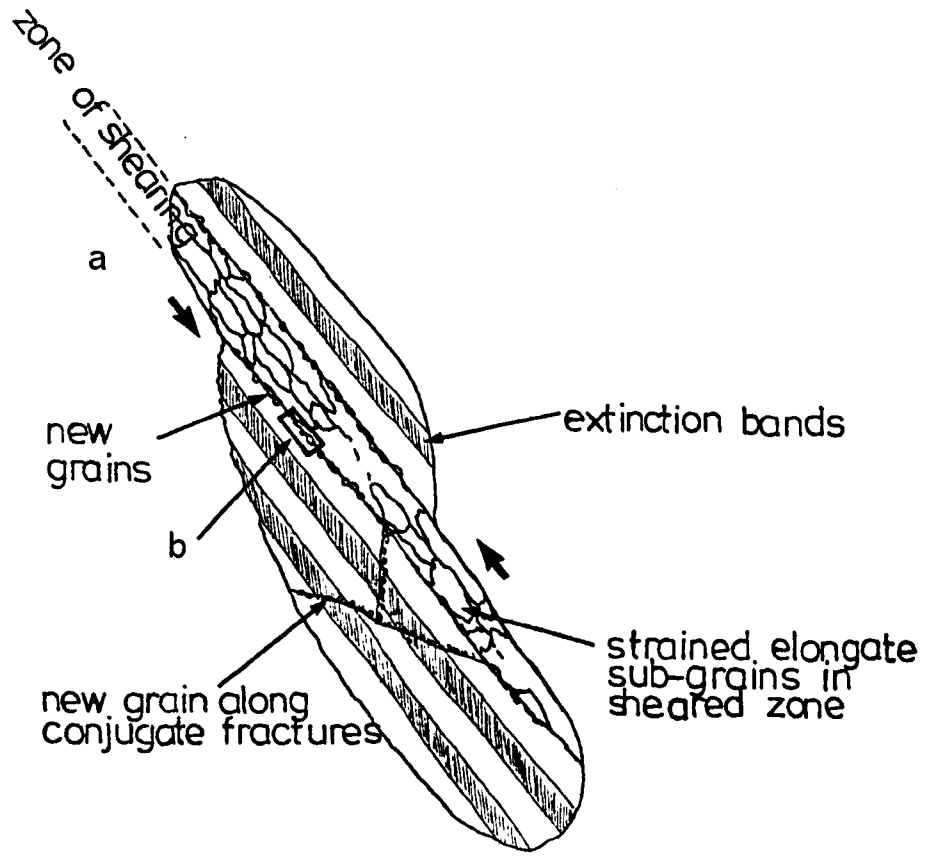
A = detrital grain

B = boundary

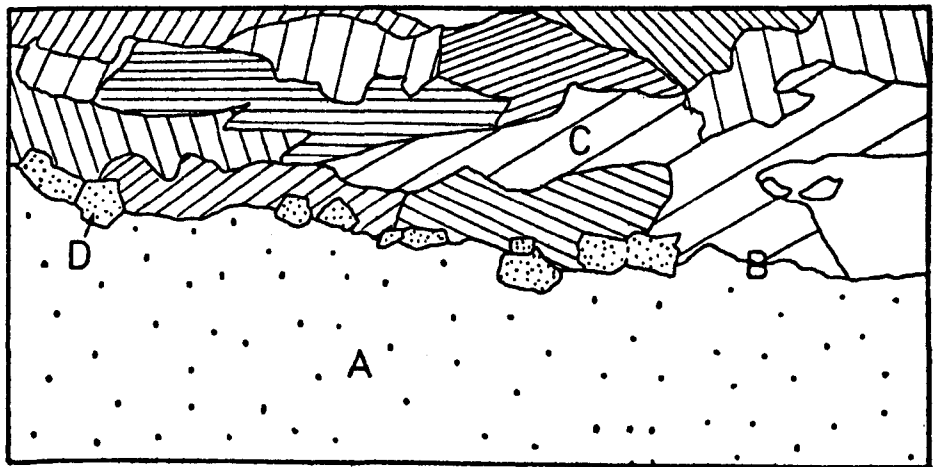
C = strained subgrains in deformation band

D = new strain-free grains

a



b



This grain shape orientation is possibly due to the growth of grains during annealing being faster in the direction parallel to pre-existing deformation bands or strained lattice (Vernon, 1976).

The strong shape fabrics developed in the impure quartzites of Central Maranhão are a result of plastic recrystallisation and pressure solution (Fig.5.14a).

In thin section the textures are largely annealed.

The grains are largely unstrained and the preferred orientation of quartz grains is weakened, while the grain aggregates retain a shape fabric. In many specimens the quartz texture is close to being granoblastic (Fig.8.6b) but the platy minerals still maintain a strong preferred orientation.

The annealed textures in these quartzites are the result of post tectonic recrystallisation in the aureole of Younger Variscan Granites (zone D, Fig.1.9) and the deformation textures must have developed at slightly higher temperatures than in the other areas.

The common equigranular nature of the present textures suggests that they did not anneal from mortar type textures, but rather from elongate grains which were either plastically deformed or the result of pressure solution.

8.5 SUMMARY

It is evident that the massive quartzites in the

Penacova Syncline are unstrained and possess original diagenetic textures. Regional metamorphism has not strongly recrystallised these quartzites although slates of the same area have new aligned platy minerals muscovite and chlorite. There is no cleavage in the quartzites and deformation in the synclinal limbs has been by flexural slip on discrete bedding planes with only a small amount of flattening (see deformed spots in marls, Chapter 4).

The quartzites of the Valongo Anticline do have a cleavage in places and display a range of textures indicative of low to moderate deformation.

The type of deformation mechanism varies from one of dominantly pressure solution, with the development of stylolites in the least deformed quartzites and discrete seams as deformation increases to one of cataclasis with grain size reduction by production of sub-grains and crystallisation of new grains. Occasionally, high strain zones have the beginnings of ribbon-quartz textures.

In the Marão Syncline, the textures are largely annealed although grain- or shape-fabrics are partially preserved.

Preferred orientations of grains in the different quartzites indicates greater deformation in the Valongo Anticline and Marão Syncline than in the Penacova Syncline (Fig.8.5).

Although these quartzites are the least strained

rocks of the region the development of quartz textures indicates a change across the fold belt east-northeastwards from undeformed to essentially brittle and pressure solution deformation, to ductile and pressure solution deformations.

LATE VARISCAN DUCTILE-BRITTLE STRUCTURES

Following the formation of the D_2 folds and cleavage further crustal shortening and thickening was achieved by ductile-brittle and brittle deformation along discrete, well-defined zones i.e. narrow shear zones and kink bands.

Similar structures occur throughout the region mainly affecting the Complejo xisto-grauvaquico, Ordovician and Silurian metasediments.

9.1 CLASSIFICATION OF STRUCTURES

Those ductile-brittle and brittle structures observed are summarised in Fig. 9.1.

This summary classifies the structures according to the following:

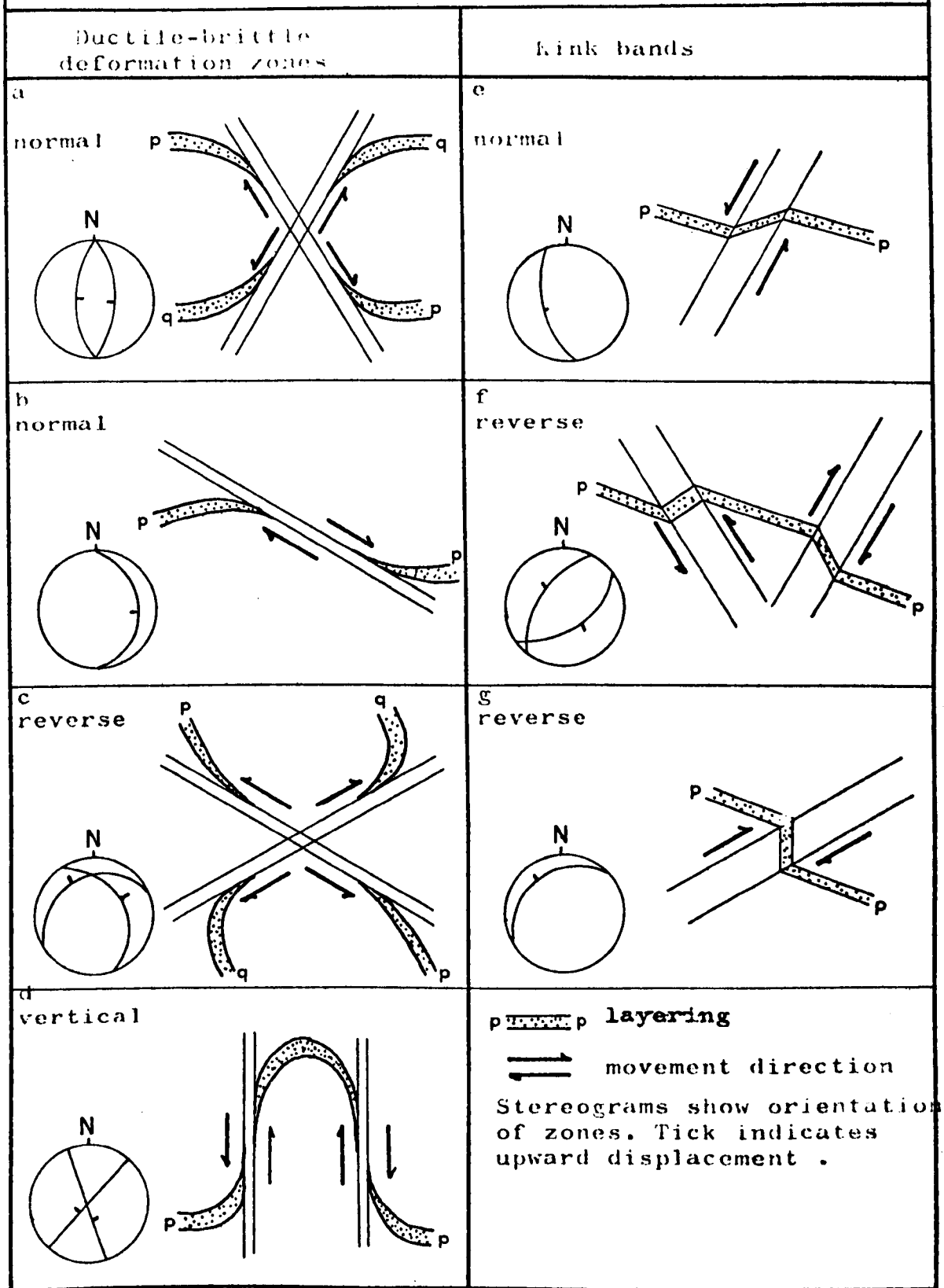
1. The internal structure of the deformation zone i.e. ductile and brittle sub-structures, brittle, or layer boundary slip structures.
2. The attitude of the deformation zone.
3. The sense and direction of movement on the deformation zone.

The two major groups of structures are described below.

FIG. 9.1

CLASSIFICATION OF LATE VARISCAN

DUCTILE-BRITTLE STRUCTURES



DUCTILE-BRITTLE DEFORMATION ZONES

Deformation in these zones is initially by ductile simple shear in the form of low angle overthrusts (Fig. 9.1c), or occasionally as high and low angle shear zones with a normal sense of movement (Fig. 9.1a, b). Brittle deformation is also an essential component of these zones.

The zones range in width from a few centimetres to two metres and usually consist of an inner unit of brittle deformation bounded sharply by two dislocation surfaces (Fig. 9.2), flanked by outer units of ductile deformation only, where layers are attenuated.

The sense of movement on each zone was deduced from the geometry of the attenuated layering and other elements e.g. lineations rotating into the zone, while some brittle deformation may be attributable to a later, separate period of movement. In most cases, however, the ductile deformation increases towards the inner unit of relative high strain such that the layers appear to have been progressively and continuously deformed passing from a ductile to a brittle mechanism.

The ductile shear strain in the outer units is low i.e. less than 1, estimated from the passive rotation of layers in the zone. Displacements across the zones are of the order of a metre (Fig. 9.2b) to estimated tens of metres for the widest zones. Pebbles are occasionally reformed

FIG. 9.2a. Vertical section through a ductile-brittle deformation zone with a normal sense of movement. The zone, dipping 35° west, deforms siltstones of the Complexo Xisto-grauvaquico. The dislocation surfaces separating the inner brittle zone from the outer ductile zones are indicated by arrows.

Location: The core region of the Valongo Anticline at Cha do Arvoredo, 1km east of Beloi.

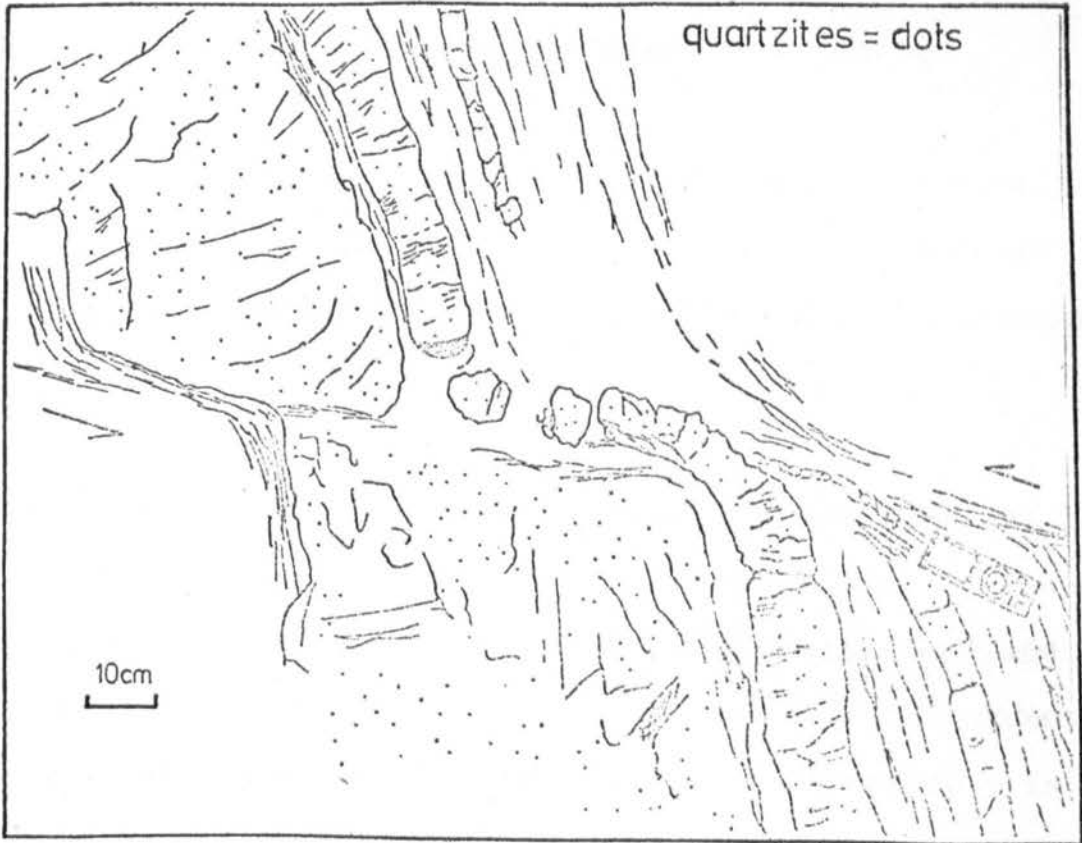
FIG. 9.2b. Low angle, ductile-brittle deformation zone with a reverse or overthrust movement developed in Ordovician quartzites and thin bedded siltstones. Note the attenuation and boudinage of quartzites.

Location: Western limb of the Valongo Anticline, 3km west of Melres on the N108 from Porto.

a



b



in such zones (Fig. 7.3) resulting in new shape fabrics. Further examples of superimposed shape fabrics result from small scale, sub-vertical, conjugate zones which reformat Ordovician conglomerate pebbles at Viana do Castelo (Fig. 3.9a).

KINK BANDS

The second group of structures described are collectively referred to as large scale kink bands or zigzag folds (Ramsay, 1967 p.436) such that the internal deformation of the material is dominantly by slip along the surfaces of the layers. These kink bands develop preferentially to the first group of structures in rocks which exhibit a strong planar anisotropy. Their development is most concentrated in the region around Arouca in strongly fissile siltstones and mudstones of the Complexo xisto-grauvaquico.

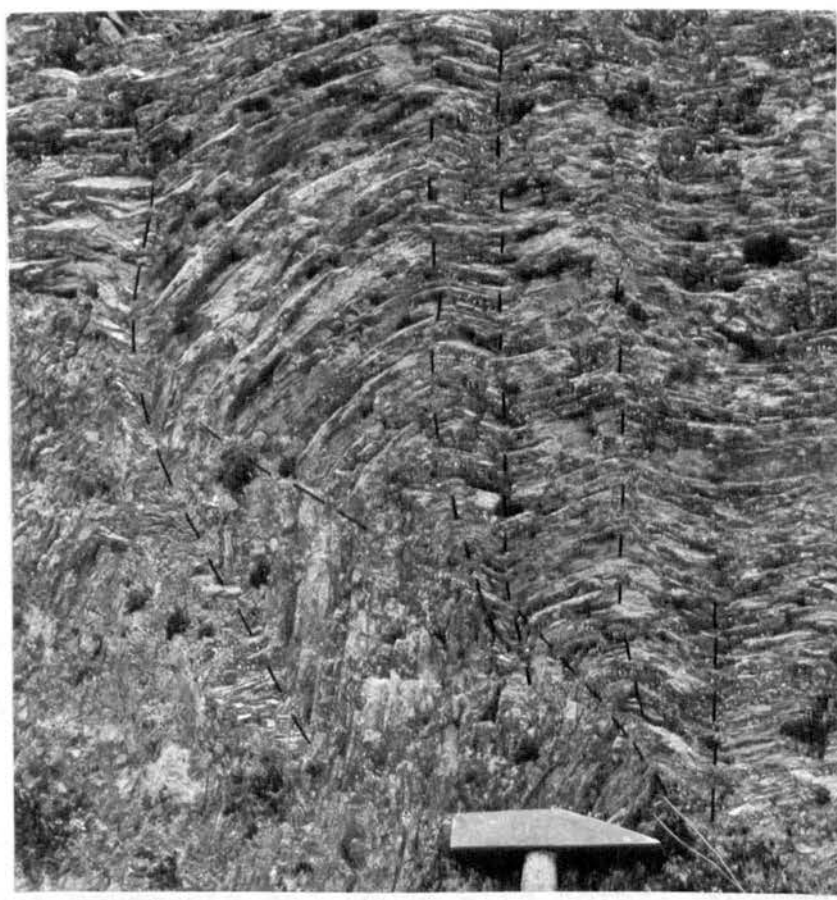
The kink bands occur either as single or multiple kinked zones (Figs. 9.3b, 9.3a respectively), but are relatively infrequent and are commonly spaced a kilometre apart.

The widths of the zones ranges between 10cm and 1.5m, 1m being the most common. The kink bands have corresponding attitudes and movement directions to the ductile-brittle zones, although the orientation of any kink structures is closely determined by the degree of anisotropy in the rock and the orientation of the layering with respect to

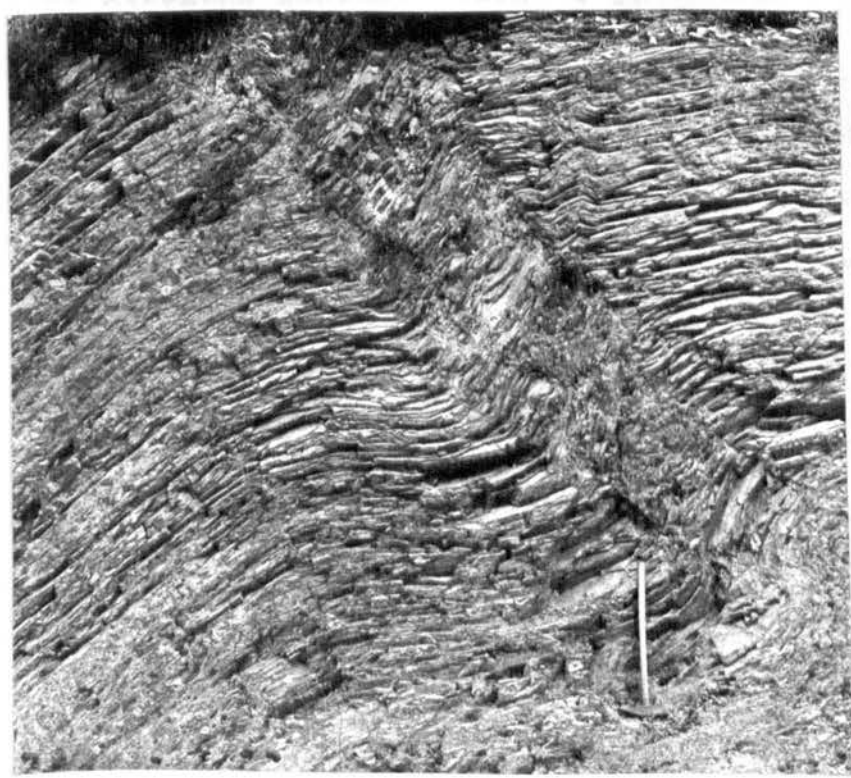
FIG. 9.3a. A multiple kink zone showing the traces of anastomosing kink surfaces developed in staurolitic mica schists of the Complexo Xisto-grauvaquico. Location: 1km east of Foz do Sousa east of Valongo.

FIG. 9.3b. A single reverse kink band developed in micaceous siltstones of the Complexo Xisto-grauvaquico. The prominent planar anisotropy is a combined cleavage S_1 and bedding. The kink band dips to the north west. Location: 500m east of the villiage of Gamarde de Cima in a cutting on the main road to Alverenga 6km north of Arouca.

a



b



the maximum compressive stress (Cosgrove, 1976).

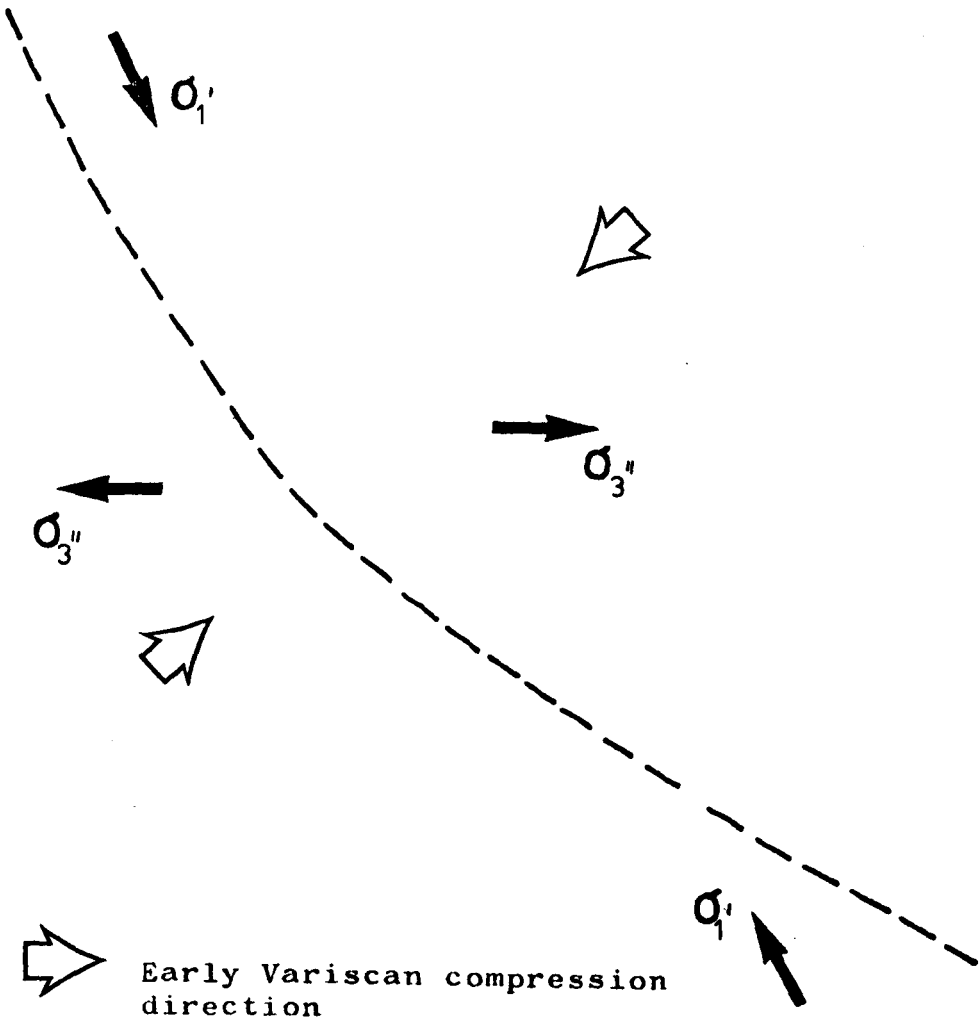
9.2 DISCUSSION



Likening all these structures to smaller scale crenulation cleavage structures and models for their formation (Cosgrove, 1976), it is argued that the two groups of structures developed contemporaneously in rocks of different anisotropy i.e. the kink band structures developed in rocks with a high anisotropy, in terms of the shear and compressive moduli (Cosgrove op.cit.), and the ductile shear zones with associated brittle deformation developed in rocks with a low anisotropy for the same stress conditions.

Grouping the structures into those with reverse or overthrust movements and those with normal movements two palaeostress patterns emerge: (Fig. 9.4)

- a. Crustal compression in a NW-SE direction sub-parallel to the fold belt resulting in high and low angle reverse movement kink bands and low angle ductile-brittle overthrusts.
- b. Crustal extension in an E-W direction resulting in high angle, normal movement, kink bands and ductile-brittle zones.

FIG. 9.4
 PALAEOSTRESS DIRECTIONS FORMING DUCTILE-
 BRITTLE STRUCTURES



-  Early Variscan compression direction
- σ_1' Compressive stress direction forming reverse movement structures
- σ_3'' Tensional stress direction forming normal movement structures
-  Trend of Variscan folds

SLATY CLEAVAGE AND CHLORITE PORPHYROBLASTS

The 'penetrative' S_1 Variscan cleavage developed in the slates of the Valongo Formation is domainal on less than a millimetre scale (Williams, 1972) and displays a post-kinematic relationship to late-diagenetic chlorite porphyroblasts.

10.1 Slaty Cleavage

The dark-blue to grey homogeneous slates of the Valongo Formation possess a slaty cleavage i.e. a planar fabric which appears penetrative in the field, which is domainal in thin section and of a similar structure to the slaty cleavages described by Williams (1972) and Hobbs et. al. (1976), consisting of two types of Domain, A and B.

In thin section at high magnification (x100) type A domains appear as an anastomosing network of thin (0.1mm) dark seams which separate type B domains. The seams comprise mainly phyllosilicates which have a strong preferred planar orientation, subordinate fine-grained quartz, opaques and some clay minerals.

Type B domains or lithons are composed of mainly quartz and phyllosilicates which have a weaker dimensional orientation than type A domains. They are

irregular or lensoidal in shape due to the sinuous and anastomosing bounding seams; their width is variable but, for the most part, is that of the diameter of the largest porphyroblast or quartz grain around which the type A seams wrap (Fig. 10.1a).

The differentiation processes resulting in this domainal structure which manifests itself as a mesoscopic cleavage include local quartz migration, probably by water assisted grain boundary diffusion (Knipe and White, 1976), as indicated by quartz overgrowths around large, competent opaque minerals and porphyroblasts. Elongate quartz grains probably derive their shape from pressure solution and syntaxial overgrowth (see pressure solution in the Armorican Quartzite in Serra do Marão, page 131).

10.2 Crenulation Cleavage

A second, crenulation cleavage (s_2) locally deforms the slaty cleavage and gives rise to a new micro-layering or domainal structure (Fig. 10.2). In most cases the S_2 lithons (c.f. type B domains) partly preserve the texture and fabric of the slaty cleavage, hence the lithons in slaty cleavage may be preserving some of the original texture of the dewatered shale such as the phyllosilicates at a high angle to the seams (type A domains).

Again a local but incipient development of crenulation cleavage (S_2) in fine-grained slates of the

FIG. 10.1a Structure of the slaty cleavage in slates of the Valongo Formation. Dark anastomosing seams (type A domain) wrapping around a lozenge shaped chlorite porphyroblast. White grains are mainly quartz.

Scale bar is 0.1mm. Crossed nicols.

Location: Quarry 200m west of road 1.5km. north of Suzao (2km north of Valongo) towards Quintarei.

Specimen no. 13V.

FIG. 10.1b Slaty cleavage (E-W) in slates of the Valongo Formation. Large white grains (arrowed) are chlorite porphyroblasts; small white grains are mainly quartz. Large opaque mineral is tailed by curved fibre growths of quartz.

Scale bar is 0.5mm. Crossed nicols

Location: 2km south of Valongo. Cutting on road to San Pedro da Cova.

Specimen no. 23V.

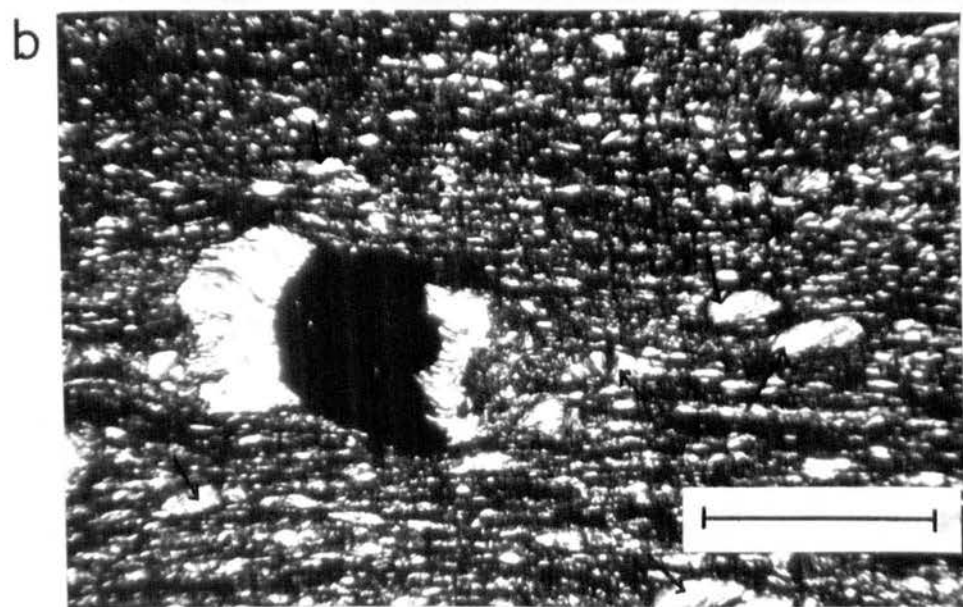
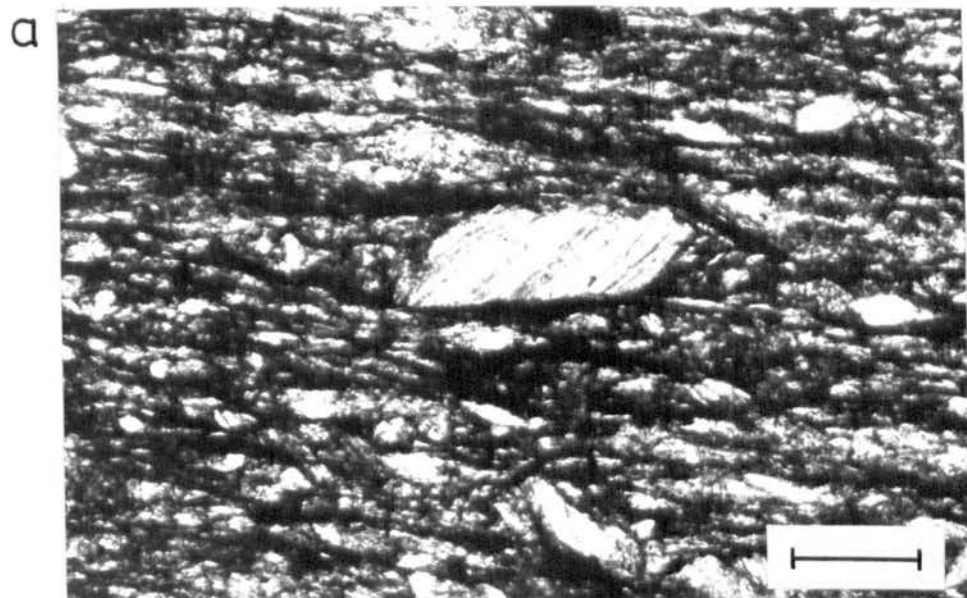


FIG.10.2 Crenulation cleavage (S_2) (N-S) giving rise to a new micro-layering in a quartz-rich siltstone at the base of the Valongo Formation. The slaty cleavage (S_1) (E-W) is partially preserved in the lithons (type B domains) between the thin, dark seams (type A domain).

Scale bar is 0.5mm Plane polarised light.

Location: 1.5km due west the peak, Freitas in the Serra do Marão. A cutting in the track leading to the summit of Marão from the N.15 road 5km west of Campea.

Specimen no. M205.

a



Complexo xisto-grauvaquico indicates ^{that} rotational strain is sometimes important in effecting differentiation to produce a micro-layering. The new cleavage can be seen in different stages of development (Fig. 10.3a,b,c) which is essentially by simple shear (Ramsay, 1967 pp. 388-391), and shows opaque minerals and phyllosilicates concentrated, aligned with some re-crystallisation in the zones of high strain forming a new spaced, domainal layering.

10.3 Nature of the Chlorite Porphyroblasts

Chlorite porphyroblasts are present in those slates of the Valongo Formation which lie outside the zone of contact metamorphism associated with the Variscan Granites within which they are upgraded to chiastolite slates (see Chapter 3, p 89). Most of the textural descriptions are of slates collected in the core of the Valongo Anticline just south of Valongo, and to the north near the small village of Calfaioma (for exact locations see figure captions) where the chlorites are best preserved.

Single porphyroblasts are between 0.1mm and 0.2mm diameter and consist of stacked chlorite crystals in optical continuity. They are anhedral varying from sub-spherical to rounded lozenge shapes. Internally, the chlorites forming sub-spherical porphyroblasts have

FIG. 10.3 a,b,c. Successive stages of development of crenulation cleavage by increasing shear along discrete zones in slates of the Complexo Xisto-grauvaquico. The mineral and shape fabrics comprising the slaty cleavage S_1 (E-W) are deformed in the narrow zones S_2 . Opaque minerals disseminated throughout the matrix are concentrated together with phyllosilicates in these narrow zones of high strain away from which quartz must have migrated .

(a) Narrow zone of low shear strain (approx. =1) (N-S) through which the S_1 fabrics can be traced. Note the elongate shape of the opaque minerals within the zone .

(b) This zone is similar in width to the zone in (a) but the strain is higher and more heterogeneous, increasing towards the centre.

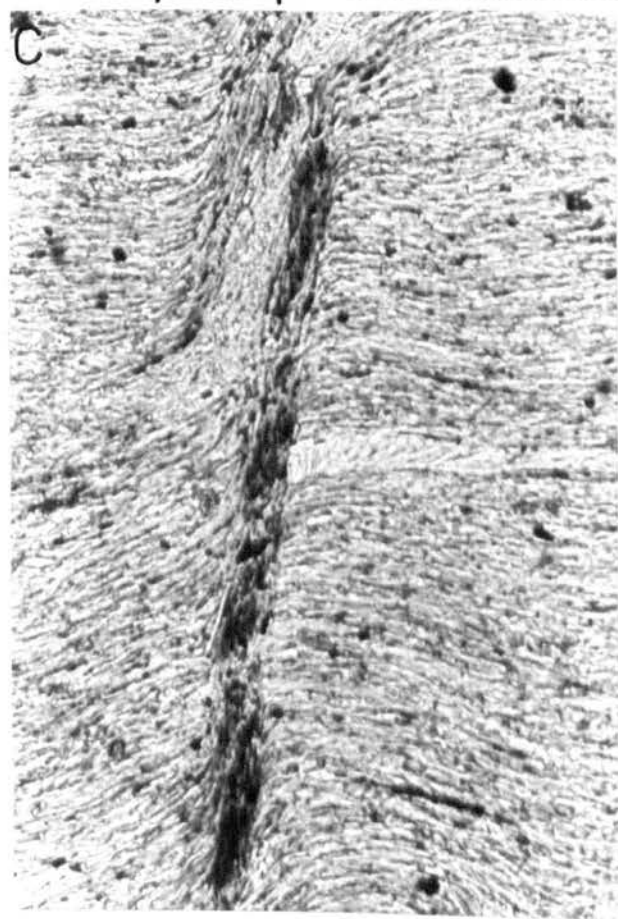
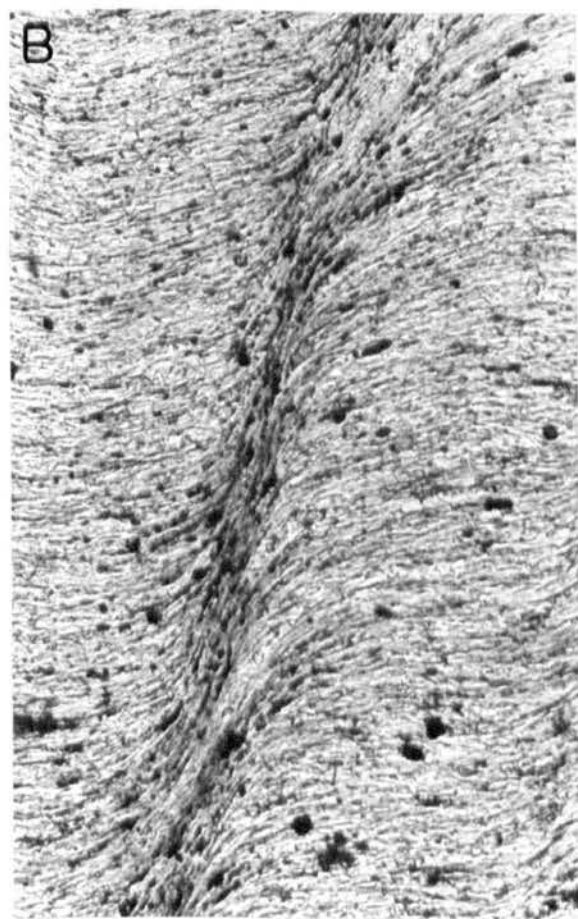
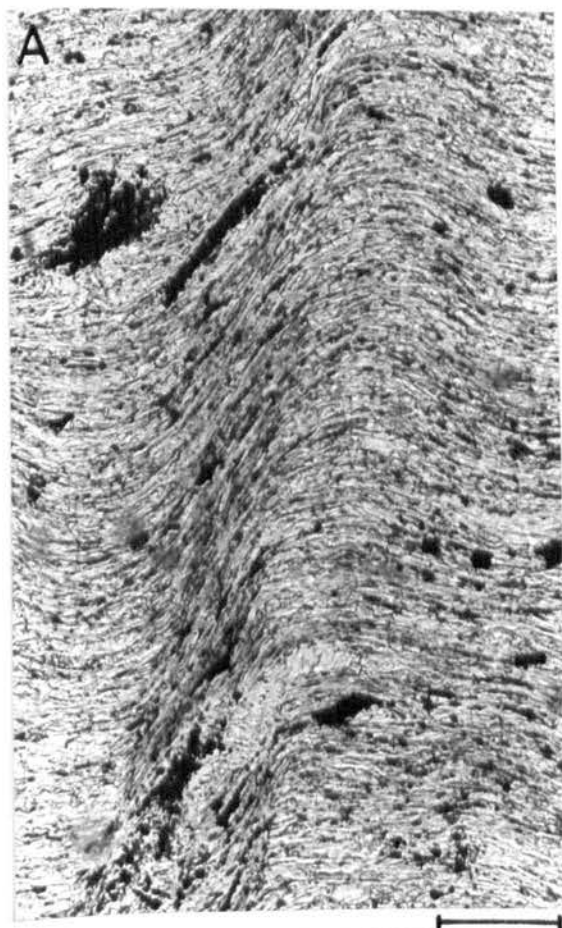
(c) Zone of very high strain where the S_1 fabric is parallel to the shear plane and can no longer be traced through the zone.

Scale bar is 0.1mm (all same scale).

Plane polarised light.

Location: At junction of the Armorican Quartzite and Complexo Xisto-grauvaquico 1km east of Aguiar de Sousa on the road south to Senande.

Specimen no. D112



(001) at high angles to S_1 , while the lozenge shapes have (001) at lower angles to S_1 (examples in Figs. 10.4, 10.5).

The chlorites are invariably intergrown with either a single or several muscovite crystals which are parallel but not in optical continuity with the chlorite (Figs. 10.4, 10.5).

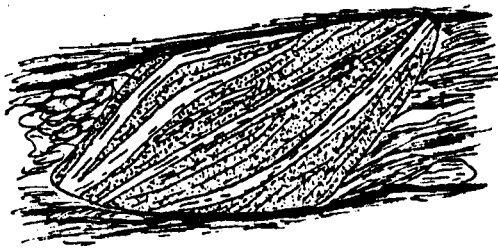
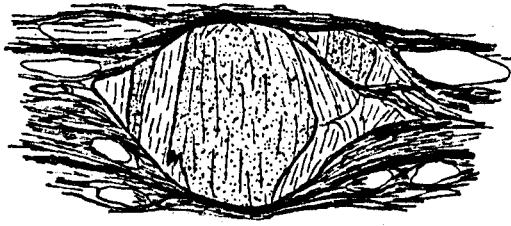
Cleavage seams of type A wrap around the porphyroblasts (Fig. 10.4) indicating their pre-cleavage origin; and occasionally the chlorites and muscovites within a porphyroblast are kinked such that the trace of the kink is parallel to the cleavage (Fig. 10.5b).

The following are descriptions of chlorite porphyroblasts, similar to those described above, which were found occurring in slates and other fine-grained sediments collected from different locations in Britain. The sediments exhibit varying degrees of cleavage or fabric development and progressively modified porphyroblast textures.

Starting with weakly deformed Devonian age, graded siltstones from Hartland, Devon these porphyroblasts are typically ellipsoidal and aligned parallel to the bedding (Fig. 10.6a). They comprise stacked chlorite crystals usually intergrown or nucleated on single muscovite crystals. Their distribution in the sediment

FIG. 10.4 Camera lucida diagrams of the most characteristic chlorite porphyroblasts in the slates of the Valongo Formation. Stipple = Chlorite, Dashed = Muscovite . Matrix comprises fine-grained muscovite , quartz and opaque minerals.

Location: In various specimens collected from the Valongo Formation on the western limb of the Valongo Anticline .



0.2 mm.

FIG. 10.5 a. Chlorite porphyroblast comprising intergrown chlorite (grey) and muscovite(white) in slate of the Valongo Formation. The central part of the porphyroblast shows chlorite around a thin muscovite grain. The cleavage(S_1) trace is E-W.

Scale bar is 0.05mm Plane polarised light

Location: Quarry 200m west of road and 1.5km north of Suzao(2km north of Valongo), between Suzao and the small villiage Quintarei.

Specimen no. 13V.

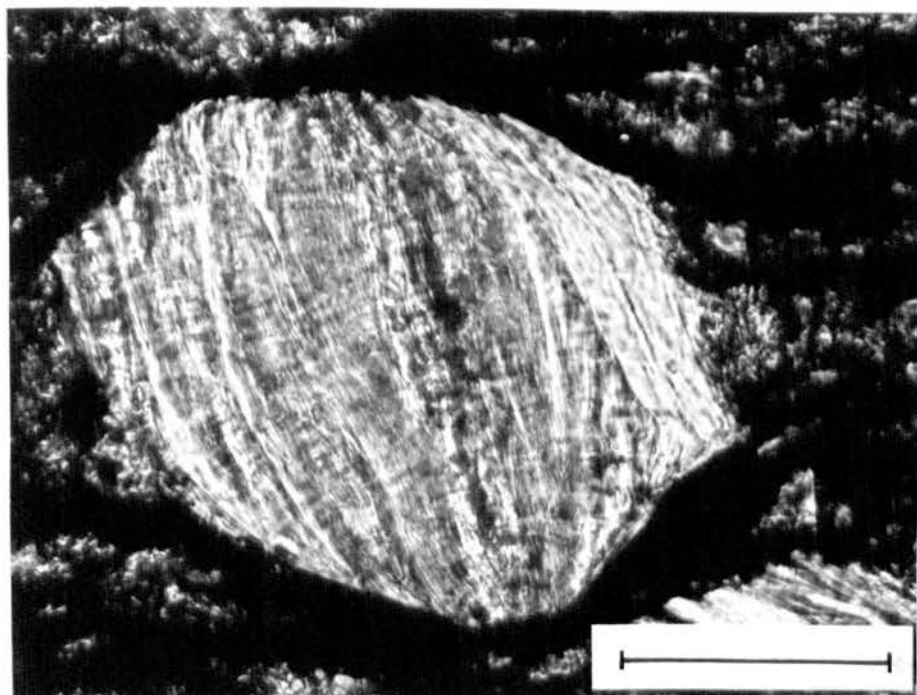
FIG. 10.5 b. Three chlorite porphyroblasts in slate of the Valongo Formation. The chlorite and muscovite grains comprising the porphyroblast in the top left part of the photomicrograph are kinked and flattened in the cleavage (E-W).

Scale bar is 0.1mm Plane polarised light

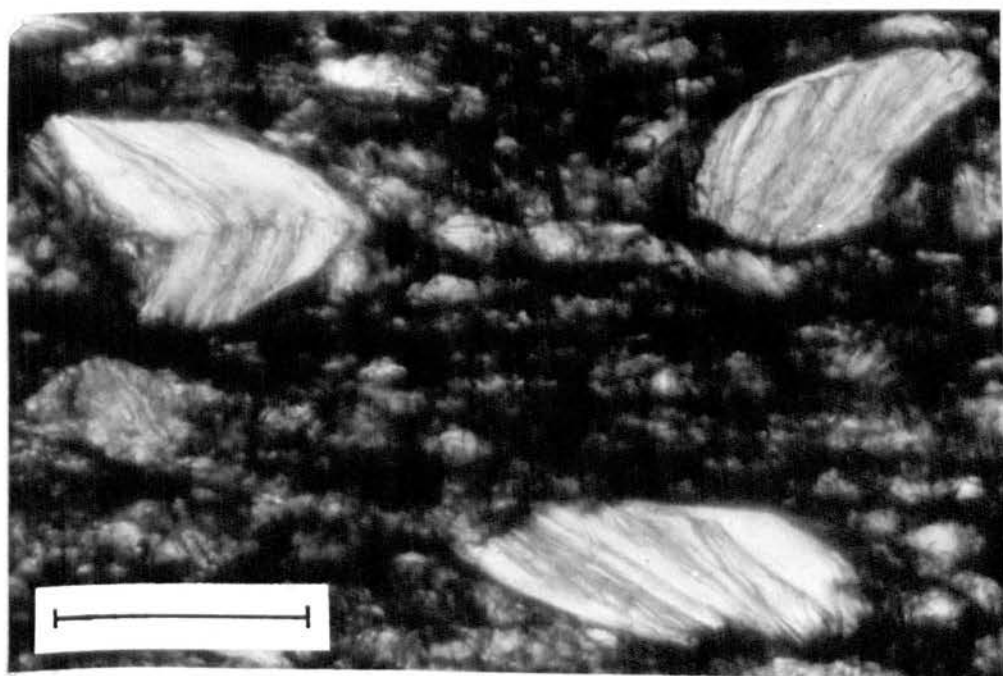
Location: 1km south of Valongo.

Specimen no. 17V.

a



b



is controlled by the composition and possibly grain size, decreasing in concentration towards the finer grained, muddier tops of beds. The cleavage is slightly deformed around the porphyroblasts although they show little or no sign of rotation.

In Ordovician greywackes from the Berwyn Hills, North Wales (collected by P. J. Brenchley) chlorite porphyroblasts are ellipsoidal and which become aligned with their long axes in the plane of the cleavage where it is most strongly developed (Fig. 10.6b). The chlorites are usually associated in growth with single muscovite crystals.

Quartzitic mudstones from Ilfracombe, Devon which are moderately cleaved contain sub-^Pspherical to ellipsoidal shaped chlorite porphyroblasts whose distribution relates to bedding which is folded. Moreover, they appear to have nucleated on single muscovite crystals which are almost certainly detrital in origin, oriented parallel to bedding planes prior to the cleavage and fold development (Fig 10.7). Although the internal structure of the porphyroblasts shows an orientational control by the bedding they are, nevertheless, rotated by small amounts on the limbs of micro-folds (Fig. 10.7a). The cleavage in these sediments is domainal in structure with type A domains or seams wrapping around the porphyroblasts.

FIG. 10.6 a. Chlorite porphyroblasts aligned with their long axes parallel to the bedding (E-W) in a graded siltstone. At the bottom of the photomicrograph the finer grained top of one graded unit is absent of porphyroblasts and passes abruptly upwards into the coarse-grained base of the overlying unit. A spaced cleavage is clearly developed in the fine-grained sediment (bottom) (at approx. 45°) but is refracted, at a higher angle to bedding, into the coarser, quartz-rich sediment where it is weakly developed. The chlorites commonly nucleate on muscovite grains (marked X). Scale bar is 0.1mm Plane polarised light
Location: Hartland, Devon.
Specimen no. H6

FIG. 10.6 b. Chlorite porphyroblasts aligned with their long axes parallel to the cleavage defined by thin, dark pressure solution seams and occasional elongate quartz grains (E-W) in a greywacke. Chlorite has highest relief (darkest grey) and matrix comprises mainly quartz with subordinate sericite and chlorite. Some chlorites nucleate on single muscovite grains (see porphyroblast top left). Scale bar is 0.1mm Plane polarised light
Location: Berwyn Hills, N. Wales. Sp. no. 28787a

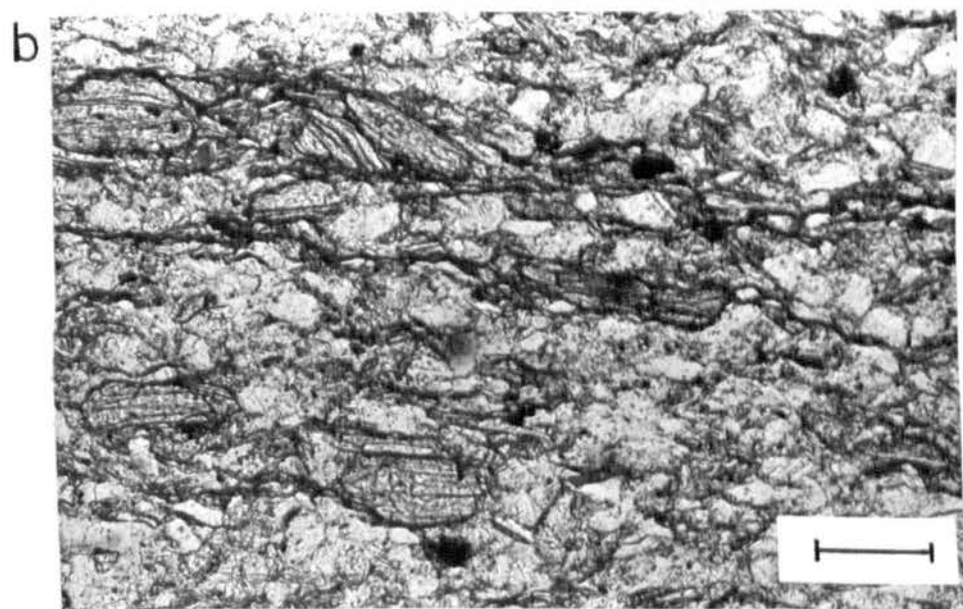
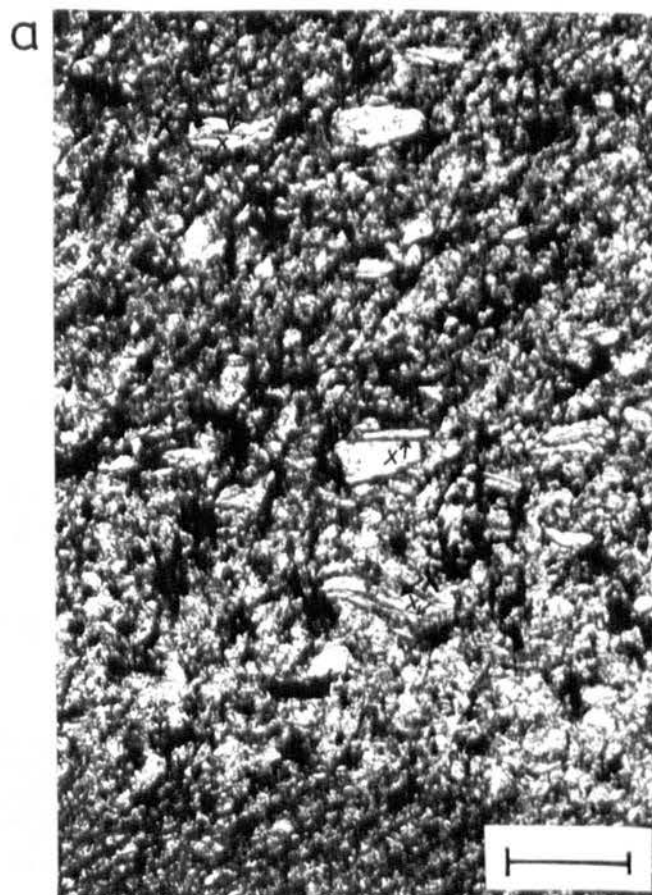


FIG. 10.7 a. Chlorite porphyroblasts which have nucleated on single muscovite grains are aligned sub-parallel to the bedding (dashed on overlay) in cleaved quartzitic mudstones. The cleavage has a domainal structure of which the dark, thin seams (type A domain) wrap around the porphyroblasts. (cleavage trace N-S). Chlorite is stippled on overlay.

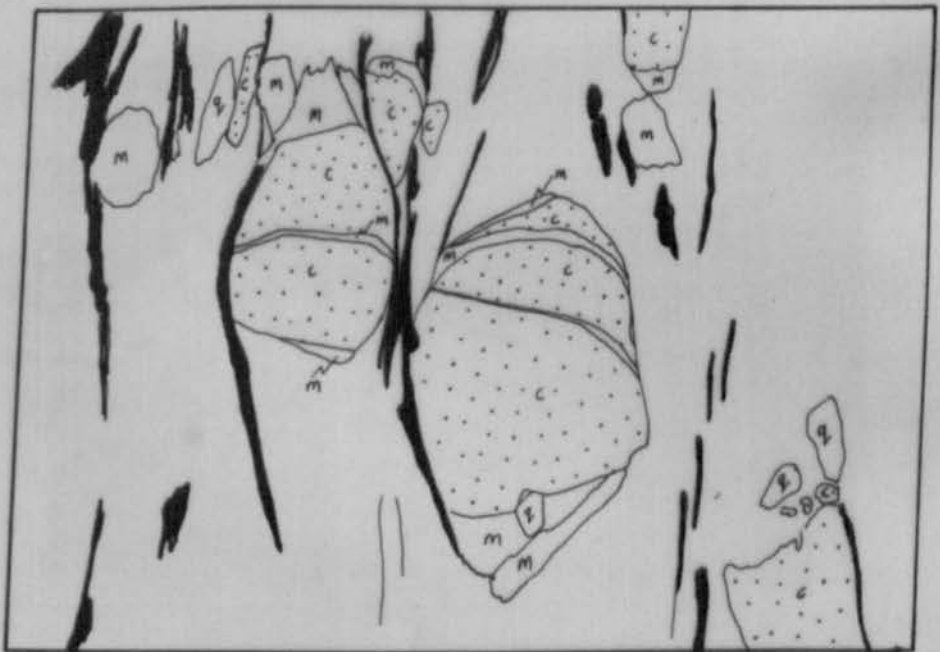
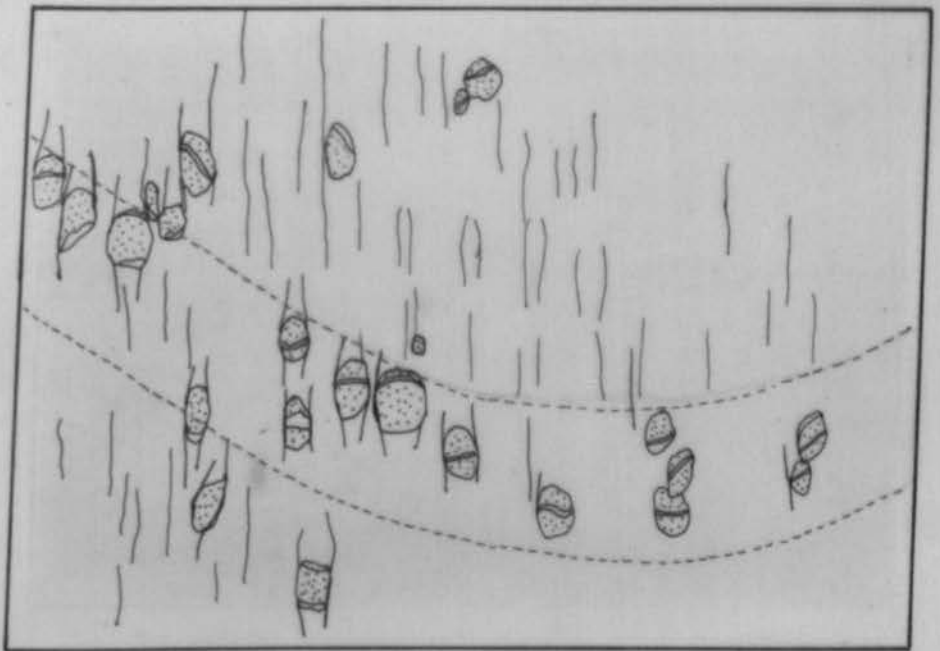
Scale bar is 0.5mm Plane polarised light

Location: Ilfracombe, Devon.

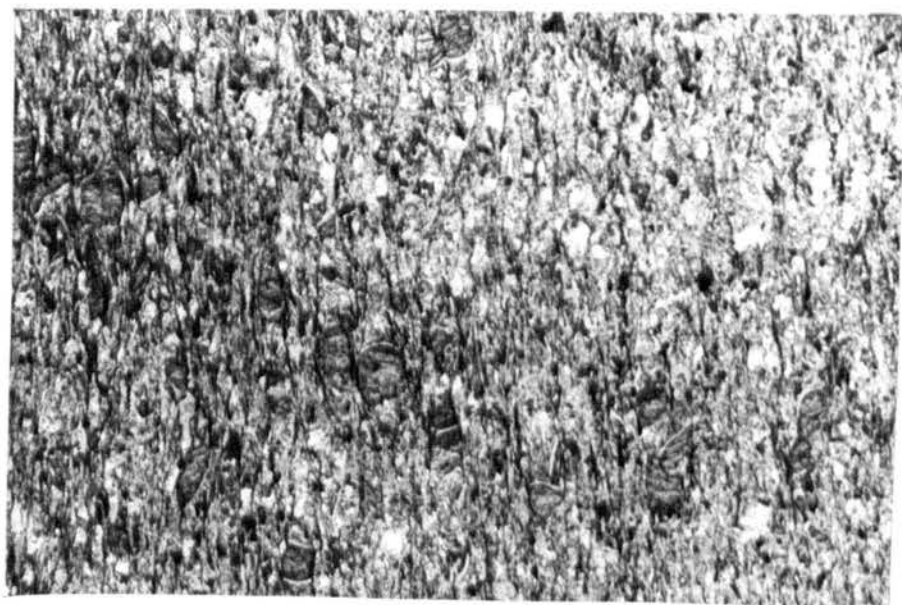
Specimen no. I19b(Y).

FIG. 10.7 b. Detail of the chlorite porphyroblasts in Fig 10.7 a. Dark seams around porphyroblasts comprises concentrated opaques and phyllosilicates (type A domain).

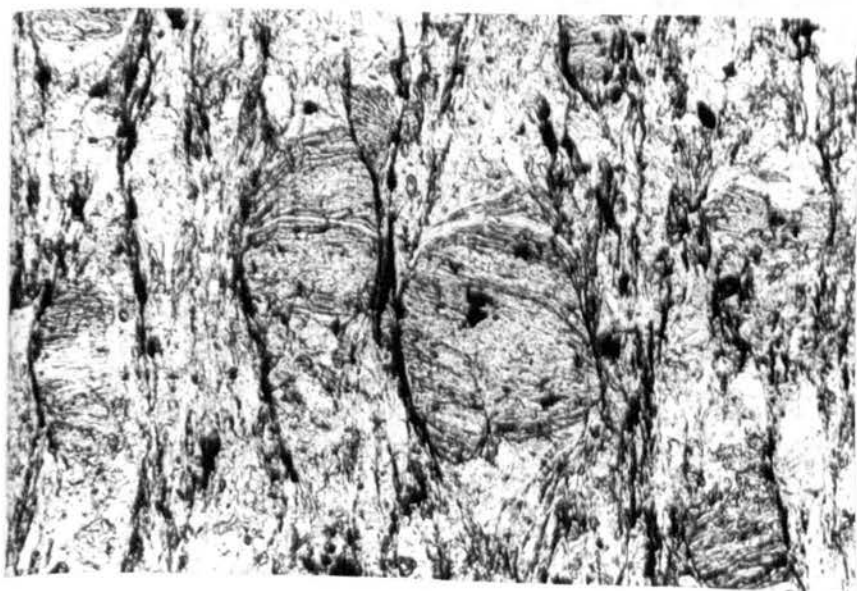
Scale bar is 0.1mm



d

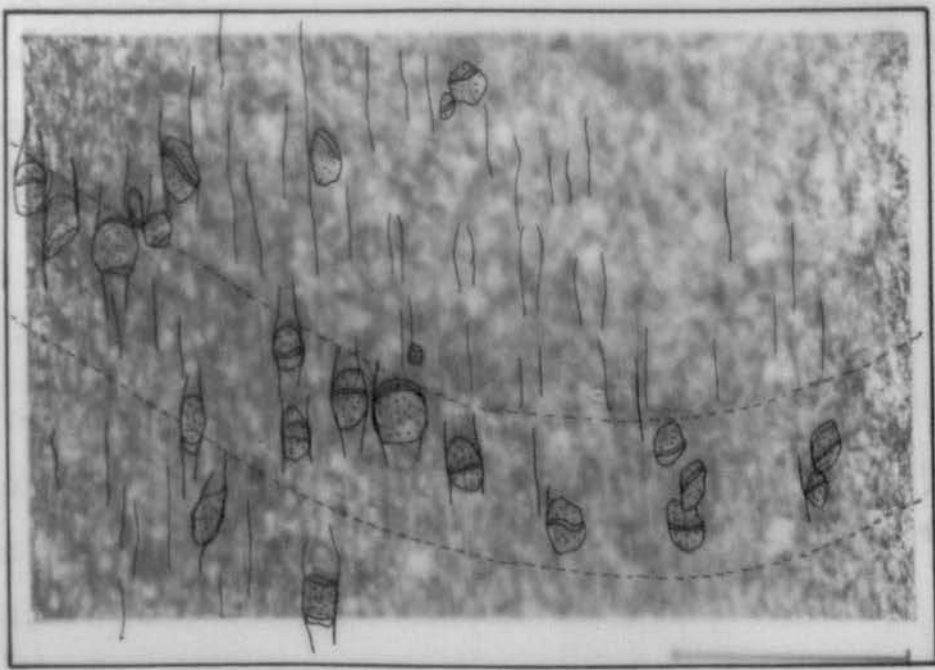


b

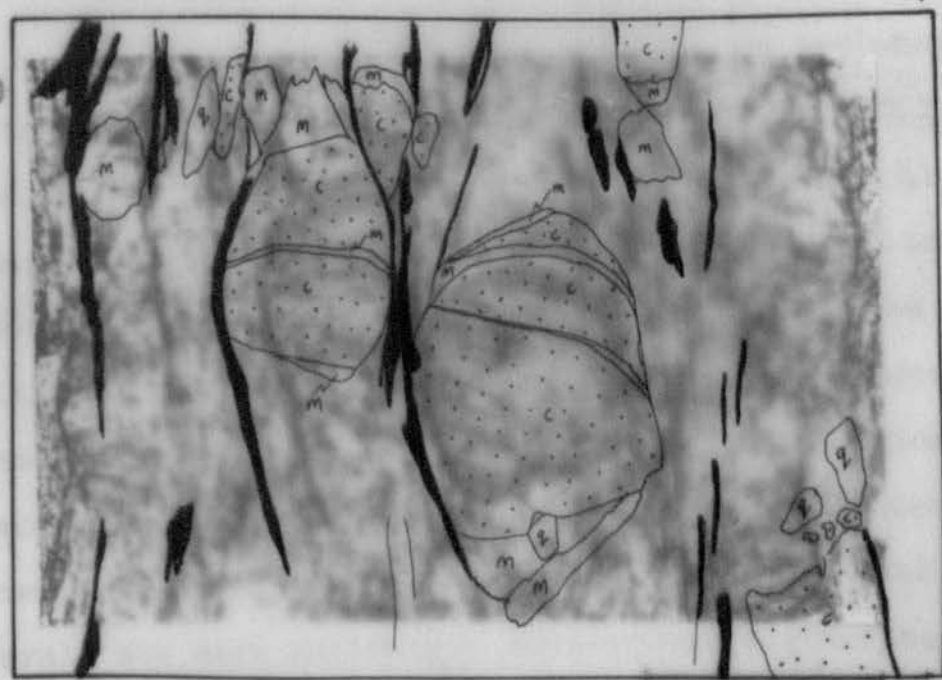


In certain places the
slates of the ...
porphyroblasts of ...

d



b



In strongly cleaved slates belonging to the Birn am Slates of the Dalradian, Obany Hill, Perthshire, Scotland porphyroblasts of intergrown chlorite and muscovite are elongate in shape and strongly aligned in the plane of the cleavage (Fig. 10.8). The chlorite in the porphyroblasts is stacked and commonly orientated at high angles to the cleavage.

10.4 CONCLUSIONS

The series of textures described above are considered to represent chlorite porphyroblasts of a similar pre-cleavage origin which have been progressively modified with increasing cleavage intensity.

The important points to note are:

The chlorite porphyroblasts are, in the sediments examined, of the same order of size i.e. between 0.1 mm and 0.2 mm, larger than the surrounding matrix. Chlorite is usually intergrown with muscovite which is considered in most cases to be detrital and must have acted as nuclei on which chlorite was able to grow as suggested by Hoepfner (1956). Clearly, the textural relationship is more complex in some cases where chlorite does not appear to have nucleated on a single muscovite crystal and the two minerals are more intimately intergrown; further, muscovite was also observed either replacing chlorite or growing on its surfaces or in pressure shadow regions with quartz.

FIG. 10.8 a. Intensely deformed chlorite porphyroblasts (arrowed C) in slates with a strong mineral and shape fabric defining a slaty cleavage (NE-SW). The matrix is composed of elongate quartz grains and lepidoblastic muscovite and chlorite.

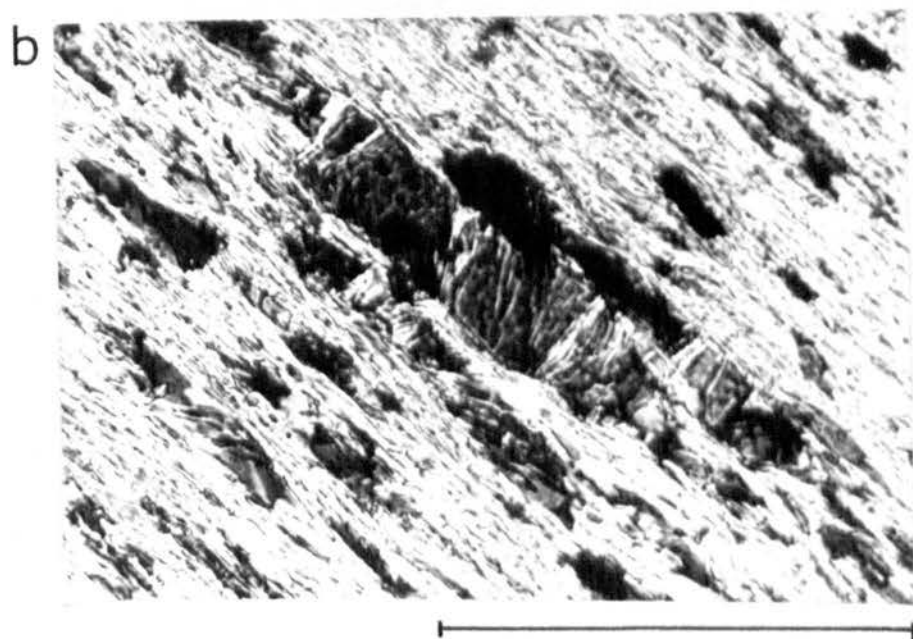
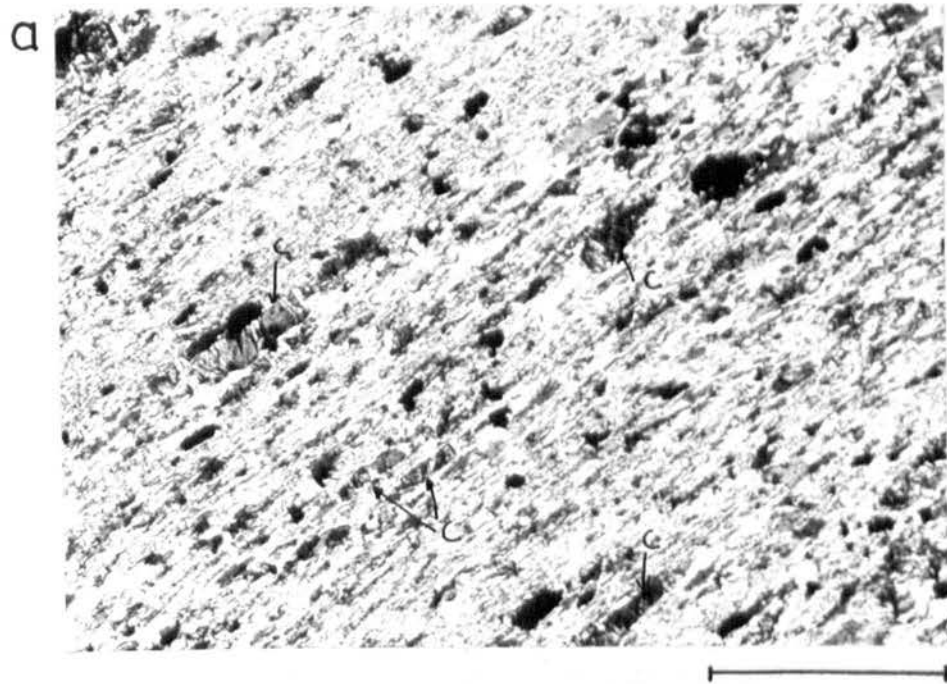
Scale bar is 0.1mm Plane polarised light

Location: Obany Hill, Perthshire, Scotland.

Specimen no. 56811

FIG. 10.8 b. Detail of a single chlorite porphyroblast from Fig. 10.8 a. Notice the high angle of the chlorite (grey) and intergrown muscovite (white) to the cleavage (NW-SE).

Scale bar is 0.05mm



It is considered that the porphyroblasts are diagenetic to early metamorphic, and pre-cleavage in origin for all the sediments described above. Brenchley (1969) assumed in the greywackes from the Berwyn Hills that the porphyroblasts are mostly diagenetically altered clay minerals, while Kirsch (1969) described the development of large chlorite-muscovite lepidoblasts in a fine groundmass, in a tectonically undeformed sedimentary pile in the zone of early metamorphism or metagenesis.

It can be observed in going from the weakly deformed to the moderately cleaved sediments that the porphyroblasts become slightly rotated. The random orientation of the stacks in the slates of the Valongo Formation is due to their progressive rotation during cleavage development. Other evidence of rotation during cleavage development in the same slates is provided by the curved fibre growth of quartz around competent opaque minerals (Fig. 10.1b) (Ramsay, 1967).

It is also considered that the chlorite porphyroblasts in the slates of Dalradian age are of a similar origin to those described in the less deformed sediments, but have had their shapes strongly modified mainly by pressure solution.

CHAPTER 11

SUMMARY AND REGIONAL CONSIDERATIONS

In Northern Portugal, part of the Central Zone A (Fig.1.3) of the Iberian Variscan Orogenic Belt (Bard et. al. 1973), a pre-Westphalian deformation DV_1 gives rise to Kilometric-scale folds (5-10 Km wavelength) that fold Lower Devonian and older rocks. The structural chronology of events is shown in figure 1.7.

In Precambrian to late Cambrian rocks, the Complexo xisto-gruavaquico, large scale Upper Cambrian folds are tightly refolded into elongate basins and domes. No cleavage is associated with the Upper Cambrian folding. A major unconformity is recognised between the Complexo xisto-grauvaquico and the Ordovician (Schermerhorn, 1955).

1. FOLDING AND CLEAVAGE

The Variscan F_1 fold axial traces trend in a broad arc from 150° in the northwest, at Viana do Castelo, to 130° in the southeast at Castro Daire.

The plunge of the tight F_1 folds in the Complexo xisto-grauvaquico is variable and controlled by the Upper Cambrian folds.

The F_1 major folds in the Ordovician and younger rocks are non-cylindrical and plunge between 20° to the northwest and horizontal. The major and minor F_1 folds are upward

facing, with either upright or moderately inclined axial planes dipping S.W.

During the DV_1 Variscan ductile deformation, the thick succession of quartzites of the Santa Justa Formation (Armorican Quartzite s.l.) behaved as a multilayered slab largely controlling the morphology of the three major folds, the Valongo Anticline, the Penacova Syncline and the Marão Syncline.

On the eastern limb of the Marão Syncline parasitic folds develop sequentially in decreasing order of wavelength in successively thinner bed units in the Armorican Quartzite. An early pre-, syn- buckling, pressure solution cleavage (S'_1), is axial planar to the parasitic folds. The regional cleavage S_1 is a pervasive, grain flattening cleavage which post-dates the development of S'_1 and is axial planar to most F_1 folds, although non-axial planar to symmetric or slightly asymmetric parasitic folds.

The S'_1 cleavage, not evident in pelitic rocks, is in most semi-pelites and psammites mainly parallel to the S_1 regional cleavage. Textural studies in the Ordovician slates show that early burial metamorphic porphyroblasts are deformed but preserved in the S_1 cleavage fabric.

2. VARISCAN STRAIN

In Ordovician rocks the Variscan finite strain approximates to plane strain ($K = 1$) with a sub-horizontal maximum elongation direction parallel to F_1 fold axes. This ductile finite strain is attributable to the DV_1 deformation only.

Deformed pebbles, fossils and other objects indicate a broad increase in the finite strain in the Ordovician rocks northeastwards from Penacova to Marão. The increase in strain is also recorded in the change in texture of Ordovician quartzites.

3. SUPERIMPOSED STRAIN IN THE COMPLEXO XISTO-GRAUVAQUICO

The finite strain recorded in deformed conglomerate pebbles in the Complexo xisto-grauvaquico is demonstrated to be the product of two deformations.

Subtraction of the Variscan ductile strain (DV_1) establishes a pre-Variscan planar-linear pebble alignment which developed by rigid rotation of the pebbles in the limbs of Upper Cambrian flexural-slip/flexural-flow folds.

The superimposed DV_1 plane strain gives rise to a variety of constrictional fabrics in the conglomerates with a maximum extension direction parallel to the plunging F_1 fold axes.

4. REGIONAL CONSIDERATIONS

The Variscan Fold Belt in Northern Portugal lies within the Central Zone (A) of the Iberian Variscan Orogenic Belt (Fig.1.3) to the west and southwest of the Galice-Castilienne sub-zone which is considered to be the axis of the orogenic belt (Lotze, 1968, Ribeiro, 1974).

Throughout the Central Zone the Variscan major first phase folds (F_1) have sub-vertical axial planes although

they commonly alternate in vergence (Bard et.al.1973).

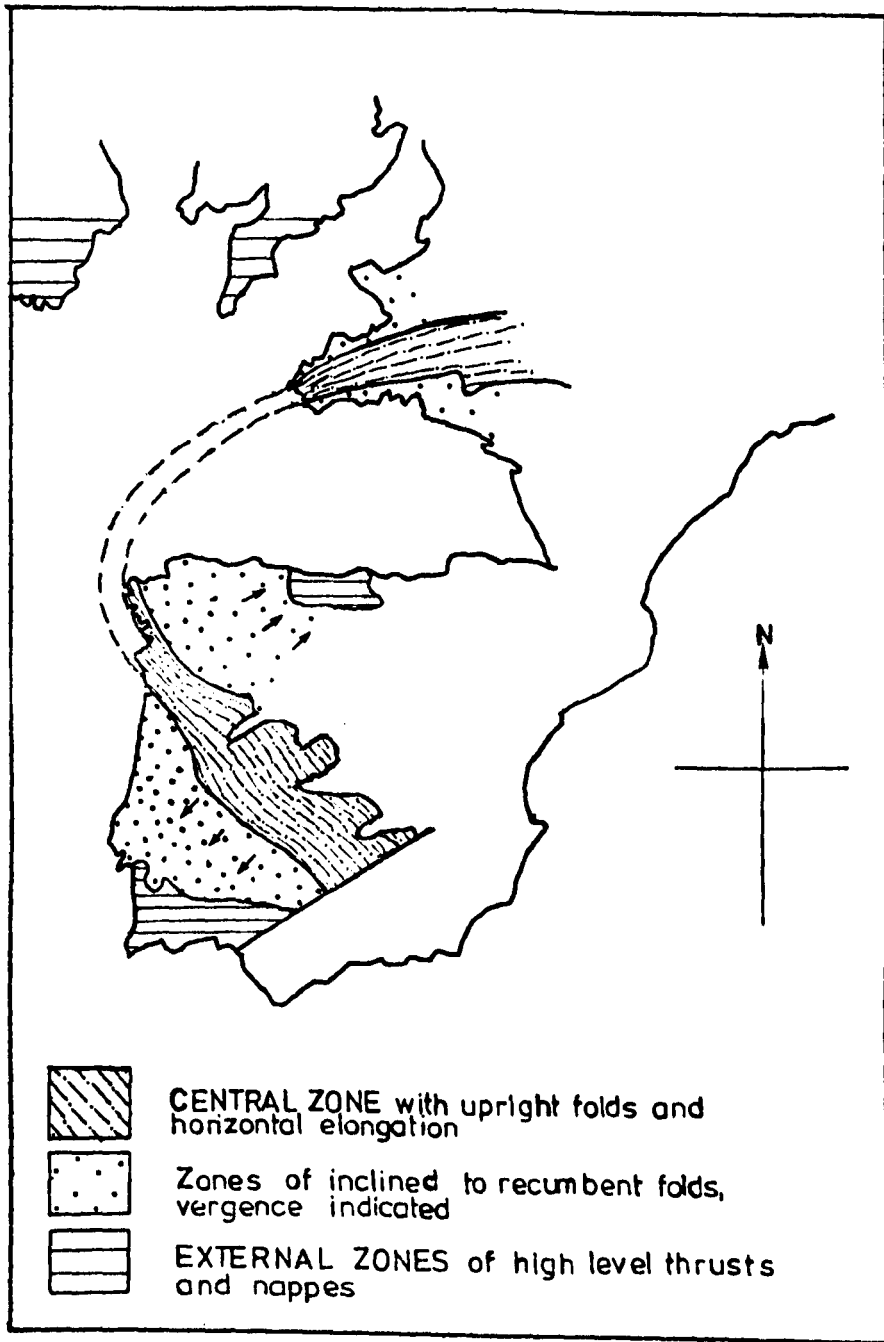
In this thesis, analysis of the Variscan structures over a large part of the Central Zone shows the cover sediments deformed essentially by buckle folding resulting from a northeast-southwest horizontal compression. The finite strains in these rocks indicate plane strain deformation and a maximum elongation in a sub-horizontal direction parallel to the fold axes. There is no significant thickening or thinning of the cover sedimentary succession by horizontal translation either by nappes or thrusts except in the Tras-os-Montes region where a change in vergence of the F_1 folds and thrusting is due to the emplacement of the ultrabasic complexes of Morais and Braganca (Ribeiro, 1974).

In the Galice-Castilienne sub-zone to the northeast of Tras-os-Montes the maximum elongation direction is also horizontal and sub-parallel to the major F_1 fold axes (Matte, 1968; Matte and Ribeiro, 1975; Ribeiro, 1974).

Structural, stratigraphic, metamorphic and magmatic zones in the Iberian Variscan Orogenic Belt have been correlated across the Bay of Biscay to Brittany and Southwest England (Cogne, 1971; Bard et.al, 1971, Bard et.al. 1973; Ries, 1974; Bless, 1977) (Fig.11.1). The opening of the Bay of Biscay is timed between late Triassic and late Cretaceous (Van der Voo, 1969), but the pole and amount of rotation has not been firmly established (Choukroune et.al, 1973; Bless, 1977).

FIG. 11.1

Tectonic zones of the Variscan Orogenic Belt
after Bard et.al. 1971



In Southern Brittany the maximum elongation is also parallel to horizontal fold axes of primary F_1 folds in the continuation of the Galice-Orientale sub-zone (Bouchez & Blaise, 1976).

Across the Galicie-Orientale sub-zone and the Asturian Arc from Zone A through Zone B of the orogen the maximum elongation direction becomes progressively more oblique to the F_1 fold axes until eventually they lie normal to each other (Matte, 1968) Fig.11.2a).

The orientation of the maximum elongation direction remains relatively constant E - W around the outer segment of the Asturian Arc (Matte, op.cit.).

In Cantabria, the external zone of the orogenic belt (Zone C, Fig.1.3), primary nappes and thrusts are refolded by two, more or less synchronous sets of folds, one radial and one curved around the arc. (Julivert, 1971). These radial and arcuate folds are considered to be the result of compression in the core of the arc (Julivert op.cit.), while the finite maximum elongation direction is normal to the arcuate folds and plunges down dip of the reclined folded nappes (Ries and Shackleton, 1976).

The southwestern external zone of the orogenic belt (Zone C, Fig.1.3) comprises primary nappes and thrusts as in Cantabria (Oliveira, pers.comm).

Two models have been put forward to explain the evolution of the finite strain pattern and arcuate form of the Variscan Orogenic Belt (Ries & Shackleton, 1976; Matte and

FIG. 11.2

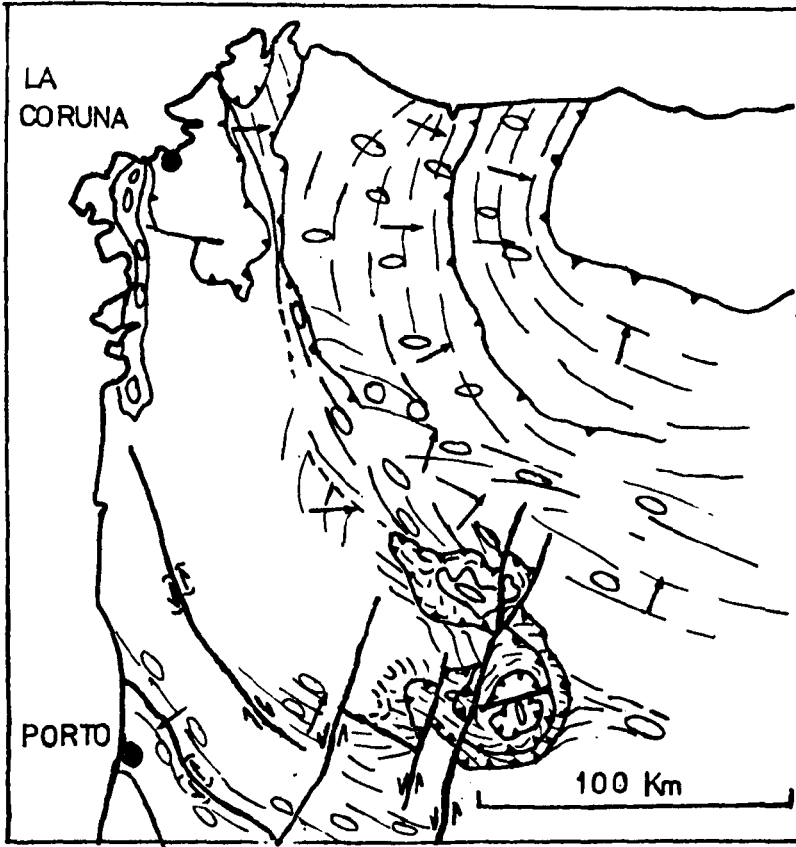
a. Relationship between major fold trend and the maximum elongation direction in the Iberian Variscan Orogenic Belt.

After Matte, 1968 and Ribeiro, 1974.

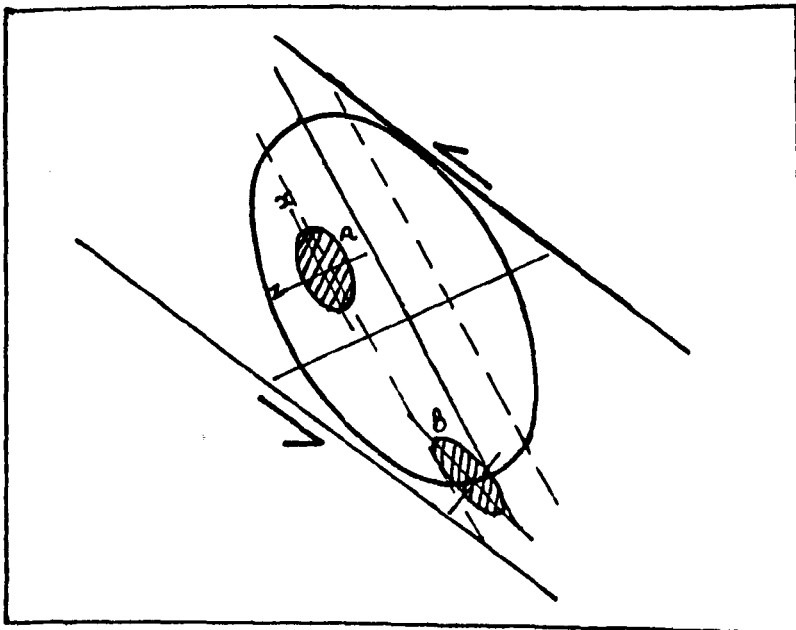
b. Schematic diagram of simple shear model for the Fold Belt in Northern Portugal .

Large ellipse represents the approximate strain in the Fold Belt . Increase in strain northeastwards and abrupt inhomogeneities in strain in deformation zones are not depicted. The strain ellipse, B is more realistic for the combined shortening by buckling and internal whole rock strain.

a



b



Ribeiro, 1975).

Ries and Shackleton (1976) propose that the Orogenic Belt is a secondary arc or orocline (Carey, 1958) formed during a counter clockwise rotation of the Iberian Peninsula relative to Brittany which resulted in an internal strain pattern analogous to that in a buckle fold produced by tangential longitudinal strain with extension in the outer arc and compression in the inner (Ramsay, 1967 p.398)

The increase in finite strain northeastwards across the fold belt in Northern Portugal is inconsistent with this model in which the strain should increase south west wards towards the outer arc from the neutral surface (Cloos, 1947; Ramsay, 1967).

In the alternative model Matte and Ribeiro (1975) propose that the arc is partly inherited from the Pre-Variscan basement crustal structure (Bard et.al, 1973) but that the strain pattern is related to simple shear with concentrated high strain along recognised major lineaments e.g. the Porto-Cordoba 'Fault' involving a northwesterly movement of the inner Cantabrian block.

The Porto-Cordoba lineament is a zone of mylonitisation involving basement gneisses in the region of Portalegre (Bladier & Laurent, 1976), and high grade metamorphism at Oliveira de Azemeis (Oen, 1970). A Variscan age is suggested for the development of the steep cleavage and main fold structures in this zone (Ries, 1974). The shearing along

this zone is considered to be dextral (Bladier & Laurent, 1976; Arthaud & Matte, 1975).

The Porto-Cordoba lineament (Fig.1.2) is correlated with the South Armorican Mylonite Zone, a branch of the Lanvaux-Angers Lineament (Nicolas et al. 1977; Bouchez & Blaise, 1976; Bless, 1977). This is a symmetrical shear zone with a horizontal maximum elongation direction parallel to fold axes. From geodynamic evidence and the strain pattern the sense of shearing is also considered to be dextral (Arthaud & Matte, 1975; Bouchez & Blaise, 1976).

The structures comprising the fold belt in Northern Portugal are considered to be the result of large-scale, transcurrent, inhomogeneous simple shear of the basement rocks and cover sediments as envisaged in the model proposed by Matte & Ribeiro (1975). The shear zone or fold belt is an extension of the complex of shear zones in Southern Brittany which has very similar, although deeper level structures (Bouchez & Blaise, 1976; Nicolas et al. 1977). In their plate reconstruction Bless (1977) propose that prior to the rotation of the Iberian Peninsula the South American Shear Zone and the Porto-Cordoba 'Shear Zone' were originally a straight zone of dextral shearing.

Commonly in pure shear compressional regimes the maximum elongation direction is vertical at a high angle to fold axes (Cloos, 1947; Wood, 1973). In contrast, the structures comprising the fold belt in Northern Portugal are more easily explained by a simple shear deformation

(Fig.11.2b). A transcurrent, horizontal, dextral, ductile simple shear zone with a shear direction parallel to NW - SE major lineaments, or zones of high strain resulted in an initial E - W compression, rotating to NE-SW with increasing strain, and a horizontal maximum elongation direction. The axes and axial planes of early formed buckle folds in the horizontal cover sediments rotated with increasing shear strain, maintaining parallelism or sub-parallelism with the maximum elongation direction (Escher and Watterson, 1974).

ACKNOWLEDGEMENTS

Foremost I would like to thank John Diggens for all his help and criticism both in the field and during the preparation of this thesis.

I am grateful to Dr. Mike Fleuty for his criticism and advice on the preparation of this thesis; also to Dr. M. Romano, Professor R. M. Shackleton, Dr. A. Ries and Dr. J. Hossack for helpful discussions in the field; and to Dr. A. Ribeiro and the late Dr. A. Madeiros for introducing me to the geology of Northern Portugal and for allowing me to use the services of the Servicos Geologicos de Portugal in Porto and Lisbon.

Also I would like to thank my many colleagues at Kingston Polytechnic and Liverpool University for their useful comments.

I am especially grateful to my wife for her help in the final compilation of this thesis.

I acknowledge receipt of a Research Award from the Natural Environment Research Council.

REFERENCES

- Arthaud, F. and Matte, Ph., 1975. Les décrochements tardi-hercyniennes du Sud-Oest de l'Europe. Geometrei et essai de reconstitution des conditions de la deformation. Tectonophysics 25, 139-171.
- Atherton, M.P., Nagär, M.H., Atkin, B.P., 1974. Kyanite in the Hercynian metamorphic rocks of the Oporto-Viseu Belt, North Portugal. Geol. Mijnbouw., 53, 189-192.
- Babin, C. 1972. Colloque Ordovician-Silurien. Bull. Soc. geol. Mineral. Bretagne., 4, No. 6.
- Bard, J.P., Capdevila, R., Matte, Ph. 1971. La eststructure de la chaine hercynienne de la Meseta Iberique: comparaison avec les segments voisins. Publ. Inst. Fr. Petr. Coll. Col. et. Sem. 22, 1-68.
- Bard, J.P., Capdevila, R., Matte, P., Ribeiro, A. 1973. Geotectonic Model for the Iberian Variscan Orogen. Nature(phys. Sci.). 241, 50-52.
- Beach, A. 1974. A geochemical investigation of pressure solution, and the formation of veins in a deformed greywacke. Contrib. Mineral. Petrol. 46, 61-68.
- Bennison, G.M. and Wright, A.E. 1969. The geological history of the British Isles. Publ. Edward Arnold. pp. 406
- Biot, M.A., 1961. Theory of folding in stratified viscoelastic media and its implications in tectonics and orogenesis. Bull. geol. Soc. Am. 72 1595-1620.

- Bladier, Y. and Laurent, Ph. 1976. La Zone mylonitique de Badajoz-Cordne Raccords avec la zone Portalegre-Coimbra. Com. Serv. geol. Portugal. LX, 267.
- Bless, M.J.M. 1977. Y-A-T-IL des hydrocarbures dans le pre-Permien de l'Europe occidentale. Ministere des Affaires Economiques. Administration de Mines. Prof. Pap. 11 , No. 148, 1-58.
- Bouchez, J.L. and Blaise, J. 1976. Une structure hercynienne liee a un accident ductile: l' anticlinal de Lanvaux-les-Pontes-de-Ce, aux environs d'Angers (massif Armoricaïn). Bull. geol Soc. France. XV111 No. 1. 145-157.
- Brace, W.F. 1955. Quartzite Pebble Deformation in Central Vermont. Am. J. Sci. 253, 129-145.
- Brenchley, P.J. 1969. Origin of matrix in Ordovician greywackes, Berwyn Hills, North Wales. J. sediment. Petrol. 39, 1297-1301.
- Burns, K.L. and Spry, A.H. 1969. Analysis of the shape of deformed pebbles. Tectonophysics. 7, 177-196.
- Carey, W.S. 1958. The orocline concept in geotectonics. Pap. Proc. R. Soc. Tasmania. 89, 255.
- Carrington da Costa, J.C.S., 1948. Tectonique du Portugal. Int. geol. Congr. London. XV111, 45-51.
- Carrington da Costa, J.C.S., 1950. Quelques remarques sur la tectonique du Portugal. Bol. Soc. geol. Portugal., 8, 193-206.
- Carta Geologica de Portugal. 1972. 1:500,000. Teixeira, C. (Servicos Geologicos de Portugal).

- Choukroune, P., le Pichon , X., Segunet, M., Sibuet, J-C. 1973. Bay of Biscay and Pyrenees. Earth planet. Sci. Lett. 18, 109-118.
- Cloos. E. 1947. Oolite deformation in the South Mountain Fold, Maryland. Bull. geol. Soc. Am. 58, 843-918.
- Coe, K., 1962. Some aspects of the Variscan Fold Belt. 9th Inter-University geol. Cong. Publ. Manchester University Press.
- Cogne, J., 1971. Le Massif Armoricaïn et sa place dans la structure des socles ouest-Europeens: l'arc Hercynien Ibero-Armoricaïn. Publ. Inst. Fr. Petr. Coll. Col. et Sem. 22 ,
- Cosgrove, J.W. 1976. The formation of crenulation cleavage. J. geol. Soc. London., 132, 155-178.
- Crimes, T.P. , 1968. CRUZIANA: a stratigraphically useful trace fossil. Geol. Mag. 105, 360-364.
- Curtis, M.L.K., 1961. Ordovician trilobites from the Valongo Area, Portugal. Bol. Soc. geol. Portugal, XIV, 1-16.
- Dahlstrom, C.D.A., 1970. Structural Geology in the Eastern Margin of the Canadian Rocky Mountains. Bull. Can Pet. Geol. 18, No. 3., 332-406.
- Delgado, J.F.N., 1908. Systeme Silurique du Portugal . Etude de Stratigraphie palaeontologique. Mem. Comm. geol. Portugal, 1-245.
- Dunnet, D., 1969. A technique of finite strain analysis using elliptical particles. Tectonophysics. 7, 117-136.

- Dunnet, D. and Siddans, A.W.B. , 1971. Non-random sedimentary fabrics and their modification by strain. *Tectonophysics*. 12, 307-325.
- Elliot, D., 1970. Determination of finite strain and initial shape from deformed elliptical objects. *Bull. geol. Soc. Am.*, 81, 2221-2236.
- Elliot, D., 1973. Diffusion Flow Laws in Metamorphic Rocks. *Bull. geol. Soc. Am.* 84, 2645-2664.
- Escher, A. and Watterson, J., 1974. Stretching Fabrics, Folds and Crustal Shortening. *Tectonophysics*. 22, 225-231.
- Fairbairn, H.W., 1949. Structural Petrology of Deformed Rocks. Publ. Cambridge Mass. Addison-Wesley. Inc.
- Fellows, R.E., 1943. Recrystallisation and flowage in Appalachian quartzite. *Bull. geol. Soc. Am.* 54, 1399.
- Fleuty, M.J. , 1964. The description of Folds. *Proc. Geol. Assoc. London.* 75, 461-492.
- Flinn, D., 1956. Deformation of the Funzie Conglomerate, Fetlar, Shetland. *J. Geol.* 64, 480-505.
- Flinn, D., 1962. On folding during three-dimensional progressive deformation. *Q. J. geol. Soc. London.*, 118, 385-433.
- Gay, N.C., 1969. Analysis of strain in the Barberton Mountain Land, Eastern Transval , using deformed pebbles, *J. Geol.* 77, 377.

- Gay, N. and Fripp, R.E.D. 1976. The control of ductility on the deformation of pebbles and conglomerates. Philos. Trans. R. Soc. London. 283, 109-128.
- Ghosh, S.K. 1974. Strain distribution in superposed buckling and the problem of reorientation of early lineations. Tectonophysics. 21, 249-272.
- Ghosh, S.K. and Ramberg, H. 1976. Re-orientation of inclusions by combination of pure and simple shear. Tectonophysics. 34, 1-70.
- Ghosh, S.K. and Sengupta, S. 1973. Compression and simple shear of test models with rigid and deformable inclusions. Tectonophysics. 17, 133-175
- Glenn, J.W., Donner, J.J., West, R.G. 1957. the mechanism by which stones in till become orientated. Am. J. Sci. 255, 194-205.
- Harris, A.L., Bradbury, H.J., McGonigal, M.H. 1976. The evolution and transport of the Tay Nappe. Scott. J. Geol., 12, 103-116.
- Hobbs, B.E., Means, W.D., Williams, P.F. 1976. An outline of Structural Geology. Publ. Wiley, pp.571.
- Hoeppener, R. 1956. Zum problem der Bruchbildung, Schieferung und Faltung. Geol. Rdsch. 45, 247-283.
- Hossack, J.R. 1968. Pebble deformation and thrusting in the Bygdin Area(Southern Norway). Tectonophysics. 5, 315-339.

- Jeffery, G.B. 1922. The motion of ellipsoidal particles immersed in a viscous fluid. Proc. R. Soc. London. 102, 161-179.
- Julivert, M. 1971. L' Evolution structural de l'Arc Asturien T. 1. Techanip.
- Julivert, M., Fontbote, J., Ribeiro, A., Conde, L. 1974. Memoria Explicativa del Mapa Tectonico de la Peninsula Iberica y Baleares. Inst. Geol. Min. Espana.
- Kisch, H.J. 1969. Coal-rank and burial metamorphic mineral facies. In 'Advances in Organic Geochemistry. Publ. Pergaman Press. 407-425.
- Knipe, R.J. and White, S.H. 1976. Microstructural development of slaty cleavage. In 'Developments in Electron Microscopy and Analysis. 537.
- Krumbein, W.C. 1939. Preferred orientation of pebbles in sedimentary deposits. J. Geol. 47, 673-706.
- Kuenen, P.H. 1942. Pitted Pebbles. Leidse. geol. Meded. 13, 189-201.
- Lotze, F. 1968. Schlusswort: Der gesamttektoische Rahman. Geotekton. Forsch. Stuttgart. 27, 147-154.
- McLeish, A.J. 1971. Strain analysis of deformed pipe rock in the Moine Thrust Zone, Northwest Scotland. Tectonophysics. 12, 469-503.
- Matte, Ph., 1968. La structure de la virgation hercynienne de Galice (Espagne). Thesis, Rev. Geol. Alpine., 44, 1-127.

- Matte, Ph. and Ribeiro, A. 1975. Forme et orientation de l'ellipsoïde de deformation dans la virgation hercynienne de Galice. Relations avec le plissement et hypotheses sur la genese de l' Arc Ibero-Armoricain. C.r. Seances Acad. Sci. Paris. 280, 2825-2828.
- Mehnert, K.R. 1939. Die meta-konglomerate des Weisenthaler Geizuges im Sächsischen Erzgebirge. Mitt, Pet. Min. 50, 194-272.
- Mitchell, W.I. 1974. An outline of the stratigraphy and palaeontology of the Ordovician rocks of Central Portugal. Geol. Mag. 111, 385-396.
- Nabais Conde, L.E. 1966. Direcções de correntes na bas do Ordoviciano do afloramento de Amendoa-Macao e sua importancia paleogeografica. Mus. Lab. Min. geol. Univ. Coimbra. 31, 61 44-55.
- Nicolas, A., Bouchez, J.L., Blaise, J., Poirier, J.P. 1977. Geological aspects of deformation in continental shear zones. Tectonophysics. 42, 55-73.
- O'Driscoll, E.S. 1964. Rheid and rigid rotations. Nature. London. 203, 832-835.
- Oen, I.S. 1958. The geology, petrology and ore deposits of the Viseu region, Northern Portugal. Com. Serv. geol. Portugal. 41, 5-199.
- Oen, I.S. 1970. Granite intrusion, folding and metamorphism in Central Northern Portugal. Bol. geol. y Minero. 81, 157-184.

- Ofte dahl, C. 1948. Deformation of quartz conglomerates in Central Norway. J. Geol. 56, 476-487.
- Pettijohn, F.J., Potter, P.E., Siever, R. 1973. Sand and Sandstone, Publ. Springer Verlag, New York. pp 618.
- Price, N.J. 1967. The initiation and development of asymmetrical buckle folds in non-metamorphosed competent sediments. Tectonophysics. 4, 173-201.
- Priem, H.N.A. 1968. Geological, petrological and mineralogical investigations in the Serra do Marao region, Northern Portugal. PhD. Thesis. University of Amsterdam.
- Priem, H.N.A., Boelrijk, N.A.I.M., Verschure, R.H., Hebeda, E.H., Verdumen, E.A.Th. 1970. Dating events of acid plutonism through the Palaeozoic of the Western Iberian Peninsula. Eclog. geol. Helv. 63, 255-274.
- Ramsay, D, 1964. Deformation of pebbles in Lower Old Red Sandstone Conglomerates adjacent to the Highland Boundary Fault. Geol. Mag. 101, 228-248.
- Ramsay, J.G. 1963. Structural investigations in the Barberton Mountain Land, Eastern Transvaal. Trans. Proc. geol. Soc. South Afr. LXVI, 353-401.
- Ramsay, J.G. 1967. Folding and Fracturing of Rocks. McGraw Hill, New York, 568 pp.
- Read, H.H. and Watson, J. 1975. Introduction to Geology. Volume 2. Earth History. Part 2 . Later Stages of Earth History. MacMillan .

- Ribeiro, A. 1974. Contribution a l'Etude Technique de
Tras-os-Montes Oriental. Mem. Serv. geol. Portugal. 24.
- Ribeiro, A., Cramez, C., da Silva, L.C., Macedo, J. 1962.
Nota sobre a geologica da Serra do Marão. Bol. Soc.
geol. Portugal. XIV, 151-170.
- Ries, A. 1974. The Variscan Orogenic Belt in Brittany and
Spain and its disruption during the formation of the
Bay of Biscay. Unpublished Ph.D. thesis. University
of London.
- Ries, A. and Shackleton, R.M. 1971. Catazonal Complexes of
North-West Spain and North Portugal, remnants of a
Hercynian Thrust Plate. Nature (phys. Sci.). 234, 65-68.
- Ries, A. and Shackleton, R.M. 1976. Patterns of strain
variation in arcuate fold belts. Philos. Trans. R.
Soc. London.A. 283, 281-288.
- Romano, M. 1974. The palaeoenvironment and Ichnology of the
Lower Ordovician rocks at Apulia, North Portugal.
Bol. Mus. Lab. mineral. geol. Univ. Lisboa. 14, 63-76.
- Romano, M. 1976. The trilobite genus Placoparia from the
Ordovician of the Valongo area, North Portugal.
Geol. Mag. 113, 11-28.
- Romano, M. and Diggens, J.N. 1974. The stratigraphy and
structure of Ordovician and associated rocks around
Valongo, north Portugal. Com. Serv. geol. Portugal.
58, 23-50.
- Schermerhorn. L.J.G. 1955. The age of the Beira Schists
(Portugal). Bol. Soc. geol. Portugal. VX11, 77-100.
- Schermerhorn. L.J.G. 1956. Geology of the Castro Daire,
São Pedro do Sul, Satão Region. PhD. thesis. Lisboa.
- Schermerhorn, L.J.G. and Stanton, W.I. 1963. Tilloids in
the West Congo Syncline. Q.J. geol.Soc.London. 119, 201-
241.

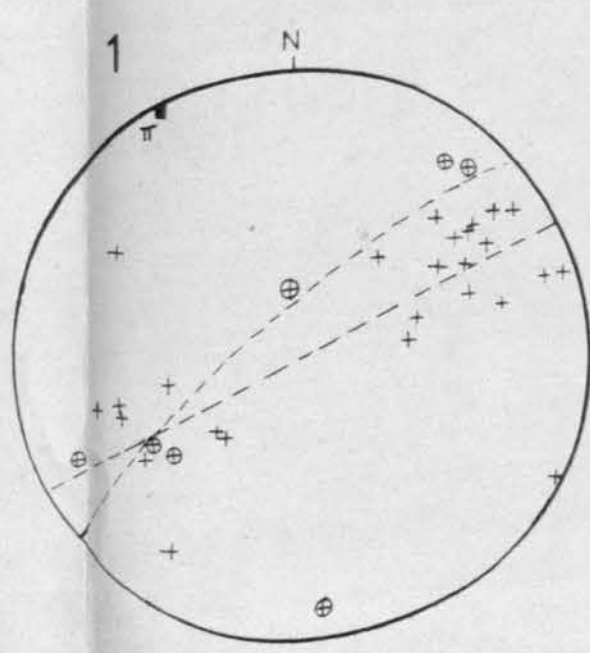
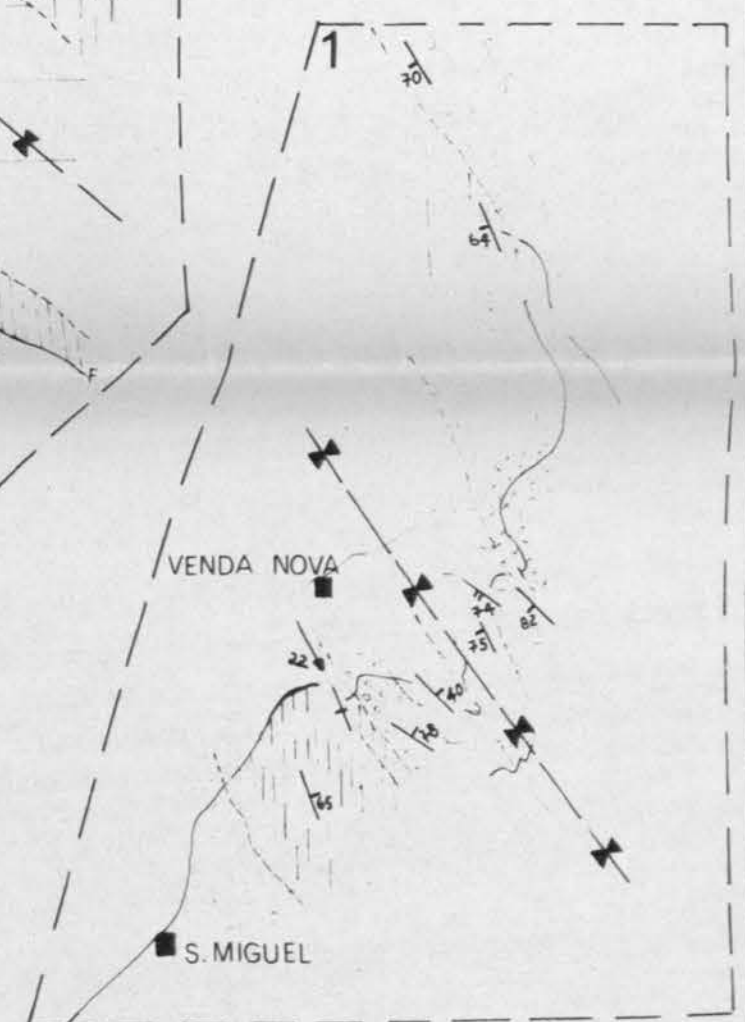
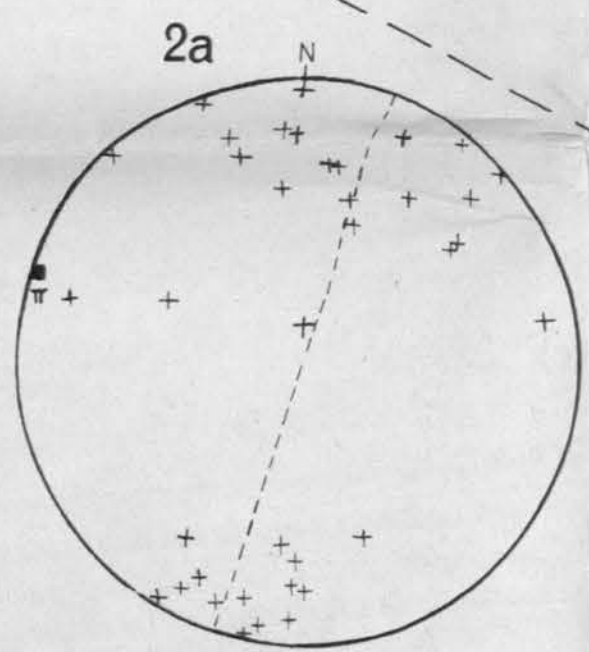
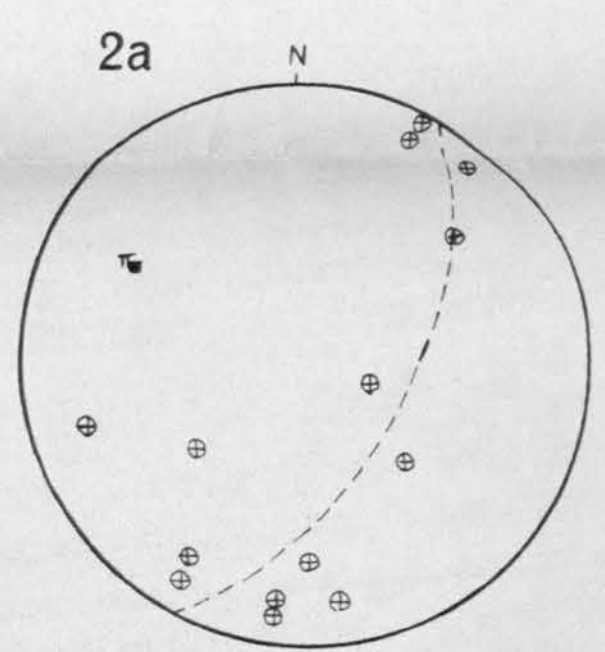
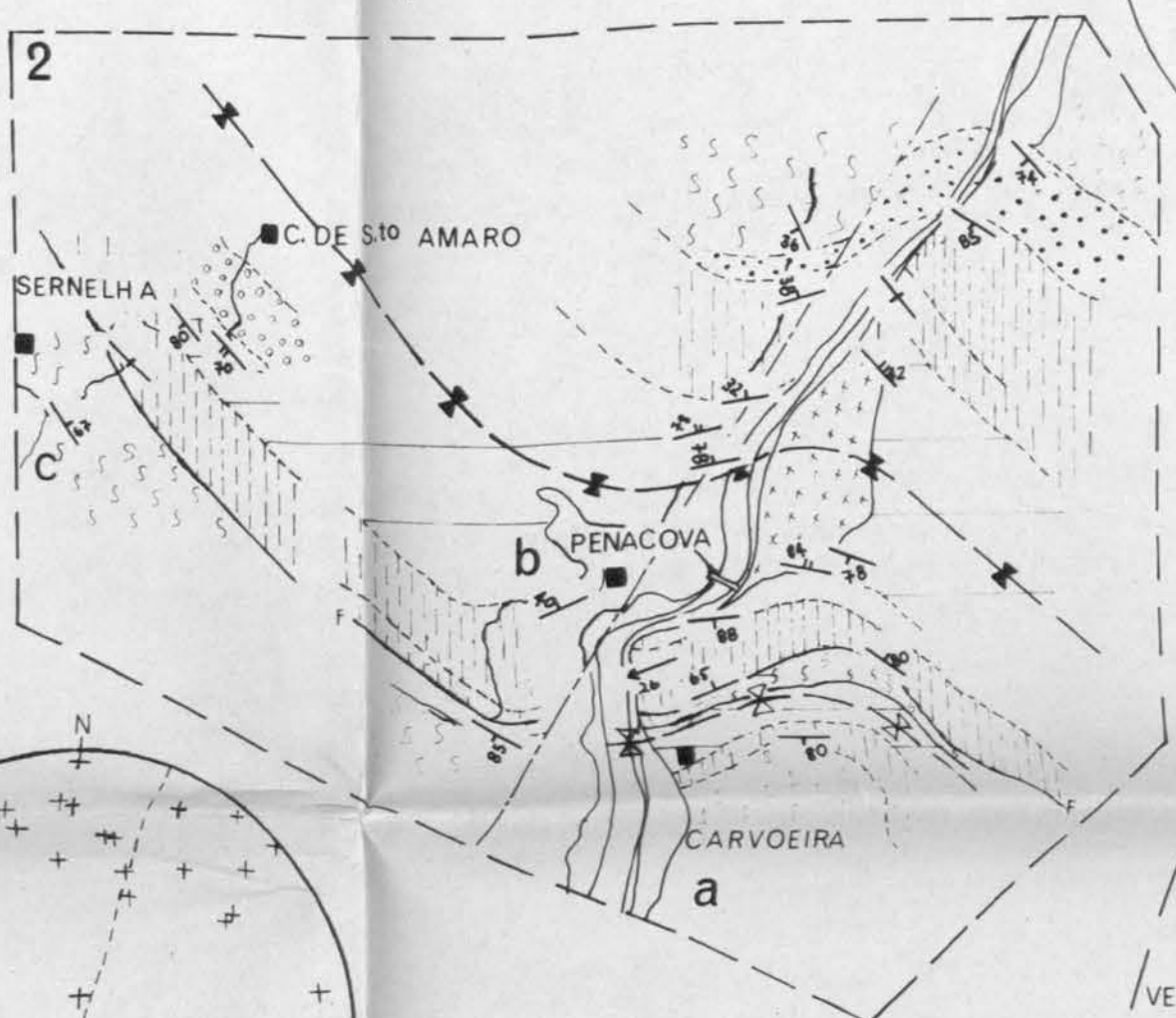
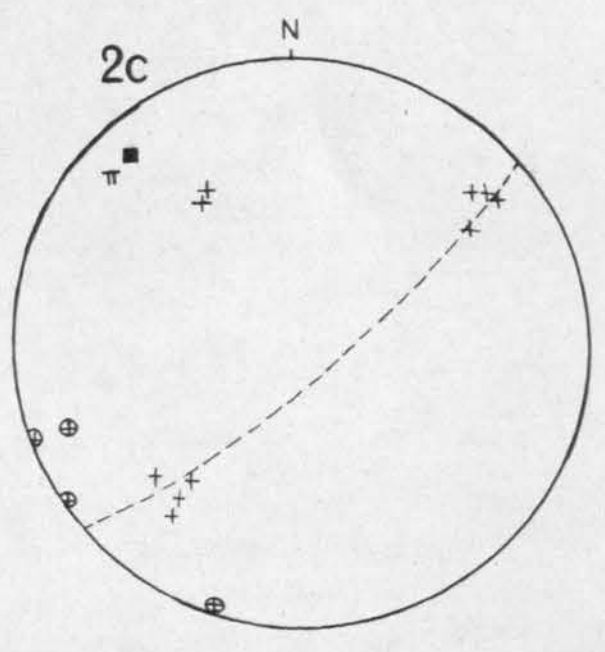
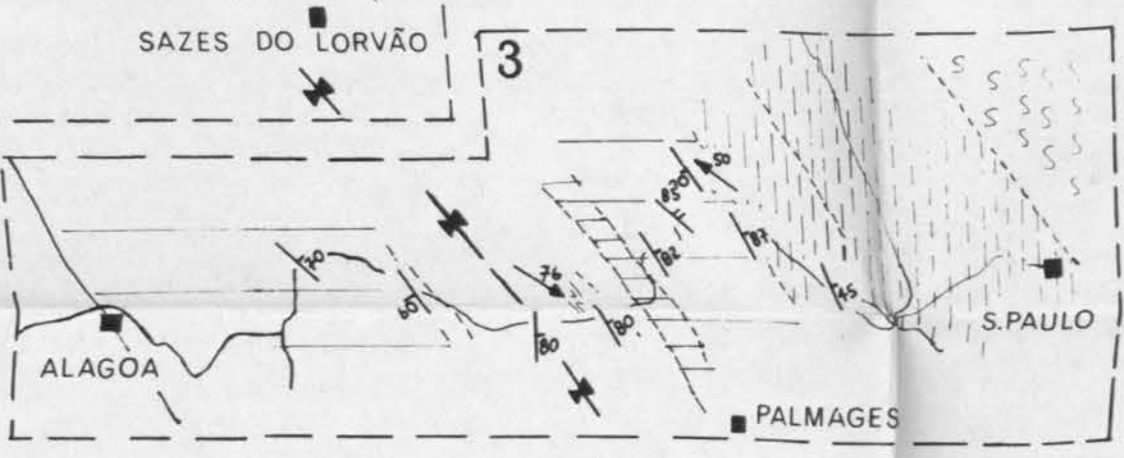
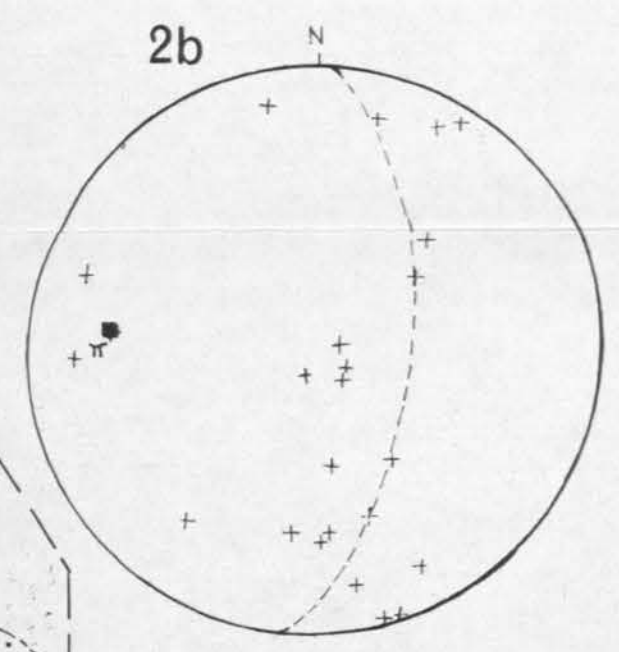
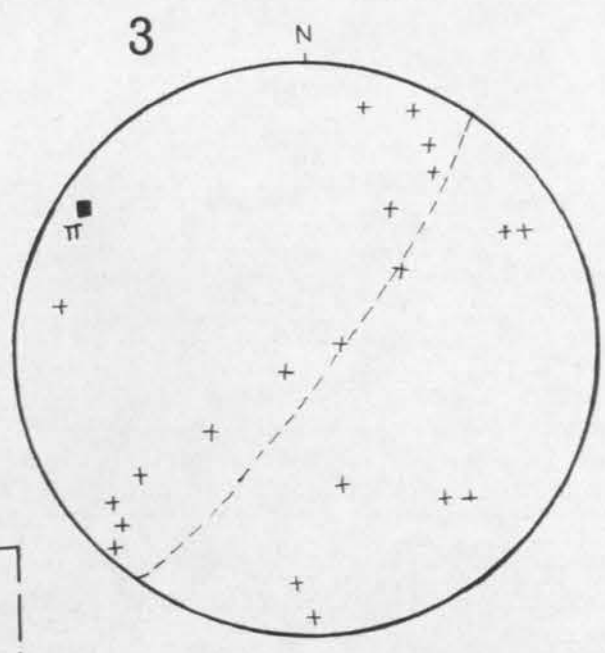
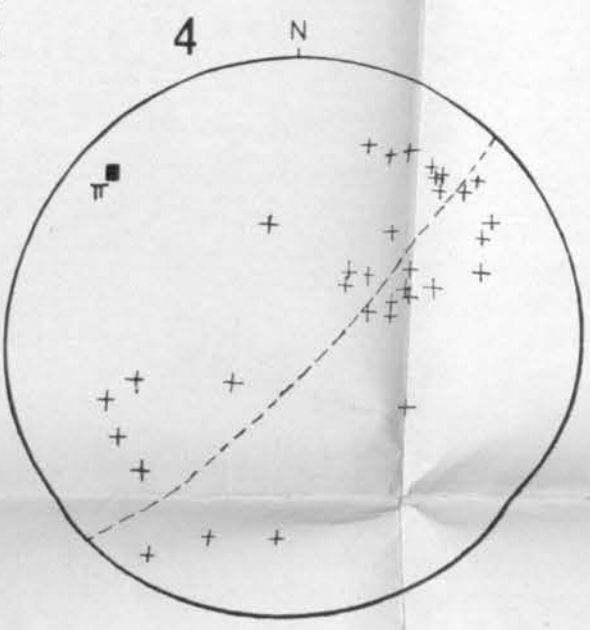
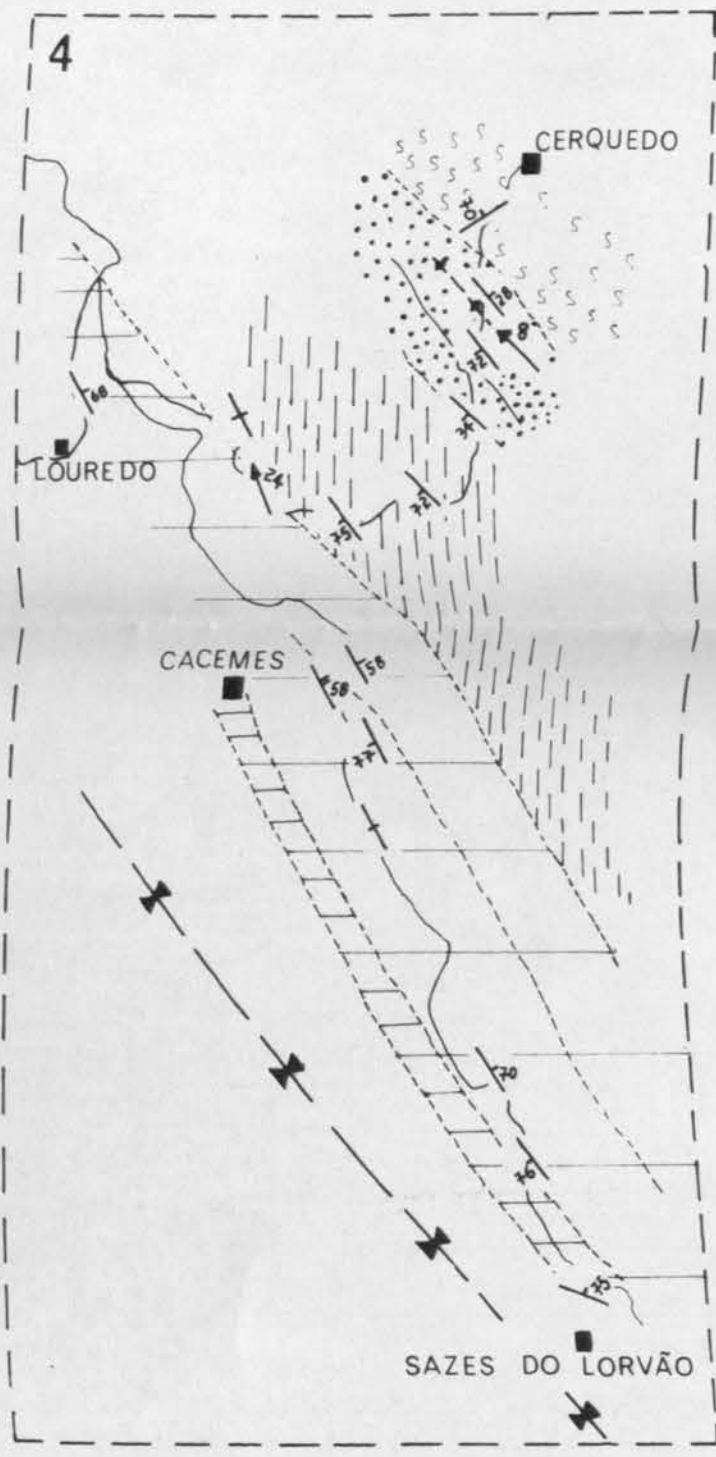
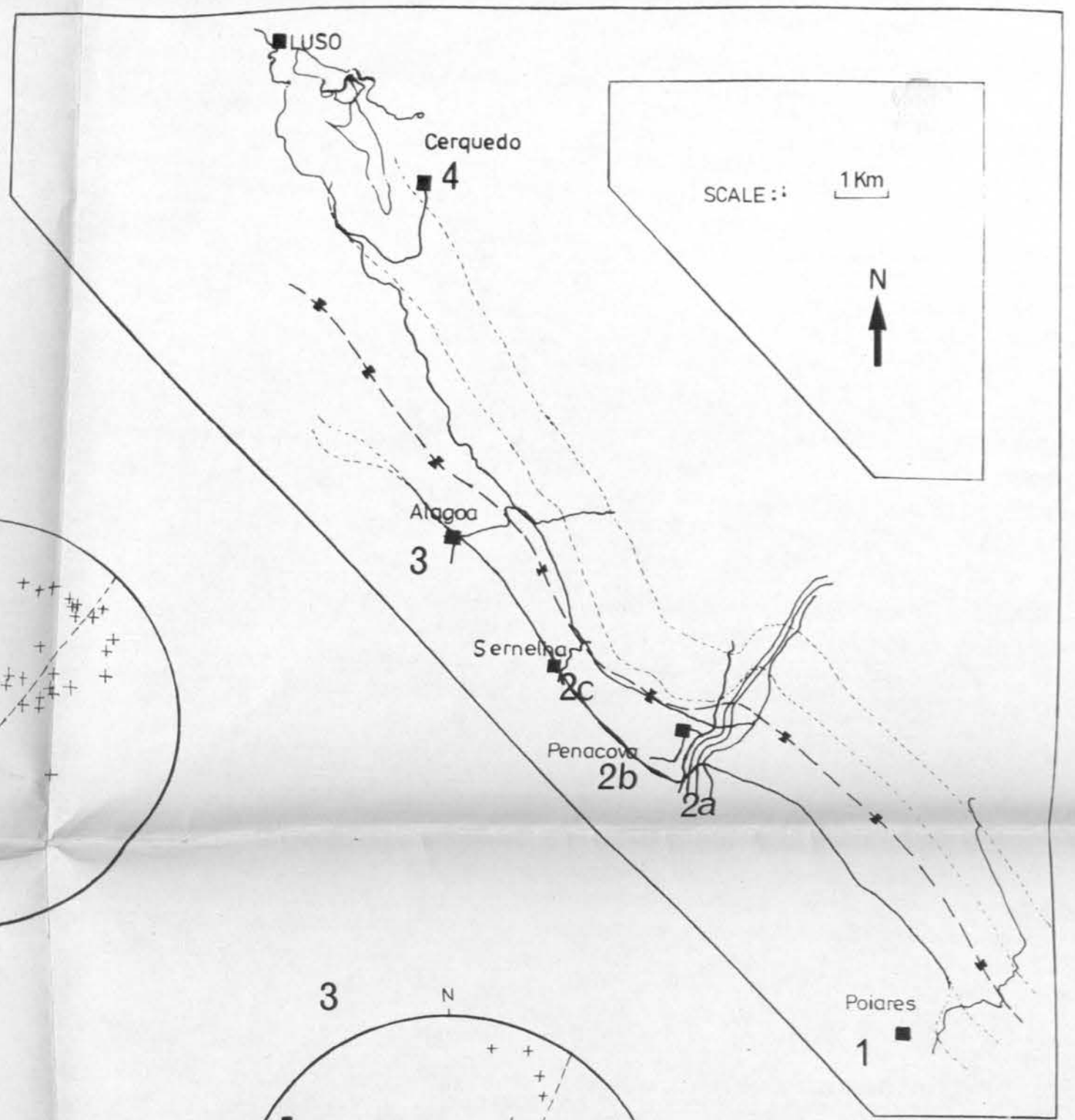
- Seilacher, A. 1970. A Cruziana Stratigraphy of 'non-Fossiliferous' Palaeozoic sandstones. In Trace Fossils. Edited by Crimes, T.C. and Harper, J.C. 447-476.
- Stille, H. 1939. Bemerkungen betreffend die 'sardischer' Faltung und den Ausdruck 'ophiolithisch'. Z. Deutsch. geol. Ges. 91, 771-773.
- Strand, T. 1944. Structural Petrology of the Bygdin conglomerate. Nor. geol. Tidsskr. 24, 14-31.
- Teixeira, C. 1943. O Palaeozoico Iberico e os movimentos Caledonicos e Hercinicos. Bol. Soc. geol. Portugal. 111, 17-47.
- Teixeira, C. 1954. Os conglomerados do Complexo xisto-grauvaquico ante-Silurico. Sua importancia geologica e paleogeografica. Com. Serv. geol. Portugal 35, 33-50.
- Teixeira, C. 1955. Notas sobre Geologica de Portugal O Complexo xisto-grauvaquico ante -Ordoviciano. Lisboa.
- Teixeira, C. 1955a. Novos elementos para o conhecimento do Silurico Portugues. Com. Serv. geol. Portugal. XXXV1, 1-12.
- Teixeira, C. 1968. Quelques problemes de la geologie du Portugal. Int. geol. Congr. Prague. Report 23, 13, 233-242.
- Teixeira, C., Ribeiro, A., Silva, L.C. da. 1964. La faune de Lingulellinae des formations ante-ordoviciennes de Marao. Bol. Soc. geol. Portugal. 15, 117-122.

- Treagus, S.H. 1973. Buckling stability of a viscous single - layer system, oblique to the principal compression. *Tectonophysics*. 19, 271-289.
- Vernon, R.H. 1976. Metamorphic Processes. Reactions and microstructure Development. George Allen Unwin. London.
- Voo, R. Van der. 1969. Palaeomagnetic evidence for the rotation of the Iberian Peninsula. *Tectonophysics*. 7, 5-56.
- Wellman, H.W. 1962, A graphical method for analysing fossil distortion caused by tectonic deformation. *Geol. Mag.* 99, 348-352.
- Wilkinson, P., Soper, N.J., Bell, A.M. 1975. Skolithos pipes as strain markers in mylonites. *Tectonophysics*. 28, 143-157.
- Williams, P.F. 1972. Development of metamorphic layering and cleavage in low grade metamorphic rocks at Bermagui, Australia. *Am. J. Sci.* 272, 1-47.
- Wood, D.S. 1971. Studies of strain and slaty cleavage in the Caledonides of North-West Europe and the Eastern United States. Unpublished PhD. thesis. University of Leeds.
- Wood, D.S. 1973. Patterns and magnitudes of natural strain in rocks. *Philos. Trans, R. Soc. London. A.* 274, 373-382.

Fig. 4.1

FIGURE 4.1

THE PENACOVA SYNCLINE



KEY			
	Post Silurian		Minor Syncline
	Silurian undifferentiated		Axial trace of Penacova Syncline
	marble volcanics		Plunge of F1 folds
	Sobredo Formation		Cleavage
	Valongo Formation		bedding inclined vertical
	quartzites		
	Santa Justa red facies Formation		
	Complexo xisto-grauvaquico		

STEREOGRAPHIC PROJECTIONS	
	bedding
	S ₁ cleavage
	TT pole to bedding

Fig. 5.1

Figure 5.1

THE EASTERN LIMB OF THE MARÃO SYNCLINE

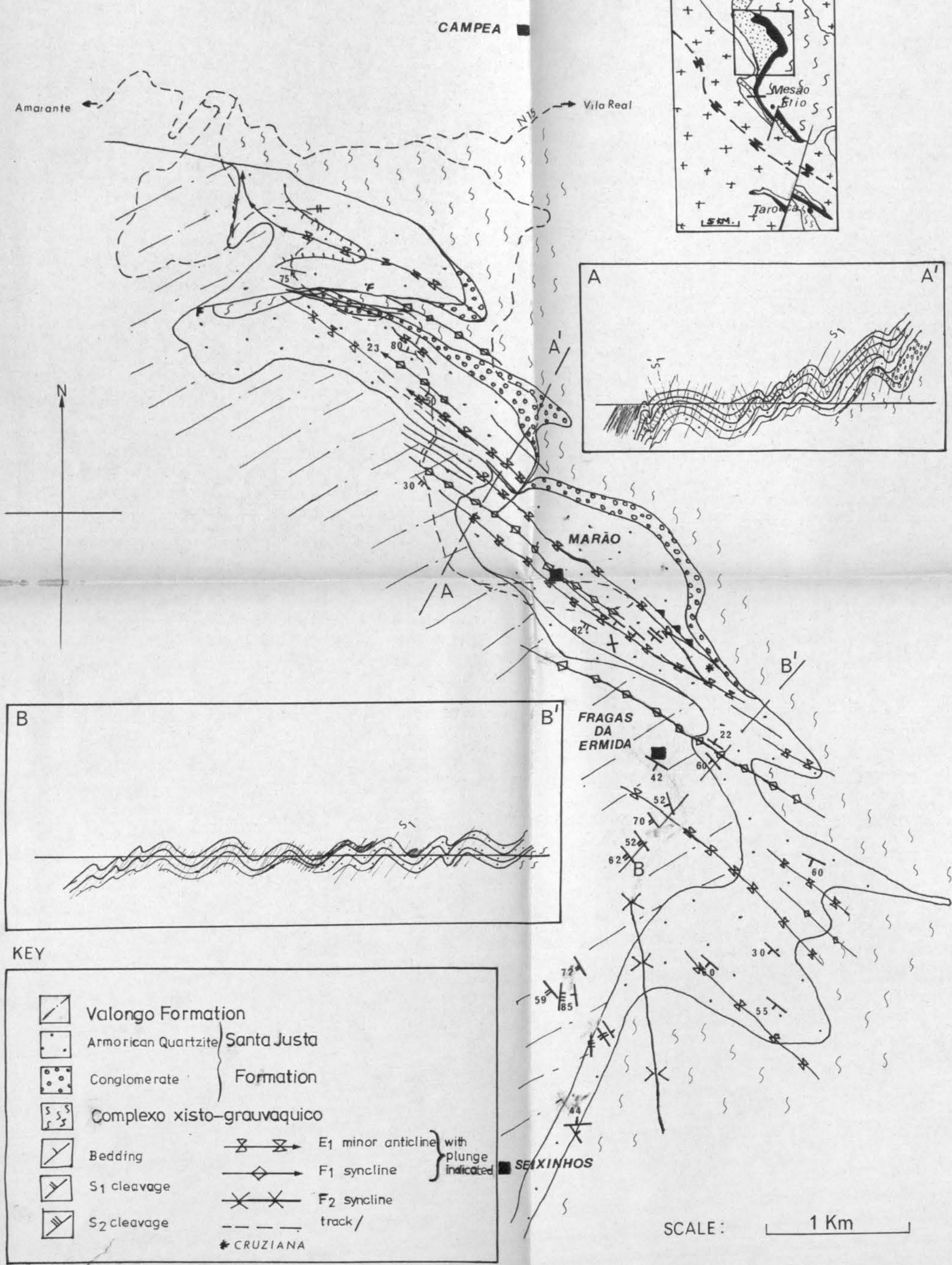
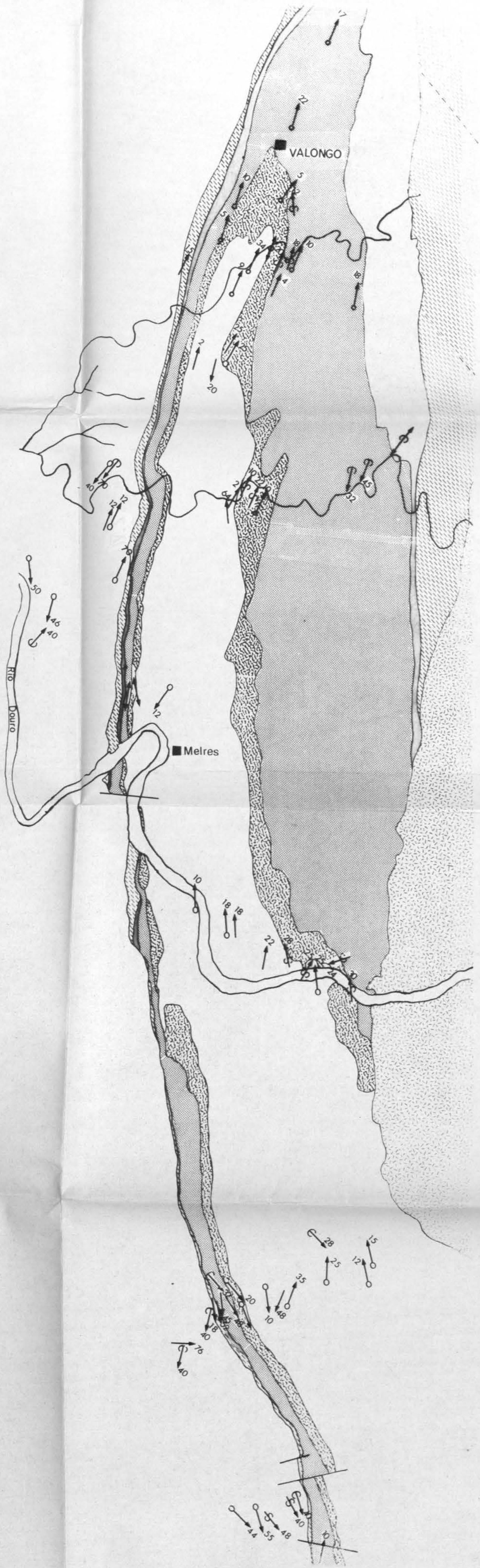
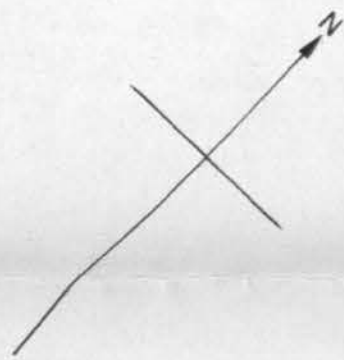


Fig. 2,7

FIGURE 2.76

THE VALONGO ANTICLINE:

Linear structures



SCALE : 1 km

KEY



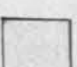



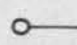
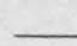
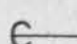

-  Granite
 -  Silurian-Carboniferous
 -  Sobredo Formation
 -  Valongo Formation
 -  Santa Justa Formation
 -  Complexo xisto-grauvaquico
 -  Elongation direction
 -  S₁/S₀ intersection lineation
 -  Plunge of F₂ crenulations
 -  Plunge of F₁ fold axes
- } Ordovician

Fig. 7.1

